

GRANT
IN-3151
137778
P-183

**Carderock Division
Naval Surface Warfare Center**

Bethesda, MD 20084-5000

CARDEROCKDIV-U-SSM-65-93/03 Axisymmetric Deformations and Stresses of Unsymmetrically Laminated Composite Cylinders in Axial Compression with Thermally-Induced Preloading Effects

CARDEROCKDIV-U-SSM-65-93/03 March 1993
Survivability, Structures and Materials Directorate
Research and Development Report

**Axisymmetric Deformations and Stresses of
Unsymmetrically Laminated Composite Cylinders in
Axial Compression with Thermally-Induced
Preloading Effects**

by
Peter J. Paraska

(NASA-CR-192788) AXISYMMETRIC
DEFORMATIONS AND STRESSES OF
UNSYMMETRICALLY LAMINATED COMPOSITE
CYLINDERS IN AXIAL COMPRESSION WITH
THERMALLY-INDUCED PRELOADING
EFFECTS (Naval Surface Warfare
Center) 183 p

N93-24912

Unclass

G3/39 0157798



Approved for public release;
unlimited distribution.

MAJOR DTRC TECHNICAL COMPONENTS

- CODE 011 DIRECTOR OF TECHNOLOGY, PLANS AND ASSESSMENT
 - 12 SHIP SYSTEMS INTEGRATION DEPARTMENT
 - 14 SHIP ELECTROMAGNETIC SIGNATURES DEPARTMENT
 - 15 SHIP HYDROMECHANICS DEPARTMENT
 - 16 AVIATION DEPARTMENT
 - 17 SHIP STRUCTURES AND PROTECTION DEPARTMENT
 - 18 COMPUTATION, MATHEMATICS & LOGISTICS DEPARTMENT
 - 19 SHIP ACOUSTICS DEPARTMENT
 - 27 PROPULSION AND AUXILIARY SYSTEMS DEPARTMENT
 - 28 SHIP MATERIALS ENGINEERING DEPARTMENT

DTRC ISSUES THREE TYPES OF REPORTS:

1. **DTRC reports, a formal series**, contain information of permanent technical value. They carry a consecutive numerical identification regardless of their classification or the originating department.
2. **Departmental reports, a semiformal series**, contain information of a preliminary, temporary, or proprietary nature or of limited interest or significance. They carry a departmental alphanumeric identification.
3. **Technical memoranda, an informal series**, contain technical documentation of limited use and interest. They are primarily working papers intended for internal use. They carry an identifying number which indicates their type and the numerical code of the originating department. Any distribution outside DTRC must be approved by the head of the originating department on a case-by-case basis.

**Carderock Division
Naval Surface Warfare Center**

Bethesda MD 20084-5000

CARDEROCKDIV-U-SSM-65-93/03 March 1993

Survivability, Structures, and Materials Directorate
Research and Development Report

**Axisymmetric Deformations and Stresses of
Unsymmetrically Laminated Composite Cylinders in
Axial Compression with Thermally-Induced
Preloading Effects**

by

Peter J. Paraska

Omit from general bibliographic listings

CONTENTS

	Page
ABSTRACT	1
ADMINISTRATIVE INFORMATION	1
I. INTRODUCTION	2
A. Cylinder Nomenclature and Geometry	5
II. DERIVATION OF THE EQUILIBRIUM EQUATIONS FOR THIN CYLINDRICAL PANELS	7
A. The Method of Minimum Total Potential Energy	7
B. Assumptions Related to Thin Shells	9
C. Specification of the Potential Energy Due to External Loads	12
D. Application of the Method of Total Potential Energy to Cylindrical Panels	24
E. Application of Integration By Parts	45
III. SIMPLIFICATION OF THE EQUILIBRIUM EQUATIONS DUE TO THE CONDITION OF AXISYMMETRY	61
A. Solution of Equations for the Case of Axial End Load	63
B. Specification of Boundary Conditions	65
1. Lubricated Boundary Conditions	68
2. Simply Supported Boundary Conditions	69
3. Clamped Boundary Conditions	70
C. Solution of the Governing Equation for $w^o(x)$	70
D. Solution of the Governing Equation for $u^o(x)$	75
E. Preloading Response Due to Thermal Effects	80
F. Numerical Results for the Case of Thermally-Induced Preloading	81
G. Cylinder Response Due to Thermally-Induced Preloading Effects and a Compressive Axial Load	84
H. Numerical Results for the Case of Thermally-Induced Preloading Effects and a Compressive Axial Load	88
1. Simply Supported Boundary Conditions with Thermally-Induced Preloading Effects and a Compressive Axial Load	88
2. Clamped Boundary Conditions with Thermally-Induced Preloading Effects and a Compressive Axial Load	92
3. Effect of Neglecting to Include the Thermally-Induced Preloading Effects	95



CONTENTS (continued)

	Page
IV. CALCULATION OF INTRALAMINAR STRESSES	100
A. Equations Describing Intralaminar Stresses	100
B. Numerical Results for Intralaminar Stresses: Case of Thermally-Induced Preloading Effects and a Compressive Axial Load with Clamped Boundary Conditions	103
C. Discussion of Intralaminar Stress Results	105
V. DERIVATION OF THE THREE-DIMENSIONAL EQUILIBRIUM EQUATIONS IN CYLINDRICAL COORDINATES	115
A. Transformation of the Three-Dimensional Equations of a Linear Elastic Body in Rectangular Coordinates to Cylindrical Coordinates	117
B. Derivation of the Displacement Gradients and Rotation Components of the Finite Strain Tensor in Cylindrical Coordinates	125
C. Specialization of the Displacement Gradients and Rotations Under the Assumption of Axisymmetry	130
D. Simplification of the Axisymmetric Displacement Gradients and Rotations Under the Assumptions of Kirchhoff and Donnell	131
E. Specialization of the Three-Dimensional Equilibrium Equations and Boundary Conditions Under the Assumption of Axisymmetry	133
F. Simplification of the Equilibrium Equations and Boundary Conditions Through Elimination of Terms of Relatively Small Magnitude	134
1. Simplification of the First Equilibrium Equation	136
2. Simplification of the Second Equilibrium Equation	137
3. Simplification of the Third Equilibrium Equation	139
4. Simplification of the Natural Boundary Conditions	141
VI. SOLUTION OF THE THREE-DIMENSIONAL EQUILIBRIUM EQUATIONS FOR THE INTERLAMINAR STRESSES	145
A. Solution of the First Equilibrium Equation	146
B. Calculation of the Interlaminar Stress Component τ^{xz}	156
C. Numerical Results for the Interlaminar Stress Component : Case of Thermally-Induced Preloading Effects and a Compressive Axial Load with Clamped Boundary Conditions	158
VII. CONCLUSIONS	166
A. Discussion of Displacement Results	166
B. Discussion of Intralaminar Stress Results	168
C. Discussion of Interlaminar Stress Results	169
REFERENCES	171

TABLES

		Page
Table I.	Layer Material Properties	81
Table II.	Laminate Properties and Thermally-Induced Stress Resultants for [+45/-45/0 ₂] _{2S} , [+45/-45/0 ₂] _{4T} , and [0 ₂ /-45/+45] _{4T} Cylinders, $\Delta T = -280^\circ\text{F}$	82
Table III.	Maximum Values of Displacement Gradients and Rotations	136
Table IV.	Comparison of the Shear Resultant Q_x as Calculated from the Interlaminar Shear Stress τ^{xz} and the Derivative of the CLT Relation for M_x	165

FIGURES

		Page
Fig. 1.	Cylinder Coordinate System, Geometry, and Nomenclature.	5
Fig. 2.	Tractions acting on the $x = +L/2$ edge.	13
Fig. 3.	Stress Resultants acting along the $x = +L/2$ edge.	14
Fig. 4.	Tractions acting along the $x = -L/2$ edge.	15
Fig. 5.	Stress Resultants acting along the $x = -L/2$ edge.	16
Fig. 6.	Tractions acting along the $\theta = +\beta/2$ edge.	17
Fig. 7.	Stress Resultants acting along the $\theta = +\beta/2$ edge.	18
Fig. 8.	Tractions acting along the $\theta = -\beta/2$ edge.	19
Fig. 9.	Stress Resultants acting along the $\theta = -\beta/2$ edge.	19
Fig. 10.	Tractions acting on the top and bottom surfaces.	20
Fig. 11.	Dimensionless Axial Mid-surface Displacement of Cylinders with Lubricated Boundary Conditions, $N=0$, $\Delta T = -280^\circ\text{F}$	82
Fig. 12.	Dimensionless Tangential Mid-surface Displacement of Cylinders with Lubricated Boundary Conditions, $N=0$, $\Delta T = -280^\circ\text{F}$	83
Fig. 13.	Dimensionless Radial Mid-surface Displacement of Cylinders with Lubricated Boundary Conditions, $N=0$, $\Delta T = -280^\circ\text{F}$	83
Fig. 14.	Dimensionless Axial Mid-surface Displacement of Cylinders with Simply Supported Ends, $N=10\%N^*$, $\Delta T = -280^\circ\text{F}$	90
Fig. 15.	Dimensionless Tangential Mid-surface Displacement of Cylinders with Simply Supported Ends, $N=10\%N^*$, $\Delta T = -280^\circ\text{F}$	90
Fig. 16.	Dimensionless Radial Mid-surface Displacement of Cylinders with Simply Supported Ends, $N=10\%N^*$, $\Delta T = -280^\circ\text{F}$	91
Fig. 17.	Dimensionless Axial Mid-surface Displacement of Cylinders with Simply Supported Ends, $N=90\%N^*$, $\Delta T = -280^\circ\text{F}$	91
Fig. 18.	Dimensionless Tangential Mid-surface Displacement of Cylinders with Simply Supported Ends, $N=90\%N^*$, $\Delta T = -280^\circ\text{F}$	91

FIGURES (continued)

		Page
Fig. 19.	Dimensionless Radial Mid-surface Displacement of Cylinders with Simply Supported Ends, $N=90\%N^*$, $\Delta T=-280^\circ\text{F}$	92
Fig. 20.	Dimensionless Axial Mid-surface Displacement of Cylinders with Clamped Ends, $N=10\%N^*$, $\Delta T=-280^\circ\text{F}$	93
Fig. 21.	Dimensionless Tangential Mid-surface Displacement of Cylinders with Clamped Ends, $N=10\%N^*$, $\Delta T=-280^\circ\text{F}$	94
Fig. 22.	Dimensionless Radial Mid-surface Displacement of Cylinders with Clamped Ends, $N=10\%N^*$, $\Delta T=-280^\circ\text{F}$	94
Fig. 23.	Dimensionless Axial Mid-surface Displacement of Cylinders with Clamped Ends, $N=90\%N^*$, $\Delta T=-280^\circ\text{F}$	94
Fig. 24.	Dimensionless Tangential Mid-surface Displacement of Cylinders with Clamped Ends, $N=90\%N^*$, $\Delta T=-280^\circ\text{F}$	95
Fig. 25.	Dimensionless Radial Mid-surface Displacement of Cylinders with Clamped Ends, $N=90\%N^*$, $\Delta T=-280^\circ\text{F}$	95
Fig. 26.	Dimensionless Axial Mid-surface Displacement of Cylinders with Simply Supported Ends, $N=10\%N^*$, $\Delta T=0^\circ\text{F}$	96
Fig. 27.	Dimensionless Tangential Mid-surface Displacement of Cylinders with Simply Supported Ends, $N=10\%N^*$, $\Delta T=0^\circ\text{F}$	97
Fig. 28.	Dimensionless Radial Mid-surface Displacement of Cylinders with Simply Supported Ends, $N=10\%N^*$, $\Delta T=0^\circ\text{F}$	97
Fig. 29.	Dimensionless Axial Mid-surface Displacement of Cylinders with Simply Supported Ends, $N=90\%N^*$, $\Delta T=0^\circ\text{F}$	97
Fig. 30.	Dimensionless Tangential Mid-surface Displacement of Cylinders with Simply Supported Ends, $N=90\%N^*$, $\Delta T=0^\circ\text{F}$	98
Fig. 31.	Dimensionless Radial Mid-surface Displacement of Cylinders with Simply Supported Ends, $N=90\%N^*$, $\Delta T=0^\circ\text{F}$	98
Fig. 32.	Dimensionless Radial Mid-surface Displacement of a $[0_8/90_8]_T$ Cylinder with Simply Supported Ends, $N=10\%N^*$, $\Delta T=0^\circ\text{F}$ and $\Delta T=-280^\circ\text{F}$	98
Fig. 33.	Dimensionless Radial Mid-surface Displacement of a $[0_8/90_8]_T$ Cylinder with Simply Supported Ends, $N=90\%N^*$, $\Delta T=0^\circ\text{F}$ and $\Delta T=-280^\circ\text{F}$	99
Fig. 34a.	σ_{11} along x/L for 0° Layers of a $[+45/-45/0_2]_{2S}$ Cylinder, $N=10\%N^*$, $\Delta T=-280^\circ\text{F}$	108
Fig. 34b.	σ_{11} along x/L for 45° Layers of a $[+45/-45/0_2]_{2S}$ Cylinder, $N=10\%N^*$, $\Delta T=-280^\circ\text{F}$	108
Fig. 34c.	σ_{22} along x/L for 0° Layers of a $[+45/-45/0_2]_{2S}$ Cylinder, $N=10\%N^*$, $\Delta T=-280^\circ\text{F}$	108
Fig. 34d.	σ_{22} along x/L for 45° Layers of a $[+45/-45/0_2]_{2S}$ Cylinder, $N=10\%N^*$, $\Delta T=-280^\circ\text{F}$	108

FIGURES (continued)

	Page
Fig. 34e.	τ_{12} along x/L for 0° Layers of a $[+45/-45/0_2]_{2S}$ Cylinder, $N=10\%N^*$, $\Delta T=-280^\circ F$ 108
Fig. 34f.	τ_{12} along x/L for 45° Layers of a $[+45/-45/0_2]_{2S}$ Cylinder, $N=10\%N^*$, $\Delta T=-280^\circ F$ 108
Fig. 35a.	σ_{11} along x/L for 0° Layers of a $[+45/-45/0_2]_{4T}$ Cylinder, $N=10\%N^*$, $\Delta T=-280^\circ F$ 109
Fig. 35b.	σ_{11} along x/L for 45° Layers of a $[+45/-45/0_2]_{4T}$ Cylinder, $N=10\%N^*$, $\Delta T=-280^\circ F$ 109
Fig. 35c.	σ_{22} along x/L for 0° Layers of a $[+45/-45/0_2]_{4T}$ Cylinder, $N=10\%N^*$, $\Delta T=-280^\circ F$ 109
Fig. 35d.	σ_{22} along x/L for 45° Layers of a $[+45/-45/0_2]_{4T}$ Cylinder, $N=10\%N^*$, $\Delta T=-280^\circ F$ 109
Fig. 35e.	τ_{12} along x/L for 0° Layers of a $[+45/-45/0_2]_{4T}$ Cylinder, $N=10\%N^*$, $\Delta T=-280^\circ F$ 109
Fig. 35f.	τ_{12} along x/L for 45° Layers of a $[+45/-45/0_2]_{4T}$ Cylinder, $N=10\%N^*$, $\Delta T=-280^\circ F$ 109
Fig. 36a.	σ_{11} along x/L for 0° Layers of a $[0_2/-45/+45]_{4T}$ Cylinder, $N=10\%N^*$, $\Delta T=-280^\circ F$ 110
Fig. 36b.	σ_{11} along x/L for 45° Layers of a $[0_2/-45/+45]_{4T}$ Cylinder, $N=10\%N^*$, $\Delta T=-280^\circ F$ 110
Fig. 36c.	σ_{22} along x/L for 0° Layers of a $[0_2/-45/+45]_{4T}$ Cylinder, $N=10\%N^*$, $\Delta T=-280^\circ F$ 110
Fig. 36d.	σ_{22} along x/L for 45° Layers of a $[0_2/-45/+45]_{4T}$ Cylinder, $N=10\%N^*$, $\Delta T=-280^\circ F$ 110
Fig. 36e.	τ_{12} along x/L for 0° Layers of a $[0_2/-45/+45]_{4T}$ Cylinder, $N=10\%N^*$, $\Delta T=-280^\circ F$ 110
Fig. 36f.	τ_{12} along x/L for 45° Layers of a $[0_2/-45/+45]_{4T}$ Cylinder, $N=10\%N^*$, $\Delta T=-280^\circ F$ 110
Fig. 37a.	σ_{11} along x/L for 0° Layers of a $[+45/-45/0_2]_{2S}$ Cylinder, $N=90\%N^*$, $\Delta T=-280^\circ F$ 111
Fig. 37b.	σ_{11} along x/L for 45° Layers of a $[+45/-45/0_2]_{2S}$ Cylinder, $N=90\%N^*$, $\Delta T=-280^\circ F$ 111
Fig. 37c.	σ_{22} along x/L for 0° Layers of a $[+45/-45/0_2]_{2S}$ Cylinder, $N=90\%N^*$, $\Delta T=-280^\circ F$ 111
Fig. 37d.	σ_{22} along x/L for 45° Layers of a $[+45/-45/0_2]_{2S}$ Cylinder, $N=90\%N^*$, $\Delta T=-280^\circ F$ 111
Fig. 37e.	τ_{12} along x/L for 0° Layers of a $[+45/-45/0_2]_{2S}$ Cylinder, $N=90\%N^*$, $\Delta T=-280^\circ F$ 111
Fig. 37f.	τ_{12} along x/L for 45° Layers of a $[+45/-45/0_2]_{2S}$ Cylinder, $N=90\%N^*$, $\Delta T=-280^\circ F$ 111

FIGURES (continued)

	Page
Fig. 38a.	σ_{11} along x/L for 0° Layers of a $[+45/-45/0_2]_{4T}$ Cylinder, $N=90\%N^*$, $\Delta T=-280^\circ F$ 112
Fig. 38b.	σ_{11} along x/L for 45° Layers of a $[+45/-45/0_2]_{4T}$ Cylinder, $N=90\%N^*$, $\Delta T=-280^\circ F$ 112
Fig. 38c.	σ_{22} along x/L for 0° Layers of a $[+45/-45/0_2]_{4T}$ Cylinder, $N=90\%N^*$, $\Delta T=-280^\circ F$ 112
Fig. 38d.	σ_{22} along x/L for 45° Layers of a $[+45/-45/0_2]_{4T}$ Cylinder, $N=90\%N^*$, $\Delta T=-280^\circ F$ 112
Fig. 38e.	τ_{12} along x/L for 0° Layers of a $[+45/-45/0_2]_{4T}$ Cylinder, $N=90\%N^*$, $\Delta T=-280^\circ F$ 112
Fig. 38f.	τ_{12} along x/L for 45° Layers of a $[+45/-45/0_2]_{4T}$ Cylinder, $N=90\%N^*$, $\Delta T=-280^\circ F$ 112
Fig. 39a.	σ_{11} along x/L for 0° Layers of a $[0_2/-45/+45]_{4T}$ Cylinder, $N=90\%N^*$, $\Delta T=-280^\circ F$ 113
Fig. 39b.	σ_{11} along x/L for 45° Layers of a $[0_2/-45/+45]_{4T}$ Cylinder, $N=90\%N^*$, $\Delta T=-280^\circ F$ 113
Fig. 39c.	σ_{22} along x/L for 0° Layers of a $[0_2/-45/+45]_{4T}$ Cylinder, $N=90\%N^*$, $\Delta T=-280^\circ F$ 113
Fig. 39d.	σ_{22} along x/L for 45° Layers of a $[0_2/-45/+45]_{4T}$ Cylinder, $N=90\%N^*$, $\Delta T=-280^\circ F$ 113
Fig. 39e.	τ_{12} along x/L for 0° Layers of a $[0_2/-45/+45]_{4T}$ Cylinder, $N=90\%N^*$, $\Delta T=-280^\circ F$ 113
Fig. 39f.	τ_{12} along x/L for 45° Layers of a $[0_2/-45/+45]_{4T}$ Cylinder, $N=90\%N^*$, $\Delta T=-280^\circ F$ 113
Fig. 40a.	σ_{11} along x/L for 0° Layers of a $[+45/-45/0_2]_{4T}$ Cylinder, $N=90\%N^*$, $\Delta T=0^\circ F$ 114
Fig. 40b.	σ_{11} along x/L for 45° Layers of a $[+45/-45/0_2]_{4T}$ Cylinder, $N=90\%N^*$, $\Delta T=0^\circ F$ 114
Fig. 40c.	σ_{22} along x/L for 0° Layers of a $[+45/-45/0_2]_{4T}$ Cylinder, $N=90\%N^*$, $\Delta T=0^\circ F$ 114
Fig. 40d.	σ_{22} along x/L for 45° Layers of a $[+45/-45/0_2]_{4T}$ Cylinder, $N=90\%N^*$, $\Delta T=0^\circ F$ 114
Fig. 40e.	τ_{12} along x/L for 0° Layers of a $[+45/-45/0_2]_{4T}$ Cylinder, $N=90\%N^*$, $\Delta T=0^\circ F$ 114
Fig. 40f.	τ_{12} along x/L for 45° Layers of a $[+45/-45/0_2]_{4T}$ Cylinder, $N=90\%N^*$, $\Delta T=0^\circ F$ 114
Fig. 41.	τ^x versus ρ at $x/L=0.5$ for $[+45/-45/0_2]_{2S}$, $[+45/-45/0_2]_{4T}$, and $[0_2/-45/+45]_{4T}$ Cylinders, $N=10\%N^*$, $\Delta T=-280^\circ F$ 162
Fig. 42.	τ^x versus ρ at $x/L=0.5$ for $[+45/-45/0_2]_{2S}$, $[+45/-45/0_2]_{4T}$, and $[0_2/-45/+45]_{4T}$ Cylinders, $N=90\%N^*$, $\Delta T=-280^\circ F$ 163

FIGURES (continued)

		Page
Fig. 43.	τ^w versus ρ at x/L locations of max. Q_x for $[+45/-45/0_2]_{2S}$, $[+45/-45/0_2]_{4T}$, and $[0_2/-45/+45]_{4T}$ Cylinders, $N=90\%N^*$, $\Delta T=-280^\circ F$.	163
Fig. 44.	τ^w versus ρ at x/L locations of maximum r_x for $[+45/-45/0_2]_{2S}$, $[+45/-45/0_2]_{4T}$, and $[0_2/-45/+45]_{4T}$ Cylinders, $N=10\%N^*$, $\Delta T=-280^\circ F$.	164
Fig. 45.	τ^w versus ρ at x/L locations of maximum r_x for $[+45/-45/0_2]_{2S}$, $[+45/-45/0_2]_{4T}$, and $[0_2/-45/+45]_{4T}$ Cylinders, $N=90\%N^*$, $\Delta T=-280^\circ F$.	164

ABSTRACT

This analytical study focuses on the response of unsymmetrically laminated cylinders subjected to thermally-induced preloading effects and compressive axial load. Attention is focused on the displacement response and three-dimensional stress state of cylinders having $[+45/-45/0_2]_{2S}$, $[+45/-45/0_2]_{4T}$, and $[0_2/-45/+45]_{4T}$ stacking sequences with clamped end conditions. The methods used in the analyses involve derivation of the plane stress and three-dimensional equilibrium equations and boundary conditions using the method of minimum total potential energy with nonlinear strain-displacement relations. The plane stress equations and boundary conditions are solved in closed-form for the displacements and intralaminar stresses. The three-dimensional equilibrium equations are then solved for the interlaminar shear stress τ^{xz} using the results of the plane stress problem. For the three cylinders analyzed, the radial deformations are observed to be larger for the unsymmetrically laminated cylinders, particularly in the boundary layer near the ends of the cylinders. With the nonlinear effects included, the boundary layer length increases with increasingly compressive axial load. If the thermally-induced preloading effects are not included, the deformations and intralaminar stresses are under-predicted. Also, it is observed that the boundary conditions for the axial load must include the thermally deformed shape of the cylinder. At low axial load levels, it was seen that both the fiber-direction intralaminar stress and the interlaminar stress τ^{xz} are dominated by the thermally-induced preloading effects. However, the intralaminar stress perpendicular to the fiber direction and the intralaminar shear stress are largely unaffected by the thermally-induced preloading effects.

ADMINISTRATIVE INFORMATION

The work described in this report was sponsored by the Survivability, Structures, and Materials Directorate, Carderock Division, Naval Surface Warfare Center, under job order number 4-1700-001-41, and the National Aeronautics and Space Administration, under NASA Grant NAG-1-901 with the Virginia Polytechnic Institute and State University. The NASA Technical Monitor was Dr. Michael P. Nemeth of the Aircraft Structures Branch, Langley Research Center. The development of the analytical work was directed by Professor Michael W. Hyer of the Department of Engineering Science and Mechanics at the Virginia Polytechnic Institute and State University.

I. INTRODUCTION

Cylinders made of composite materials are structurally efficient and well suited to manufacture by automated fiber-placement techniques such as filament winding. Composite cylinders are also more tolerant of unsymmetric stacking sequences than are flat plates. Unsymmetrically laminated plates warp when cooled from the consolidation temperature during manufacture. This effect becomes problematic for the designer, since the degree of warp must be anticipated and accounted for before manufacture. Because of the difficulties brought about by the manufacture of unsymmetrically laminated plates, there is a tendency to view the idea of unsymmetrically laminated cylinders with the same skepticism. However, due to the axisymmetric geometry inherent in the cylindrical form, cylinders resist much of the warping observed in the manufacture of plates. In practice, cylinders which are manufactured with the filament winding process are sometimes purposely made with unsymmetric stacking sequences because it is easier and less costly to complete the winding process without changing the fiber orientation on the outer layers of the cylinder.

One of the benefits of designing a structure with composite materials is the ability to tailor the structural properties of a member not only through changing the material type or thickness, but also by taking advantage of the couplings between bending, stretching, and shearing possible through changes in the stacking sequence of the wall of the structure. These couplings may impart a structure with behaviors which are beneficial under certain types of loadings, for example, increased buckling resistance to

compressive axial loads. For tubular members such as cylinders, these couplings will also impart to the structure a nonuniform shape as a result of cooling from consolidation temperature to ambient temperature. Although considerable attention to the response of composite cylinders has been given by others in the past, the combined effects of thermally-induced preloading effects and a compressive axial load on unsymmetrically laminated cylinders have previously received little or no attention. In fact, buckling analyses of unsymmetric cylinders are available in the literature which completely and erroneously ignore thermally-induced deformation (ref. 1).

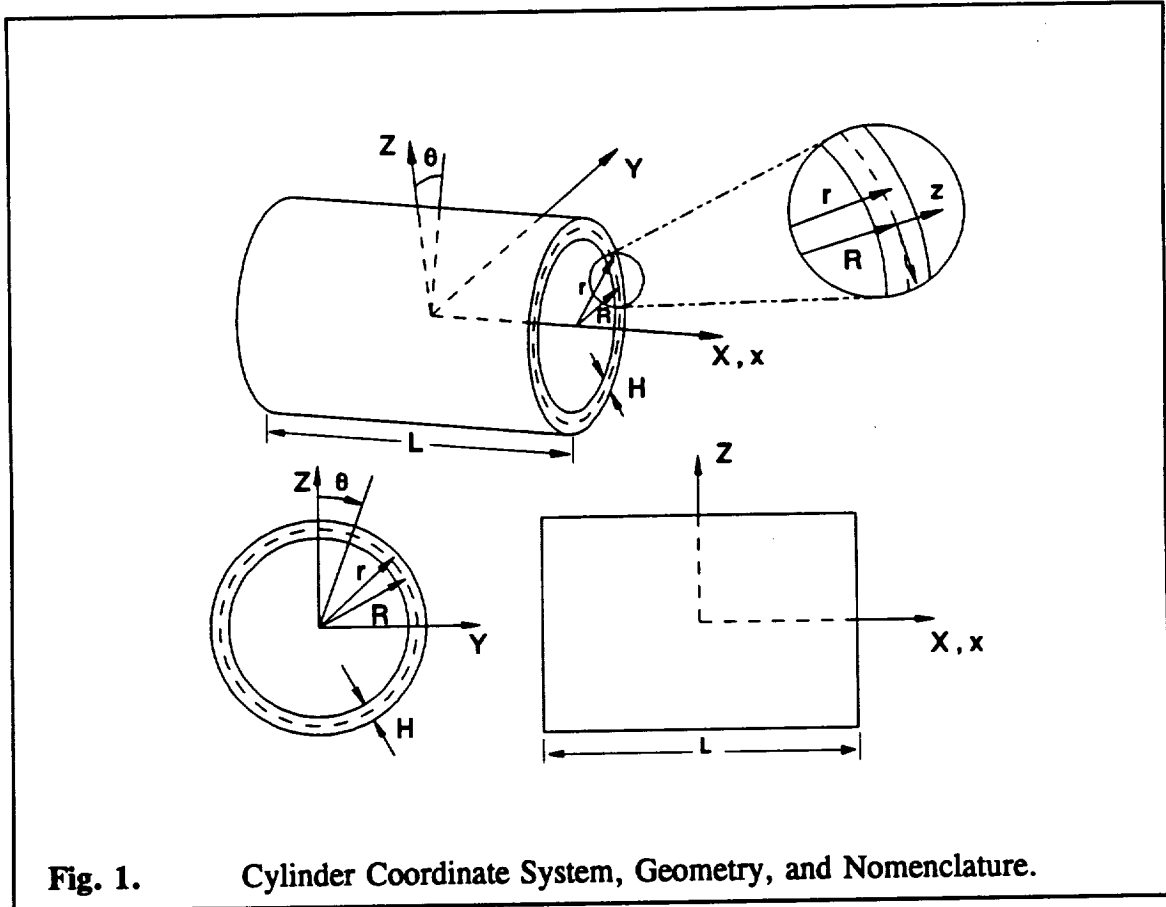
The purpose of this work is to investigate the effect of applying a compressive axial load to an unsymmetrically laminated cylinder which has already deformed in a nonuniform manner due to a temperature change from the consolidation temperature to ambient temperature. The work is important because cylinders subjected to a compressive axial load are prone to buckle. Analysis of the buckling phenomenon is a difficult problem. However, a key component of the buckling analysis is the prebuckling analysis. The predicted prebuckling state for an unsymmetrically laminated cylinder deformed by thermal effects before loading could be significantly different than the prebuckling state for that cylinder predicted by an analysis which ignores thermal effects. Though interest here will not extend to a buckling analysis, as it is considerably beyond the scope of the present effort, the formulation addressed here must be considered if a buckling analysis is to be developed. The analysis developed here is indeed a prebuckling analysis. Implicitly, it will be possible to determine if ignoring thermally-induced deformations may have an impact on predicting buckling loads. Towards this

end, the equilibrium equations and consistent boundary conditions which govern the response of thin cylindrical panels under general loadings will be derived in the second chapter. In the third chapter, these equations will be simplified due to conditions of axisymmetric geometry and response for the case of compressive axial end loading. The equations will be solved, to include the thermally-induced preloading effects, for the axial, tangential, and radial displacements as a function of the cylinder's length coordinate. These displacements will be calculated for three cylinders with different stacking sequences and are presented in graphical form.

In the fourth chapter, the solutions derived previously for the displacements will be used to obtain relations for the intralaminar stress components within each layer of the cylinder. Relations between the stress components and the radial coordinate for clamped boundary conditions and several axial load levels will be graphically presented for the three cylinders. In the fifth chapter, the equilibrium equations and boundary conditions in cylindrical coordinates for a three-dimensional stress state will be presented and simplified based on an investigation of the magnitudes of the coupling terms in the equations. The sixth chapter will present a solution of the simplified three-dimensional equilibrium equations and boundary conditions by making use of the stress-strain relations of the fourth chapter, which are of closed form. The significant interlaminar stress component will be calculated for each of three cylinders and the results will be graphically presented.

A. Cylinder Nomenclature and Geometry

The cylinder is referenced to a rectangular coordinate system with the axis of the cylinder centerline coincident with the X axis, as shown in Fig. 1.



For convenience, the origin of the global coordinate system is chosen to be at the midspan of the cylinder. Naturally, a cylindrical coordinate system is used for the analysis. The cylindrical coordinate system consists of an x axis which is coincident with the X axis, θ , which is measured positive from the $+Z$ axis toward the $+Y$ axis, and r , which is measured outward from the X axis. The cylinder has a length L , a mean radius R , and wall thickness H . Within the cylinder wall, a z coordinate is defined as being positive outward, measured from the mean radius R . The axial, tangential, and radial

displacement components of a point in the cylinder wall are denoted by $u(x,\theta,r)$, $v(x,\theta,r)$, and $w(x,\theta,r)$, respectively. The axial displacement $u(x,\theta,r)$ is measured positive along the $+X$ axis, the tangential displacement $v(x,\theta,r)$ is measured positive in the $+\theta$ direction, and the radial displacement $w(x,\theta,r)$ is measured positive outward in the r coordinate direction.

The derivation of the governing equations follows in the next chapter.

II. DERIVATION OF THE EQUILIBRIUM EQUATIONS FOR THIN CYLINDRICAL PANELS

A. The Method of Minimum Total Potential Energy

The total potential energy of a body is given by

$$\Pi = U + \Pi_{load}, \quad (1)$$

where U is the strain energy of the body given by

$$U = \frac{1}{2} \iiint_V \tau_{ij} \epsilon_{ij} dV, \quad (2)$$

τ_{ij} and ϵ_{ij} being the stress and strain tensors. The potential energy Π_{load} is defined as

$$\Pi_{load} = - \iiint_V B_i u_i dv - \iint_S T_i u_i ds, \quad (3)$$

where B_i is the body force distribution acting on the volume V of the body, T_i are the surface tractions acting over the boundary S of the body, and u_i is the displacement field.

For thin cylindrical shells, the strain energy expression of eq. (1) can be simplified by assuming a state of plane stress, i.e., by assuming that σ_{rr} , $\tau_{\theta r}$, and τ_{xr} are zero. As a further simplification, the body force distribution will also be assumed to be zero. Considering preloading deformations and including these two restrictions, eq. (1) can be expanded to yield

$$\begin{aligned} \Pi = & \frac{1}{2} \iiint_V [(\sigma_x - \sigma_x^P) \epsilon_x + (\sigma_\theta - \sigma_\theta^P) \epsilon_\theta + (\tau_{x\theta} - \tau_{x\theta}^P) \gamma_{x\theta}] dV \\ & - \iint_S (T_x u + T_\theta v + T_z w) dS. \end{aligned} \quad (4)$$

For a cylindrical panel with mean radius R , length L , opening angle β , thickness H , bounded by the six surfaces $x = -\frac{L}{2}$, $x = +\frac{L}{2}$, $\theta = -\frac{\beta}{2}$, $\theta = +\frac{\beta}{2}$, $r = R - \frac{H}{2}$, and $r = R + \frac{H}{2}$, eq. (4) becomes

$$\Pi = \frac{1}{2} \int_{r=R-\frac{H}{2}}^{r=R+\frac{H}{2}} \int_{x=-\frac{L}{2}}^{x=+\frac{L}{2}} \int_{\theta=-\frac{\beta}{2}}^{\theta=+\frac{\beta}{2}} [(\sigma_x - \sigma_x^P) \epsilon_x + (\sigma_\theta - \sigma_\theta^P) \epsilon_\theta + (\tau_{x\theta} - \tau_{x\theta}^P) \gamma_{x\theta}] r d\theta dx dr + \Pi_{load}, \quad (5)$$

where

$$\Pi_{load} = - \iint_S (T_x u + T_\theta v + T_z w) ds \quad (6)$$

is the potential energy of the applied loads. The stress components superscripted with a "P" denote preloading effects. These components could be due to imperfect cylinder geometry, thermally-induced deformations, or any other influence unrelated to the loading.

The functional in eqs. (5) and (6) represent the total potential energy of a cylindrical panel under the assumption of plane stress. This functional will be minimized in a later section through the methods of variational calculus.

B. Assumptions Related to Thin Shells

The following are Donnell's assumptions for the kinematics of deformation :

$$\begin{aligned} u(x,\theta,r) &= u^o(x,\theta) + z\beta_x^o(x,\theta) \\ v(x,\theta,r) &= v^o(x,\theta) + z\beta_\theta^o(x,\theta) \\ w(x,\theta,r) &= w^o(x,\theta) . \end{aligned} \tag{7}$$

In the above, the local thickness coordinate z is given by

$$z = r - R, \tag{8}$$

the superscript zero denotes displacements of the cylindrical panel's reference surface taken at the mean radius R , and the β 's are the rotations at the reference surface given by

$$\begin{aligned} \beta_x^o &= -\frac{\partial w^o}{\partial x} \\ \beta_\theta^o &= -\frac{\partial w^o}{R\partial\theta} . \end{aligned} \tag{9}$$

Note that the displacements u^o , v^o , and w^o and the rotations β_x^o and β_θ^o are relative to a perfectly cylindrical panel before any preloading effects. The pertinent strain-displacement relations in cylindrical coordinates are

$$\begin{aligned} \epsilon_x &= \frac{\partial u}{\partial x} + \frac{1}{2} \left(\frac{\partial w}{\partial x} \right)^2 \\ \epsilon_\theta &= \frac{\partial v}{R\partial\theta} + \frac{w}{r} + \frac{1}{2} \left(\frac{\partial w}{r\partial\theta} \right)^2 \\ \gamma_{x\theta} &= \frac{\partial v}{\partial x} + \frac{\partial u}{r\partial\theta} + \frac{\partial w}{r\partial\theta} \frac{\partial w}{\partial x} . \end{aligned} \tag{10}$$

For thin cylindrical panels, the approximation

$$r = R \tag{11}$$

can be made with sufficient accuracy. Substituting eqs. (7) and (9) into eq. (10) using eq. (11), the strains become

$$\begin{aligned}\epsilon_x &= \epsilon_x^o + z\kappa_x^o \\ \epsilon_\theta &= \epsilon_\theta^o + z\kappa_\theta^o \\ \gamma_{x\theta} &= \gamma_{x\theta}^o + z\kappa_{x\theta}^o ,\end{aligned}\tag{12}$$

where

$$\begin{aligned}\epsilon_x^o &= \frac{\partial u^o}{\partial x} + \frac{1}{2}\beta_x^{o^2} \\ \epsilon_\theta^o &= \frac{\partial v^o}{R\partial\theta} + \frac{w^o}{R} + \frac{1}{2}\beta_\theta^{o^2} \\ \gamma_{x\theta}^o &= \frac{\partial v^o}{\partial x} + \frac{\partial u^o}{R\partial\theta} + \beta_x^o\beta_\theta^o \\ \kappa_x^o &= \frac{\partial\beta_x^o}{\partial x} ; \quad \kappa_\theta^o = \frac{\partial\beta_\theta^o}{R\partial\theta} ; \quad \kappa_{x\theta}^o = \frac{\partial\beta_\theta^o}{\partial x} + \frac{\partial\beta_x^o}{R\partial\theta} .\end{aligned}\tag{13}$$

The stresses within the cylindrical panel are given by

$$\begin{aligned}\sigma_x &= \bar{Q}_{11}(\epsilon_x - \epsilon_x^P) + \bar{Q}_{12}(\epsilon_\theta - \epsilon_\theta^P) + \bar{Q}_{16}(\gamma_{x\theta} - \gamma_{x\theta}^P) \\ \sigma_\theta &= \bar{Q}_{12}(\epsilon_x - \epsilon_x^P) + \bar{Q}_{22}(\epsilon_\theta - \epsilon_\theta^P) + \bar{Q}_{26}(\gamma_{x\theta} - \gamma_{x\theta}^P) \\ \tau_{x\theta} &= \bar{Q}_{16}(\epsilon_x - \epsilon_x^P) + \bar{Q}_{26}(\epsilon_\theta - \epsilon_\theta^P) + \bar{Q}_{66}(\gamma_{x\theta} - \gamma_{x\theta}^P) ,\end{aligned}\tag{14}$$

where ϵ_x^P , ϵ_θ^P and $\gamma_{x\theta}^P$ are the strains due to preloading effects.

Equation (14) can be rewritten as

$$\begin{aligned}\sigma_x &= \bar{Q}_{11}\epsilon_x + \bar{Q}_{12}\epsilon_\theta + \bar{Q}_{16}\gamma_{x\theta} - \sigma_x^P \\ \sigma_\theta &= \bar{Q}_{12}\epsilon_x + \bar{Q}_{22}\epsilon_\theta + \bar{Q}_{26}\gamma_{x\theta} - \sigma_\theta^P \\ \tau_{x\theta} &= \bar{Q}_{16}\epsilon_x + \bar{Q}_{26}\epsilon_\theta + \bar{Q}_{66}\gamma_{x\theta} - \tau_{x\theta}^P ,\end{aligned}\tag{15}$$

where

$$\begin{aligned}
\sigma_x^P &= (\bar{Q}_{11}\epsilon_x^P + \bar{Q}_{12}\epsilon_\theta^P + \bar{Q}_{16}\gamma_{x\theta}^P) \\
\sigma_\theta^P &= (\bar{Q}_{12}\epsilon_x^P + \bar{Q}_{22}\epsilon_\theta^P + \bar{Q}_{26}\gamma_{x\theta}^P) \\
\tau_{x\theta}^P &= (\bar{Q}_{16}\epsilon_x^P + \bar{Q}_{26}\epsilon_\theta^P + \bar{Q}_{66}\gamma_{x\theta}^P).
\end{aligned} \tag{16}$$

If the preloading effects are due to thermally-induced deformations (from a temperature change such as from consolidation temperature to room temperature, for example), then

$$\begin{aligned}
\epsilon_x^P &= \alpha_x \Delta T \\
\epsilon_\theta^P &= \alpha_\theta \Delta T \\
\gamma_{x\theta}^P &= \alpha_{x\theta} \Delta T,
\end{aligned} \tag{17}$$

where α_x , α_θ and $\alpha_{x\theta}$ are the coefficients of thermal expansion of the material in the cylindrical coordinate system. If this is the case, then the stress-strain relation of eq. (14) can be written as

$$\begin{aligned}
\sigma_x &= \bar{Q}_{11}(\epsilon_x - \alpha_x \Delta T) + \bar{Q}_{12}(\epsilon_\theta - \alpha_\theta \Delta T) + \bar{Q}_{16}(\gamma_{x\theta} - \alpha_{x\theta} \Delta T) \\
\sigma_\theta &= \bar{Q}_{12}(\epsilon_x - \alpha_x \Delta T) + \bar{Q}_{22}(\epsilon_\theta - \alpha_\theta \Delta T) + \bar{Q}_{26}(\gamma_{x\theta} - \alpha_{x\theta} \Delta T) \\
\tau_{x\theta} &= \bar{Q}_{16}(\epsilon_x - \alpha_x \Delta T) + \bar{Q}_{26}(\epsilon_\theta - \alpha_\theta \Delta T) + \bar{Q}_{66}(\gamma_{x\theta} - \alpha_{x\theta} \Delta T),
\end{aligned} \tag{18}$$

or

$$\begin{aligned}
\sigma_x &= \bar{Q}_{11}\epsilon_x + \bar{Q}_{12}\epsilon_\theta + \bar{Q}_{16}\gamma_{x\theta} - \sigma_x^T \\
\sigma_\theta &= \bar{Q}_{12}\epsilon_x + \bar{Q}_{22}\epsilon_\theta + \bar{Q}_{26}\gamma_{x\theta} - \sigma_\theta^T \\
\tau_{x\theta} &= \bar{Q}_{16}\epsilon_x + \bar{Q}_{26}\epsilon_\theta + \bar{Q}_{66}\gamma_{x\theta} - \tau_{x\theta}^T,
\end{aligned} \tag{19}$$

where

$$\begin{aligned}
\sigma_x^T &= (\bar{Q}_{11}\alpha_x + \bar{Q}_{12}\alpha_\theta + \bar{Q}_{16}\alpha_{x\theta})\Delta T \\
\sigma_\theta^T &= (\bar{Q}_{12}\alpha_x + \bar{Q}_{22}\alpha_\theta + \bar{Q}_{26}\alpha_{x\theta})\Delta T \\
\tau_{x\theta}^T &= (\bar{Q}_{16}\alpha_x + \bar{Q}_{26}\alpha_\theta + \bar{Q}_{66}\alpha_{x\theta})\Delta T.
\end{aligned} \tag{20}$$

Here the superscript "T" denotes that the preloading effects are thermally-induced. The stresses σ_x^T , σ_θ^T , $\tau_{x\theta}^T$ would be the stresses at a point arising from a temperature

change if the composite is fully constrained from any deformation. Since, in general, each layer in the laminated cylindrical panel has unique values for \bar{Q}_{ij} , α_x , α_θ , and $\alpha_{x\theta}$, there are separate equations, eqs. (19) and (20), relating the strains ϵ_x , ϵ_θ , and $\gamma_{x\theta}$, and the temperature change, ΔT , to the stresses in each layer.

C. Specification of the Potential Energy Due to External Loads

In the absence of body forces, the potential energy due to applied tractions is given by

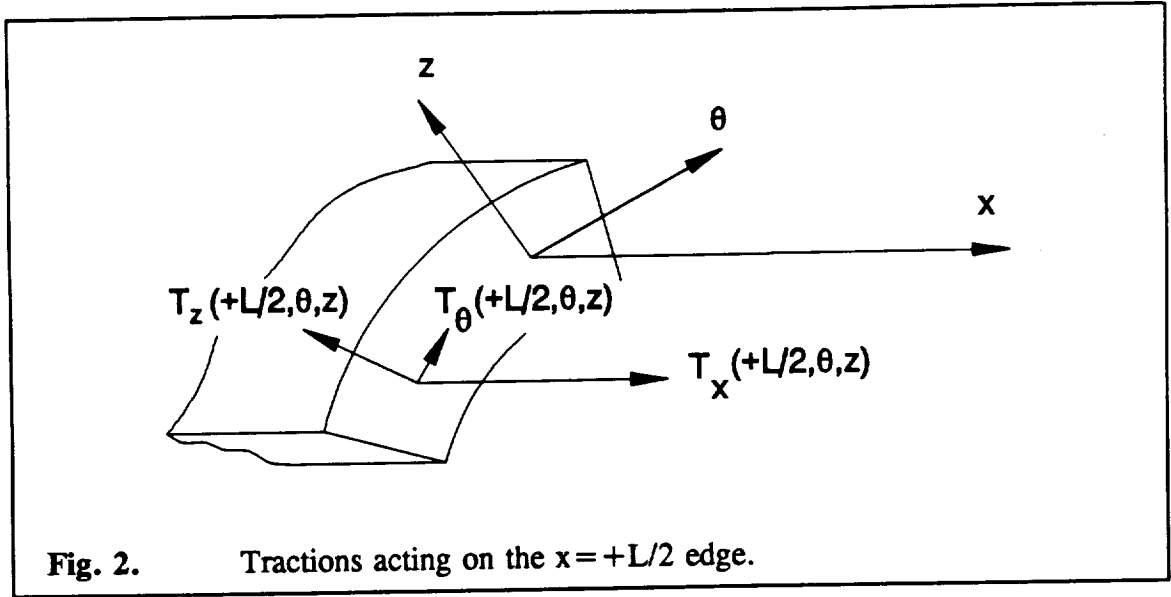
$$\Pi_{load} = - \iint_S [T_x u + T_\theta v + T_z w] ds , \quad (21)$$

where T_x , T_θ , and T_z are the known applied tractions acting on the surfaces of the cylindrical panel and the tractions and displacements u and v are functions of x , θ , and z , and w is a function of x and θ . Substituting eq. (7) into the above,

$$\begin{aligned} \Pi_{load} = - \iint_S [& T_x(x,\theta,z) (u^o(x,\theta) + z\beta_x^o(x,\theta)) \\ & + T_\theta(x,\theta,z) (v^o(x,\theta) + z\beta_\theta^o(x,\theta)) \\ & + T_z(x,\theta,z) w^o(x,\theta)] ds . \end{aligned} \quad (22)$$

As shown in Fig. 2, considering the tractions acting along the $x = +L/2$ edge of the cylindrical panel, the contribution towards Π_{load} is

$$\begin{aligned} \Pi_{load} \Big|_{x=+L/2} = - \int_{\theta=-\beta/2}^{+\beta/2} \int_{z=-H/2}^{+H/2} \left\{ & T_x \left(+\frac{L}{2}, \theta, z \right) \left[u^o \left(+\frac{L}{2}, \theta \right) + z\beta_x^o \left(+\frac{L}{2}, \theta \right) \right] \right. \\ & T_\theta \left(+\frac{L}{2}, \theta, z \right) \left[v^o \left(+\frac{L}{2}, \theta \right) + z\beta_\theta^o \left(+\frac{L}{2}, \theta \right) \right] \\ & \left. T_z \left(+\frac{L}{2}, \theta, z \right) w^o \left(+\frac{L}{2}, \theta \right) \right\} R d\theta dz . \end{aligned} \quad (23)$$

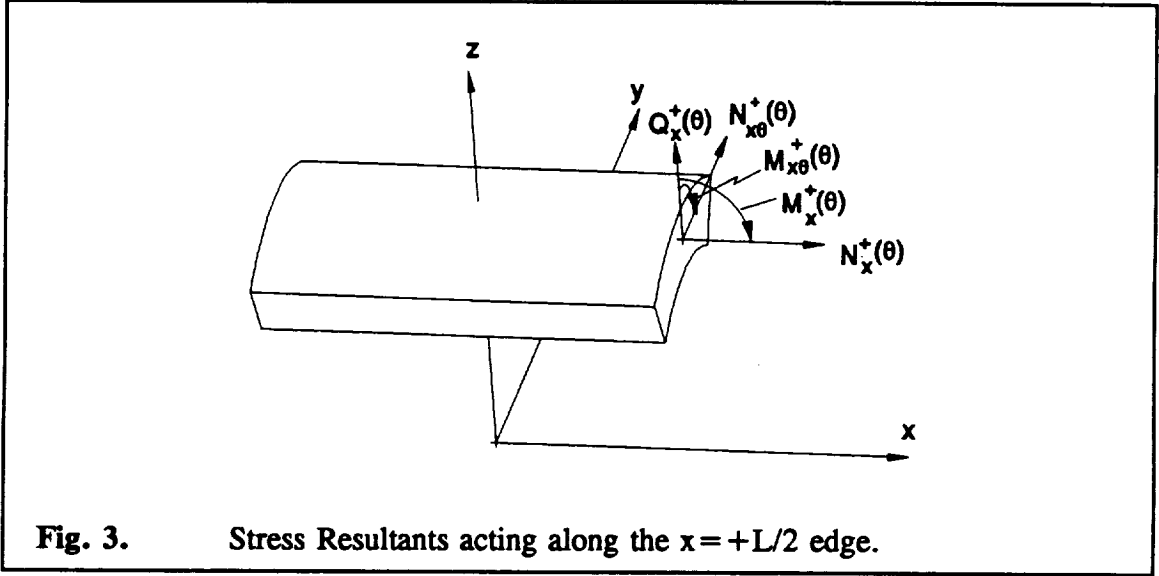


Since u^o , v^o , w^o , β_x^o , and β_θ^o are not functions of z , the integration with respect to z can be distributed, resulting in

$$\begin{aligned}
 \Pi_{load} \Big|_{x=+L/2} = & - \int_{\theta=-\frac{\theta}{2}}^{+\frac{\theta}{2}} \left\{ \int_{-\frac{H}{2}}^{+\frac{H}{2}} T_x \left(+\frac{L}{2}, \theta, z \right) dz \right\} u^o \left(+\frac{L}{2}, \theta \right) \\
 & + \left\{ \int_{-\frac{H}{2}}^{+\frac{H}{2}} T_x \left(+\frac{L}{2}, \theta, z \right) z dz \right\} \beta_x^o \left(+\frac{L}{2}, \theta \right) + \left\{ \int_{-\frac{H}{2}}^{+\frac{H}{2}} T_\theta \left(+\frac{L}{2}, \theta, z \right) dz \right\} v^o \left(+\frac{L}{2}, \theta \right) \\
 & + \left\{ \int_{-\frac{H}{2}}^{+\frac{H}{2}} T_\theta \left(+\frac{L}{2}, \theta, z \right) z dz \right\} \beta_\theta^o \left(+\frac{L}{2}, \theta \right) + \left\{ \int_{-\frac{H}{2}}^{+\frac{H}{2}} T_z \left(+\frac{L}{2}, \theta, z \right) dz \right\} w^o \left(+\frac{L}{2}, \theta \right) \Big\} R d\theta .
 \end{aligned} \tag{24}$$

The integrals with respect to z are the resultant forces and moments acting along the $x = +L/2$ edge and are defined by

$$\begin{aligned}
N_x^+(\theta) &= \int_{-\frac{H}{2}}^{+\frac{H}{2}} T_x\left(+\frac{L}{2}, \theta, z\right) dz ; & M_x^+(\theta) &= \int_{-\frac{H}{2}}^{+\frac{H}{2}} T_x\left(+\frac{L}{2}, \theta, z\right) z dz \\
N_{x\theta}^+(\theta) &= \int_{-\frac{H}{2}}^{+\frac{H}{2}} T_\theta\left(+\frac{L}{2}, \theta, z\right) dz ; & M_{x\theta}^+(\theta) &= \int_{-\frac{H}{2}}^{+\frac{H}{2}} T_\theta\left(+\frac{L}{2}, \theta, z\right) z dz \\
Q_x^+(\theta) &= \int_{-\frac{H}{2}}^{+\frac{H}{2}} T_z\left(+\frac{L}{2}, \theta, z\right) dz .
\end{aligned} \tag{25}$$



These resultants have the dimension of force or moment per unit circumferential length and they are illustrated in Fig. 3. Substituting the definitions of eq. (25) into eq. (24), the contribution towards Π_{load} due to the tractions acting along the $x = +L/2$ edge can be written as

$$\begin{aligned}
\Pi_{load}\Big|_{x=+\frac{L}{2}} &= -\int_{\theta=-\frac{\beta}{2}}^{+\frac{\beta}{2}} \left\{ N_x^+(\theta) u^o\left(+\frac{L}{2}, \theta\right) + M_x^+(\theta) \beta_x^o\left(+\frac{L}{2}, \theta\right) \right. \\
&\quad \left. + N_{x\theta}^+(\theta) v^o\left(+\frac{L}{2}, \theta\right) + M_{x\theta}^+(\theta) \beta_\theta^o\left(+\frac{L}{2}, \theta\right) + Q_x^+(\theta) w^o\left(+\frac{L}{2}, \theta\right) \right\} R d\theta .
\end{aligned} \tag{26}$$

In a similar fashion, the contribution to Π_{load} due to tractions acting along the $x = -L/2$

edge can be written as

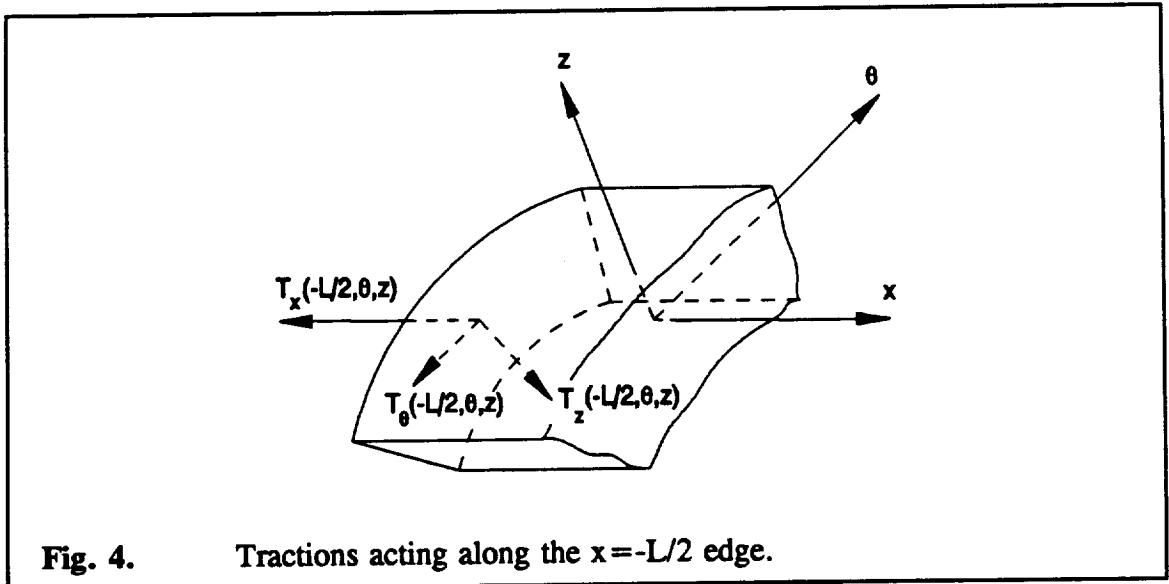
$$\begin{aligned} \Pi_{load}|_{x=-\frac{L}{2}} = \int_{\theta=-\frac{\beta}{2}}^{+\frac{\beta}{2}} \left\{ N_x^-(\theta) u^\circ\left(-\frac{L}{2}, \theta\right) + M_x^-(\theta) \beta_x^\circ\left(-\frac{L}{2}, \theta\right) \right. \\ \left. + N_{x\theta}^-(\theta) v^\circ\left(-\frac{L}{2}, \theta\right) + M_{x\theta}^-(\theta) \beta_\theta^\circ\left(-\frac{L}{2}, \theta\right) + Q_x^-(\theta) w^\circ\left(-\frac{L}{2}, \theta\right) \right\} R d\theta, \end{aligned} \quad (27)$$

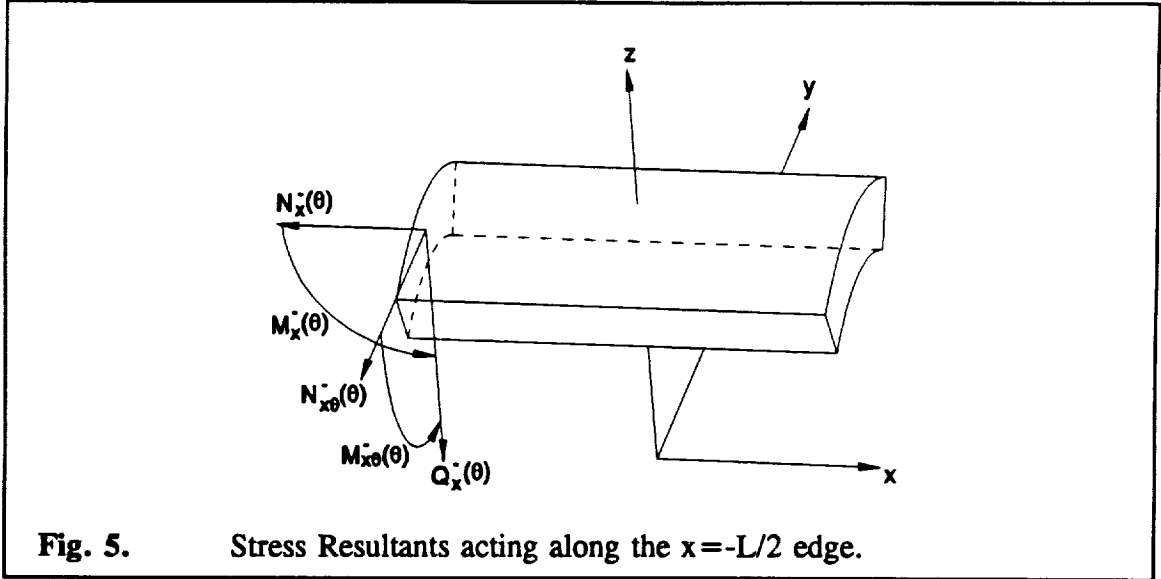
where the resultant forces and moments along the $x=-L/2$ edge are given by

$$\begin{aligned} N_x^-(\theta) &= \int_{-\frac{H}{2}}^{+\frac{H}{2}} T_x\left(-\frac{L}{2}, \theta, z\right) dz; & M_x^-(\theta) &= \int_{-\frac{H}{2}}^{+\frac{H}{2}} T_x\left(-\frac{L}{2}, \theta, z\right) z dz \\ N_{x\theta}^-(\theta) &= \int_{-\frac{H}{2}}^{+\frac{H}{2}} T_\theta\left(-\frac{L}{2}, \theta, z\right) dz; & M_{x\theta}^-(\theta) &= \int_{-\frac{H}{2}}^{+\frac{H}{2}} T_\theta\left(-\frac{L}{2}, \theta, z\right) z dz \\ Q_x^-(\theta) &= \int_{-\frac{H}{2}}^{+\frac{H}{2}} T_z\left(-\frac{L}{2}, \theta, z\right) dz. \end{aligned} \quad (28)$$

These resultants have the dimension of force or moment per unit circumferential length.

The tractions and associated resultants at $x=-L/2$ are shown in Fig. 4 and Fig. 5.

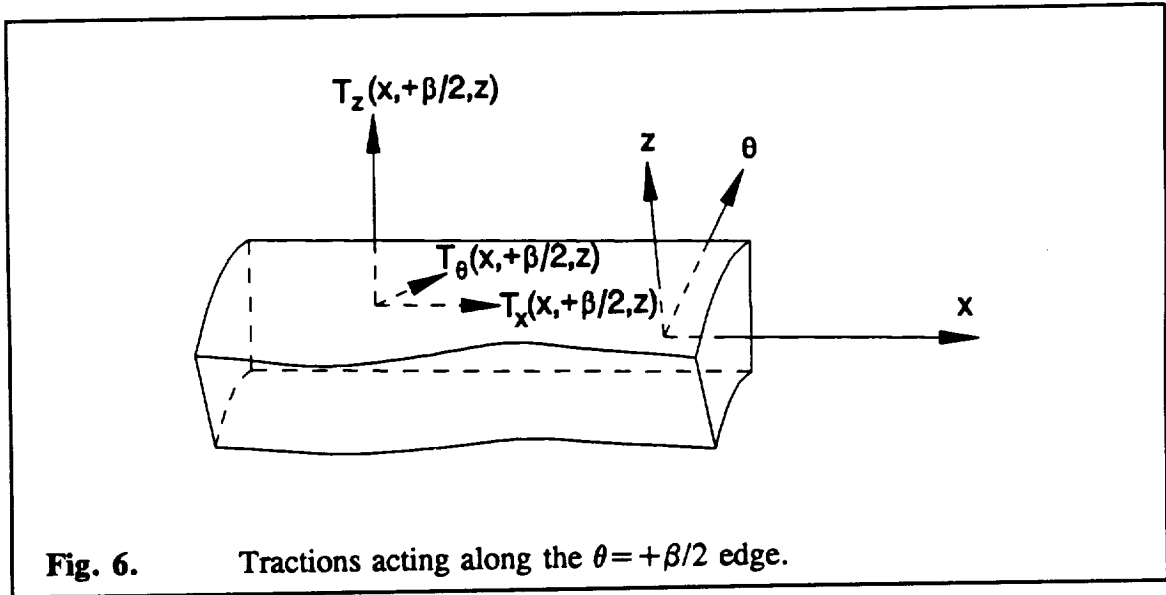




Referring to Fig. 6 and considering the tractions acting along the $\theta = +\beta/2$ edge of the cylindrical panel, the contribution towards Π_{load} is

$$\begin{aligned} \Pi_{load} \Big|_{\theta = +\frac{\beta}{2}} = & - \int_{x = -\frac{L}{2}}^{+\frac{L}{2}} \int_{z = -\frac{H}{2}}^{+\frac{H}{2}} \left\{ T_x \left(x, +\frac{\beta}{2}, z \right) \left[u^o \left(x, +\frac{\beta}{2} \right) + z \beta_x^o \left(x, +\frac{\beta}{2} \right) \right] \right. \\ & T_\theta \left(x, +\frac{\beta}{2}, z \right) \left[v^o \left(x, +\frac{\beta}{2} \right) + z \beta_\theta^o \left(x, +\frac{\beta}{2} \right) \right] \\ & \left. T_z \left(x, +\frac{\beta}{2}, z \right) w^o \left(x, +\frac{\beta}{2} \right) \right\} dx dz . \end{aligned} \quad (29)$$

Since u^o , v^o , w^o , β_x^o , and β_θ^o are not functions of z , the integration with respect to z can be distributed, resulting in



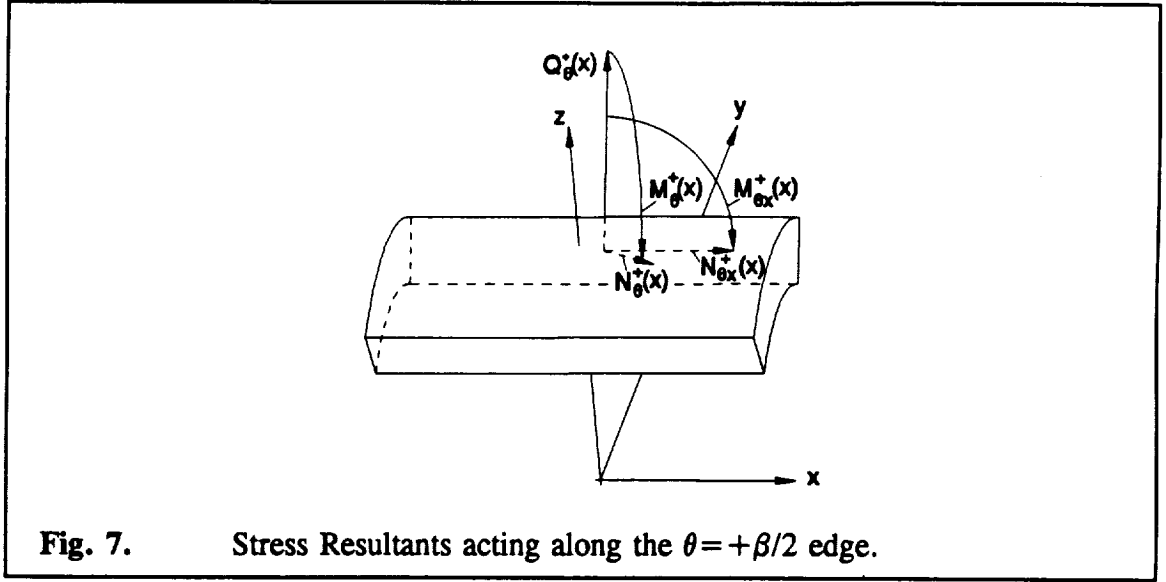
$$\begin{aligned}
 \Pi_{load} |_{\theta = +\beta/2} = & - \int_{x=-L/2}^{+L/2} \left\{ \left\{ \int_{-H/2}^{+H/2} T_x \left(x, +\frac{\beta}{2}, z \right) dz \right\} u^o \left(x, +\frac{\beta}{2} \right) \right. \\
 & + \left\{ \int_{-H/2}^{+H/2} T_x \left(x, +\frac{\beta}{2}, z \right) z dz \right\} \beta_x^o \left(x, +\frac{\beta}{2} \right) + \left\{ \int_{-H/2}^{+H/2} T_\theta \left(x, +\frac{\beta}{2}, z \right) dz \right\} v^o \left(x, +\frac{\beta}{2} \right) \\
 & \left. + \left\{ \int_{-H/2}^{+H/2} T_\theta \left(x, +\frac{\beta}{2}, z \right) z dz \right\} \beta_\theta^o \left(x, +\frac{\beta}{2} \right) + \left\{ \int_{-H/2}^{+H/2} T_z \left(x, +\frac{\beta}{2}, z \right) dz \right\} w^o \left(x, +\frac{\beta}{2} \right) \right\} dx .
 \end{aligned} \tag{30}$$

The integrals with respect to z are the resultant forces and moments acting along the $\theta = +\beta/2$ edge. They are defined as

$$\begin{aligned}
 N_{\theta x}^+(x) &= \int_{-H/2}^{+H/2} T_x \left(x, +\frac{\beta}{2}, z \right) dz ; & M_{\theta x}^+(x) &= \int_{-H/2}^{+H/2} T_x \left(x, +\frac{\beta}{2}, z \right) z dz \\
 N_\theta^+(x) &= \int_{-H/2}^{+H/2} T_\theta \left(x, +\frac{\beta}{2}, z \right) dz ; & M_\theta^+(x) &= \int_{-H/2}^{+H/2} T_\theta \left(x, +\frac{\beta}{2}, z \right) z dz \\
 Q_\theta^+(x) &= \int_{-H/2}^{+H/2} T_z \left(x, +\frac{\beta}{2}, z \right) dz .
 \end{aligned} \tag{31}$$

These resultants have the dimension of force or moment per unit length. The orientation

of these stress resultants is shown in Fig. 7.



The contribution towards Π_{load} due to the tractions acting along the $\theta = +\beta/2$ edge can therefore be written as

$$\begin{aligned} \Pi_{load}|_{\theta=+\frac{\beta}{2}} = & - \int_{x=-\frac{L}{2}}^{+\frac{L}{2}} \left\{ N_{\theta_x}^+(x) u^o \left(x, +\frac{\beta}{2} \right) + M_{\theta_x}^+(x) \beta_x^o \left(x, +\frac{\beta}{2} \right) \right. \\ & \left. + N_{\theta}^+(x) v^o \left(x, +\frac{\beta}{2} \right) + M_{\theta}^+(x) \beta_{\theta}^o \left(x, +\frac{\beta}{2} \right) + Q_{\theta}^+(x) w^o \left(x, +\frac{\beta}{2} \right) \right\} dx . \end{aligned} \quad (32)$$

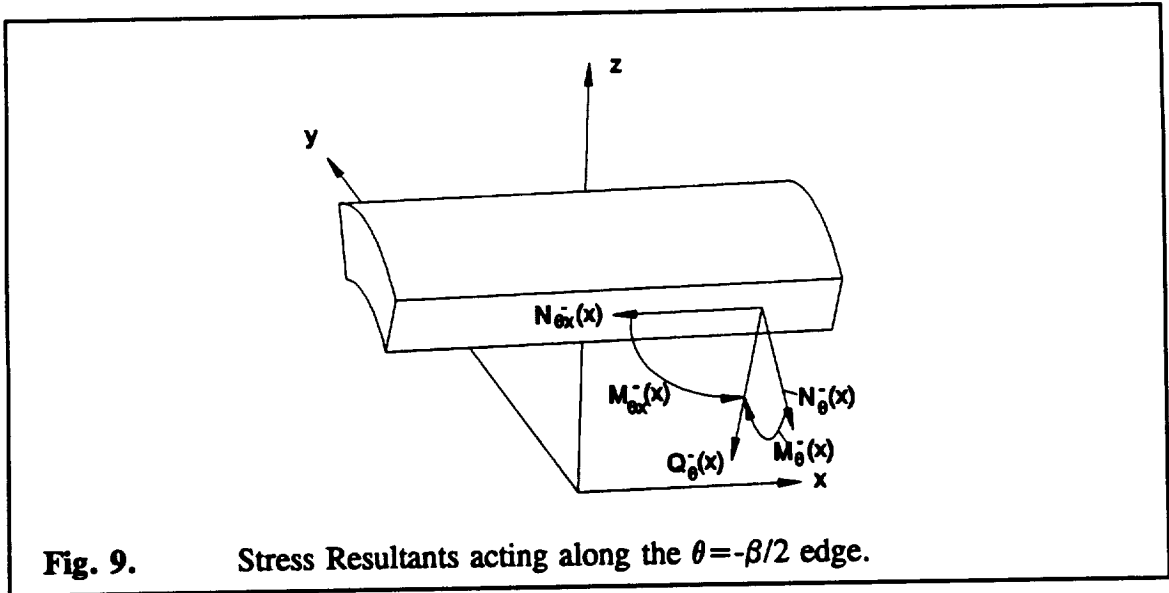
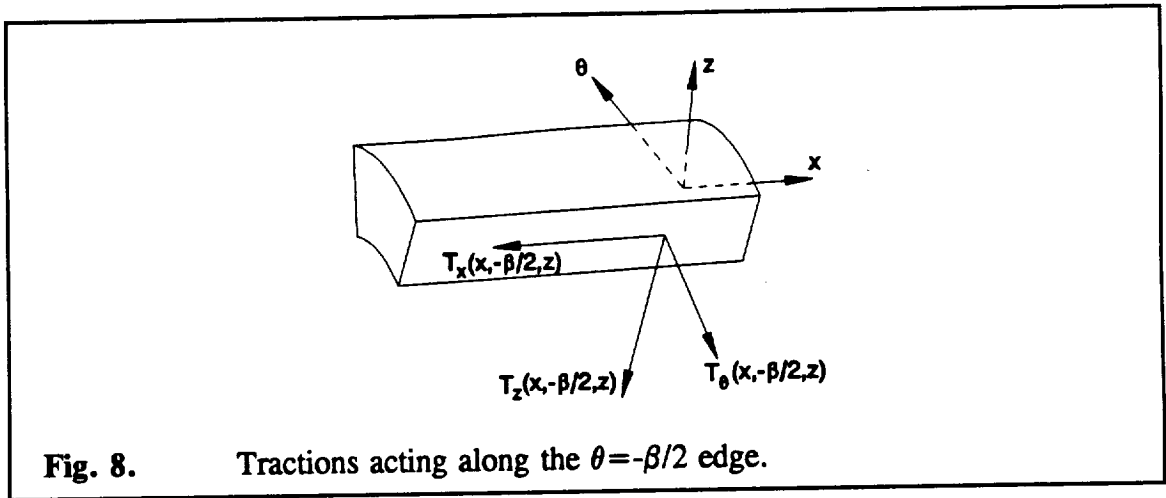
In a similar fashion, the contribution to Π_{load} due to tractions acting along the $\theta = -\beta/2$ edge can be written as

$$\begin{aligned} \Pi_{load}|_{\theta=-\frac{\beta}{2}} = & \int_{x=-\frac{L}{2}}^{+\frac{L}{2}} \left\{ N_{\theta_x}^-(x) u^o \left(x, -\frac{\beta}{2} \right) + M_{\theta_x}^-(x) \beta_x^o \left(x, -\frac{\beta}{2} \right) \right. \\ & \left. + N_{\theta}^-(x) v^o \left(x, -\frac{\beta}{2} \right) + M_{\theta}^-(x) \beta_{\theta}^o \left(x, -\frac{\beta}{2} \right) + Q_{\theta}^-(x) w^o \left(x, -\frac{\beta}{2} \right) \right\} dx , \end{aligned} \quad (33)$$

where the resultant forces and moments along the $\theta = -\beta/2$ edge are given by

$$\begin{aligned}
 N_{\theta x}^{-}(x) &= \int_{-\frac{H}{2}}^{+\frac{H}{2}} T_x\left(x, -\frac{\beta}{2}, z\right) dz ; & M_{\theta x}^{-}(x) &= \int_{-\frac{H}{2}}^{+\frac{H}{2}} T_x\left(x, -\frac{\beta}{2}, z\right) z dz \\
 N_{\theta}^{-}(x) &= \int_{-\frac{H}{2}}^{+\frac{H}{2}} T_{\theta}\left(x, -\frac{\beta}{2}, z\right) dz ; & M_{\theta}^{-}(x) &= \int_{-\frac{H}{2}}^{+\frac{H}{2}} T_{\theta}\left(x, -\frac{\beta}{2}, z\right) z dz \\
 Q_{\theta}^{-}(x) &= \int_{-\frac{H}{2}}^{+\frac{H}{2}} T_z\left(x, -\frac{\beta}{2}, z\right) dz .
 \end{aligned} \tag{34}$$

Fig. 8 and Fig. 9 show the tractions and associated resultants acting on the $\theta = -\beta/2$ edge.



Finally, the tractions acting on the top and bottom surfaces of the cylindrical panel shall be considered. In this work, only loadings normal to these surfaces will be considered, i.e., T_x and T_θ will be taken as zero. These are illustrated in Fig. 10.

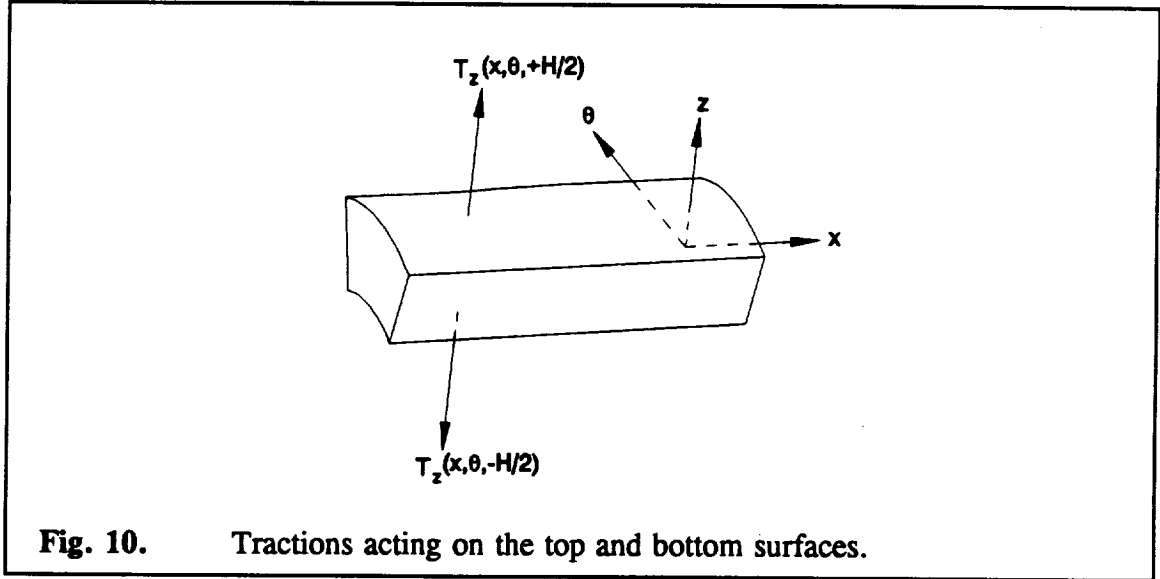


Fig. 10. Tractions acting on the top and bottom surfaces.

With this limitation in the loading on the top and bottom surfaces, the contribution to Π_{load} due to normal tractions acting on the top surface is

$$\Pi_{load}|_{z=+\frac{H}{2}} = - \int_{x=-\frac{L}{2}}^{+\frac{L}{2}} \int_{\theta=-\frac{\beta}{2}}^{+\frac{\beta}{2}} T_z\left(x, \theta, +\frac{H}{2}\right) w^o(x, \theta) R d\theta dx \quad . \quad (35a)$$

The contribution towards Π_{load} due to normal tractions acting on the bottom surface is

$$\Pi_{load}|_{z=-\frac{H}{2}} = \int_{x=-\frac{L}{2}}^{+\frac{L}{2}} \int_{\theta=-\frac{\beta}{2}}^{+\frac{\beta}{2}} T_z\left(x, \theta, -\frac{H}{2}\right) w^o(x, \theta) R d\theta dx \quad . \quad (35b)$$

The definitions

$$q^+(x, \theta) \equiv T_z\left(x, \theta, +\frac{H}{2}\right) \quad (36a)$$

and

$$q^-(x,\theta) \equiv T_z\left(x,\theta,-\frac{H}{2}\right) \quad (36b)$$

are introduced here to give a more familiar meaning to these loadings, i.e., that of a distributed normal pressure loading with dimensions of force per unit area. Substituting eqs. (36) into eqs. (35),

$$\Pi_{load}|_{z=+\frac{H}{2}} = - \int_{x=-\frac{L}{2}}^{+\frac{L}{2}} \int_{\theta=-\frac{\beta}{2}}^{+\frac{\beta}{2}} q^+(x,\theta) w^o(x,\theta) R d\theta dx \quad , \quad (37a)$$

and

$$\Pi_{load}|_{z=-\frac{H}{2}} = \int_{x=-\frac{L}{2}}^{+\frac{L}{2}} \int_{\theta=-\frac{\beta}{2}}^{+\frac{\beta}{2}} q^-(x,\theta) w^o(x,\theta) R d\theta dx \quad . \quad (37b)$$

For convenience, and for ease of discussion, commonly occurring loadings will be partitioned from the general form of the potential energy due to surface tractions. For the case of known axial loads applied at the $x=-L/2$ and $x=+L/2$ edges of the cylindrical panel,

$$\Pi_{load} = \int_{\theta=-\frac{\beta}{2}}^{+\frac{\beta}{2}} N_x^-(\theta) u^o\left(-\frac{L}{2},\theta\right) R d\theta - \int_{\theta=-\frac{\beta}{2}}^{+\frac{\beta}{2}} N_x^+(\theta) u^o\left(+\frac{L}{2},\theta\right) R d\theta \quad . \quad (38a)$$

For bending moments applied along the $x=-L/2$ and $x=+L/2$ edges,

$$\Pi_{load} = \int_{\theta=-\frac{\beta}{2}}^{+\frac{\beta}{2}} M_x^-(\theta) \beta_x^o\left(-\frac{L}{2},\theta\right) R d\theta - \int_{\theta=-\frac{\beta}{2}}^{+\frac{\beta}{2}} M_x^+(\theta) \beta_x^o\left(+\frac{L}{2},\theta\right) R d\theta \quad . \quad (38b)$$

For inplane shearing loads applied along the $x=-L/2$ and $x=+L/2$ edges, and along the $\theta=-\beta/2$ and $\theta=+\beta/2$ edges of the cylindrical panel,

$$\begin{aligned} \Pi_{load} = & \int_{\theta=-\frac{\beta}{2}}^{+\frac{\beta}{2}} N_{x\theta}^-(\theta) v^o\left(-\frac{L}{2}, \theta\right) R d\theta - \int_{\theta=-\frac{\beta}{2}}^{+\frac{\beta}{2}} N_{x\theta}^+(\theta) v^o\left(+\frac{L}{2}, \theta\right) R d\theta \\ & + \int_{x=-\frac{L}{2}}^{+\frac{L}{2}} N_{\theta x}^-(x) u^o\left(x, -\frac{\beta}{2}\right) dx - \int_{x=-\frac{L}{2}}^{+\frac{L}{2}} N_{\theta x}^+(x) u^o\left(x, +\frac{\beta}{2}\right) dx . \end{aligned} \quad (38c)$$

For shearing moments applied along the $x=-L/2$ and $x=+L/2$ edges, and along the $\theta=-\beta/2$ and $\theta=+\beta/2$ edges,

$$\begin{aligned} \Pi_{load} = & \int_{\theta=-\frac{\beta}{2}}^{+\frac{\beta}{2}} M_{x\theta}^-(\theta) \beta_\theta^o\left(-\frac{L}{2}, \theta\right) R d\theta - \int_{\theta=-\frac{\beta}{2}}^{+\frac{\beta}{2}} M_{x\theta}^+(\theta) \beta_\theta^o\left(+\frac{L}{2}, \theta\right) R d\theta \\ & + \int_{x=-\frac{L}{2}}^{+\frac{L}{2}} M_{\theta x}^-(x) \beta_x^o\left(x, -\frac{\beta}{2}\right) dx - \int_{x=-\frac{L}{2}}^{+\frac{L}{2}} M_{\theta x}^+(x) \beta_x^o\left(x, +\frac{\beta}{2}\right) dx . \end{aligned} \quad (38d)$$

For out-of-plane shear loadings applied along the $x=-L/2$ and $x=+L/2$ edges,

$$\Pi_{load} = \int_{\theta=-\frac{\beta}{2}}^{+\frac{\beta}{2}} Q_x^-(\theta) w^o\left(-\frac{L}{2}, \theta\right) R d\theta - \int_{\theta=-\frac{\beta}{2}}^{+\frac{\beta}{2}} Q_x^+(\theta) w^o\left(+\frac{L}{2}, \theta\right) R d\theta . \quad (38e)$$

For circumferential loadings applied along the $\theta=-\beta/2$ and $\theta=+\beta/2$ edges,

$$\Pi_{load} = \int_{x=-\frac{L}{2}}^{+\frac{L}{2}} N_\theta^-(x) v^o\left(x, -\frac{\beta}{2}\right) dx - \int_{x=-\frac{L}{2}}^{+\frac{L}{2}} N_\theta^+(x) v^o\left(x, +\frac{\beta}{2}\right) dx . \quad (38f)$$

For bending moments applied along the $\theta=-\beta/2$ and $\theta=+\beta/2$ edges,

$$\Pi_{load} = \int_{x=-\frac{L}{2}}^{+\frac{L}{2}} M_\theta^-(x) \beta_\theta^o\left(x, -\frac{\beta}{2}\right) dx - \int_{x=-\frac{L}{2}}^{+\frac{L}{2}} M_\theta^+(x) \beta_\theta^o\left(x, +\frac{\beta}{2}\right) dx . \quad (38g)$$

For out-of-plane shear loadings applied along the $\theta=-\beta/2$ and $\theta=+\beta/2$ edges,

$$\Pi_{load} = \int_{x=-\frac{L}{2}}^{+\frac{L}{2}} Q_{\theta}^{-}(x) w^{\circ}\left(x, -\frac{\beta}{2}\right) dx - \int_{x=-\frac{L}{2}}^{+\frac{L}{2}} Q_{\theta}^{+}(x) w^{\circ}\left(x, +\frac{\beta}{2}\right) dx . \quad (38h)$$

For normal distributed loadings $q^{-}(x, \theta)$ and $q^{+}(x, \theta)$ applied to the bottom and top surfaces of the cylindrical panel, respectively,

$$\Pi_{load} = \int_{\theta=-\frac{\beta}{2}}^{+\frac{\beta}{2}} \int_{x=-\frac{L}{2}}^{+\frac{L}{2}} (q^{-}(x, \theta) - q^{+}(x, \theta)) w^{\circ}(x, \theta) R d\theta dx . \quad (38i)$$

Note that, in this theory, the difference between the normal distributed loadings $q^{-}(x, \theta)$ and $q^{+}(x, \theta)$ has an effect, not the individual distributed loadings themselves. In other words, distributed normal loadings of $q^{-}(x, \theta) = -q$ and $q^{+}(x, \theta) = 0$ would have the same effect as distributed normal loadings of $q^{-}(x, \theta) = 0$ and $q^{+}(x, \theta) = q$. Hence, since the theory utilizes only the difference in the loadings, only the difference

$$q = q^{+} - q^{-} \quad (39)$$

shall be used in the following. The sense of this net distributed load q is outward positive and it acts normal to the surfaces of the cylindrical panel.

It is important to note that, in general, the end loads N_x^{-} and N_x^{+} , the inplane shearing loads $N_{x\theta}^{-}$ and $N_{x\theta}^{+}$, the out-of-plane shear loads Q_x^{-} and Q_x^{+} , the bending moments M_x^{-} and M_x^{+} , and the shearing moments $M_{x\theta}^{-}$ and $M_{x\theta}^{+}$ can be known functions of θ . Also, the inplane shearing loads $N_{\theta x}^{-}$ and $N_{\theta x}^{+}$, the circumferential loads N_{θ}^{-} and N_{θ}^{+} , the out-of-plane shear loads Q_{θ}^{-} and Q_{θ}^{+} , the bending moments M_{θ}^{-} and M_{θ}^{+} , and the shearing moments $M_{\theta x}^{-}$ and $M_{\theta x}^{+}$ can be known functions of x . The net distributed normal load $q = q^{+} - q^{-}$ can be a function of x and θ .

D. Application of the Method of Total Potential Energy to Cylindrical Panels

Substituting the expressions for the strains given in eq. (12) into the energy expression for the cylindrical panel, eq. (5), and including the nine loading terms being considered, results in a rather lengthy but complete expression for the total potential energy, namely,

$$\begin{aligned}
\Pi(u^\circ, v^\circ, w^\circ) = & \frac{1}{2} \int_{z=-\frac{H}{2}}^{+\frac{H}{2}} \int_{x=-\frac{L}{2}}^{+\frac{L}{2}} \int_{\theta=-\frac{\beta}{2}}^{+\frac{\beta}{2}} \left[(\sigma_x - \sigma_x^P)(\varepsilon_x^\circ + z\kappa_x^\circ) + (\sigma_\theta - \sigma_\theta^P)(\varepsilon_\theta^\circ + z\kappa_\theta^\circ) \right. \\
& \left. + (\tau_{x\theta} - \tau_{x\theta}^P)(\gamma_{x\theta}^\circ + z\kappa_{x\theta}^\circ) \right] R d\theta dx dz \\
& + \int_{\theta=-\frac{\beta}{2}}^{+\frac{\beta}{2}} N_x^-(\theta) u^\circ \left(-\frac{L}{2}, \theta \right) R d\theta - \int_{\theta=-\frac{\beta}{2}}^{+\frac{\beta}{2}} N_x^+(\theta) u^\circ \left(+\frac{L}{2}, \theta \right) R d\theta \\
& + \int_{\theta=-\frac{\beta}{2}}^{+\frac{\beta}{2}} M_x^-(\theta) \beta_x^\circ \left(-\frac{L}{2}, \theta \right) R d\theta - \int_{\theta=-\frac{\beta}{2}}^{+\frac{\beta}{2}} M_x^+(\theta) \beta_x^\circ \left(+\frac{L}{2}, \theta \right) R d\theta \\
& + \int_{\theta=-\frac{\beta}{2}}^{+\frac{\beta}{2}} N_{x\theta}^-(\theta) v^\circ \left(-\frac{L}{2}, \theta \right) R d\theta - \int_{\theta=-\frac{\beta}{2}}^{+\frac{\beta}{2}} N_{x\theta}^+(\theta) v^\circ \left(+\frac{L}{2}, \theta \right) R d\theta \\
& + \int_{\theta=-\frac{\beta}{2}}^{+\frac{\beta}{2}} M_{x\theta}^-(\theta) \beta_\theta^\circ \left(-\frac{L}{2}, \theta \right) R d\theta - \int_{\theta=-\frac{\beta}{2}}^{+\frac{\beta}{2}} M_{x\theta}^+(\theta) \beta_\theta^\circ \left(+\frac{L}{2}, \theta \right) R d\theta \\
& + \int_{\theta=-\frac{\beta}{2}}^{+\frac{\beta}{2}} Q_x^-(\theta) w^\circ \left(-\frac{L}{2}, \theta \right) R d\theta - \int_{\theta=-\frac{\beta}{2}}^{+\frac{\beta}{2}} Q_x^+(\theta) w^\circ \left(+\frac{L}{2}, \theta \right) R d\theta \\
& + \int_{x=-\frac{L}{2}}^{+\frac{L}{2}} N_{\theta x}^-(x) u^\circ \left(x, -\frac{\beta}{2} \right) dx - \int_{x=-\frac{L}{2}}^{+\frac{L}{2}} N_{\theta x}^+(x) u^\circ \left(x, +\frac{\beta}{2} \right) dx \\
& + \int_{x=-\frac{L}{2}}^{+\frac{L}{2}} M_{\theta x}^-(x) \beta_x^\circ \left(x, -\frac{\beta}{2} \right) dx - \int_{x=-\frac{L}{2}}^{+\frac{L}{2}} M_{\theta x}^+(x) \beta_x^\circ \left(x, +\frac{\beta}{2} \right) dx \\
& + \int_{x=-\frac{L}{2}}^{+\frac{L}{2}} N_\theta^-(x) v^\circ \left(x, -\frac{\beta}{2} \right) dx - \int_{x=-\frac{L}{2}}^{+\frac{L}{2}} N_\theta^+(x) v^\circ \left(x, +\frac{\beta}{2} \right) dx \\
& + \int_{x=-\frac{L}{2}}^{+\frac{L}{2}} M_\theta^-(x) \beta_\theta^\circ \left(x, -\frac{\beta}{2} \right) dx - \int_{x=-\frac{L}{2}}^{+\frac{L}{2}} M_\theta^+(x) \beta_\theta^\circ \left(x, +\frac{\beta}{2} \right) dx \\
& + \int_{x=-\frac{L}{2}}^{+\frac{L}{2}} Q_\theta^-(x) w^\circ \left(x, -\frac{\beta}{2} \right) dx - \int_{x=-\frac{L}{2}}^{+\frac{L}{2}} Q_\theta^+(x) w^\circ \left(x, +\frac{\beta}{2} \right) dx \\
& - \int_{x=-\frac{L}{2}}^{+\frac{L}{2}} \int_{\theta=-\frac{\beta}{2}}^{+\frac{\beta}{2}} q w^\circ(x, \theta) R d\theta dx .
\end{aligned} \tag{40}$$

In the eq. (40), use has been made of eq. (11) and the fact that

$$dr = dz . \quad (41)$$

and the integration with respect to r in the volume integral has been replaced with integration with respect to z . Grouping terms under single integrals and integrating with respect to z leads to the expression

$$\begin{aligned}
\Pi(u^o, v^o, w^o) = & \frac{1}{2} \int_{x=-\frac{L}{2}}^{+\frac{L}{2}} \int_{\theta=-\frac{\beta}{2}}^{+\frac{\beta}{2}} \left[(N_x - N_x^P) \varepsilon_x^o + (N_\theta - N_\theta^P) \varepsilon_\theta^o + (N_{x\theta} - N_{x\theta}^P) \gamma_{x\theta}^o + \right. \\
& + (M_x - M_x^P) \kappa_x^o + (M_\theta - M_\theta^P) \kappa_\theta^o + (M_{x\theta} - M_{x\theta}^P) \kappa_{x\theta}^o \\
& \left. - q w^o \right] R d\theta dx \\
& + \int_{\theta=-\frac{\beta}{2}}^{+\frac{\beta}{2}} \left\{ \left[N_x^-(\theta) u^o \left(-\frac{L}{2}, \theta \right) - N_x^+(\theta) u^o \left(+\frac{L}{2}, \theta \right) \right] \right. \\
& + \left[M_x^-(\theta) \beta_x^o \left(-\frac{L}{2}, \theta \right) - M_x^+(\theta) \beta_x^o \left(+\frac{L}{2}, \theta \right) \right] \\
& + \left[N_{x\theta}^-(\theta) v^o \left(-\frac{L}{2}, \theta \right) - N_{x\theta}^+(\theta) v^o \left(+\frac{L}{2}, \theta \right) \right] \\
& + \left[M_{x\theta}^-(\theta) \beta_\theta^o \left(-\frac{L}{2}, \theta \right) - M_{x\theta}^+(\theta) \beta_\theta^o \left(+\frac{L}{2}, \theta \right) \right] \\
& \left. + \left[Q_x^-(\theta) w^o \left(-\frac{L}{2}, \theta \right) - Q_x^+(\theta) w^o \left(+\frac{L}{2}, \theta \right) \right] \right\} R d\theta \\
& + \int_{x=-\frac{L}{2}}^{+\frac{L}{2}} \left\{ \left[N_{\theta x}^-(x) u^o \left(x, -\frac{\beta}{2} \right) - N_{\theta x}^+(x) u^o \left(x, +\frac{\beta}{2} \right) \right] \right. \\
& + \left[M_{\theta x}^-(x) \beta_x^o \left(x, -\frac{\beta}{2} \right) - M_{\theta x}^+(x) \beta_x^o \left(x, +\frac{\beta}{2} \right) \right] \\
& + \left[N_\theta^-(x) v^o \left(x, -\frac{\beta}{2} \right) - N_\theta^+(x) v^o \left(x, +\frac{\beta}{2} \right) \right] \\
& + \left[M_\theta^-(x) \beta_\theta^o \left(x, -\frac{\beta}{2} \right) - M_\theta^+(x) \beta_\theta^o \left(x, +\frac{\beta}{2} \right) \right] \\
& \left. + \left[Q_\theta^-(x) w^o \left(x, -\frac{\beta}{2} \right) - Q_\theta^+(x) w^o \left(x, +\frac{\beta}{2} \right) \right] \right\} dx . \quad (42)
\end{aligned}$$

The stress resultants in eq. (42) are defined as

$$\begin{aligned}
N_x &\equiv \int_{z=-\frac{H}{2}}^{+\frac{H}{2}} \sigma_x dz = A_{11} \varepsilon_x^0 + A_{12} \varepsilon_\theta^0 + A_{16} \gamma_{x\theta}^0 + B_{11} \kappa_x^0 + B_{12} \kappa_\theta^0 + B_{16} \kappa_{x\theta}^0 - N_x^P \\
N_\theta &\equiv \int_{z=-\frac{H}{2}}^{+\frac{H}{2}} \sigma_\theta dz = A_{12} \varepsilon_x^0 + A_{22} \varepsilon_\theta^0 + A_{26} \gamma_{x\theta}^0 + B_{12} \kappa_x^0 + B_{22} \kappa_\theta^0 + B_{26} \kappa_{x\theta}^0 - N_\theta^P \\
N_{x\theta} &\equiv \int_{z=-\frac{H}{2}}^{+\frac{H}{2}} \tau_{x\theta} dz = A_{16} \varepsilon_x^0 + A_{26} \varepsilon_\theta^0 + A_{66} \gamma_{x\theta}^0 + B_{16} \kappa_x^0 + B_{26} \kappa_\theta^0 + B_{66} \kappa_{x\theta}^0 - N_{x\theta}^P \\
M_x &\equiv \int_{z=-\frac{H}{2}}^{+\frac{H}{2}} z \sigma_x dz = B_{11} \varepsilon_x^0 + B_{12} \varepsilon_\theta^0 + B_{16} \gamma_{x\theta}^0 + D_{11} \kappa_x^0 + D_{12} \kappa_\theta^0 + D_{16} \kappa_{x\theta}^0 - M_x^P \\
M_\theta &\equiv \int_{z=-\frac{H}{2}}^{+\frac{H}{2}} z \sigma_\theta dz = B_{12} \varepsilon_x^0 + B_{22} \varepsilon_\theta^0 + B_{26} \gamma_{x\theta}^0 + D_{12} \kappa_x^0 + D_{22} \kappa_\theta^0 + D_{26} \kappa_{x\theta}^0 - M_\theta^P \\
M_{x\theta} &\equiv \int_{z=-\frac{H}{2}}^{+\frac{H}{2}} z \tau_{x\theta} dz = B_{16} \varepsilon_x^0 + B_{26} \varepsilon_\theta^0 + B_{66} \gamma_{x\theta}^0 + D_{16} \kappa_x^0 + D_{26} \kappa_\theta^0 + D_{66} \kappa_{x\theta}^0 - M_{x\theta}^P .
\end{aligned} \tag{43}$$

In the above

$$\begin{aligned}
N_x^P &\equiv \int_{z=-\frac{H}{2}}^{+\frac{H}{2}} \sigma_x^P dz = \int_{z=-\frac{H}{2}}^{+\frac{H}{2}} (\bar{Q}_{11} \varepsilon_x^P + \bar{Q}_{12} \varepsilon_\theta^P + \bar{Q}_{16} \gamma_{x\theta}^P) dz \\
N_\theta^P &\equiv \int_{z=-\frac{H}{2}}^{+\frac{H}{2}} \sigma_\theta^P dz = \int_{z=-\frac{H}{2}}^{+\frac{H}{2}} (\bar{Q}_{12} \varepsilon_x^P + \bar{Q}_{22} \varepsilon_\theta^P + \bar{Q}_{26} \gamma_{x\theta}^P) dz \\
N_{x\theta}^P &\equiv \int_{z=-\frac{H}{2}}^{+\frac{H}{2}} \tau_{x\theta}^P dz = \int_{z=-\frac{H}{2}}^{+\frac{H}{2}} (\bar{Q}_{16} \varepsilon_x^P + \bar{Q}_{26} \varepsilon_\theta^P + \bar{Q}_{66} \gamma_{x\theta}^P) dz \\
M_x^P &\equiv \int_{z=-\frac{H}{2}}^{+\frac{H}{2}} z \sigma_x^P dz = \int_{z=-\frac{H}{2}}^{+\frac{H}{2}} (\bar{Q}_{11} \varepsilon_x^P + \bar{Q}_{12} \varepsilon_\theta^P + \bar{Q}_{16} \gamma_{x\theta}^P) z dz \\
M_\theta^P &\equiv \int_{z=-\frac{H}{2}}^{+\frac{H}{2}} z \sigma_\theta^P dz = \int_{z=-\frac{H}{2}}^{+\frac{H}{2}} (\bar{Q}_{12} \varepsilon_x^P + \bar{Q}_{22} \varepsilon_\theta^P + \bar{Q}_{26} \gamma_{x\theta}^P) z dz \\
M_{x\theta}^P &\equiv \int_{z=-\frac{H}{2}}^{+\frac{H}{2}} z \tau_{x\theta}^P dz = \int_{z=-\frac{H}{2}}^{+\frac{H}{2}} (\bar{Q}_{16} \varepsilon_x^P + \bar{Q}_{26} \varepsilon_\theta^P + \bar{Q}_{66} \gamma_{x\theta}^P) z dz .
\end{aligned} \tag{44}$$

The superscript "P" denotes a preloading effect, and therefore, these expressions are the so-called equivalent preloading stress resultants. If the preloading effects are thermally induced,

$$\begin{aligned}
N_x^P &= N_x^T \equiv \int_{z=-\frac{H}{2}}^{+\frac{H}{2}} \sigma_x^T dz = \int_{z=-\frac{H}{2}}^{+\frac{H}{2}} (\bar{Q}_{11}\alpha_x + \bar{Q}_{12}\alpha_\theta + \bar{Q}_{16}\alpha_{x\theta}) \Delta T dz \\
N_\theta^P &= N_\theta^T \equiv \int_{z=-\frac{H}{2}}^{+\frac{H}{2}} \sigma_\theta^T dz = \int_{z=-\frac{H}{2}}^{+\frac{H}{2}} (\bar{Q}_{12}\alpha_x + \bar{Q}_{22}\alpha_\theta + \bar{Q}_{26}\alpha_{x\theta}) \Delta T dz \\
N_{x\theta}^P &= N_{x\theta}^T \equiv \int_{z=-\frac{H}{2}}^{+\frac{H}{2}} \tau_{x\theta}^T dz = \int_{z=-\frac{H}{2}}^{+\frac{H}{2}} (\bar{Q}_{16}\alpha_x + \bar{Q}_{26}\alpha_\theta + \bar{Q}_{66}\alpha_{x\theta}) \Delta T dz \\
M_x^P &= M_x^T \equiv \int_{z=-\frac{H}{2}}^{+\frac{H}{2}} z \sigma_x^T dz = \int_{z=-\frac{H}{2}}^{+\frac{H}{2}} (\bar{Q}_{11}\alpha_x + \bar{Q}_{12}\alpha_\theta + \bar{Q}_{16}\alpha_{x\theta}) \Delta T z dz \\
M_\theta^P &= M_\theta^T \equiv \int_{z=-\frac{H}{2}}^{+\frac{H}{2}} z \sigma_\theta^T dz = \int_{z=-\frac{H}{2}}^{+\frac{H}{2}} (\bar{Q}_{12}\alpha_x + \bar{Q}_{22}\alpha_\theta + \bar{Q}_{26}\alpha_{x\theta}) \Delta T z dz \\
M_{x\theta}^P &= M_{x\theta}^T \equiv \int_{z=-\frac{H}{2}}^{+\frac{H}{2}} z \tau_{x\theta}^T dz = \int_{z=-\frac{H}{2}}^{+\frac{H}{2}} (\bar{Q}_{16}\alpha_x + \bar{Q}_{26}\alpha_\theta + \bar{Q}_{66}\alpha_{x\theta}) \Delta T z dz .
\end{aligned} \tag{45}$$

These expressions are the so-called equivalent thermal stress resultants.

The notation

$$\Pi = \Pi(u^o, v^o, w^o) \tag{46}$$

is being used in eq. (40) and (42) to emphasize the fact that the total potential energy is a function of the displacements, the superscript zero indicating that the displacements of interest are the displacements of the cylindrical reference surface. The governing equilibrium equations and consistent boundary conditions will be derived by examining the variations, or increment, in the total potential energy due to variations, or increments, in these displacements. Then, considering increments in the displacements of the form

$$u^o + \varepsilon u_1^o ; \quad v^o + \varepsilon v_1^o ; \quad w^o + \varepsilon w_1^o , \quad (47)$$

the increment of the total potential energy will be of the form

$$\Pi + \Delta\Pi = \Pi(u^o + \varepsilon u_1^o, v^o + \varepsilon v_1^o, w^o + \varepsilon w_1^o) , \quad (48)$$

where ε is a small parameter and the quantities u_1^o , v_1^o , and w_1^o satisfy all the kinematic requirements of the problem.

The incremented total potential energy can be expanded using eq. (42) as follows:

$$\begin{aligned}
\Pi + \Delta\Pi &= \frac{1}{2} \int_{x=-\frac{L}{2}}^{+\frac{L}{2}} \int_{\theta=-\frac{\beta}{2}}^{+\frac{\beta}{2}} \left\{ (N_x + \Delta N_x - N_x^P)(\epsilon_x^o + \Delta \epsilon_x^o) + (N_\theta + \Delta N_\theta - N_\theta^P)(\epsilon_\theta^o + \Delta \epsilon_\theta^o) \right. \\
&\quad + (N_{x\theta} + \Delta N_{x\theta} - N_{x\theta}^P)(\gamma_{x\theta}^o + \Delta \gamma_{x\theta}^o) + (M_x + \Delta M_x - M_x^P)(\kappa_x^o + \Delta \kappa_x^o) \\
&\quad + (M_\theta + \Delta M_\theta - M_\theta^P)(\kappa_\theta^o + \Delta \kappa_\theta^o) + (M_{x\theta} + \Delta M_{x\theta} - M_{x\theta}^P)(\kappa_{x\theta}^o + \Delta \kappa_{x\theta}^o) \\
&\quad \left. - q\{w^o(x, \theta) + \epsilon w_1^o(x, \theta)\} \right\} R d\theta dx \\
&+ \int_{\theta=-\frac{\beta}{2}}^{+\frac{\beta}{2}} \left[N_x^-(\theta) \left\{ \mu^o\left(-\frac{L}{2}, \theta\right) + \epsilon u_1^o\left(-\frac{L}{2}, \theta\right) \right\} - N_x^+(\theta) \left\{ \mu^o\left(+\frac{L}{2}, \theta\right) + \epsilon u_1^o\left(+\frac{L}{2}, \theta\right) \right\} \right. \\
&\quad + M_x^-(\theta) \left\{ \beta_x^o\left(-\frac{L}{2}, \theta\right) + \epsilon \beta_{x_1}^o\left(-\frac{L}{2}, \theta\right) \right\} - M_x^+(\theta) \left\{ \beta_x^o\left(+\frac{L}{2}, \theta\right) + \epsilon \beta_{x_1}^o\left(+\frac{L}{2}, \theta\right) \right\} \\
&\quad + N_{x\theta}^-(\theta) \left\{ \nu^o\left(-\frac{L}{2}, \theta\right) + \epsilon \nu_1^o\left(-\frac{L}{2}, \theta\right) \right\} - N_{x\theta}^+(\theta) \left\{ \nu^o\left(+\frac{L}{2}, \theta\right) + \epsilon \nu_1^o\left(+\frac{L}{2}, \theta\right) \right\} \\
&\quad + M_{x\theta}^-(\theta) \left\{ \beta_\theta^o\left(-\frac{L}{2}, \theta\right) + \epsilon \beta_{\theta_1}^o\left(-\frac{L}{2}, \theta\right) \right\} - M_{x\theta}^+(\theta) \left\{ \beta_\theta^o\left(+\frac{L}{2}, \theta\right) + \epsilon \beta_{\theta_1}^o\left(+\frac{L}{2}, \theta\right) \right\} \\
&\quad \left. + Q_x^-(\theta) \left\{ w^o\left(-\frac{L}{2}, \theta\right) + \epsilon w_1^o\left(-\frac{L}{2}, \theta\right) \right\} - Q_x^+(\theta) \left\{ w^o\left(+\frac{L}{2}, \theta\right) + \epsilon w_1^o\left(+\frac{L}{2}, \theta\right) \right\} \right] R d\theta \\
&+ \int_{x=-\frac{L}{2}}^{+\frac{L}{2}} \left[N_{\theta x}^-(x) \left\{ \mu^o\left(x, -\frac{\beta}{2}\right) + \epsilon u_1^o\left(x, -\frac{\beta}{2}\right) \right\} - N_{\theta x}^+(x) \left\{ \mu^o\left(x, +\frac{\beta}{2}\right) + \epsilon u_1^o\left(x, +\frac{\beta}{2}\right) \right\} \right. \\
&\quad + M_{\theta x}^-(x) \left\{ \beta_x^o\left(x, -\frac{\beta}{2}\right) + \epsilon \beta_{x_1}^o\left(x, -\frac{\beta}{2}\right) \right\} - M_{\theta x}^+(x) \left\{ \beta_x^o\left(x, +\frac{\beta}{2}\right) + \epsilon \beta_{x_1}^o\left(x, +\frac{\beta}{2}\right) \right\} \\
&\quad + N_\theta^-(x) \left\{ \nu^o\left(x, -\frac{\beta}{2}\right) + \epsilon \nu_1^o\left(x, -\frac{\beta}{2}\right) \right\} - N_\theta^+(x) \left\{ \nu^o\left(x, +\frac{\beta}{2}\right) + \epsilon \nu_1^o\left(x, +\frac{\beta}{2}\right) \right\} \\
&\quad + M_\theta^-(x) \left\{ \beta_\theta^o\left(x, -\frac{\beta}{2}\right) + \epsilon \beta_{\theta_1}^o\left(x, -\frac{\beta}{2}\right) \right\} - M_\theta^+(x) \left\{ \beta_\theta^o\left(x, +\frac{\beta}{2}\right) + \epsilon \beta_{\theta_1}^o\left(x, +\frac{\beta}{2}\right) \right\} \\
&\quad \left. + Q_\theta^-(x) \left\{ w^o\left(x, -\frac{\beta}{2}\right) + \epsilon w_1^o\left(x, -\frac{\beta}{2}\right) \right\} - Q_\theta^+(x) \left\{ w^o\left(x, +\frac{\beta}{2}\right) + \epsilon w_1^o\left(x, +\frac{\beta}{2}\right) \right\} \right] dx .
\end{aligned} \tag{49}$$

It should be noted that the equivalent preloading stress resultants do not have increments because they depend only on the material properties, temperature, and initial displacements, not the displacements due to the applied forces. Subtracting eq. (42) from

eq. (49) leads to an expression for the increment in the total potential energy, namely,

$$\begin{aligned}
\Delta \Pi = & \frac{1}{2} \int_{x=-\frac{L}{2}}^{+\frac{L}{2}} \int_{\theta=-\frac{\beta}{2}}^{+\frac{\beta}{2}} \left\{ (N_x - N_x^P) \Delta \varepsilon_x^o + \Delta N_x \varepsilon_x^o + \Delta N_x \Delta \varepsilon_x^o + (N_\theta - N_\theta^P) \Delta \varepsilon_\theta^o \right. \\
& + \Delta N_\theta \varepsilon_\theta^o + \Delta N_\theta \Delta \varepsilon_\theta^o + (N_{x\theta} - N_{x\theta}^P) \Delta \gamma_{x\theta}^o + \Delta N_{x\theta} \gamma_{x\theta}^o + \Delta N_{x\theta} \Delta \gamma_{x\theta}^o \\
& + (M_x - M_x^P) \Delta \kappa_x^o + \Delta M_x \kappa_x^o + \Delta M_x \Delta \kappa_x^o + (M_\theta - M_\theta^P) \Delta \kappa_\theta^o + \Delta M_\theta \kappa_\theta^o \\
& + \Delta M_\theta \Delta \kappa_\theta^o + (M_{x\theta} - M_{x\theta}^P) \Delta \kappa_{x\theta}^o + \Delta M_{x\theta} \kappa_{x\theta}^o + \Delta M_{x\theta} \Delta \kappa_{x\theta}^o \\
& \left. - \varepsilon q w^o(x, \theta) \right\} R d\theta dx \\
& + \varepsilon \left\{ \int_{\theta=-\frac{\beta}{2}}^{+\frac{\beta}{2}} \left\{ \left[N_x^-(\theta) u_1^o\left(-\frac{L}{2}, \theta\right) - N_x^+(\theta) u_1^o\left(+\frac{L}{2}, \theta\right) \right] \right. \right. \\
& \quad + \left[M_x^-(\theta) \beta_{x_1}^o\left(-\frac{L}{2}, \theta\right) - M_x^+(\theta) \beta_{x_1}^o\left(+\frac{L}{2}, \theta\right) \right] \\
& \quad + \left[N_{x\theta}^-(\theta) v_1^o\left(-\frac{L}{2}, \theta\right) - N_{x\theta}^+(\theta) v_1^o\left(+\frac{L}{2}, \theta\right) \right] \\
& \quad + \left[M_{x\theta}^-(\theta) \beta_{\theta_1}^o\left(-\frac{L}{2}, \theta\right) - M_{x\theta}^+(\theta) \beta_{\theta_1}^o\left(+\frac{L}{2}, \theta\right) \right] \\
& \quad \left. \left. + \left[Q_x^-(\theta) w_1^o\left(-\frac{L}{2}, \theta\right) - Q_x^+(\theta) w_1^o\left(+\frac{L}{2}, \theta\right) \right] \right\} R d\theta \right\} \\
& + \varepsilon \left\{ \int_{x=-\frac{L}{2}}^{+\frac{L}{2}} \left\{ \left[N_{\theta x}^-(x) u_1^o\left(x, -\frac{\beta}{2}\right) - N_{\theta x}^+(x) u_1^o\left(x, +\frac{\beta}{2}\right) \right] \right. \right. \\
& \quad + \left[M_{\theta x}^-(x) \beta_{x_1}^o\left(x, -\frac{\beta}{2}\right) - M_{\theta x}^+(x) \beta_{x_1}^o\left(x, +\frac{\beta}{2}\right) \right] \\
& \quad + \left[N_\theta^-(x) v_1^o\left(x, -\frac{\beta}{2}\right) - N_\theta^+(x) v_1^o\left(x, +\frac{\beta}{2}\right) \right] \\
& \quad + \left[M_\theta^-(x) \beta_{\theta_1}^o\left(x, -\frac{\beta}{2}\right) - M_\theta^+(x) \beta_{\theta_1}^o\left(x, +\frac{\beta}{2}\right) \right] \\
& \quad \left. \left. + \left[Q_\theta^-(x) w_1^o\left(x, -\frac{\beta}{2}\right) - Q_\theta^+(x) w_1^o\left(x, +\frac{\beta}{2}\right) \right] \right\} dx \right\} .
\end{aligned} \tag{50}$$

The various strain increments in eq. (50) arise from the basic definitions of the strains and curvatures, i.e., eq. (13), by substituting the increments in the displacements, eq. (47), for the displacements in the original definitions. Such a substitution for ϵ_x^o leads to

$$\epsilon_x^o + \Delta \epsilon_x^o = \frac{\partial(u^o + \epsilon u_1^o)}{\partial x} + \frac{1}{2}(\beta_x^o + \epsilon \beta_{x_1}^o)^2. \quad (51)$$

Discarding the superscript zero for convenience and expanding,

$$\epsilon_x + \Delta \epsilon_x = \frac{\partial u}{\partial x} + \epsilon \frac{\partial u_1}{\partial x} + \frac{1}{2}\beta_x^2 + \epsilon \beta_x \beta_{x_1} + \frac{1}{2}\epsilon^2 \beta_{x_1}^2. \quad (52)$$

Substituting eq. (13) for ϵ_x ,

$$\Delta \epsilon_x = \epsilon \left(\frac{\partial u_1}{\partial x} + \beta_x \beta_{x_1} \right) + \frac{1}{2}\epsilon^2 \beta_{x_1}^2, \quad (53)$$

which can be written as

$$\Delta \epsilon_x = \epsilon \epsilon_{x_1} + \epsilon^2 \epsilon_{x_2}, \quad (54)$$

where ϵ_{x_1} and ϵ_{x_2} are defined as

$$\epsilon_{x_1} = \frac{\partial u_1}{\partial x} + \beta_x \beta_{x_1} \quad (55)$$

$$\epsilon_{x_2} = \frac{1}{2}\beta_{x_1}^2. \quad (56)$$

In a similar fashion

$$\epsilon_\theta + \Delta \epsilon_\theta = \frac{\partial(v + \epsilon v_1)}{R\partial\theta} + \frac{w + \epsilon w_1}{R} + \frac{1}{2}(\beta_\theta + \epsilon \beta_{\theta_1})^2 \quad (57)$$

$$= \frac{\partial v}{R\partial\theta} + \epsilon \frac{\partial v_1}{R\partial\theta} + \frac{w}{R} + \epsilon \frac{w_1}{R} + \frac{1}{2}\beta_\theta^2 + \epsilon \beta_\theta \beta_{\theta_1} + \frac{1}{2}\epsilon^2 \beta_{\theta_1}^2, \quad (58)$$

or

$$\Delta \epsilon_\theta = \epsilon \epsilon_{\theta_1} + \epsilon^2 \epsilon_{\theta_2}, \quad (59)$$

where

$$\epsilon_{\theta_1} = \left(\frac{\partial v_1}{R \partial \theta} + \frac{w_1}{R} + \beta_{\theta} \beta_{\theta_1} \right) \quad (60)$$

$$\epsilon_{\theta_2} = \frac{1}{2} \beta_{\theta_1}^2 . \quad (61)$$

Likewise, the increment in $\gamma_{x\theta}$ is given by

$$\gamma_{x\theta} + \Delta \gamma_{x\theta} = \frac{\partial(v + \epsilon v_1)}{\partial x} + \frac{\partial(u + \epsilon u_1)}{R \partial \theta} + (\beta_x + \epsilon \beta_{x_1})(\beta_{\theta} + \epsilon \beta_{\theta_1}) \quad (62)$$

$$\begin{aligned} \gamma_{x\theta} + \Delta \gamma_{x\theta} &= \frac{\partial v}{\partial x} + \epsilon \frac{\partial v_1}{\partial x} + \frac{\partial u}{R \partial \theta} + \epsilon \frac{\partial u_1}{R \partial \theta} + \beta_x \beta_{\theta} \\ &\quad + \epsilon (\beta_x \beta_{\theta_1} + \beta_{\theta} \beta_{x_1}) + \epsilon^2 \beta_{x_1} \beta_{\theta_1} , \end{aligned} \quad (63)$$

which can be written as

$$\Delta \gamma_{x\theta} = \epsilon \gamma_{x\theta_1} + \epsilon^2 \gamma_{x\theta_2} , \quad (64)$$

where

$$\gamma_{x\theta_1} = \left(\frac{\partial v_1}{\partial x} + \frac{\partial u_1}{R \partial \theta} + \beta_x \beta_{\theta_1} + \beta_{\theta} \beta_{x_1} \right) \quad (65)$$

$$\gamma_{x\theta_2} = \beta_{x_1} \beta_{\theta_1} . \quad (66)$$

Finally,

$$\Delta \kappa_x = \epsilon \kappa_{x_1} ; \quad \Delta \kappa_{\theta} = \epsilon \kappa_{\theta_1} ; \quad \Delta \kappa_{x\theta} = \epsilon \kappa_{x\theta_1} , \quad (67)$$

where

$$\kappa_{x_1} = \frac{\partial \beta_{x_1}}{\partial x} , \quad (68)$$

$$\kappa_{\theta_1} = \frac{\partial \beta_{\theta_1}}{R \partial \theta} , \quad (69)$$

$$\kappa_{x\theta_1} = \left(\frac{\partial \beta_{\theta_1}}{\partial x} + \frac{\partial \beta_{x_1}}{R \partial \theta} \right) . \quad (70)$$

In the above, use has been made of the definitions

$$\beta_{x_1} = -\frac{\partial w_1}{\partial x} ; \quad \beta_{\theta_1} = -\frac{\partial w_1}{R\partial\theta} . \quad (71)$$

The increments in the stress resultants, in terms of the strain increments just defined, are given by:

$$\begin{aligned} \Delta N_x &= A_{11}\Delta\epsilon_x + A_{12}\Delta\epsilon_\theta + A_{16}\Delta\gamma_{x\theta} + B_{11}\Delta\kappa_x + B_{12}\Delta\kappa_\theta + B_{16}\Delta\kappa_{x\theta} \\ \Delta N_\theta &= A_{12}\Delta\epsilon_x + A_{22}\Delta\epsilon_\theta + A_{26}\Delta\gamma_{x\theta} + B_{12}\Delta\kappa_x + B_{22}\Delta\kappa_\theta + B_{26}\Delta\kappa_{x\theta} \\ \Delta N_{x\theta} &= A_{16}\Delta\epsilon_x + A_{26}\Delta\epsilon_\theta + A_{66}\Delta\gamma_{x\theta} + B_{16}\Delta\kappa_x + B_{26}\Delta\kappa_\theta + B_{66}\Delta\kappa_{x\theta} \\ \Delta M_x &= B_{11}\Delta\epsilon_x + B_{12}\Delta\epsilon_\theta + B_{16}\Delta\gamma_{x\theta} + D_{11}\Delta\kappa_x + D_{12}\Delta\kappa_\theta + D_{16}\Delta\kappa_{x\theta} \\ \Delta M_\theta &= B_{12}\Delta\epsilon_x + B_{22}\Delta\epsilon_\theta + B_{26}\Delta\gamma_{x\theta} + D_{12}\Delta\kappa_x + D_{22}\Delta\kappa_\theta + D_{26}\Delta\kappa_{x\theta} \\ \Delta M_{x\theta} &= B_{16}\Delta\epsilon_x + B_{26}\Delta\epsilon_\theta + B_{66}\Delta\gamma_{x\theta} + D_{16}\Delta\kappa_x + D_{26}\Delta\kappa_\theta + D_{66}\Delta\kappa_{x\theta} . \end{aligned} \quad (72)$$

In order to separate the first, second, etc. variations of the total potential energy at a later point, it is convenient to expand the increments in the stress resultants in terms of the displacements and redefine those increments in terms of powers of ϵ . Incorporating the definitions for the strain increments, eqs. (51)-(70), the stress resultant increments from eq. (72) are

$$\begin{aligned} \Delta N_x &= A_{11}(\epsilon\epsilon_{x_1} + \epsilon^2\epsilon_{x_2}) + A_{12}(\epsilon\epsilon_{\theta_1} + \epsilon^2\epsilon_{\theta_2}) + A_{16}(\epsilon\gamma_{x\theta_1} + \epsilon^2\gamma_{x\theta_2}) \\ &\quad + B_{11}\epsilon\kappa_{x_1} + B_{12}\epsilon\kappa_{\theta_1} + B_{16}\epsilon\kappa_{x\theta_1} . \end{aligned} \quad (73a)$$

These terms can be redefined to give

$$\Delta N_x = \epsilon N_{x_1} + \epsilon^2 N_{x_2} , \quad (73b)$$

where

$$N_{x_1} = A_{11}\epsilon_{x_1} + A_{12}\epsilon_{\theta_1} + A_{16}\gamma_{x\theta_1} + B_{11}\kappa_{x_1} + B_{12}\kappa_{\theta_1} + B_{16}\kappa_{x\theta_1} , \quad (73c)$$

and

$$N_{x_2} = A_{11}\epsilon_{x_2} + A_{12}\epsilon_{\theta_2} + A_{16}\gamma_{x\theta_2} . \quad (73d)$$

Expanding for future reference,

$$\begin{aligned}
 N_{x_1} = & A_{11} \left(\frac{\partial u_1}{\partial x} + \beta_x \beta_{x_1} \right) + A_{12} \left(\frac{\partial v_1}{R \partial \theta} + \frac{w_1}{R} + \beta_\theta \beta_{\theta_1} \right) \\
 & + A_{16} \left(\frac{\partial v_1}{\partial x} + \frac{\partial u_1}{R \partial \theta} + \beta_x \beta_{\theta_1} + \beta_\theta \beta_{x_1} \right) \\
 & + B_{11} \frac{\partial \beta_{x_1}}{\partial x} + B_{12} \frac{\partial \beta_{\theta_1}}{R \partial \theta} + B_{16} \left(\frac{\partial \beta_{\theta_1}}{\partial x} + \frac{\partial \beta_{x_1}}{R \partial \theta} \right)
 \end{aligned} \tag{73e}$$

and

$$N_{x_2} = \left(\frac{1}{2} A_{11} \beta_{x_1}^2 + \frac{1}{2} A_{12} \beta_{\theta_1}^2 + A_{16} \beta_{x_1} \beta_{\theta_1} \right). \tag{73f}$$

Using this procedure for the remaining stress resultants,

$$\begin{aligned}
 \Delta N_\theta = & A_{12} (\epsilon \epsilon_{x_1} + \epsilon^2 \epsilon_{x_2}) + A_{22} (\epsilon \epsilon_{\theta_1} + \epsilon^2 \epsilon_{\theta_2}) + A_{26} (\epsilon \gamma_{x\theta_1} + \epsilon^2 \gamma_{x\theta_2}) \\
 & + B_{12} \epsilon \kappa_{x_1} + B_{22} \epsilon \kappa_{\theta_1} + B_{26} \epsilon \kappa_{x\theta_1}.
 \end{aligned} \tag{74a}$$

Redefining,

$$\Delta N_\theta = \epsilon N_{\theta_1} + \epsilon^2 N_{\theta_2}, \tag{74b}$$

with

$$N_{\theta_1} = A_{12} \epsilon_{x_1} + A_{22} \epsilon_{\theta_1} + A_{26} \gamma_{x\theta_1} + B_{12} \kappa_{x_1} + B_{22} \kappa_{\theta_1} + B_{26} \kappa_{x\theta_1} \tag{74c}$$

and

$$N_{\theta_2} = A_{12} \epsilon_{x_2} + A_{22} \epsilon_{\theta_2} + A_{26} \gamma_{x\theta_2}. \tag{74d}$$

Expanding for future reference,

$$\begin{aligned}
 N_{\theta_1} = & A_{12} \left(\frac{\partial u_1}{\partial x} + \beta_x \beta_{x_1} \right) + A_{22} \left(\frac{\partial v_1}{R \partial \theta} + \frac{w_1}{R} + \beta_\theta \beta_{\theta_1} \right) \\
 & + A_{26} \left(\frac{\partial v_1}{\partial x} + \frac{\partial u_1}{R \partial \theta} + \beta_x \beta_{\theta_1} + \beta_\theta \beta_{x_1} \right) \\
 & + B_{12} \frac{\partial \beta_{x_1}}{\partial x} + B_{22} \frac{\partial \beta_{\theta_1}}{R \partial \theta} + B_{26} \left(\frac{\partial \beta_{\theta_1}}{\partial x} + \frac{\partial \beta_{x_1}}{R \partial \theta} \right)
 \end{aligned} \tag{74e}$$

and

$$N_{\theta_2} = \left(\frac{1}{2} A_{12} \beta_{x_1}^2 + \frac{1}{2} A_{22} \beta_{\theta_1}^2 + A_{26} \beta_{x_1} \beta_{\theta_1} \right). \quad (74f)$$

Likewise,

$$\begin{aligned} \Delta N_{x\theta} = & A_{16}(\epsilon \epsilon_{x_1} + \epsilon^2 \epsilon_{x_2}) + A_{26}(\epsilon \epsilon_{\theta_1} + \epsilon^2 \epsilon_{\theta_2}) + A_{66}(\epsilon \gamma_{x\theta_1} + \epsilon^2 \gamma_{x\theta_2}) \\ & + B_{16} \epsilon \kappa_{x_1} + B_{26} \epsilon \kappa_{\theta_1} + B_{66} \epsilon \kappa_{x\theta_1}, \end{aligned} \quad (75a)$$

or

$$\Delta N_{x\theta} = \epsilon N_{x\theta_1} + \epsilon^2 N_{x\theta_2}, \quad (75b)$$

where

$$N_{x\theta_1} = A_{16} \epsilon_{x_1} + A_{26} \epsilon_{\theta_1} + A_{66} \gamma_{x\theta_1} + B_{16} \kappa_{x_1} + B_{26} \kappa_{\theta_1} + B_{66} \kappa_{x\theta_1}, \quad (75c)$$

and

$$N_{x\theta_2} = A_{16} \epsilon_{x_2} + A_{26} \epsilon_{\theta_2} + A_{66} \gamma_{x\theta_2}. \quad (75d)$$

Expanding,

$$\begin{aligned} N_{x\theta_1} = & A_{16} \left(\frac{\partial u_1}{\partial x} + \beta_x \beta_{x_1} \right) + A_{26} \left(\frac{\partial v_1}{R \partial \theta} + \frac{w_1}{R} + \beta_\theta \beta_{\theta_1} \right) \\ & + A_{66} \left(\frac{\partial v_1}{\partial x} + \frac{\partial u_1}{R \partial \theta} + \beta_x \beta_{\theta_1} + \beta_\theta \beta_{x_1} \right) \\ & + B_{16} \frac{\partial \beta_{x_1}}{\partial x} + B_{26} \frac{\partial \beta_{\theta_1}}{R \partial \theta} + B_{66} \left(\frac{\partial \beta_{\theta_1}}{\partial x} + \frac{\partial \beta_{x_1}}{R \partial \theta} \right) \end{aligned} \quad (75e)$$

and

$$N_{x\theta_2} = \left(\frac{1}{2} A_{16} \beta_{x_1}^2 + \frac{1}{2} A_{26} \beta_{\theta_1}^2 + A_{66} \beta_{x_1} \beta_{\theta_1} \right). \quad (75f)$$

The increments in the moments can be similarly defined, namely,

$$\begin{aligned} \Delta M_x = & B_{11}(\epsilon \epsilon_{x_1} + \epsilon^2 \epsilon_{x_2}) + B_{12}(\epsilon \epsilon_{\theta_1} + \epsilon^2 \epsilon_{\theta_2}) + B_{16}(\epsilon \gamma_{x\theta_1} + \epsilon^2 \gamma_{x\theta_2}) \\ & + D_{11} \epsilon \kappa_{x_1} + D_{12} \epsilon \kappa_{\theta_1} + D_{16} \epsilon \kappa_{x\theta_1}, \end{aligned} \quad (76a)$$

or

$$\Delta M_x = \epsilon M_{x_1} + \epsilon^2 M_{x_2}, \quad (76b)$$

with

$$M_{x_1} = B_{11} \epsilon_{x_1} + B_{12} \epsilon_{\theta_1} + B_{16} \gamma_{x\theta_1} + D_{11} \kappa_{x_1} + D_{12} \kappa_{\theta_1} + D_{16} \kappa_{x\theta_1}, \quad (76c)$$

and

$$M_{x_2} = B_{11}\epsilon_{x_2} + B_{12}\epsilon_{\theta_2} + B_{16}\gamma_{x\theta_2}, \quad (76d)$$

where

$$\begin{aligned} M_{x_1} = & B_{11}\left(\frac{\partial u_1}{\partial x} + \beta_x \beta_{x_1}\right) + B_{12}\left(\frac{\partial v_1}{R\partial\theta} + \frac{w_1}{R} + \beta_\theta \beta_{\theta_1}\right) \\ & + B_{16}\left(\frac{\partial v_1}{\partial x} + \frac{\partial u_1}{R\partial\theta} + \beta_x \beta_{\theta_1} + \beta_\theta \beta_{x_1}\right) \\ & + D_{11}\frac{\partial \beta_{x_1}}{\partial x} + D_{12}\frac{\partial \beta_{\theta_1}}{R\partial\theta} + D_{16}\left(\frac{\partial \beta_{\theta_1}}{\partial x} + \frac{\partial \beta_{x_1}}{R\partial\theta}\right) \end{aligned} \quad (76e)$$

and

$$M_{x_2} = \left(\frac{1}{2}B_{11}\beta_{x_1}^2 + \frac{1}{2}B_{12}\beta_{\theta_1}^2 + B_{16}\beta_{x_1}\beta_{\theta_1}\right). \quad (76f)$$

In a similar manner,

$$\begin{aligned} \Delta M_\theta = & B_{12}(\epsilon\epsilon_{x_1} + \epsilon^2\epsilon_{x_2}) + B_{22}(\epsilon\epsilon_{\theta_1} + \epsilon^2\epsilon_{\theta_2}) + B_{26}(\epsilon\gamma_{x\theta_1} + \epsilon^2\gamma_{x\theta_2}) \\ & + D_{12}\epsilon\kappa_{x_1} + D_{22}\epsilon\kappa_{\theta_1} + D_{26}\epsilon\kappa_{x\theta_1}, \end{aligned} \quad (77a)$$

or

$$\Delta M_\theta = \epsilon M_{\theta_1} + \epsilon^2 M_{\theta_2}, \quad (77b)$$

with

$$M_{\theta_1} = B_{12}\epsilon_{x_1} + B_{22}\epsilon_{\theta_1} + B_{26}\gamma_{x\theta_1} + D_{12}\kappa_{x_1} + D_{22}\kappa_{\theta_1} + D_{26}\kappa_{x\theta_1} \quad (77c)$$

and

$$M_{\theta_2} = B_{12}\epsilon_{x_2} + B_{22}\epsilon_{\theta_2} + B_{26}\gamma_{x\theta_2}, \quad (77d)$$

where

$$\begin{aligned} M_{\theta_1} = & B_{12}\left(\frac{\partial u_1}{\partial x} + \beta_x \beta_{x_1}\right) + B_{22}\left(\frac{\partial v_1}{R\partial\theta} + \frac{w_1}{R} + \beta_\theta \beta_{\theta_1}\right) \\ & + B_{26}\left(\frac{\partial v_1}{\partial x} + \frac{\partial u_1}{R\partial\theta} + \beta_x \beta_{\theta_1} + \beta_\theta \beta_{x_1}\right) \\ & + D_{12}\frac{\partial \beta_{x_1}}{\partial x} + D_{22}\frac{\partial \beta_{\theta_1}}{R\partial\theta} + D_{26}\left(\frac{\partial \beta_{\theta_1}}{\partial x} + \frac{\partial \beta_{x_1}}{R\partial\theta}\right) \end{aligned} \quad (77e)$$

and

$$M_{\theta_2} = \left(\frac{1}{2} B_{12} \beta_{x_1}^2 + \frac{1}{2} B_{22} \beta_{\theta_1}^2 + B_{26} \beta_{x_1} \beta_{\theta_1} \right). \quad (77f)$$

Finally,

$$\begin{aligned} \Delta M_{x\theta} = & B_{16}(\epsilon \epsilon_{x_1} + \epsilon^2 \epsilon_{x_2}) + B_{26}(\epsilon \epsilon_{\theta_1} + \epsilon^2 \epsilon_{\theta_2}) + B_{66}(\epsilon \gamma_{x\theta_1} + \epsilon^2 \gamma_{x\theta_2}) \\ & + D_{16} \epsilon \kappa_{x_1} + D_{26} \epsilon \kappa_{\theta_1} + D_{66} \epsilon \kappa_{x\theta_1}, \end{aligned} \quad (78a)$$

where

$$\Delta M_{x\theta} = \epsilon M_{x\theta_1} + \epsilon^2 M_{x\theta_2}, \quad (78b)$$

with

$$M_{x\theta_1} = B_{16} \epsilon_{x_1} + B_{26} \epsilon_{\theta_1} + B_{66} \gamma_{x\theta_1} + D_{16} \kappa_{x_1} + D_{26} \kappa_{\theta_1} + D_{66} \kappa_{x\theta_1} \quad (78c)$$

and

$$M_{x\theta_2} = B_{16} \epsilon_{x_2} + B_{26} \epsilon_{\theta_2} + B_{66} \gamma_{x\theta_2}. \quad (78d)$$

Expanding for future reference

$$\begin{aligned} M_{x\theta_1} = & B_{16} \left(\frac{\partial u_1}{\partial x} + \beta_x \beta_{x_1} \right) + B_{26} \left(\frac{\partial v_1}{R \partial \theta} + \frac{w_1}{R} + \beta_\theta \beta_{\theta_1} \right) \\ & + B_{66} \left(\frac{\partial v_1}{\partial x} + \frac{\partial u_1}{R \partial \theta} + \beta_x \beta_{\theta_1} + \beta_\theta \beta_{x_1} \right) \\ & + D_{16} \frac{\partial \beta_{x_1}}{\partial x} + D_{26} \frac{\partial \beta_{\theta_1}}{R \partial \theta} + D_{66} \left(\frac{\partial \beta_{\theta_1}}{\partial x} + \frac{\partial \beta_{x_1}}{R \partial \theta} \right) \end{aligned} \quad (78e)$$

and

$$M_{x\theta_2} = \left(\frac{1}{2} B_{16} \beta_{x_1}^2 + \frac{1}{2} B_{26} \beta_{\theta_1}^2 + B_{66} \beta_{x_1} \beta_{\theta_1} \right). \quad (78f)$$

With the strain and stress resultant increments defined and expanded, the definitions can be substituted into eq. (50). This results in

$$\begin{aligned}
\Delta \Pi = & \frac{1}{2} \int_{x=-\frac{L}{2}}^{+\frac{L}{2}} \int_{\theta=-\frac{\beta}{2}}^{+\frac{\beta}{2}} \left\{ (N_x - N_x^P)(\varepsilon \varepsilon_{x_1} + \varepsilon^2 \varepsilon_{x_2}) + (\varepsilon N_{x_1} + \varepsilon^2 N_{x_2}) \varepsilon_x \right. \\
& + (\varepsilon N_{x_1} + \varepsilon^2 N_{x_2})(\varepsilon \varepsilon_{x_1} + \varepsilon^2 \varepsilon_{x_2}) + (N_\theta - N_\theta^P)(\varepsilon \varepsilon_{\theta_1} + \varepsilon^2 \varepsilon_{\theta_2}) \\
& + (\varepsilon N_{\theta_1} + \varepsilon^2 N_{\theta_2}) \varepsilon_\theta + (\varepsilon N_{\theta_1} + \varepsilon^2 N_{\theta_2})(\varepsilon \varepsilon_{\theta_1} + \varepsilon^2 \varepsilon_{\theta_2}) \\
& + (N_{x\theta} - N_{x\theta}^P)(\varepsilon \gamma_{x\theta_1} + \varepsilon^2 \gamma_{x\theta_2}) + (\varepsilon N_{x\theta} + \varepsilon^2 N_{x\theta_2}) \gamma_{x\theta} \\
& + (\varepsilon N_{x\theta_1} + \varepsilon^2 N_{x\theta_2})(\varepsilon \gamma_{x\theta_1} + \varepsilon^2 \gamma_{x\theta_2}) + (M_x - M_x^P) \varepsilon \kappa_{x_1} \\
& + (\varepsilon M_{x_1} + \varepsilon^2 M_{x_2}) \kappa_x + (\varepsilon M_{x_1} + \varepsilon^2 M_{x_2}) \varepsilon \kappa_{x_1} + (M_\theta - M_\theta^P) \varepsilon \kappa_{\theta_1} \\
& + (\varepsilon M_{\theta_1} + \varepsilon^2 M_{\theta_2}) \kappa_\theta + (\varepsilon M_{\theta_1} + \varepsilon^2 M_{\theta_2}) \varepsilon \kappa_{\theta_1} + (M_{x\theta} - M_{x\theta}^P) \varepsilon \kappa_{x\theta_1} \\
& \left. + (\varepsilon M_{x\theta_1} + \varepsilon^2 M_{x\theta_2}) \kappa_{x\theta} + (\varepsilon M_{x\theta_1} + \varepsilon^2 M_{x\theta_2}) \varepsilon \kappa_{x\theta_1} - \varepsilon q w_1^0 \right\} R d\theta dx \\
& + \varepsilon \left\{ \int_{\theta=-\frac{\beta}{2}}^{+\frac{\beta}{2}} \left\{ \left[N_x^-(\theta) u_1^0 \left(-\frac{L}{2}, \theta \right) - N_x^+(\theta) u_1^0 \left(+\frac{L}{2}, \theta \right) \right] \right. \right. \\
& \quad + \left[M_x^-(\theta) \beta_{x_1}^0 \left(-\frac{L}{2}, \theta \right) - M_x^+(\theta) \beta_{x_1}^0 \left(+\frac{L}{2}, \theta \right) \right] \\
& \quad + \left[N_{x\theta}^-(\theta) v_1^0 \left(-\frac{L}{2}, \theta \right) - N_{x\theta}^+(\theta) v_1^0 \left(+\frac{L}{2}, \theta \right) \right] \\
& \quad + \left[M_{x\theta}^-(\theta) \beta_{\theta_1}^0 \left(-\frac{L}{2}, \theta \right) - M_{x\theta}^+(\theta) \beta_{\theta_1}^0 \left(+\frac{L}{2}, \theta \right) \right] \\
& \quad \left. \left. + \left[Q_x^-(\theta) w_1^0 \left(-\frac{L}{2}, \theta \right) - Q_x^+(\theta) w_1^0 \left(+\frac{L}{2}, \theta \right) \right] \right\} R d\theta \right\} \\
& + \varepsilon \left\{ \int_{x=-\frac{L}{2}}^{+\frac{L}{2}} \left\{ \left[N_{\theta x}^-(x) u_1^0 \left(x, -\frac{\beta}{2} \right) - N_{\theta x}^+(x) u_1^0 \left(x, +\frac{\beta}{2} \right) \right] \right. \right. \\
& \quad + \left[M_{\theta x}^-(x) \beta_{x_1}^0 \left(x, -\frac{\beta}{2} \right) - M_{\theta x}^+(x) \beta_{x_1}^0 \left(x, +\frac{\beta}{2} \right) \right] \\
& \quad + \left[N_\theta^-(x) v_1^0 \left(x, -\frac{\beta}{2} \right) - N_\theta^+(x) v_1^0 \left(x, +\frac{\beta}{2} \right) \right] \\
& \quad + \left[M_\theta^-(x) \beta_{\theta_1}^0 \left(x, -\frac{\beta}{2} \right) - M_\theta^+(x) \beta_{\theta_1}^0 \left(x, +\frac{\beta}{2} \right) \right] \\
& \quad \left. \left. + \left[Q_\theta^-(x) w_1^0 \left(x, -\frac{\beta}{2} \right) - Q_\theta^+(x) w_1^0 \left(x, +\frac{\beta}{2} \right) \right] \right\} dx \right\} .
\end{aligned} \tag{79}$$

Expanding and regrouping in powers of ε leads to

$$\begin{aligned}
\Delta \Pi = & \frac{1}{2} \int_{x=-\frac{L}{2}}^{+\frac{L}{2}} \int_{\theta=-\frac{\beta}{2}}^{+\frac{\beta}{2}} \left[\varepsilon \left\{ (N_x - N_x^F) \varepsilon_{x_1} + N_{x_1} \varepsilon + (N_\theta - N_\theta^F) \varepsilon_{\theta_1} + N_{\theta_1} \varepsilon_\theta \right. \right. \\
& + (N_{x\theta} - N_{x\theta}^F) \gamma_{x\theta_1} + N_{x\theta_1} \gamma_{x\theta} + (M_x - M_x^F) \kappa_{x_1} + M_{x_1} \kappa_x \\
& + (M_\theta - M_\theta^F) \kappa_{\theta_1} + M_{\theta_1} \kappa_\theta + (M_{x\theta} - M_{x\theta}^F) \kappa_{x\theta_1} + M_{x\theta_1} \kappa_{x\theta} - q w_1^o \left. \right\} \\
& + \varepsilon^2 \left\{ (N_x - N_x^F) \varepsilon_{x_2} + N_{x_2} \varepsilon_x + N_{x_1} \varepsilon_{x_1} + (N_\theta - N_\theta^F) \varepsilon_{\theta_2} \right. \\
& + N_{\theta_2} \varepsilon_\theta + N_{\theta_1} \varepsilon_{\theta_1} + (N_{x\theta} - N_{x\theta}^F) \gamma_{x\theta} + N_{x\theta_2} \gamma_{x\theta} + N_{x\theta_1} \gamma_{x\theta_1} \\
& + M_{x_2} \kappa_x + M_{x_1} \kappa_{x_1} + M_{\theta_2} \kappa_\theta + M_{\theta_1} \kappa_{\theta_1} + M_{x\theta_2} \kappa_{x\theta} + M_{x\theta_1} \kappa_{x\theta_1} \left. \right\} \\
& + \varepsilon^3 \left\{ N_{x_1} \varepsilon_{x_2} + N_{x_2} \varepsilon_{x_1} + N_{\theta_2} \varepsilon_{\theta_1} + N_{\theta_1} \varepsilon_{\theta_2} + N_{x\theta_1} \gamma_{x\theta_2} \right. \\
& + N_{x\theta_2} \gamma_{x\theta_1} + M_{x_2} \kappa_{x_1} + M_{\theta_2} \kappa_{\theta_1} + M_{x\theta_2} \kappa_{x\theta_1} \left. \right\} \\
& + \varepsilon^4 \left\{ N_{x_2} \varepsilon_{x_2} + N_{\theta_2} \varepsilon_{\theta_2} + N_{x\theta_2} \gamma_{x\theta_2} \right\} R d\theta dx \\
& + \varepsilon \left\{ \int_{\theta=-\frac{\beta}{2}}^{+\frac{\beta}{2}} \left\{ \left[N_x^-(\theta) u_1^o \left(-\frac{L}{2}, \theta \right) - N_x^+(\theta) u_1^o \left(+\frac{L}{2}, \theta \right) \right] \right. \right. \\
& \quad + \left[M_x^-(\theta) \beta_{x_1}^o \left(-\frac{L}{2}, \theta \right) - M_x^+(\theta) \beta_{x_1}^o \left(+\frac{L}{2}, \theta \right) \right] \\
& \quad + \left[N_{x\theta}^-(\theta) v_1^o \left(-\frac{L}{2}, \theta \right) - N_{x\theta}^+(\theta) v_1^o \left(+\frac{L}{2}, \theta \right) \right] \\
& \quad + \left[M_{x\theta}^-(\theta) \beta_{\theta_1}^o \left(-\frac{L}{2}, \theta \right) - M_{x\theta}^+(\theta) \beta_{\theta_1}^o \left(+\frac{L}{2}, \theta \right) \right] \\
& \quad \left. \left. + \left[Q_x^-(\theta) w_1^o \left(-\frac{L}{2}, \theta \right) - Q_x^+(\theta) w_1^o \left(+\frac{L}{2}, \theta \right) \right] \right\} R d\theta \right\} \\
& + \varepsilon \left\{ \int_{x=-\frac{L}{2}}^{+\frac{L}{2}} \left\{ \left[N_{\theta x}^-(x) u_1^o \left(x, -\frac{\beta}{2} \right) - N_{\theta x}^+(x) u_1^o \left(x, +\frac{\beta}{2} \right) \right] \right. \right. \\
& \quad + \left[M_{\theta x}^-(x) \beta_{x_1}^o \left(x, -\frac{\beta}{2} \right) - M_{\theta x}^+(x) \beta_{x_1}^o \left(x, +\frac{\beta}{2} \right) \right] \\
& \quad + \left[N_\theta^-(x) v_1^o \left(x, -\frac{\beta}{2} \right) - N_\theta^+(x) v_1^o \left(x, +\frac{\beta}{2} \right) \right] \\
& \quad + \left[M_\theta^-(x) \beta_{\theta_1}^o \left(x, -\frac{\beta}{2} \right) - M_\theta^+(x) \beta_{\theta_1}^o \left(x, +\frac{\beta}{2} \right) \right] \\
& \quad \left. \left. + \left[Q_\theta^-(x) w_1^o \left(x, -\frac{\beta}{2} \right) - Q_\theta^+(x) w_1^o \left(x, +\frac{\beta}{2} \right) \right] \right\} dx \right\} .
\end{aligned} \tag{80}$$

The increment in the total potential energy can be written as

$$\Delta \Pi = \varepsilon \Pi_1 + \varepsilon^2 \Pi_2 + \varepsilon^3 \Pi_3 + \varepsilon^4 \Pi_4 \quad . \quad (81)$$

The quantities $\varepsilon \Pi_1$, $\varepsilon^2 \Pi_2$, $\varepsilon^3 \Pi_3$, and $\varepsilon^4 \Pi_4$ are defined to be the first, second, third, and fourth variations of total potential energy, respectively. The equilibrium conditions for a cylindrical panel are obtained from the condition

$$\varepsilon \Pi_1(u_1, v_1, w_1) = 0 \rightarrow \Pi_1(u_1, v_1, w_1) = 0 \quad , \quad (82)$$

where the notation indicates Π_1 is to be stationary with respect to the displacements u_1 , v_1 , w_1 . These displacements are the variations in the equilibrium displacements. The second variation is used to examine stability of the equilibrium displacements. According to the Trefftz stability criterion, transition from a stable equilibrium configuration to an unstable one is characterized by

$$\delta \varepsilon^2 \Pi_2(u_1, v_1, w_1) = 0 \rightarrow \delta \Pi_2(u_1, v_1, w_1) = 0 \quad . \quad (83)$$

This states that the second variation of the total potential energy should be stationary with respect to variations in u_1 , v_1 , w_1 .

Interest in the present study focusses on equilibrium rather than stability. Hence, the first variation, Π_1 , shall be studied further. The higher order variations, however, will not be discussed beyond this point.

The first variation can be identified with Π_1 and that quantity is given by

$$\begin{aligned}
\Pi_1 = & \frac{1}{2} \int_{x=-\frac{L}{2}}^{+\frac{L}{2}} \int_{\theta=-\frac{\beta}{2}}^{+\frac{\beta}{2}} \left[(N_x - N_x^P) \varepsilon_{x_1} + N_{x_1} \varepsilon_x + (N_\theta - N_\theta^P) \varepsilon_{\theta_1} + N_{\theta_1} \varepsilon_\theta \right. \\
& + (N_{x\theta} - N_{x\theta}^P) \gamma_{x\theta_1} + N_{x\theta_1} \gamma_{x\theta} + (M_x - M_x^P) \kappa_{x_1} + M_{x_1} \kappa_x \\
& \left. + (M_\theta - M_\theta^P) \kappa_{\theta_1} + M_{\theta_1} \kappa_\theta + (M_{x\theta} - M_{x\theta}^P) \kappa_{x\theta_1} + M_{x\theta_1} \kappa_{x\theta} - q w_1^\circ \right] R d\theta dx \\
& + \int_{\theta=-\frac{\beta}{2}}^{+\frac{\beta}{2}} \left\{ \left[N_x^-(\theta) u_1^\circ \left(-\frac{L}{2}, \theta \right) - N_x^+(\theta) u_1^\circ \left(+\frac{L}{2}, \theta \right) \right] \right. \\
& + \left[M_x^-(\theta) \beta_{x_1}^\circ \left(-\frac{L}{2}, \theta \right) - M_x^+(\theta) \beta_{x_1}^\circ \left(+\frac{L}{2}, \theta \right) \right] \\
& + \left[N_{x\theta}^-(\theta) v_1^\circ \left(-\frac{L}{2}, \theta \right) - N_{x\theta}^+(\theta) v_1^\circ \left(+\frac{L}{2}, \theta \right) \right] \\
& + \left[M_{x\theta}^-(\theta) \beta_{\theta_1}^\circ \left(-\frac{L}{2}, \theta \right) - M_{x\theta}^+(\theta) \beta_{\theta_1}^\circ \left(+\frac{L}{2}, \theta \right) \right] \\
& \left. + \left[Q_x^-(\theta) w_1^\circ \left(-\frac{L}{2}, \theta \right) - Q_x^+(\theta) w_1^\circ \left(+\frac{L}{2}, \theta \right) \right] \right\} R d\theta \\
& + \int_{x=-\frac{L}{2}}^{+\frac{L}{2}} \left\{ \left[N_{\theta x}^-(x) u_1^\circ \left(x, -\frac{\beta}{2} \right) - N_{\theta x}^+(x) u_1^\circ \left(x, +\frac{\beta}{2} \right) \right] \right. \\
& + \left[M_{\theta x}^-(x) \beta_{x_1}^\circ \left(x, -\frac{\beta}{2} \right) - M_{\theta x}^+(x) \beta_{x_1}^\circ \left(x, +\frac{\beta}{2} \right) \right] \\
& + \left[N_\theta^-(x) v_1^\circ \left(x, -\frac{\beta}{2} \right) - N_\theta^+(x) v_1^\circ \left(x, +\frac{\beta}{2} \right) \right] \\
& + \left[M_\theta^-(x) \beta_{\theta_1}^\circ \left(x, -\frac{\beta}{2} \right) - M_\theta^+(x) \beta_{\theta_1}^\circ \left(x, +\frac{\beta}{2} \right) \right] \\
& \left. + \left[Q_\theta^-(x) w_1^\circ \left(x, -\frac{\beta}{2} \right) - Q_\theta^+(x) w_1^\circ \left(x, +\frac{\beta}{2} \right) \right] \right\} dx .
\end{aligned} \tag{84}$$

A more useful form of the first variation can be obtained by substituting for N_{x_1} , N_{θ_1} , $N_{x\theta_1}$, M_{x_1} , M_{θ_1} , and $M_{x\theta_1}$ from eqs. (73e), (74e), (75e), (76e), (77e), and (78e). If this is done and the various terms in this expanded form of Π_1 are regrouped, the result is

$$\begin{aligned}
\Pi_1 = & \int_{x=-\frac{L}{2}}^{+\frac{L}{2}} \int_{\theta=-\frac{\beta}{2}}^{+\frac{\beta}{2}} \left\{ N_x \varepsilon_{x_1} + N_{\theta} \varepsilon_{\theta_1} + N_{x\theta} \gamma_{x\theta_1} + M_x \kappa_{x_1} \right. \\
& \left. + M_{\theta} \kappa_{\theta_1} + M_{x\theta} \kappa_{x\theta_1} - q w_1^{\circ} \right\} R d\theta dx \\
& + \int_{\theta=-\frac{\beta}{2}}^{+\frac{\beta}{2}} \left\{ \left[N_x^-(\theta) u_1^{\circ}\left(-\frac{L}{2}, \theta\right) - N_x^+(\theta) u_1^{\circ}\left(+\frac{L}{2}, \theta\right) \right] \right. \\
& \left. + \left[M_x^-(\theta) \beta_{x_1}^{\circ}\left(-\frac{L}{2}, \theta\right) - M_x^+(\theta) \beta_{x_1}^{\circ}\left(+\frac{L}{2}, \theta\right) \right] \right. \\
& \left. + \left[N_{x\theta}^-(\theta) v_1^{\circ}\left(-\frac{L}{2}, \theta\right) - N_{x\theta}^+(\theta) v_1^{\circ}\left(+\frac{L}{2}, \theta\right) \right] \right. \\
& \left. + \left[M_{x\theta}^-(\theta) \beta_{\theta_1}^{\circ}\left(-\frac{L}{2}, \theta\right) - M_{x\theta}^+(\theta) \beta_{\theta_1}^{\circ}\left(+\frac{L}{2}, \theta\right) \right] \right. \\
& \left. + \left[Q_x^-(\theta) w_1^{\circ}\left(-\frac{L}{2}, \theta\right) - Q_x^+(\theta) w_1^{\circ}\left(+\frac{L}{2}, \theta\right) \right] \right\} R d\theta \\
& + \int_{x=-\frac{L}{2}}^{+\frac{L}{2}} \left\{ \left[N_{\theta x}^-(x) u_1^{\circ}\left(x, -\frac{\beta}{2}\right) - N_{\theta x}^+(x) u_1^{\circ}\left(x, +\frac{\beta}{2}\right) \right] \right. \\
& \left. + \left[M_{\theta x}^-(x) \beta_{x_1}^{\circ}\left(x, -\frac{\beta}{2}\right) - M_{\theta x}^+(x) \beta_{x_1}^{\circ}\left(x, +\frac{\beta}{2}\right) \right] \right. \\
& \left. + \left[N_{\theta}^-(x) v_1^{\circ}\left(x, -\frac{\beta}{2}\right) - N_{\theta}^+(x) v_1^{\circ}\left(x, +\frac{\beta}{2}\right) \right] \right. \\
& \left. + \left[M_{\theta}^-(x) \beta_{\theta_1}^{\circ}\left(x, -\frac{\beta}{2}\right) - M_{\theta}^+(x) \beta_{\theta_1}^{\circ}\left(x, +\frac{\beta}{2}\right) \right] \right. \\
& \left. + \left[Q_{\theta}^-(x) w_1^{\circ}\left(x, -\frac{\beta}{2}\right) - Q_{\theta}^+(x) w_1^{\circ}\left(x, +\frac{\beta}{2}\right) \right] \right\} dx .
\end{aligned} \tag{85}$$

Note the quantities $N_x^P, \dots, M_{x\theta}^P$ have disappeared, as has the factor of 1/2 in front of the two-dimensional integral. Substituting the strain-displacement and curvature-displacement relations, eqs. (55), (60), (65), and (68)-(70), into the above, the first variation takes the form

$$\begin{aligned}
\Pi_1 = & \int_{x=-\frac{L}{2}}^{+\frac{L}{2}} \int_{\theta=-\frac{\beta}{2}}^{+\frac{\beta}{2}} \left\{ N_x \left(\frac{\partial u_1}{\partial x} + \beta_x \beta_{x_1} \right) + N_\theta \left(\frac{\partial v_1}{R \partial \theta} + \frac{w_1}{R} + \beta_\theta \beta_{\theta_1} \right) \right. \\
& + N_{x\theta} \left(\frac{\partial v_1}{\partial x} + \frac{\partial u_1}{R \partial \theta} + \beta_x \beta_{\theta_1} + \beta_\theta \beta_{x_1} \right) + M_x \frac{\partial \beta_{x_1}}{\partial x} + M_\theta \frac{\partial \beta_{\theta_1}}{R \partial \theta} \\
& \left. + M_{x\theta} \left(\frac{\partial \beta_{\theta_1}}{\partial x} + \frac{\partial \beta_{x_1}}{R \partial \theta} \right) - q w_1 \right\} R d\theta dx \\
& + \int_{\theta=-\frac{\beta}{2}}^{+\frac{\beta}{2}} \left\{ \left[N_x^-(\theta) u_1^\circ \left(-\frac{L}{2}, \theta \right) - N_x^+(\theta) u_1^\circ \left(+\frac{L}{2}, \theta \right) \right] \right. \\
& + \left[M_x^-(\theta) \beta_{x_1}^\circ \left(-\frac{L}{2}, \theta \right) - M_x^+(\theta) \beta_{x_1}^\circ \left(+\frac{L}{2}, \theta \right) \right] \\
& + \left[N_{x\theta}^-(\theta) v_1^\circ \left(-\frac{L}{2}, \theta \right) - N_{x\theta}^+(\theta) v_1^\circ \left(+\frac{L}{2}, \theta \right) \right] \\
& + \left[M_{x\theta}^-(\theta) \beta_{\theta_1}^\circ \left(-\frac{L}{2}, \theta \right) - M_{x\theta}^+(\theta) \beta_{\theta_1}^\circ \left(+\frac{L}{2}, \theta \right) \right] \\
& \left. + \left[Q_x^-(\theta) w_1^\circ \left(-\frac{L}{2}, \theta \right) - Q_x^+(\theta) w_1^\circ \left(+\frac{L}{2}, \theta \right) \right] \right\} R d\theta \\
& + \int_{x=-\frac{L}{2}}^{+\frac{L}{2}} \left\{ \left[N_{\theta x}^-(x) u_1^\circ \left(x, -\frac{\beta}{2} \right) - N_{\theta x}^+(x) u_1^\circ \left(x, +\frac{\beta}{2} \right) \right] \right. \\
& + \left[M_{\theta x}^-(x) \beta_{x_1}^\circ \left(x, -\frac{\beta}{2} \right) - M_{\theta x}^+(x) \beta_{x_1}^\circ \left(x, +\frac{\beta}{2} \right) \right] \\
& + \left[N_\theta^-(x) v_1^\circ \left(x, -\frac{\beta}{2} \right) - N_\theta^+(x) v_1^\circ \left(x, +\frac{\beta}{2} \right) \right] \\
& + \left[M_\theta^-(x) \beta_{\theta_1}^\circ \left(x, -\frac{\beta}{2} \right) - M_\theta^+(x) \beta_{\theta_1}^\circ \left(x, +\frac{\beta}{2} \right) \right] \\
& \left. + \left[Q_\theta^-(x) w_1^\circ \left(x, -\frac{\beta}{2} \right) - Q_\theta^+(x) w_1^\circ \left(x, +\frac{\beta}{2} \right) \right] \right\} dx .
\end{aligned} \tag{86}$$

This is one of the fundamental forms of the first variation for determining the response of a cylindrical panel. This form can be used directly in approximate schemes such as the Rayleigh-Ritz method. Further steps, however, are required to obtain the equilibrium

equations and associated boundary conditions which are of interest here.

E. Application of Integration By Parts

To determine the equilibrium equations and the associated boundary conditions, differentiation of u_1 , v_1 , and w_1 with respect to the spatial variables x and θ must be eliminated. This is done by applying integration by parts to the various terms in eq. (86). This procedure follows, the results being given on a term-by-term basis:

first term

$$\begin{aligned} \int_{x=-\frac{L}{2}}^{+\frac{L}{2}} \int_{\theta=-\frac{\beta}{2}}^{+\frac{\beta}{2}} N_x \frac{\partial u_1}{\partial x} R d\theta dx &= \int_{\theta=-\frac{\beta}{2}}^{+\frac{\beta}{2}} (N_x u_1) \Big|_{x=-\frac{L}{2}}^{x=+\frac{L}{2}} R d\theta \\ &- \int_{x=-\frac{L}{2}}^{+\frac{L}{2}} \int_{\theta=-\frac{\beta}{2}}^{+\frac{\beta}{2}} \frac{\partial N_x}{\partial x} u_1 R d\theta dx \end{aligned} \quad (87)$$

second term

$$\begin{aligned} \int_{x=-\frac{L}{2}}^{+\frac{L}{2}} \int_{\theta=-\frac{\beta}{2}}^{+\frac{\beta}{2}} N_x \beta_x \beta_{x_1} R d\theta dx &= \int_{x=-\frac{L}{2}}^{+\frac{L}{2}} \int_{\theta=-\frac{\beta}{2}}^{+\frac{\beta}{2}} N_x \frac{\partial w}{\partial x} \frac{\partial w_1}{\partial x} R d\theta dx \\ &= \int_{\theta=-\frac{\beta}{2}}^{+\frac{\beta}{2}} \left(N_x \frac{\partial w}{\partial x} w_1 \right) \Big|_{x=-\frac{L}{2}}^{x=+\frac{L}{2}} R d\theta \\ &- \int_{x=-\frac{L}{2}}^{+\frac{L}{2}} \int_{\theta=-\frac{\beta}{2}}^{+\frac{\beta}{2}} \frac{\partial}{\partial x} \left(N_x \frac{\partial w}{\partial x} \right) w_1 R d\theta dx \end{aligned} \quad (88)$$

third term

$$\begin{aligned} \int_{x=-\frac{L}{2}}^{+\frac{L}{2}} \int_{\theta=-\frac{\beta}{2}}^{+\frac{\beta}{2}} N_\theta \frac{\partial v_1}{R \partial \theta} R d\theta dx &= \int_{x=-\frac{L}{2}}^{+\frac{L}{2}} (N_\theta v_1) \Big|_{\theta=-\frac{\beta}{2}}^{\theta=+\frac{\beta}{2}} dx \\ &- \int_{x=-\frac{L}{2}}^{+\frac{L}{2}} \int_{\theta=-\frac{\beta}{2}}^{+\frac{\beta}{2}} \frac{\partial N_\theta}{R \partial \theta} v_1 R d\theta dx \end{aligned} \quad (89)$$

fifth term

$$\begin{aligned}
 \int_{x=-\frac{L}{2}}^{+\frac{L}{2}} \int_{\theta=-\frac{\beta}{2}}^{+\frac{\beta}{2}} N_{\theta} \beta_{\theta} \beta_{\theta_1} R d\theta dx &= \int_{x=-\frac{L}{2}}^{+\frac{L}{2}} \int_{\theta=-\frac{\beta}{2}}^{+\frac{\beta}{2}} N_{\theta} \frac{\partial w}{R \partial \theta} \frac{\partial w_1}{R \partial \theta} R d\theta dx \\
 &= \int_{x=-\frac{L}{2}}^{+\frac{L}{2}} \left(N_{\theta} \frac{\partial w}{R \partial \theta} w_1 \right) \Big|_{\theta=-\frac{\beta}{2}}^{\theta=+\frac{\beta}{2}} dx \\
 &\quad - \int_{x=-\frac{L}{2}}^{+\frac{L}{2}} \int_{\theta=-\frac{\beta}{2}}^{+\frac{\beta}{2}} \frac{\partial}{R \partial \theta} \left(N_{\theta} \frac{\partial w}{R \partial \theta} \right) w_1 R d\theta dx
 \end{aligned} \tag{90}$$

sixth term

$$\begin{aligned}
 \int_{x=-\frac{L}{2}}^{+\frac{L}{2}} \int_{\theta=-\frac{\beta}{2}}^{+\frac{\beta}{2}} N_{x\theta} \frac{\partial v_1}{\partial x} R d\theta dx &= \int_{\theta=-\frac{\beta}{2}}^{+\frac{\beta}{2}} (N_{x\theta} v_1) \Big|_{x=-\frac{L}{2}}^{x=+\frac{L}{2}} R d\theta \\
 &\quad - \int_{x=-\frac{L}{2}}^{+\frac{L}{2}} \int_{\theta=-\frac{\beta}{2}}^{+\frac{\beta}{2}} \frac{\partial N_{x\theta}}{\partial x} v_1 R d\theta dx
 \end{aligned} \tag{91}$$

seventh term

$$\begin{aligned}
 \int_{x=-\frac{L}{2}}^{+\frac{L}{2}} \int_{\theta=-\frac{\beta}{2}}^{+\frac{\beta}{2}} N_{x\theta} \frac{\partial u_1}{R \partial \theta} R d\theta dx &= \int_{x=-\frac{L}{2}}^{+\frac{L}{2}} (N_{x\theta} u_1) \Big|_{\theta=-\frac{\beta}{2}}^{\theta=+\frac{\beta}{2}} dx \\
 &\quad - \int_{x=-\frac{L}{2}}^{+\frac{L}{2}} \int_{\theta=-\frac{\beta}{2}}^{+\frac{\beta}{2}} \frac{\partial N_{x\theta}}{R \partial \theta} u_1 R d\theta dx
 \end{aligned} \tag{92}$$

eighth term

$$\begin{aligned}
 \int_{x=-\frac{L}{2}}^{+\frac{L}{2}} \int_{\theta=-\frac{\beta}{2}}^{+\frac{\beta}{2}} N_{x\theta} \beta_x \beta_{\theta_1} R d\theta dx &= \int_{x=-\frac{L}{2}}^{+\frac{L}{2}} \int_{\theta=-\frac{\beta}{2}}^{+\frac{\beta}{2}} N_{x\theta} \frac{\partial w}{\partial x} \frac{\partial w_1}{R \partial \theta} R d\theta dx \\
 &= \int_{x=-\frac{L}{2}}^{+\frac{L}{2}} \left(N_{x\theta} \frac{\partial w}{\partial x} w_1 \right) \Big|_{\theta=-\frac{\beta}{2}}^{\theta=+\frac{\beta}{2}} dx \\
 &\quad - \int_{x=-\frac{L}{2}}^{+\frac{L}{2}} \int_{\theta=-\frac{\beta}{2}}^{+\frac{\beta}{2}} \frac{\partial}{R \partial \theta} \left(N_{x\theta} \frac{\partial w}{\partial x} \right) w_1 R d\theta dx
 \end{aligned} \tag{93}$$

ninth term

$$\begin{aligned}
 \int_{x=-\frac{L}{2}}^{+\frac{L}{2}} \int_{\theta=-\frac{\beta}{2}}^{+\frac{\beta}{2}} N_{x\theta} \beta_{\theta} \beta_{x_1} R d\theta dx &= \int_{x=-\frac{L}{2}}^{+\frac{L}{2}} \int_{\theta=-\frac{\beta}{2}}^{+\frac{\beta}{2}} N_{x\theta} \frac{\partial w}{R \partial \theta} \frac{\partial w_1}{\partial x} R d\theta dx \\
 &= \int_{\theta=-\frac{\beta}{2}}^{+\frac{\beta}{2}} \left(N_{x\theta} \frac{\partial w}{R \partial \theta} w_1 \right) \Big|_{x=-\frac{L}{2}}^{x=+\frac{L}{2}} R d\theta \\
 &\quad - \int_{x=-\frac{L}{2}}^{+\frac{L}{2}} \int_{\theta=-\frac{\beta}{2}}^{+\frac{\beta}{2}} \frac{\partial}{\partial x} \left(N_{x\theta} \frac{\partial w}{R \partial \theta} \right) w_1 R d\theta dx
 \end{aligned} \tag{94}$$

tenth term

$$\begin{aligned}
 \int_{x=-\frac{L}{2}}^{+\frac{L}{2}} \int_{\theta=-\frac{\beta}{2}}^{+\frac{\beta}{2}} M_x \frac{\partial \beta_{x_1}}{\partial x} R d\theta dx &= \int_{\theta=-\frac{\beta}{2}}^{+\frac{\beta}{2}} \left(M_x \beta_{x_1} \right) \Big|_{x=-\frac{L}{2}}^{x=+\frac{L}{2}} R d\theta \\
 &\quad - \int_{x=-\frac{L}{2}}^{+\frac{L}{2}} \int_{\theta=-\frac{\beta}{2}}^{+\frac{\beta}{2}} \frac{\partial M_x}{\partial x} \beta_{x_1} R d\theta dx
 \end{aligned} \tag{95}$$

The last term on the right can be expanded further by substituting the definition for β_{x_1} , from eq. (71), into eq. (95), namely,

$$- \int_{x=-\frac{L}{2}}^{+\frac{L}{2}} \int_{\theta=-\frac{\beta}{2}}^{+\frac{\beta}{2}} \frac{\partial M_x}{\partial x} \beta_{x_1} R d\theta dx = \int_{x=-\frac{L}{2}}^{+\frac{L}{2}} \int_{\theta=-\frac{\beta}{2}}^{+\frac{\beta}{2}} \frac{\partial M_x}{\partial x} \frac{\partial w_1}{\partial x} R d\theta dx . \tag{96}$$

Using integration by parts yields

$$\begin{aligned}
 - \int_{x=-\frac{L}{2}}^{+\frac{L}{2}} \int_{\theta=-\frac{\beta}{2}}^{+\frac{\beta}{2}} \frac{\partial M_x}{\partial x} \beta_{x_1} R d\theta dx &= \int_{\theta=-\frac{\beta}{2}}^{+\frac{\beta}{2}} \left(\frac{\partial M_x}{\partial x} w_1 \right) \Big|_{x=-\frac{L}{2}}^{x=+\frac{L}{2}} R d\theta \\
 &\quad - \int_{x=-\frac{L}{2}}^{+\frac{L}{2}} \int_{\theta=-\frac{\beta}{2}}^{+\frac{\beta}{2}} \frac{\partial^2 M_x}{\partial x^2} w_1 R d\theta dx .
 \end{aligned} \tag{97}$$

The tenth term can, therefore, be written as

$$\begin{aligned}
\int_{x=-\frac{L}{2}}^{+\frac{L}{2}} \int_{\theta=-\frac{\beta}{2}}^{+\frac{\beta}{2}} M_x \frac{\partial \beta_{x_1}}{\partial x} R d\theta dx &= - \int_{\theta=-\frac{\beta}{2}}^{+\frac{\beta}{2}} \left(M_x \frac{\partial w_1}{\partial x} \right) \Big|_{x=-\frac{L}{2}}^{x=+\frac{L}{2}} R d\theta \\
&+ \int_{\theta=-\frac{\beta}{2}}^{+\frac{\beta}{2}} \left(\frac{\partial M_x}{\partial x} w_1 \right) \Big|_{x=-\frac{L}{2}}^{x=+\frac{L}{2}} R d\theta \\
&- \int_{x=-\frac{L}{2}}^{+\frac{L}{2}} \int_{\theta=-\frac{\beta}{2}}^{+\frac{\beta}{2}} \frac{\partial^2 M_x}{\partial x^2} w_1 R d\theta dx .
\end{aligned} \tag{98}$$

eleventh term

$$\begin{aligned}
\int_{x=-\frac{L}{2}}^{+\frac{L}{2}} \int_{\theta=-\frac{\beta}{2}}^{+\frac{\beta}{2}} M_\theta \frac{\partial \beta_{\theta_1}}{R \partial \theta} R d\theta dx &= \int_{x=-\frac{L}{2}}^{+\frac{L}{2}} \left(M_\theta \beta_{\theta_1} \right) \Big|_{\theta=-\frac{\beta}{2}}^{\theta=+\frac{\beta}{2}} dx \\
&- \int_{x=-\frac{L}{2}}^{+\frac{L}{2}} \int_{\theta=-\frac{\beta}{2}}^{+\frac{\beta}{2}} \frac{\partial M_\theta}{R \partial \theta} \beta_{\theta_1} R d\theta dx
\end{aligned} \tag{99}$$

This can be expanded further by substituting the definition for β_{θ_1} , from eq. (71), into eq. (99), namely,

$$- \int_{x=-\frac{L}{2}}^{+\frac{L}{2}} \frac{\partial M_\theta}{R \partial \theta} \beta_{\theta_1} R d\theta dx = \int_{x=-\frac{L}{2}}^{+\frac{L}{2}} \frac{\partial M_\theta}{R \partial \theta} \frac{\partial w_1}{R \partial \theta} R d\theta dx . \tag{100}$$

Using integration by parts and substituting into eq. (99), the eleventh term becomes

$$\begin{aligned}
&\int_{x=-\frac{L}{2}}^{+\frac{L}{2}} \int_{\theta=-\frac{\beta}{2}}^{+\frac{\beta}{2}} M_\theta \frac{\partial \beta_{\theta_1}}{R \partial \theta} R d\theta dx \\
&= - \int_{x=-\frac{L}{2}}^{+\frac{L}{2}} \left(M_\theta \frac{\partial w_1}{R \partial \theta} \right) \Big|_{\theta=-\frac{\beta}{2}}^{\theta=+\frac{\beta}{2}} dx + \int_{x=-\frac{L}{2}}^{+\frac{L}{2}} \int_{\theta=-\frac{\beta}{2}}^{+\frac{\beta}{2}} \frac{\partial M_\theta}{R \partial \theta} \frac{\partial w_1}{R \partial \theta} R d\theta dx \\
&= - \int_{x=-\frac{L}{2}}^{+\frac{L}{2}} \left(M_\theta \frac{\partial w_1}{R \partial \theta} \right) \Big|_{\theta=-\frac{\beta}{2}}^{\theta=+\frac{\beta}{2}} dx + \int_{x=-\frac{L}{2}}^{+\frac{L}{2}} \left(\frac{\partial M_\theta}{R \partial \theta} w_1 \right) \Big|_{\theta=-\frac{\beta}{2}}^{\theta=+\frac{\beta}{2}} dx \\
&\quad - \int_{x=-\frac{L}{2}}^{+\frac{L}{2}} \int_{\theta=-\frac{\beta}{2}}^{+\frac{\beta}{2}} \frac{\partial^2 M_\theta}{R^2 \partial \theta^2} w_1 R d\theta dx .
\end{aligned} \tag{101}$$

twelfth term

$$\int_{x=-\frac{L}{2}}^{+\frac{L}{2}} \int_{\theta=-\frac{\beta}{2}}^{+\frac{\beta}{2}} M_{x\theta} \frac{\partial \beta_{\theta_1}}{\partial x} R d\theta dx = \int_{\theta=-\frac{\beta}{2}}^{+\frac{\beta}{2}} \left(M_{x\theta} \beta_{\theta_1} \right) \Big|_{x=-\frac{L}{2}}^{x=+\frac{L}{2}} R d\theta$$

$$- \int_{x=-\frac{L}{2}}^{+\frac{L}{2}} \int_{\theta=-\frac{\beta}{2}}^{+\frac{\beta}{2}} \frac{\partial M_{x\theta}}{\partial x} \beta_{\theta_1} R d\theta dx$$
(102)

Using the definition of β_{θ_1} , in eq. (102),

$$\int_{x=-\frac{L}{2}}^{+\frac{L}{2}} \int_{\theta=-\frac{\beta}{2}}^{+\frac{\beta}{2}} M_{x\theta} \frac{\partial \beta_{\theta_1}}{\partial x} R d\theta dx = - \int_{\theta=-\frac{\beta}{2}}^{+\frac{\beta}{2}} \left(M_{x\theta} \frac{\partial w_1}{R \partial \theta} \right) \Big|_{x=-\frac{L}{2}}^{x=+\frac{L}{2}} R d\theta$$

$$+ \int_{x=-\frac{L}{2}}^{+\frac{L}{2}} \int_{\theta=-\frac{\beta}{2}}^{+\frac{\beta}{2}} \frac{\partial M_{x\theta}}{\partial x} \frac{\partial w_1}{R \partial \theta} R d\theta dx .$$
(103)

Expanding the second term on the right using integration by parts,

$$\int_{x=-\frac{L}{2}}^{+\frac{L}{2}} \int_{\theta=-\frac{\beta}{2}}^{+\frac{\beta}{2}} M_{x\theta} \frac{\partial \beta_{\theta_1}}{\partial x} R d\theta dx = - \int_{\theta=-\frac{\beta}{2}}^{+\frac{\beta}{2}} \left(M_{x\theta} \frac{\partial w_1}{R \partial \theta} \right) \Big|_{x=-\frac{L}{2}}^{x=+\frac{L}{2}} R d\theta$$

$$+ \int_{x=-\frac{L}{2}}^{+\frac{L}{2}} \left(\frac{\partial M_{x\theta}}{\partial x} w_1 \right) \Big|_{\theta=-\frac{\beta}{2}}^{\theta=+\frac{\beta}{2}} dx$$

$$- \int_{x=-\frac{L}{2}}^{+\frac{L}{2}} \int_{\theta=-\frac{\beta}{2}}^{+\frac{\beta}{2}} \frac{\partial^2 M_{x\theta}}{R \partial \theta \partial x} w_1 R d\theta dx .$$
(104)

Applying integration by parts to the first term on the right,

$$\begin{aligned}
& \int_{\theta=-\frac{\beta}{2}}^{+\frac{\beta}{2}} \left(M_{x\theta} \frac{\partial w_1}{R\partial\theta} \right) \Big|_{x=-\frac{L}{2}}^{x=+\frac{L}{2}} R d\theta \\
&= \int_{\theta=-\frac{\beta}{2}}^{+\frac{\beta}{2}} M_{x\theta} \left(+\frac{L}{2}, \theta \right) \frac{\partial w_1}{R\partial\theta} \left(+\frac{L}{2}, \theta \right) R d\theta - \int_{\theta=-\frac{\beta}{2}}^{+\frac{\beta}{2}} M_{x\theta} \left(-\frac{L}{2}, \theta \right) \frac{\partial w_1}{R\partial\theta} \left(-\frac{L}{2}, \theta \right) R d\theta \quad (105) \\
&= \left\{ \left(M_{x\theta} \left(+\frac{L}{2}, \theta \right) w_1 \left(+\frac{L}{2}, \theta \right) \right) \Big|_{\theta=-\frac{\beta}{2}}^{\theta=+\frac{\beta}{2}} - \int_{\theta=-\frac{\beta}{2}}^{+\frac{\beta}{2}} \frac{\partial M_{x\theta}}{R\partial\theta} \left(+\frac{L}{2}, \theta \right) w_1 \left(+\frac{L}{2}, \theta \right) R d\theta \right\} \\
&\quad - \left\{ \left(M_{x\theta} \left(-\frac{L}{2}, \theta \right) w_1 \left(-\frac{L}{2}, \theta \right) \right) \Big|_{\theta=-\frac{\beta}{2}}^{\theta=+\frac{\beta}{2}} - \int_{\theta=-\frac{\beta}{2}}^{+\frac{\beta}{2}} \frac{\partial M_{x\theta}}{R\partial\theta} \left(-\frac{L}{2}, \theta \right) w_1 \left(-\frac{L}{2}, \theta \right) R d\theta \right\} .
\end{aligned}$$

Collecting terms evaluated at $-L/2$ and $+L/2$, the first term on the right in eq. (104)

becomes

$$\begin{aligned}
& \int_{\theta=-\frac{\beta}{2}}^{+\frac{\beta}{2}} \left(M_{x\theta} \frac{\partial w_1}{R\partial\theta} \right) \Big|_{x=-\frac{L}{2}}^{x=+\frac{L}{2}} R d\theta \\
&= \left[M_{x\theta} \left(\frac{L}{2}, \theta \right) w_1 \left(\frac{L}{2}, \theta \right) \right] \Big|_{\theta=-\frac{\beta}{2}}^{\theta=+\frac{\beta}{2}} - \left[M_{x\theta} \left(-\frac{L}{2}, \theta \right) w_1 \left(-\frac{L}{2}, \theta \right) \right] \Big|_{\theta=-\frac{\beta}{2}}^{\theta=+\frac{\beta}{2}} \quad (106) \\
&\quad - \int_{\theta=-\frac{\beta}{2}}^{+\frac{\beta}{2}} \left(\frac{\partial M_{x\theta}}{R\partial\theta} w_1 \right) \Big|_{x=-\frac{L}{2}}^{x=+\frac{L}{2}} R d\theta .
\end{aligned}$$

The twelfth term can thus be written

$$\begin{aligned}
& \int_{x=-\frac{L}{2}}^{+\frac{L}{2}} \int_{\theta=-\frac{\beta}{2}}^{+\frac{\beta}{2}} M_{x\theta} \frac{\partial \beta_{\theta_1}}{\partial x} R d\theta dx \\
&= - \left[M_{x\theta} \left(\frac{L}{2}, \theta \right) w_1 \left(\frac{L}{2}, \theta \right) \right] \Big|_{\theta=-\frac{\beta}{2}}^{\theta=+\frac{\beta}{2}} + \left[M_{x\theta} \left(-\frac{L}{2}, \theta \right) w_1 \left(-\frac{L}{2}, \theta \right) \right] \Big|_{\theta=-\frac{\beta}{2}}^{\theta=+\frac{\beta}{2}} \quad (107) \\
&+ \int_{\theta=-\frac{\beta}{2}}^{+\frac{\beta}{2}} \left[\frac{\partial M_{x\theta}}{R\partial\theta} w_1 \right] \Big|_{x=-\frac{L}{2}}^{x=+\frac{L}{2}} R d\theta + \int_{x=-\frac{L}{2}}^{+\frac{L}{2}} \left[\frac{\partial M_{x\theta}}{\partial x} w_1 \right] \Big|_{\theta=-\frac{\beta}{2}}^{\theta=+\frac{\beta}{2}} dx \\
&- \int_{x=-\frac{L}{2}}^{+\frac{L}{2}} \int_{\theta=-\frac{\beta}{2}}^{+\frac{\beta}{2}} \frac{\partial^2 M_{x\theta}}{R\partial\theta \partial x} w_1 R d\theta dx .
\end{aligned}$$

Expanding the first two terms on the right for future use, the twelfth term becomes

$$\begin{aligned}
& \int_{x=-\frac{L}{2}}^{+\frac{L}{2}} \int_{\theta=-\frac{\beta}{2}}^{+\frac{\beta}{2}} M_{x\theta} \frac{\partial \beta_{\theta_1}}{\partial x} R d\theta dx \\
&= \left[-M_{x\theta} \left(+\frac{L}{2}, +\frac{\beta}{2} \right) w_1 \left(+\frac{L}{2}, +\frac{\beta}{2} \right) + M_{x\theta} \left(+\frac{L}{2}, -\frac{\beta}{2} \right) w_1 \left(+\frac{L}{2}, -\frac{\beta}{2} \right) \right. \\
&\quad \left. + M_{x\theta} \left(-\frac{L}{2}, +\frac{\beta}{2} \right) w_1 \left(-\frac{L}{2}, +\frac{\beta}{2} \right) - M_{x\theta} \left(-\frac{L}{2}, -\frac{\beta}{2} \right) w_1 \left(-\frac{L}{2}, -\frac{\beta}{2} \right) \right] \\
&\quad + \int_{\theta=-\frac{\beta}{2}}^{+\frac{\beta}{2}} \left[\frac{\partial M_{x\theta}}{\partial \theta} w_1 \right]_{x=-\frac{L}{2}}^{x=+\frac{L}{2}} R d\theta + \int_{x=-\frac{L}{2}}^{+\frac{L}{2}} \left[\frac{\partial M_{x\theta}}{\partial x} w_1 \right]_{\theta=-\frac{\beta}{2}}^{\theta=+\frac{\beta}{2}} dx \\
&\quad - \int_{x=-\frac{L}{2}}^{+\frac{L}{2}} \int_{\theta=-\frac{\beta}{2}}^{+\frac{\beta}{2}} \frac{\partial^2 M_{x\theta}}{R \partial \theta \partial x} w_1 R d\theta dx .
\end{aligned} \tag{108}$$

Thirteenth term

$$\begin{aligned}
\int_{x=-\frac{L}{2}}^{+\frac{L}{2}} \int_{\theta=-\frac{\beta}{2}}^{+\frac{\beta}{2}} M_{x\theta} \frac{\partial \beta_{x_1}}{R \partial \theta} R d\theta dx &= \int_{x=-\frac{L}{2}}^{+\frac{L}{2}} [M_{x\theta} \beta_{x_1}]_{\theta=-\frac{\beta}{2}}^{\theta=+\frac{\beta}{2}} dx \\
&\quad - \int_{x=-\frac{L}{2}}^{+\frac{L}{2}} \int_{\theta=-\frac{\beta}{2}}^{+\frac{\beta}{2}} \frac{\partial M_{x\theta}}{R \partial \theta} \beta_{x_1} R d\theta dx
\end{aligned} \tag{109}$$

Substituting the definition of β_{x_1} into the first term on the right above and integrating by

parts:

$$\begin{aligned}
& \int_{x=-\frac{L}{2}}^{+\frac{L}{2}} [M_{x\theta} \beta_{x_1}]_{\theta=-\frac{\beta}{2}}^{\theta=+\frac{\beta}{2}} dx = - \int_{x=-\frac{L}{2}}^{+\frac{L}{2}} \left[M_{x\theta} \frac{\partial w_1}{\partial x} \right]_{\theta=-\frac{\beta}{2}}^{\theta=+\frac{\beta}{2}} dx \\
&= - \int_{x=-\frac{L}{2}}^{+\frac{L}{2}} \left[M_{x\theta} \left(x, +\frac{\beta}{2} \right) \frac{\partial w_1}{\partial x} \left(x, +\frac{\beta}{2} \right) \right] dx + \int_{x=-\frac{L}{2}}^{+\frac{L}{2}} \left[M_{x\theta} \left(x, -\frac{\beta}{2} \right) \frac{\partial w_1}{\partial x} \left(x, -\frac{\beta}{2} \right) \right] dx \\
&= - \left[M_{x\theta} \left(x, +\frac{\beta}{2} \right) w_1 \left(x, +\frac{\beta}{2} \right) \right]_{x=-\frac{L}{2}}^{x=+\frac{L}{2}} + \int_{x=-\frac{L}{2}}^{+\frac{L}{2}} \left[\frac{\partial M_{x\theta}}{\partial x} w_1 \right]_{\theta=-\frac{\beta}{2}}^{\theta=+\frac{\beta}{2}} dx \\
&\quad + \left[M_{x\theta} \left(x, -\frac{\beta}{2} \right) w_1 \left(x, -\frac{\beta}{2} \right) \right]_{x=-\frac{L}{2}}^{x=+\frac{L}{2}} - \int_{x=-\frac{L}{2}}^{+\frac{L}{2}} \left[\frac{\partial M_{x\theta}}{\partial x} w_1 \right]_{\theta=-\frac{\beta}{2}}^{\theta=+\frac{\beta}{2}} dx ,
\end{aligned} \tag{110}$$

or

$$\begin{aligned}
& \int_{x=-\frac{L}{2}}^{+\frac{L}{2}} \left[M_{x\theta} \beta_{x_1} \right]_{\theta=-\frac{\beta}{2}}^{\theta=+\frac{\beta}{2}} dx = \\
& - \left[M_{x\theta} \left(x, +\frac{\beta}{2} \right) w_1 \left(x, +\frac{\beta}{2} \right) \right]_{x=-\frac{L}{2}}^{x=+\frac{L}{2}} + \left[M_{x\theta} \left(x, -\frac{\beta}{2} \right) w_1 \left(x, -\frac{\beta}{2} \right) \right]_{x=-\frac{L}{2}}^{x=+\frac{L}{2}} \\
& + \int_{x=-\frac{L}{2}}^{+\frac{L}{2}} \left[\frac{\partial M_{x\theta}}{\partial x} w_1 \right]_{\theta=-\frac{\beta}{2}}^{\theta=+\frac{\beta}{2}} dx .
\end{aligned} \tag{111}$$

Substituting the definition of β_{x_1} into the second term on the right of eq. (109),

$$\begin{aligned}
& - \int_{x=-\frac{L}{2}}^{+\frac{L}{2}} \int_{\theta=-\frac{\beta}{2}}^{+\frac{\beta}{2}} \frac{\partial M_{x\theta}}{R\partial\theta} \beta_{x_1} R d\theta dx = \int_{x=-\frac{L}{2}}^{+\frac{L}{2}} \int_{\theta=-\frac{\beta}{2}}^{+\frac{\beta}{2}} \frac{\partial M_{x\theta}}{R\partial\theta} \frac{\partial w_1}{\partial x} R d\theta dx \\
& = \int_{\theta=-\frac{\beta}{2}}^{+\frac{\beta}{2}} \left[\frac{\partial M_{x\theta}}{R\partial\theta} w_1 \right]_{x=-\frac{L}{2}}^{x=+\frac{L}{2}} R d\theta - \int_{x=-\frac{L}{2}}^{+\frac{L}{2}} \int_{\theta=-\frac{\beta}{2}}^{+\frac{\beta}{2}} \frac{\partial^2 M_{x\theta}}{R\partial\theta \partial x} w_1 R d\theta dx .
\end{aligned} \tag{112}$$

Substituting the results of eq. (111) and eq. (112) into eq. (109), the thirteenth term can be written as

$$\begin{aligned}
& \int_{x=-\frac{L}{2}}^{+\frac{L}{2}} \int_{\theta=-\frac{\beta}{2}}^{+\frac{\beta}{2}} M_{x\theta} \frac{\partial \beta_{x_1}}{R\partial\theta} R d\theta dx = \\
& - \left[M_{x\theta} \left(x, +\frac{\beta}{2} \right) w_1 \left(x, +\frac{\beta}{2} \right) \right]_{x=-\frac{L}{2}}^{x=+\frac{L}{2}} + \left[M_{x\theta} \left(x, -\frac{\beta}{2} \right) w_1 \left(x, -\frac{\beta}{2} \right) \right]_{x=-\frac{L}{2}}^{x=+\frac{L}{2}} \\
& + \int_{x=-\frac{L}{2}}^{+\frac{L}{2}} \left[\frac{\partial M_{x\theta}}{\partial x} w_1 \right]_{\theta=-\frac{\beta}{2}}^{\theta=+\frac{\beta}{2}} dx + \int_{\theta=-\frac{\beta}{2}}^{+\frac{\beta}{2}} \left[\frac{\partial M_{x\theta}}{R\partial\theta} w_1 \right]_{x=-\frac{L}{2}}^{x=+\frac{L}{2}} R d\theta \\
& - \int_{x=-\frac{L}{2}}^{+\frac{L}{2}} \int_{\theta=-\frac{\beta}{2}}^{+\frac{\beta}{2}} \frac{\partial^2 M_{x\theta}}{R\partial\theta \partial x} w_1 R d\theta dx .
\end{aligned} \tag{113}$$

Expanding the first two terms on the right for future use,

$$\begin{aligned}
& \int_{x=-\frac{L}{2}}^{+\frac{L}{2}} \int_{\theta=-\frac{\beta}{2}}^{+\frac{\beta}{2}} M_{x\theta} \frac{\partial \beta_{x_1}}{R \partial \theta} R d\theta dx = \\
& + \left[-M_{x\theta} \left(+\frac{L}{2}, +\frac{\beta}{2} \right) w_1 \left(+\frac{L}{2}, +\frac{\beta}{2} \right) + M_{x\theta} \left(-\frac{L}{2}, +\frac{\beta}{2} \right) w_1 \left(-\frac{L}{2}, +\frac{\beta}{2} \right) \right. \\
& \left. + M_{x\theta} \left(+\frac{L}{2}, -\frac{\beta}{2} \right) w_1 \left(+\frac{L}{2}, -\frac{\beta}{2} \right) - M_{x\theta} \left(-\frac{L}{2}, -\frac{\beta}{2} \right) w_1 \left(-\frac{L}{2}, -\frac{\beta}{2} \right) \right] \\
& + \int_{x=-\frac{L}{2}}^{+\frac{L}{2}} \left[\frac{\partial M_{x\theta}}{\partial x} w_1 \right]_{\theta=-\frac{\beta}{2}}^{\theta=+\frac{\beta}{2}} dx + \int_{\theta=-\frac{\beta}{2}}^{+\frac{\beta}{2}} \left[\frac{\partial M_{x\theta}}{R \partial \theta} w_1 \right]_{x=-\frac{L}{2}}^{x=+\frac{L}{2}} R d\theta \\
& - \int_{x=-\frac{L}{2}}^{+\frac{L}{2}} \int_{\theta=-\frac{\beta}{2}}^{+\frac{\beta}{2}} \frac{\partial^2 M_{x\theta}}{R \partial \theta \partial x} w_1 R d\theta dx .
\end{aligned} \tag{114}$$

The terms involving $M_{x\theta}^-$, $M_{x\theta}^+$, $M_{\theta x}^-$ and $M_{\theta x}^+$ in the line integrals in eq. (86) must be expanded in terms of w_1 and integrated by parts also. These two terms follow.

Term involving $M_{x\theta}^-$ and $M_{x\theta}^+$ in line integral from $\theta = -\beta/2$ to $\theta = +\beta/2$:

Substituting the definition of β_{θ_1} into this term and integrating by parts,

$$\begin{aligned}
& \int_{\theta=-\frac{\beta}{2}}^{+\frac{\beta}{2}} \left[M_{x\theta}^-(\theta) \beta_{\theta_1} \left(-\frac{L}{2}, \theta \right) - M_{x\theta}^+(\theta) \beta_{\theta_1} \left(+\frac{L}{2}, \theta \right) \right] R d\theta \\
& = - \int_{\theta=-\frac{\beta}{2}}^{+\frac{\beta}{2}} M_{x\theta}^-(\theta) \frac{\partial w_1}{R \partial \theta} \left(-\frac{L}{2}, \theta \right) R d\theta + \int_{\theta=-\frac{\beta}{2}}^{+\frac{\beta}{2}} M_{x\theta}^+(\theta) \frac{\partial w_1}{R \partial \theta} \left(+\frac{L}{2}, \theta \right) R d\theta \\
& = - \left[M_{x\theta}^-(\theta) w_1 \left(-\frac{L}{2}, \theta \right) \right]_{\theta=-\frac{\beta}{2}}^{\theta=+\frac{\beta}{2}} + \int_{\theta=-\frac{\beta}{2}}^{+\frac{\beta}{2}} \frac{\partial M_{x\theta}^-(\theta)}{R \partial \theta} w_1 \left(-\frac{L}{2}, \theta \right) R d\theta \\
& + \left[M_{x\theta}^+(\theta) w_1 \left(+\frac{L}{2}, \theta \right) \right]_{\theta=-\frac{\beta}{2}}^{\theta=+\frac{\beta}{2}} - \int_{\theta=-\frac{\beta}{2}}^{+\frac{\beta}{2}} \frac{\partial M_{x\theta}^+(\theta)}{R \partial \theta} w_1 \left(+\frac{L}{2}, \theta \right) R d\theta .
\end{aligned} \tag{115}$$

Expanding the first and third terms on the right-hand side,

$$\begin{aligned}
& \int_{\theta=-\frac{\beta}{2}}^{+\frac{\beta}{2}} \left[M_{x\theta}^-(\theta) \beta_{\theta_1} \left(-\frac{L}{2}, \theta \right) - M_{x\theta}^+(\theta) \beta_{\theta_1} \left(+\frac{L}{2}, \theta \right) \right] R d\theta \\
&= \left[-M_{x\theta}^- \left(+\frac{\beta}{2} \right) w_1 \left(-\frac{L}{2}, +\frac{\beta}{2} \right) + M_{x\theta}^- \left(-\frac{\beta}{2} \right) w_1 \left(-\frac{L}{2}, -\frac{\beta}{2} \right) \right. \\
&\quad \left. + M_{x\theta}^+ \left(+\frac{\beta}{2} \right) w_1 \left(+\frac{L}{2}, +\frac{\beta}{2} \right) - M_{x\theta}^+ \left(-\frac{\beta}{2} \right) w_1 \left(+\frac{L}{2}, -\frac{\beta}{2} \right) \right] \\
&\quad + \int_{\theta=-\frac{\beta}{2}}^{+\frac{\beta}{2}} \frac{\partial M_{x\theta}^-(\theta)}{R \partial \theta} w_1 \left(-\frac{L}{2}, \theta \right) R d\theta - \int_{\theta=-\frac{\beta}{2}}^{+\frac{\beta}{2}} \frac{\partial M_{x\theta}^+(\theta)}{R \partial \theta} w_1 \left(+\frac{L}{2}, \theta \right) R d\theta .
\end{aligned} \tag{116}$$

Term involving $M_{\theta x}^-$ and $M_{\theta x}^+$ in line integral from $x=-L/2$ to $x=+L/2$:

Substituting the definition of β_{x_1} into this term and integrating by parts,

$$\begin{aligned}
& \int_{x=-\frac{L}{2}}^{+\frac{L}{2}} \left[M_{\theta x}^-(x) \beta_{x_1} \left(x, -\frac{\beta}{2} \right) - M_{\theta x}^+(x) \beta_{x_1} \left(x, +\frac{\beta}{2} \right) \right] dx \\
&= - \int_{x=-\frac{L}{2}}^{+\frac{L}{2}} M_{\theta x}^-(x) \frac{\partial w_1}{\partial x} \left(x, -\frac{\beta}{2} \right) dx + \int_{x=-\frac{L}{2}}^{+\frac{L}{2}} M_{\theta x}^+(x) \frac{\partial w_1}{\partial x} \left(x, +\frac{\beta}{2} \right) dx \\
&= - \left[M_{\theta x}^-(x) w_1 \left(x, -\frac{\beta}{2} \right) \right]_{x=-\frac{L}{2}}^{x=+\frac{L}{2}} + \int_{x=-\frac{L}{2}}^{+\frac{L}{2}} \frac{\partial M_{\theta x}^-(x)}{\partial x} w_1 \left(x, -\frac{\beta}{2} \right) dx \\
&\quad + \left[M_{\theta x}^+(x) w_1 \left(x, +\frac{\beta}{2} \right) \right]_{x=-\frac{L}{2}}^{x=+\frac{L}{2}} - \int_{x=-\frac{L}{2}}^{+\frac{L}{2}} \frac{\partial M_{\theta x}^+(x)}{\partial x} w_1 \left(x, +\frac{\beta}{2} \right) dx .
\end{aligned} \tag{117}$$

Expanding the first and third terms on the right-hand side,

$$\begin{aligned}
& \int_{x=-\frac{L}{2}}^{+\frac{L}{2}} \left[M_{\theta x}^-(x) \beta_{x_1} \left(x, -\frac{\beta}{2} \right) - M_{\theta x}^+(x) \beta_{x_1} \left(x, +\frac{\beta}{2} \right) \right] dx \\
&= \left[-M_{\theta x}^- \left(+\frac{L}{2} \right) w_1 \left(+\frac{L}{2}, -\frac{\beta}{2} \right) + M_{\theta x}^- \left(-\frac{L}{2} \right) w_1 \left(-\frac{L}{2}, -\frac{\beta}{2} \right) \right. \\
&\quad \left. + M_{\theta x}^+ \left(+\frac{L}{2} \right) w_1 \left(+\frac{L}{2}, +\frac{\beta}{2} \right) - M_{\theta x}^+ \left(-\frac{L}{2} \right) w_1 \left(-\frac{L}{2}, +\frac{\beta}{2} \right) \right] \\
&\quad + \int_{x=-\frac{L}{2}}^{+\frac{L}{2}} \frac{\partial M_{\theta x}^-(x)}{\partial x} w_1 \left(x, -\frac{\beta}{2} \right) dx - \int_{x=-\frac{L}{2}}^{+\frac{L}{2}} \frac{\partial M_{\theta x}^+(x)}{\partial x} w_1 \left(x, +\frac{\beta}{2} \right) dx .
\end{aligned} \tag{118}$$

Substituting eqs. (87), (88), (89), (90), (91), (92), (93), (94), (98), (101), (108), (114), (116), and (118) into the expression for the first variation, eq. (86), and combining the boundary terms (i.e., integrals with respect to θ and integrals with respect to x), results in

$$\begin{aligned}
\Pi_1 = & \int_{x=-\frac{L}{2}}^{+\frac{L}{2}} \int_{\theta=-\frac{\beta}{2}}^{+\frac{\beta}{2}} \left[\left\{ -\frac{\partial N_x}{\partial x} - \frac{\partial N_{x\theta}}{R\partial\theta} \right\} u_1 + \left\{ -\frac{\partial N_\theta}{R\partial\theta} - \frac{\partial N_{x\theta}}{\partial x} \right\} v_1 \right. \\
& + \left. \left\{ -\frac{\partial}{\partial x} \left(N_x \frac{\partial w}{\partial x} \right) + \frac{N_\theta}{R} - \frac{\partial}{R\partial\theta} \left(N_\theta \frac{\partial w}{R\partial\theta} \right) - \frac{\partial}{R\partial\theta} \left(N_{x\theta} \frac{\partial w}{\partial x} \right) - \frac{\partial}{\partial x} \left(N_{x\theta} \frac{\partial w}{R\partial\theta} \right) \right. \right. \\
& \quad \left. \left. - \frac{\partial^2 M_x}{\partial x^2} - \frac{\partial^2 M_\theta}{R^2 \partial \theta^2} - 2 \frac{\partial^2 M_{x\theta}}{R\partial\theta \partial x} - q \right\} w_1 \right] R d\theta dx \\
& + \int_{\theta=-\frac{\beta}{2}}^{+\frac{\beta}{2}} \left[\left(N_x \left(+\frac{L}{2}, \theta \right) - N_x^+(\theta) \right) u_1 \left(+\frac{L}{2}, \theta \right) - \left(N_x \left(-\frac{L}{2}, \theta \right) - N_x^-(\theta) \right) u_1 \left(-\frac{L}{2}, \theta \right) \right. \\
& \quad + \left(N_{x\theta} \left(+\frac{L}{2}, \theta \right) - N_{x\theta}^+(\theta) \right) v_1 \left(+\frac{L}{2}, \theta \right) - \left(N_{x\theta} \left(-\frac{L}{2}, \theta \right) - N_{x\theta}^-(\theta) \right) v_1 \left(-\frac{L}{2}, \theta \right) \\
& \quad + \left. \left(N_x \frac{\partial w}{\partial x} + N_{x\theta} \frac{\partial w}{R\partial\theta} + \frac{\partial M_x}{\partial x} + 2 \frac{\partial M_{x\theta}}{R\partial\theta} - Q_x^+ - \frac{\partial M_{x\theta}^+}{R\partial\theta} \right) \right|_{x=+\frac{L}{2}} w_1 \left(+\frac{L}{2}, \theta \right) \\
& \quad - \left. \left(N_x \frac{\partial w}{\partial x} + N_{x\theta} \frac{\partial w}{R\partial\theta} + \frac{\partial M_x}{\partial x} + 2 \frac{\partial M_{x\theta}}{R\partial\theta} - Q_x^- - \frac{\partial M_{x\theta}^-}{R\partial\theta} \right) \right|_{x=-\frac{L}{2}} w_1 \left(-\frac{L}{2}, \theta \right) \\
& \quad - \left. \left(M_x \left(+\frac{L}{2}, \theta \right) - M_x^+(\theta) \right) \frac{\partial w_1}{\partial x} \left(+\frac{L}{2}, \theta \right) + \left(M_x \left(-\frac{L}{2}, \theta \right) - M_x^-(\theta) \right) \frac{\partial w_1}{\partial x} \left(-\frac{L}{2}, \theta \right) \right] R d\theta \\
& + \int_{x=-\frac{L}{2}}^{+\frac{L}{2}} \left[\left(N_{x\theta} \left(x, +\frac{\beta}{2} \right) - N_{\theta x}^+(x) \right) u_1 \left(x, +\frac{\beta}{2} \right) - \left(N_{x\theta} \left(x, -\frac{\beta}{2} \right) - N_{\theta x}^-(x) \right) u_1 \left(x, -\frac{\beta}{2} \right) \right. \\
& \quad + \left(N_\theta \left(x, +\frac{\beta}{2} \right) - N_\theta^+(x) \right) v_1 \left(x, +\frac{\beta}{2} \right) - \left(N_\theta \left(x, -\frac{\beta}{2} \right) - N_\theta^-(x) \right) v_1 \left(x, -\frac{\beta}{2} \right) \\
& \quad + \left. \left(N_\theta \frac{\partial w}{R\partial\theta} + N_{x\theta} \frac{\partial w}{\partial x} + \frac{\partial M_\theta}{R\partial\theta} + 2 \frac{\partial M_{x\theta}}{\partial x} - Q_\theta^+ - \frac{\partial M_{\theta x}^+}{\partial x} \right) \right|_{\theta=+\frac{\beta}{2}} w_1 \left(x, +\frac{\beta}{2} \right) \\
& \quad - \left. \left(N_\theta \frac{\partial w}{R\partial\theta} + N_{x\theta} \frac{\partial w}{\partial x} + \frac{\partial M_\theta}{R\partial\theta} + 2 \frac{\partial M_{x\theta}}{\partial x} - Q_\theta^- - \frac{\partial M_{\theta x}^-}{\partial x} \right) \right|_{\theta=-\frac{\beta}{2}} w_1 \left(x, -\frac{\beta}{2} \right) \\
& \quad - \left. \left(M_\theta \left(x, +\frac{\beta}{2} \right) - M_\theta^+(x) \right) \frac{\partial w_1}{R\partial\theta} \left(x, +\frac{\beta}{2} \right) + \left(M_\theta \left(x, -\frac{\beta}{2} \right) - M_\theta^-(x) \right) \frac{\partial w_1}{R\partial\theta} \left(x, -\frac{\beta}{2} \right) \right] dx \\
& - \left[2M_{x\theta} \left(+\frac{L}{2}, +\frac{\beta}{2} \right) - M_{x\theta}^+ \left(+\frac{\beta}{2} \right) - M_{\theta x}^+ \left(+\frac{L}{2} \right) \right] w_1 \left(+\frac{L}{2}, +\frac{\beta}{2} \right) \\
& + \left[2M_{x\theta} \left(+\frac{L}{2}, -\frac{\beta}{2} \right) - M_{x\theta}^+ \left(-\frac{\beta}{2} \right) - M_{\theta x}^- \left(+\frac{L}{2} \right) \right] w_1 \left(+\frac{L}{2}, -\frac{\beta}{2} \right) \\
& + \left[2M_{x\theta} \left(-\frac{L}{2}, +\frac{\beta}{2} \right) - M_{x\theta}^- \left(+\frac{\beta}{2} \right) - M_{\theta x}^+ \left(-\frac{L}{2} \right) \right] w_1 \left(-\frac{L}{2}, +\frac{\beta}{2} \right) \\
& - \left[2M_{x\theta} \left(-\frac{L}{2}, -\frac{\beta}{2} \right) - M_{x\theta}^- \left(-\frac{\beta}{2} \right) - M_{\theta x}^- \left(-\frac{L}{2} \right) \right] w_1 \left(-\frac{L}{2}, -\frac{\beta}{2} \right) .
\end{aligned} \tag{119}$$

For the first variation to be zero, each term which is a product involving an increment in the displacement, in each of the integrals, must be zero. The Euler equations come from the two-dimensional integral and the boundary conditions come from the line integrals along the x and θ edges. Thus, the three governing equilibrium equations are

$$\frac{\partial N_x}{\partial x} + \frac{\partial N_{x\theta}}{R\partial\theta} = 0 \quad (120a)$$

$$\frac{\partial N_{x\theta}}{\partial x} + \frac{\partial N_\theta}{R\partial\theta} = 0 \quad (120b)$$

$$\begin{aligned} & \frac{\partial^2 M_x}{\partial x^2} + 2 \frac{\partial^2 M_{x\theta}}{R\partial\theta\partial x} + \frac{\partial^2 M_\theta}{R^2\partial\theta^2} + \frac{\partial}{\partial x} \left(N_x \frac{\partial w}{\partial x} \right) \\ & + \frac{\partial}{R\partial\theta} \left(N_\theta \frac{\partial w}{R\partial\theta} \right) + \frac{\partial}{R\partial\theta} \left(N_{x\theta} \frac{\partial w}{\partial x} \right) + \frac{\partial}{\partial x} \left(N_{x\theta} \frac{\partial w}{R\partial\theta} \right) \\ & - \frac{N_\theta}{R} + q = 0 \quad . \end{aligned} \quad (120c)$$

Using the first two equations in the third one, the three equations can be written as

$$\frac{\partial N_x}{\partial x} + \frac{\partial N_{x\theta}}{R\partial\theta} = 0 \quad (121a)$$

$$\frac{\partial N_{x\theta}}{\partial x} + \frac{\partial N_\theta}{R\partial\theta} = 0 \quad (121b)$$

$$\begin{aligned} & \frac{\partial^2 M_x}{\partial x^2} + 2 \frac{\partial^2 M_{x\theta}}{R\partial\theta\partial x} + \frac{\partial^2 M_\theta}{R^2\partial\theta^2} + N_x \frac{\partial^2 w}{\partial x^2} \\ & + 2 N_{x\theta} \frac{\partial^2 w}{R\partial\theta\partial x} + N_\theta \frac{\partial^2 w}{R^2\partial\theta^2} - \frac{N_\theta}{R} + q = 0 \quad . \end{aligned} \quad (121c)$$

The variationally consistent boundary conditions at the $x=-L/2$ and $x=+L/2$ edges of

the cylindrical panel are

along the $x = -L/2$ edge:

$$\begin{aligned}
 \text{i) } N_x &= N_x^- , & \text{or } u &\text{ must be specified,} \\
 \text{ii) } N_{x\theta} &= N_{x\theta}^- , & \text{or } v &\text{ must be specified,} \\
 \text{iii) } N_x \frac{\partial w}{\partial x} + N_{x\theta} \frac{\partial w}{R\partial\theta} + \frac{\partial M_x}{\partial x} + 2 \frac{\partial M_{x\theta}}{R\partial\theta} &= Q_x^- + \frac{\partial M_{x\theta}^-}{R\partial\theta} , & (122a) \\
 & \text{or } w &\text{ must be specified,} \\
 \text{iv) } M_x &= M_x^- , & \text{or } \frac{\partial w}{\partial x} &\text{ must be specified.}
 \end{aligned}$$

along the $x = +L/2$ edge:

$$\begin{aligned}
 \text{i) } N_x &= N_x^+ , & \text{or } u &\text{ must be specified,} \\
 \text{ii) } N_{x\theta} &= N_{x\theta}^+ , & \text{or } v &\text{ must be specified,} \\
 \text{iii) } N_x \frac{\partial w}{\partial x} + N_{x\theta} \frac{\partial w}{R\partial\theta} + \frac{\partial M_x}{\partial x} + 2 \frac{\partial M_{x\theta}}{R\partial\theta} &= Q_x^+ + \frac{\partial M_{x\theta}^+}{R\partial\theta} , & (122b) \\
 & \text{or } w &\text{ must be specified,} \\
 \text{iv) } M_x &= M_x^+ , & \text{or } \frac{\partial w}{\partial x} &\text{ must be specified.}
 \end{aligned}$$

The variationally consistent boundary conditions at the $\theta = -\beta/2$ and $\theta = +\beta/2$ edges are:

along the $\theta = -\beta/2$ edge:

$$\begin{aligned}
 \text{i) } N_{\theta x} &= N_{\theta x}^- , & \text{or } u &\text{ must be specified,} \\
 \text{ii) } N_\theta &= N_\theta^- , & \text{or } v &\text{ must be specified,} \\
 \text{iii) } N_\theta \frac{\partial w}{R\partial\theta} + N_{x\theta} \frac{\partial w}{\partial x} + \frac{\partial M_\theta}{R\partial\theta} + 2 \frac{\partial M_{x\theta}}{\partial x} &= Q_\theta^- + \frac{\partial M_{\theta x}^-}{\partial x} , & (123a) \\
 & \text{or } w &\text{ must be specified,} \\
 \text{iv) } M_\theta &= M_\theta^- , & \text{or } \frac{\partial w}{\partial x} &\text{ must be specified.}
 \end{aligned}$$

along the $\theta = +\beta/2$ edge:

$$\begin{aligned}
 \text{i) } N_{\theta x} &= N_{\theta x}^+, & \text{or } u &\text{ must be specified,} \\
 \text{ii) } N_{\theta} &= N_{\theta}^+, & \text{or } v &\text{ must be specified,} \\
 \text{iii) } N_{\theta} \frac{\partial w}{R \partial \theta} + N_{x\theta} \frac{\partial w}{\partial x} + \frac{\partial M_{\theta}}{R \partial \theta} + 2 \frac{\partial M_{x\theta}}{\partial x} &= Q_{\theta}^+ + \frac{\partial M_{\theta x}^+}{\partial x}, & (123b) \\
 & & \text{or } w &\text{ must be specified,} \\
 \text{iv) } M_{\theta} &= M_{\theta}^+, & \text{or } \frac{\partial w}{\partial x} &\text{ must be specified.}
 \end{aligned}$$

Note that the expression for the first variation of the total potential energy also involves four non-integral terms. These are "corner" conditions. Therefore,

at the corner ($x = +L/2, \theta = +\beta/2$):

$$2M_{x\theta} = M_{x\theta}^+ + M_{\theta x}^+, \quad \text{or } w \text{ must be specified,} \quad (124a)$$

at the corner ($x = +L/2, \theta = -\beta/2$):

$$2M_{x\theta} = M_{x\theta}^+ + M_{\theta x}^-, \quad \text{or } w \text{ must be specified,} \quad (124b)$$

at the corner ($x = -L/2, \theta = +\beta/2$):

$$2M_{x\theta} = M_{x\theta}^- + M_{\theta x}^+, \quad \text{or } w \text{ must be specified,} \quad (124c)$$

at the corner ($x = -L/2, \theta = -\beta/2$):

$$2M_{x\theta} = M_{x\theta}^- + M_{\theta x}^-, \quad \text{or } w \text{ must be specified.} \quad (124d)$$

At this point, the problem can be specialized to that of a complete cylinder, that is,

$$\beta = 2\pi \quad \rightarrow \quad -\frac{\beta}{2} = -\pi, \quad +\frac{\beta}{2} = +\pi. \quad (125)$$

Because the cylinder is complete, the response is a continuous function along $\theta = \pi$, and

the displacements at the $-\beta/2$ and $+\beta/2$ "edges" are unique and therefore can be interpreted as being specified. Equations (123) do not have to be explicitly enforced. This also holds for the "corner" conditions. However, a by-product of the eqs. (123) is an expression for the out-of-plane stress resultant, Q_θ , which could be used as a check of a calculation of the interlaminar stress component $\tau_{\theta r}$. Specifically,

$$Q_\theta = N_\theta \frac{\partial w}{R \partial \theta} + N_{x\theta} \frac{\partial w}{\partial x} + \frac{\partial M_\theta}{R \partial \theta} + \frac{\partial M_{x\theta}}{\partial x} . \quad (126a)$$

This shear stress resultant compliments the other out-of-plane shear stress resultant, Q_x , which is given by

$$Q_x = N_x \frac{\partial w}{\partial x} + N_{x\theta} \frac{\partial w}{R \partial \theta} + \frac{\partial M_x}{\partial x} + \frac{\partial M_{x\theta}}{R \partial \theta} . \quad (126b)$$

This out-of-plane stress resultant will be used as a check of a calculation of the interlaminar stress component τ_{xr} in chapter VI.

Attention now turns to specializing the equations for the condition of axisymmetry.

III. SIMPLIFICATION OF THE EQUILIBRIUM EQUATIONS DUE TO THE CONDITION OF AXISYMMETRY

The derivations which follow focus on complete cylinders (i.e., $\beta = 2\pi$) subjected to an axisymmetric loading and responding in an axisymmetric manner. In particular, the loading considered will be applied axisymmetric end loads $N_x^+(\theta) = N_x^+$ and $N_x^-(\theta) = N_x^-$. Therefore, the relations of the previous chapter will be simplified by

$$\frac{\partial(\)}{\partial\theta} = 0 \text{ and } \frac{\partial(\)}{\partial x} = \frac{d(\)}{dx}, \quad (127)$$

() being any response quantity. Under these conditions the kinematic relations simplify considerably. Specifically, eqs. (9) and (13) become

$$\begin{aligned} \beta_x^o &= -\frac{dw^o}{dx}; \quad \beta_\theta^o = 0 \\ \epsilon_x^o &= \frac{du^o}{dx} + \frac{1}{2}\beta_x^{o^2}; \quad \epsilon_\theta^o = \frac{w^o}{R}; \quad \gamma_{x\theta}^o = \frac{dv^o}{dx} \\ \kappa_x^o &= \frac{d\beta_x^o}{dx}; \quad \kappa_\theta^o = 0; \quad \kappa_{x\theta}^o = 0. \end{aligned} \quad (128)$$

The equilibrium equations, eq. (121) simplify to:

$$\frac{dN_x}{dx} = 0 \quad (129a)$$

$$\frac{dN_{x\theta}}{dx} = 0 \quad (129b)$$

$$\frac{d^2 M_x}{dx^2} + N_x \frac{d^2 w^o}{dx^2} - \frac{N_\theta}{R} = 0 . \quad (129c)$$

The accompanying boundary conditions at the $x=-L/2$ and $x=+L/2$ boundaries are

at $x = -L/2$

$$\begin{aligned} \text{i) } N_x &= N_x^- , & \text{or } u &\text{ must be specified,} \\ \text{ii) } N_{x\theta} &= N_{x\theta}^- , & \text{or } v &\text{ must be specified,} \\ \text{iii) } \frac{dM_x}{dx} + N_x \frac{dw}{dx} &= Q_x^- , & \text{or } w &\text{ must be specified,} \\ \text{iv) } M_x &= M_x^- , & \text{or } \frac{dw}{dx} &\text{ must be specified.} \end{aligned} \quad (130a)$$

at $x = +L/2$

$$\begin{aligned} \text{i) } N_x &= N_x^+ , & \text{or } u &\text{ must be specified,} \\ \text{ii) } N_{x\theta} &= N_{x\theta}^+ , & \text{or } v &\text{ must be specified,} \\ \text{iii) } \frac{dM_x}{dx} + N_x \frac{dw}{dx} &= Q_x^+ , & \text{or } w &\text{ must be specified,} \\ \text{iv) } M_x &= M_x^+ , & \text{or } \frac{dw}{dx} &\text{ must be specified.} \end{aligned} \quad (130b)$$

Note that for a complete cylinder, the boundary conditions at $\theta=-\beta/2$ and $\theta=+\beta/2$ are meaningless. Equations (129) and (130) will be the focus of the remainder of the this chapter and the following chapter. In the next section, the solution of these equations for the case of a known axial end load will be derived.

A. Solution of Equations for the Case of Axial End Load

The first equilibrium equation, eq. (129a), integrates to

$$N_x = \text{constant} . \quad (131)$$

Since the axial load is known at the ends of the cylinder, this constant is the applied end load. It will be referred to simply as N . The second equation, eq. (129b), integrates to

$$N_{x\theta} = \text{another constant} . \quad (132)$$

In this study there will be no external torsional load applied explicitly to the ends of the cylinder. Rather, the tangential displacement of the end will be specified. Enforcement of the tangential end displacement may well require a torsional load, S , on the end. This torsional load will be solved for as part of the analysis. Thus, as a result of eq. (132),

$$N_{x\theta} = S \text{ (a constant)} . \quad (133)$$

To solve the third equilibrium equation, eq. (129c), it is convenient to express all quantities in that equation in terms of the midplane displacement w^o . Here, the stress resultants, eq. (43), with the preloading condition being thermal according to eq. (45), will be used. Only cylinders which are balanced, i.e., those with A_{16} , A_{26} , and $N_{x\theta}^T$ equal to zero, will be considered. This is the situation of many laminates of practical interest. Such laminates are called balanced laminates. Expanding N_x , N_θ , $N_{x\theta}$, and M_x in terms of w^o , ϵ_x^o , and $\gamma_{x\theta}^o$ results in

$$\begin{aligned}
N_x &= A_{11}\epsilon_x^\circ + A_{12}\frac{w^\circ}{R} - B_{11}\frac{d^2w^\circ}{dx^2} - N_x^T = N \\
N_\theta &= A_{12}\epsilon_x^\circ + A_{22}\frac{w^\circ}{R} - B_{12}\frac{d^2w^\circ}{dx^2} - N_\theta^T \\
N_{x\theta} &= A_{66}\gamma_{x\theta}^\circ - B_{16}\frac{d^2w^\circ}{dx^2} = S \\
M_x &= B_{11}\epsilon_x^\circ + B_{12}\frac{w^\circ}{R} + B_{16}\gamma_{x\theta}^\circ - D_{11}\frac{d^2w^\circ}{dx^2} - M_x^T .
\end{aligned} \tag{134}$$

Solving the equation for N_x for ϵ_x° , and the equation for $N_{x\theta}$ for $\gamma_{x\theta}^\circ$ yields

$$\epsilon_x^\circ = \frac{1}{A_{11}} \left(N + N_x^T - A_{12}\frac{w^\circ}{R} + B_{11}\frac{d^2w^\circ}{dx^2} \right), \tag{135a}$$

and

$$\gamma_{x\theta}^\circ = \left(\frac{B_{16}}{A_{66}} \frac{d^2w^\circ}{dx^2} + \frac{S}{A_{66}} \right). \tag{135b}$$

Substituting these results into the equations for N_θ and M_x in eq. (134) yields

$$\begin{aligned}
N_\theta &= \left(A_{22} - \frac{A_{12}^2}{A_{11}} \right) \frac{w^\circ}{R} - \left(B_{12} - \frac{B_{11}A_{12}}{A_{11}} \right) \frac{d^2w^\circ}{dx^2} \\
&\quad + \frac{A_{12}}{A_{11}} (N + N_x^T) - N_\theta^T,
\end{aligned} \tag{136a}$$

and

$$\begin{aligned}
M_x &= \left(B_{12} - \frac{B_{11}A_{12}}{A_{11}} \right) \frac{w^\circ}{R} - \left(D_{11} - \frac{B_{16}^2}{A_{66}} - \frac{B_{11}^2}{A_{11}} \right) \frac{d^2w^\circ}{dx^2} \\
&\quad + \frac{B_{11}}{A_{11}} (N + N_x^T) - M_x^T + \frac{B_{16}}{A_{66}} S.
\end{aligned} \tag{136b}$$

Substituting eq. (136a) and (136b) into the third equilibrium equation, eq. (129c), leads to the equation governing w° :

$$\begin{aligned} & \left(D_{11} - \frac{B_{11}^2}{A_{11}} - \frac{B_{16}^2}{A_{66}} \right) \frac{d^4 w^o}{dx^4} + \left(2 \frac{B_{11} A_{12}}{A_{11} R} - 2 \frac{B_{12}}{R} - N \right) \frac{d^2 w^o}{dx^2} \\ & + \left(A_{22} - \frac{A_{12}^2}{A_{11}} \right) \frac{w^o}{R^2} = \frac{N_{\theta}^T}{R} - \frac{A_{12}}{R A_{11}} (N + N_x^T) . \end{aligned} \quad (137)$$

This is a linear differential equation with constant and known coefficients which depend on material properties, equivalent thermal loads, geometry, and a known applied axial load N . Hence, this structurally nonlinear problem results in a mathematically linear problem. Note, however, that the coefficients vary as the applied axial load N varies. This will be addressed in a later section.

B. Specification of Boundary Conditions

Attention now will be focused on the boundary conditions. A statement has been made regarding N_x . This statement satisfies one of the four boundary conditions, namely, eqs. (130a) and (130b), i. For the problem to be properly posed, the three remaining boundary conditions, eqs. (130a) and (130b), ii, iii, and iv, must be satisfied. Within the context of the admissible conditions of thermal preloading, general balanced laminates, and no explicitly applied torsional loads, three physically plausible boundary conditions can be imposed on the ends of the cylinder, namely:

- 1 - lubricated boundaries;
- 2 - simply supported boundaries; and,
- 3 - clamped boundaries.

In the remainder of this work, it will be assumed that the same boundary conditions

will be enforced at both ends of the cylinder. Hence, the discussions which follow will focus on the $x=+L/2$ boundary only. Since the same boundary conditions will be enforced at either end, the radial response of the cylinder will be assumed to be symmetric about the $x=0$ plane. Therefore, the radial displacement, $w^o(x)$, of the cylinder is an even function of x .

For lubricated boundaries, the ends of the cylinder are free to rotate about the cylinder's centerline, implying that $N_{x0} = S = 0$. Also, the out-of-plane shear force Q_x and moment M_x at the ends are zero. For simply supported boundaries, the tangential displacement v^o and the radial displacement w^o at the ends of the cylinder are specified, and the moment M_x is zero. For clamped boundaries, the tangential displacement v^o , the radial displacement w^o , and slope $\frac{dw^o}{dx}$ at the ends of the cylinder are specified. The terminology 'lubricated' comes from the fact that there is no restraint on the tangential or radial displacement or slope at the cylinder ends, as if the ends of the cylinder were being pushed together axially with perfectly lubricated plates.

From eq. (130), the formal boundary conditions for lubricated boundaries are

$$N_{x0} \Big|_{x \rightarrow \pm \frac{L}{2}} = S = 0 , \quad (138a)$$

$$\frac{dM_x}{dx} \Big|_{x \rightarrow \pm \frac{L}{2}} + N \frac{dw^o}{dx} \Big|_{x \rightarrow \pm \frac{L}{2}} = 0 , \quad (138b)$$

and

$$M_x \Big|_{x \rightarrow \frac{L}{2}} = 0 . \quad (138c)$$

For simply supported boundaries the conditions are

$$v^o \Big|_{x \rightarrow \frac{L}{2}} \text{ is specified ,} \quad (139a)$$

$$w^o \Big|_{x \rightarrow \frac{L}{2}} \text{ is specified ,} \quad (139b)$$

and

$$M_x \Big|_{x \rightarrow \frac{L}{2}} = 0 . \quad (139c)$$

For clamped boundaries the conditions are

$$v^o \Big|_{x \rightarrow \frac{L}{2}} \text{ is specified ,} \quad (140a)$$

$$w^o \Big|_{x \rightarrow \frac{L}{2}} \text{ is specified ,} \quad (140b)$$

and

$$\frac{dw^o}{dx} \Big|_{x \rightarrow \frac{L}{2}} \text{ is specified .} \quad (140c)$$

In order to conveniently impose these boundary conditions, they will be expressed in terms of the radial displacement $w^o(x)$ and its derivatives. Therefore, the tangential displacement $v^o(x)$ is required as a function of $w^o(x)$ and its derivatives. From eq. (128), it follows that

$$\frac{dv^o}{dx} = \gamma_{x\theta}^o \quad \rightarrow \quad v^o(x) = \int (\gamma_{x\theta}^o(x)) dx + C_v, \quad (141)$$

where C_v is a constant of integration. Substituting eq. (135b) into eq. (141) and integrating results in,

$$v^o(x) = \frac{B_{16}}{A_{66}} \frac{dw^o(x)}{dx} + \frac{S}{A_{66}} x + C_v. \quad (142)$$

For convenience, and since we expect $v^o(x)$ to be odd since $w^o(x)$ is even in x ,

$$C_v = 0. \quad (143)$$

In the following, each of the three sets of boundary condition equations, eqs. (138), (139), and (140), will be presented in terms of the radial displacement $w^o(x)$.

1. Lubricated Boundary Conditions

Despite the desire to write the boundary conditions in terms of the displacements, the first of the equations, eqs. (138), which specify lubricated boundary conditions, i.e., eq. (138a), can be represented most simply as

$$S = 0. \quad (144)$$

The two remaining equations, eqs. (138b) and (138c), can be expanded to yield

$$\left(D_{11} - \frac{B_{16}^2}{A_{66}} - \frac{B_{11}^2}{A_{11}} \right) \frac{d^3 w^o}{dx^3} \Big|_{x \rightarrow \frac{L}{2}} + \left(\frac{B_{11} A_{12}}{A_{11} R} - \frac{B_{12}}{R} \right) \frac{dw^o}{dx} \Big|_{x \rightarrow \frac{L}{2}} = 0, \quad (145a)$$

and

$$\left(D_{11} - \frac{B_{16}^2}{A_{66}} - \frac{B_{11}^2}{A_{11}} \right) \frac{d^2 w^o}{dx^2} \Big|_{x=\frac{L}{2}} + \left(\frac{B_{11}A_{12}}{A_{11}R} - \frac{B_{12}}{R} \right) w^o \Big|_{x=\frac{L}{2}} - \frac{B_{11}}{A_{11}} (N + N_x^T) + M_x^T + \frac{B_{16}}{A_{66}} S = 0 \quad (145b)$$

Equation (145b) can be simplified by enforcing the first equation, i.e., by setting $S = 0$.

Due to these simplifications, the case of lubricated boundary conditions results in the following two equations,

$$\left(D_{11} - \frac{B_{16}^2}{A_{66}} - \frac{B_{11}^2}{A_{11}} \right) \frac{d^3 w^o}{dx^3} \Big|_{x=\frac{L}{2}} + \left(\frac{B_{11}A_{12}}{A_{11}R} - \frac{B_{12}}{R} \right) \frac{dw^o}{dx} \Big|_{x=\frac{L}{2}} = 0, \quad (146a)$$

and

$$\left(D_{11} - \frac{B_{16}^2}{A_{66}} - \frac{B_{11}^2}{A_{11}} \right) \frac{d^2 w^o}{dx^2} \Big|_{x=\frac{L}{2}} + \left(\frac{B_{11}A_{12}}{A_{11}R} - \frac{B_{12}}{R} \right) w^o \Big|_{x=\frac{L}{2}} - \frac{B_{11}}{A_{11}} (N + N_x^T) + M_x^T = 0 \quad (146b)$$

2. Simply Supported Boundary Conditions

Expanding eqs. (139) in terms of w^o yields

$$v^o \Big|_{x=\frac{L}{2}} = \frac{B_{16}}{A_{66}} \frac{dw^o}{dx} \Big|_{x=\frac{L}{2}} + \frac{S}{A_{66}} \left(+\frac{L}{2} \right) \quad \text{is specified,} \quad (147a)$$

$$w^o \Big|_{x=\frac{L}{2}} \quad \text{is specified,} \quad (147b)$$

and

$$\left(D_{11} - \frac{B_{16}^2}{A_{66}} - \frac{B_{11}^2}{A_{11}} \right) \frac{d^2 w^o}{dx^2} \Big|_{x \rightarrow \frac{L}{2}} + \left(\frac{B_{11} A_{12}}{A_{11} R} - \frac{B_{12}}{R} \right) w^o \Big|_{x \rightarrow \frac{L}{2}} - \frac{B_{11}}{A_{11}} (N + N_x^T) + M_x^T + \frac{B_{16}}{A_{66}} S = 0 \quad (147c)$$

3. Clamped Boundary Conditions

Expanding eq. (140) in terms of $w^o(x)$ yields

$$v^o \Big|_{x \rightarrow \frac{L}{2}} = \frac{B_{16}}{A_{66}} \frac{dw^o}{dx} \Big|_{x \rightarrow \frac{L}{2}} + \frac{S}{A_{66}} \left(+ \frac{L}{2} \right) \quad \text{is specified ,} \quad (148a)$$

$$w^o \Big|_{x \rightarrow \frac{L}{2}} \quad \text{is specified ,} \quad (148b)$$

and

$$\frac{dw^o}{dx} \Big|_{x \rightarrow \frac{L}{2}} \quad \text{is specified .} \quad (148c)$$

C. Solution of the Governing Equation for $w^o(x)$

Equation (137) will now be solved for $w^o(x)$. The complete solution to eq. (137) consists of homogenous and particular parts, i.e.,

$$w^o(x) = w_{\text{homo.}}^o(x) + w_{\text{part.}}^o(x) \quad (149)$$

The particular solution is simply the right hand side of eq. (137) divided by the coefficient of w^o , or

$$w_{part}^o(x) = \frac{R(A_{11}N_0^T - A_{12}(N - N_x^T))}{A_{11}A_{22} - A_{12}^2} = w_{part} \quad , \quad (150)$$

where the notation w_{part} denotes the particular solution. Note that it is not a function of x .

The homogeneous solution is of the form

$$w_{homo}^o(x) = A e^{\lambda x} \quad . \quad (151)$$

Substituting this assumed form into eq. (137) results in the characteristic equation:

$$\left(D_{11} - \frac{B_{11}^2}{A_{11}} - \frac{B_{16}^2}{A_{66}}\right)\lambda^4 + \left(2\frac{B_{11}A_{12}}{A_{11}R} - 2\frac{B_{12}}{R} - N\right)\lambda^2 + \left(A_{22} - \frac{A_{12}^2}{A_{11}}\right) = 0 \quad ,$$

or

$$R\left(D_{11}A_{11} - B_{11}^2 - \frac{B_{16}^2A_{11}}{A_{66}}\right)\lambda^4 + (2B_{11}A_{12} - 2B_{12}A_{11} - A_{11}RN)\lambda^2 + \left(\frac{A_{11}A_{22} - A_{12}^2}{R}\right) = 0 \quad . \quad (152)$$

There are four roots to this equation, namely

$\lambda_{1,2,3,4} =$

$$\pm \sqrt{\frac{(A_{11}RN + 2A_{11}B_{12} - 2A_{12}B_{11}) \pm \sqrt{(2A_{12}B_{11} - 2A_{11}B_{12} - A_{11}RN)^2 - 4\left(D_{11}A_{11} - B_{11}^2 - \frac{B_{16}^2A_{11}}{A_{66}}\right)(A_{11}A_{22} - A_{12}^2)}}{2\left(D_{11}A_{11} - B_{11}^2 - \frac{B_{16}^2A_{11}}{A_{66}}\right)R}} \quad . \quad (153)$$

Though it is not totally obvious, there is an interesting character to the roots given above. This is due to the dependence of the roots on the level of the applied axial load, N . The character of these roots can be examined by studying λ^2 instead of λ , i.e.,

$$(\lambda^2)_{1,2} = \frac{(A_{11}RN + 2A_{11}B_{12} - 2A_{12}B_{11}) \pm \sqrt{(2A_{12}B_{11} - 2A_{11}B_{12} - A_{11}RN)^2 - 4\left(D_{11}A_{11} - B_{11}^2 - \frac{B_{16}^2A_{11}}{A_{66}}\right)(A_{11}A_{22} - A_{12}^2)}}{2\left(D_{11}A_{11} - B_{11}^2 - \frac{B_{16}^2A_{11}}{A_{66}}\right)R} \quad (154)$$

The first important character to observe is that the discriminant in eq. (154) will be zero for a certain level of applied axial load N . This load will be denoted by N^* , given as

$$N^* = \frac{2}{A_{11}R} \left\{ \pm \sqrt{(A_{11}A_{22} - A_{12}^2) \left(D_{11}A_{11} - B_{11}^2 - \frac{B_{16}^2A_{11}}{A_{66}} \right) + A_{12}B_{11} - A_{11}B_{12}} \right\} \quad (155)$$

In general, eq. (155) will yield one positive and one negative value for N^* . In this investigation, attention will be focused on compressive loading of the cylinder and, therefore, on the negative value of N^* . Hence, N^* will be given by

$$N^* = \frac{2}{A_{11}R} \left\{ - \sqrt{(A_{11}A_{22} - A_{12}^2) \left(D_{11}A_{11} - B_{11}^2 - \frac{B_{16}^2A_{11}}{A_{66}} \right) + A_{12}B_{11} - A_{11}B_{12}} \right\} \quad (156)$$

For varying values of N , the roots $(\lambda^2)_{1,2}$ have the following characters:

- 1) For $0 \geq N > N^*$, the roots $(\lambda^2)_{1,2}$ are complex conjugates given by

$$\begin{aligned}
(\lambda^2)_{1,2} &= \Re((\lambda^2)_{1,2}) \pm i\Im((\lambda^2)_{1,2}) \\
&= \frac{A_{11}RN + 2A_{11}B_{12} - 2A_{12}B_{11}}{2\left(D_{11}A_{11} - B_{11}^2 - \frac{B_{16}^2A_{11}}{A_{66}}\right)R} \pm i \frac{\sqrt{-(2A_{12}B_{11} - 2A_{11}B_{12} - A_{11}RN)^2 + 4\left(D_{11}A_{11} - B_{11}^2 - \frac{B_{16}^2A_{11}}{A_{66}}\right)(A_{11}A_{22} - A_{12}^2)}}{2\left(D_{11}A_{11} - B_{11}^2 - \frac{B_{16}^2A_{11}}{A_{66}}\right)R}
\end{aligned} \tag{157}$$

The roots λ are thus of the form

$$\lambda_{1,2,3,4} = \pm \sqrt{(\lambda^2)_{1,2}} = \pm \alpha \pm i\beta . \tag{158}$$

2) For $N = N^*$, the roots $(\lambda^2)_{1,2}$ are negative repeating real roots given by

$$(\lambda^2)_{1,2} = \frac{(A_{11}RN + 2A_{11}B_{12} - 2A_{12}B_{11})}{2\left(D_{11}A_{11} - B_{11}^2 - \frac{B_{16}^2A_{11}}{A_{66}}\right)R} . \tag{159}$$

Therefore, the four roots λ are two pure imaginary repeating roots of the form

$$\lambda_{1,2,3,4} = \pm \sqrt{(\lambda^2)_{1,2}} = \pm i\beta, \pm i\beta . \tag{160}$$

3) For $N < N^*$, the roots $(\lambda^2)_{1,2}$ are negative distinct real roots given by

$$\begin{aligned}
(\lambda^2)_{1,2} &= \\
&= \frac{(A_{11}RN + 2A_{11}B_{12} - 2A_{12}B_{11}) \pm \sqrt{(2A_{12}B_{11} - 2A_{11}B_{12} - A_{11}RN)^2 - 4\left(D_{11}A_{11} - B_{11}^2 - \frac{B_{16}^2A_{11}}{A_{66}}\right)(A_{11}A_{22} - A_{12}^2)}}{2\left(D_{11}A_{11} - B_{11}^2 - \frac{B_{16}^2A_{11}}{A_{66}}\right)R}
\end{aligned} \tag{161}$$

The roots λ are thus of the form

$$\lambda_{1,2,3,4} = \pm \sqrt{(\lambda^2)_{1,2}} = \pm i\beta_1, \pm i\beta_2 . \quad (162)$$

Because of these three different forms for the roots of the characteristic equation (152), depending on the value of N relative to N^* , the functional form of the x dependence of the homogeneous solution depends on the value of N . Therefore, the value of N defines the shape, as well as the amplitude of the deformed cylinder. For the linear problem where the $N_x \frac{d^2w}{dx^2}$ term in eq. (129c) is not present, only the amplitude, not the shape, is dependent on the value of N .

The functional form of the homogeneous solution, eq. (151), is as follows:

For $0 \geq N > N^*$, from eq. (158)

$$w_{\text{homo.}}^o(x) = A_1 e^{(\alpha+i\beta)x} + A_2 e^{(\alpha-i\beta)x} + A_3 e^{(-\alpha+i\beta)x} + A_4 e^{(-\alpha-i\beta)x} . \quad (163)$$

For $N = N^*$, from eq. (160)

$$w_{\text{homo.}}^o(x) = (A_1 + A_2 x) e^{i\beta x} + (A_3 + A_4 x) e^{-i\beta x} . \quad (164)$$

For $N < N^*$, from eq. (162)

$$w_{\text{homo.}}^o(x) = A_1 e^{i\beta_1 x} + A_2 e^{i\beta_2 x} + A_3 e^{-i\beta_1 x} + A_4 e^{-i\beta_2 x} . \quad (165)$$

Combining these homogeneous solutions with the particular solution, eq. (150), and considering only the portion of the solution that is symmetric about $x=0$, the three forms of the solution of $w^o(x)$ are:

For $0 \geq N > N^*$,

$$w^o(x) = F \cosh(\alpha x) \cos(\beta x) + G \sinh(\alpha x) \sin(\beta x) + \frac{R(A_{11}N_0^T - A_{12}(N - N_x^T))}{A_{11}A_{22} - A_{12}^2}. \quad (166)$$

For $N = N^*$,

$$w^o(x) = F \cos(\beta x) + G x \sin(\beta x) + \frac{R(A_{11}N_0^T - A_{12}(N - N_x^T))}{A_{11}A_{22} - A_{12}^2}. \quad (167)$$

For $N < N^*$,

$$w^o(x) = F \cos(\beta_1 x) + G \cos(\beta_2 x) + \frac{R(A_{11}N_0^T - A_{12}(N - N_x^T))}{A_{11}A_{22} - A_{12}^2}. \quad (168)$$

The constants F and G can be determined from the application of the boundary conditions, eq. (146), (147), and (148), for lubricated, simply supported, and clamped boundary conditions, respectively.

D. Solution of the Governing Equation for $u^o(x)$

The remaining displacement variable $u^o(x)$ can be obtained from the definition of the midplane axial strain $\epsilon_x^o(x)$, given by eq. (135a), in terms of the material properties, cylinder geometry, and equivalent thermal loads, along with the solution for $w^o(x)$ and its derivatives. From eq. (128), it follows that

$$\frac{du^o(x)}{dx} = \epsilon_x^o(x) - \frac{1}{2} \left(\frac{dw^o(x)}{dx} \right)^2 \rightarrow u^o(x) = \int \left[\epsilon_x^o(x) - \frac{1}{2} \left(\frac{dw^o(x)}{dx} \right)^2 \right] dx + C_u, \quad (169)$$

where C_u is a constant integration. By substituting eq. (135a) into eq. (169),

$$\frac{du^o(x)}{dx} = \frac{1}{A_{11}} \left(N + N_x^T - \frac{A_{12}}{R} w^o(x) + B_{11} \frac{d^2 w^o(x)}{dx^2} \right) - \frac{1}{2} \left(\frac{dw^o(x)}{dx} \right)^2 . \quad (170)$$

This expression involves constants and the closed-form solution for $w^o(x)$ and its first two derivatives. Therefore, this expression can be integrated analytically as characterized in eqs. (169), i.e.,

$$\begin{aligned} u^o(x) = & \left[\frac{1}{A_{11}} (N + N_x^T) \right] x - \left[\frac{A_{12}}{A_{11} R} \right] \int w^o(x) dx \\ & + \left[\frac{B_{11}}{A_{11}} \right] \int \frac{d^2 w^o(x)}{dx^2} dx - \frac{1}{2} \int \left(\frac{dw^o(x)}{dx} \right)^2 dx + C_u . \end{aligned} \quad (171)$$

Note that the solution for $u^o(x)$ involves the three terms which are the integral of $w^o(x)$, its first derivative, and the integral of the square of its first derivative. Since $w^o(x)$ is an even function of x , these three terms are odd functions of x . Therefore, since symmetry about $x = 0$ has been assumed, and constants are even functions,

$$C_u = 0 . \quad (172)$$

Since the solutions for $w^o(x)$ comprise three different functional forms which depend on the magnitude of the compressive axial load N , so will the solution for $u^o(x)$. The solution for $v^o(x)$ was presented in the previous section in eq. (142) and (143), and involves the first derivative of the solution for $w^o(x)$, given by eqs. (166), (167), and (168).

Since the expression for $u^o(x)$, eq. (171), involves the integration of the square of the first derivative of $w^o(x)$, the solution is not easily obtainable. However, after much

algebra, it can be shown that,

for $0 \geq N > N^*$,

$$\begin{aligned} u^o(x) = & C_1 x + C_2 \sinh(\alpha x) \cos(\beta x) + C_3 \cosh(\alpha x) \sin(\beta x) \\ & + C_4 \sinh(2\alpha x) \cos(2\beta x) + C_5 \cosh(2\alpha x) \sin(2\beta x) \\ & + C_6 \sinh(2\alpha x) + C_7 \sin(2\beta x) \end{aligned}$$

where

$$\begin{aligned} C_1 = & \left(1 + \frac{A_{12}^2}{A_{11}A_{22} - A_{12}^2} \right) \left(\frac{N + N_x^T}{A_{11}} \right) - \frac{A_{12}}{A_{11}A_{22} - A_{12}^2} N_0^T + \frac{FG\alpha\beta}{2} \\ C_2 = & \frac{B_{11}(F\alpha + G\beta) + \frac{A_{12}}{R} F(\beta - \alpha)}{A_{11}(\alpha^2 + \beta^2)} \\ C_3 = & \frac{B_{11}(G\alpha - F\beta) + \frac{A_{12}}{R} F(\alpha + \beta)}{A_{11}(\alpha^2 + \beta^2)} \\ C_4 = & \frac{(G^2 - F^2)\alpha\beta^2 - FG(\alpha^2\beta + \beta^3)}{8(\alpha^2 + \beta^2)} \\ C_5 = & \frac{(G^2 - F^2)\alpha^2\beta - FG(\alpha^3 + \alpha\beta^2)}{8(\alpha^2 + \beta^2)} \\ C_6 = & -(F^2\alpha^2 + G^2\beta^2)/(8\alpha) \\ C_7 = & \frac{(F^2\alpha^2 + G^2\beta^2)(\alpha^2 + \beta^2)}{8(\alpha^2\beta + \beta^3)} \end{aligned} \tag{173a}$$

and

$$\begin{aligned} v^o(x) = & \frac{B_{16}}{A_{66}} \left\{ F[\alpha \sinh(\alpha x) \cos(\beta x) - \beta \cosh(\alpha x) \sin(\beta x)] \right. \\ & \left. - G[\alpha \cosh(\alpha x) \sin(\beta x) - \beta \sinh(\alpha x) \cos(\beta x)] \right\} \\ & + \frac{S}{A_{66}} x \end{aligned} \tag{173b}$$

For $N = N^*$,

$$u^o(x) = C_1 x + C_2 x^3 + C_3 \sin(\beta x) + C_4 \sin(2\beta x) \\ + C_5 x \cos(\beta x) + C_6 x \cos(2\beta x) + C_7 x^2 \sin(2\beta x)$$

where

$$C_1 = \left(1 + \frac{A_{12}^2}{A_{11}A_{22} - A_{12}^2} \right) \left(\frac{N + N_x^T}{A_{11}} \right) - \frac{A_{12}}{A_{11}A_{22} - A_{12}^2} N_0^T + \frac{F^2 \beta^2 + FG\beta - G^2}{4} \quad (174a)$$

$$C_2 = -\frac{G^2 \beta^2}{12} \quad ; \quad C_3 = \frac{B_{11}(G - F\beta) + \frac{A_{12}}{R} \left(F - \frac{G}{\beta^2} \right)}{A_{11}}$$

$$C_4 = \frac{(2G^2 - 2F^2 \beta^2 - FG\beta)}{16\beta} \quad ; \quad C_5 = \frac{\left(B_{11} G \beta + \frac{A_{12}}{R} \frac{G}{\beta} \right)}{A_{11}}$$

$$C_6 = -FG\beta/8 \quad ; \quad C_7 = -G^2 \beta/8$$

and

$$v^o(x) = \frac{B_{16}}{A_{66}} \left\{ F [-\beta \sin(\beta x)] + G [\sin(\beta x) + \beta x \cos(\beta x)] \right\} \\ + \frac{S}{A_{66}} x \quad (174b)$$

For $N < N^*$,

$$u^o(x) = C_1 x + C_2 \sin(\beta_1 x) + C_3 \sin(\beta_2 x) + C_4 \sin(2\beta_1 x) + C_5 \sin(2\beta_2 x) \\ + C_6 \sin[(\beta_1 - \beta_2)x] + C_7 \sin[(\beta_1 + \beta_2)x]$$

where

$$C_1 = \left(1 + \frac{A_{12}^2}{A_{11}A_{22} - A_{12}^2} \right) \left(\frac{N + N_x^T}{A_{11}} \right) - \frac{A_{12}}{A_{11}A_{22} - A_{12}^2} N_\theta^T - \frac{F^2 \beta_1^2 + G^2 \beta_2^2}{4} \quad (175a)$$

$$C_2 = \frac{\left(-B_{11} F \beta_1 - \frac{A_{12} F}{R \beta_1} \right)}{A_{11}} ; \quad C_3 = \frac{\left(-B_{11} G \beta_2 - \frac{A_{12} G}{R \beta_2} \right)}{A_{11}}$$

$$C_4 = \frac{F^2 \beta_1}{8} ; \quad C_5 = \frac{G^2 \beta_2}{8}$$

$$C_6 = -\frac{FG \beta_1 \beta_2}{4(\beta_1 - \beta_2)} ; \quad C_7 = -\frac{FG \beta_1 \beta_2}{4(\beta_1 + \beta_2)}$$

and

$$v^o(x) = \frac{B_{16}}{A_{66}} \left\{ F [-\beta_1 \sin(\beta_1 x)] + G [-\beta_2 \sin(\beta_2 x)] \right\} + \frac{S}{A_{66}} x \quad (175b)$$

The axial compressive load N^* , which corresponds to the load at which the character of the roots to the characteristic equation, eq. (152), changes from the roots being complex conjugates to the roots being repeating pure imaginary roots, has been shown to correspond to the collapse load of the cylinder by Booton (ref. 2). Since application of a compressive axial load corresponding to the collapse load would cause catastrophic failure of the cylinder, the analyses and results discussed in the remainder of this work will focus only on compressive axial loads in the range $0 \geq N > N^*$.

E. Preloading Response Due to Thermal Effects

Composite cylinders are usually fabricated on a male mandrel and are consolidated at an elevated temperature. After consolidation, the temperature is lowered to ambient temperature and the male mandrel is removed from the cured cylinder. If the fabrication and consolidation are assumed to be axisymmetric, the cured shape of the cylinder can be determined using the solutions from the previous sections.

Since there are no loads applied to the cylinder after the mandrel is removed, N is set equal to zero, as is S , and the response is given by eq. (166). Also, the roots are given by eqs. (158) and (157). Note that the roots are only functions of the material properties and cylinder geometry, since N is set equal to zero. Therefore, the shape of the deformed cylinder is a function of the material properties and geometry only. The particular solution, eq. (150), which is a function of the material properties, cylinder geometry, and the temperature change, governs the radial deformation of the cylinder away from the ends.

Since the boundaries of the cylinder are unrestrained after the mandrel is removed, the appropriate boundary conditions for this case are the lubricated boundary conditions, eq. (146), with N set equal to zero.

In summary, from the material properties and geometry of the cylinder, the root parts α and β of eq. (166) are known. By enforcing the lubricated end boundary condition, the constants F and G of eq. (166) can be solved using eqs. (146). From the material properties, cylinder geometry, and temperature change, the particular solution, eq. (150), with N set equal to zero, is known. Therefore, the deformed shape $w^o(x)$ can be

calculated.

F. Numerical Results for the Case of Thermally-Induced Preloading

Relations between $\frac{u^o(x)}{H}$, $\frac{v^o(x)}{H}$, $\frac{w^o(x)}{H}$ and $\frac{x}{L}$ for three 16 layer cylinders are presented in Fig. 11, Fig. 12, and Fig. 13, respectively. These cylinders have stacking sequences of $[+45/-45/0_2]_{2s}$, $[+45/-45/0_2]_{4T}$, and $[0_2/-45/+45]_{4T}$, a length to radius ratio, L/R , of 3 and radius to thickness ratio, R/H , of 125. The value of these parameters are representative of thin, moderately long cylinders. The results are felt to be valid for any cylinder with $L/R \geq 2$ and $R/H \geq 100$. Specific dimensions used herein can be determined knowing a single layer of fiber reinforced material is 0.005 in. thick. The layer material properties used in the calculations are given in Table I.

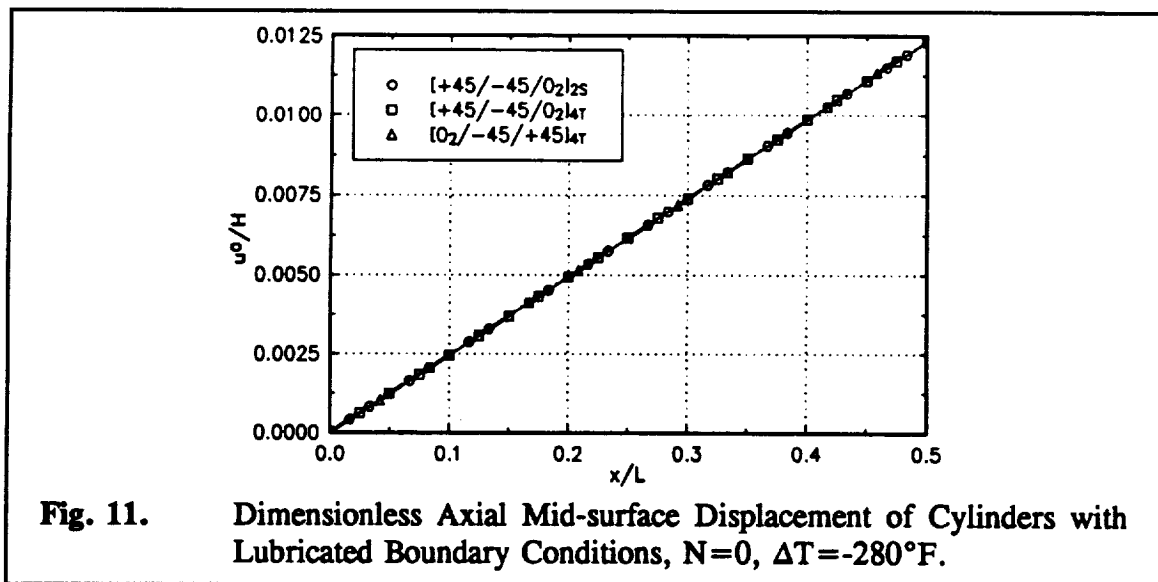
Table I. Layer Material Properties

E_1 (Msi)	E_2 (Msi)	G_{12} (Msi)	ν_{12}	layer thickness, h (in.)	α_1 (in./in.)/°F	α_2 (in./in.)/°F
20.	1.3	1.03	.3	.005	$-.167 \times 10^{-6}$	15.6×10^{-6}

The first stacking sequence represents an often-used slightly orthotropic lay-up, while the second and third stacking sequences represent two unsymmetric variants of the first one. If unsymmetric laminates are to gain favor, slight deviations from symmetry, as with the second laminates, are most likely to initially be used. The laminate properties and thermally-induced equivalent stress resultants with $\Delta T = -280^\circ\text{F}$ for these three cylinders are given in Table II.

Table II. Laminate Properties and Thermally-Induced Stress Resultants for $[+45/-45/0_2]_{2S}$, $[+45/-45/0_2]_{4T}$, and $[0_2/-45/+45]_{4T}$ Cylinders, $\Delta T = -280^\circ\text{F}$.

Laminate Property	$[+45/-45/0_2]_{2S}$	$[+45/-45/0_2]_{4T}$	$[0_2/-45/+45]_{4T}$
A_{11} (lb/in)	1.068×10^6	1.068×10^6	1.068×10^6
A_{12} (lb/in)	$.1966 \times 10^6$	$.1966 \times 10^6$	$.1966 \times 10^6$
A_{22} (lb/in)	$.3156 \times 10^6$	$.3156 \times 10^6$	$.3156 \times 10^6$
A_{66} (lb/in)	$.2476 \times 10^6$	$.2476 \times 10^6$	$.2476 \times 10^6$
B_{11} (lb-in/in)	0	2,707.	-2707.
B_{12} (lb-in/in)	0	-826.0	826.0
B_{16} (lb-in/in)	0	-470.3	470.3
D_{11} (lb-in ² /in)	461.3	569.6	569.6
N_x^T (lb/in)	-160.2	-160.2	-160.2
N_θ^T (lb/in)	-357.1	-357.1	-357.1
M_x^T (lb-in/in)	0	.4921	-.4921



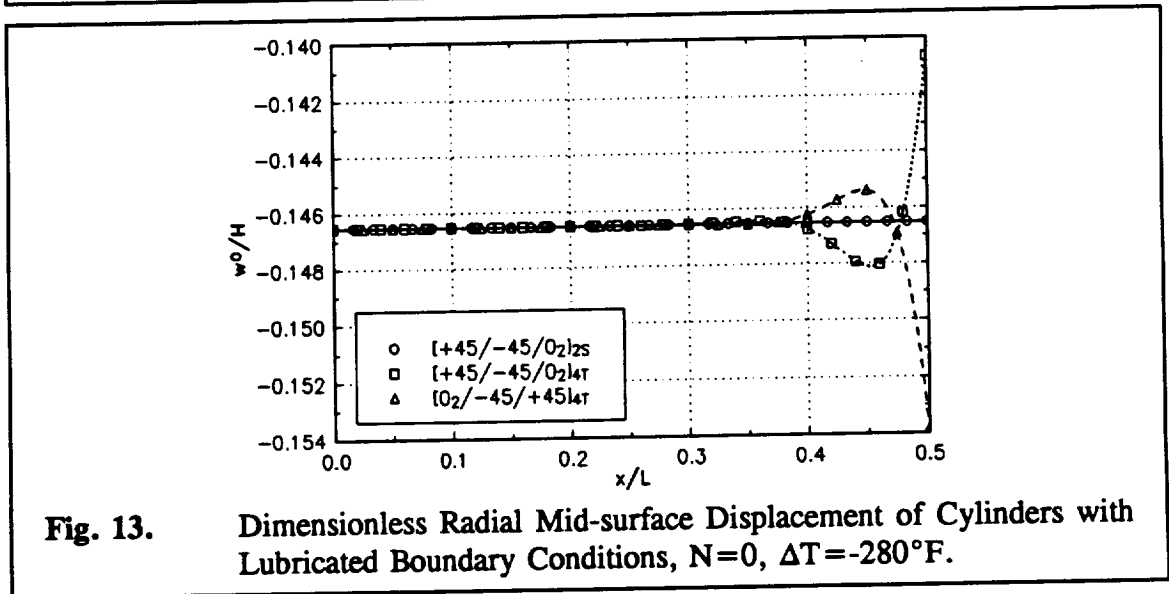
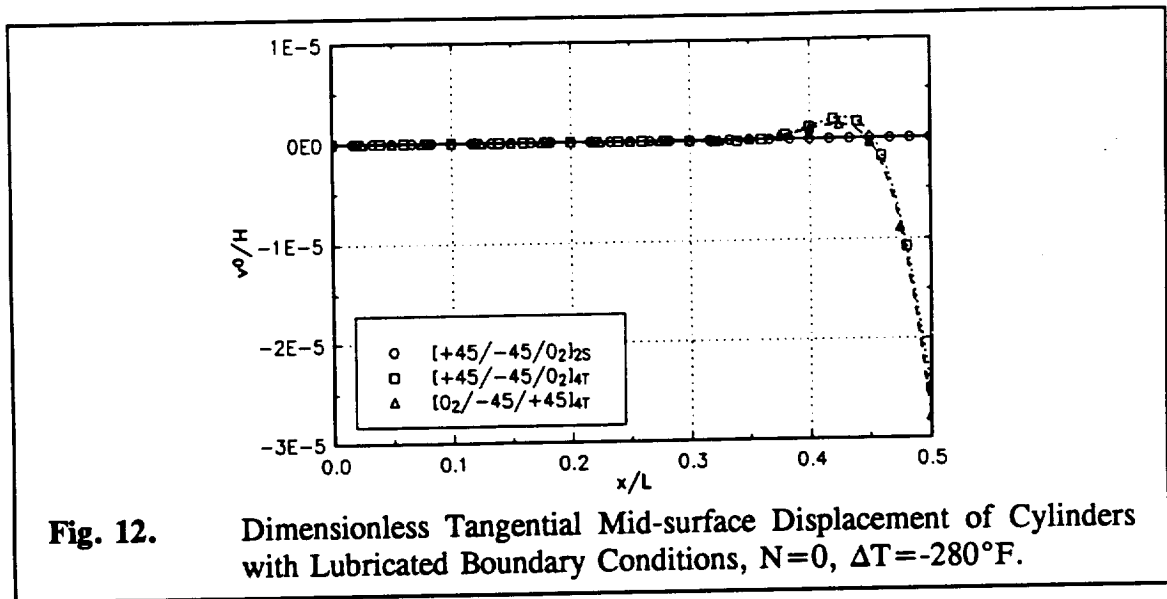


Fig. 11 reveals that the axial displacement of the cylinder mid-surface for all three cylinders is essentially a linear function of x and that the magnitudes of the responses for these cylinders is the same. Since the effective axial coefficient of thermal expansion of the cylinders is the same. Since the effective axial coefficient of thermal expansion of the cylinders is negative, they respond to the temperature change of $\Delta T = -280^\circ\text{F}$ by expanding axially.

By examination of Fig. 12 and Fig. 13, it is seen that for the symmetric cylinder, the

tangential displacements of the mid-surface are zero over the entire cylinder length, and radial displacements of the mid-surface of the symmetric cylinder are constant.

Comparing the results of the unsymmetric $[+45/-45/0_2]_{4T}$ cylinder to the results of the $[0_2/-45/+45]_{4T}$ cylinder, it is seen that the tangential and radial displacements vary along the half-length of the cylinders, particularly toward the cylinders' ends. The ends of the unsymmetric cylinders curl radially and twist, producing a boundary layer effect. The direction of the radial curl is a function of the sign of the thermally induced moment M_x^T , resulting from the opposite stacking sequences of the cylinders. The $[+45/-45/0_2]_{4T}$ cylinder curls outward, while the $[0_2/-45/+45]_{4T}$ cylinder curls inward. Fig. 12 illustrates that both unsymmetric cylinders twist in the same direction due to the thermally-induced preloading, although the $[0_2/-45/+45]_{4T}$ cylinder exhibits a slightly larger tangential displacement at the end. It is important to realize that the study of unsymmetrically laminated cylinders would not be correct without including this thermally-induced deformation due to cooling from the consolidation temperature.

G. Cylinder Response Due to Thermally-Induced Preloading Effects and a Compressive Axial Load

In order to correctly model the response of the cylinder due to thermal preloading effects and a compressive axial end load, the thermally-induced preloading deformation at the end of the cylinder must be taken into account when enforcing the end conditions under axial load. Since the cylinder deforms due to cooling from consolidation temperature to ambient temperature, any fixture used to apply the axial end load to the

thermally deformed cylinder must take into account the thermally-induced tangential and radial deformation and slope at the end of the cylinder before loading. This impacts the specification of the simply supported and clamped boundary conditions, eq. (147) and (148), respectively. Stated in another way, simply supported or clamped end conditions would resist any tangential and radial end displacements relative to the thermally-induced preloading value, and clamped end conditions would also resist rotation of the ends relative to the thermally-induced preloading value. As observed in the previous section, under thermally-induced preloading effects, for unsymmetric laminates, the radius at the end of the cylinder will most likely be different from the radius of the cylinder away from the ends. Therefore, the axial load N would be applied eccentrically relative to the mid-length of the cylinder. This could have an influence on the response of the cylinder near the ends.

Since the boundary conditions associated with the thermal-induced preloading effects are those of lubricated ends, it follows that the thermally-induced torsional load, S_T , is zero. Therefore, the tangential displacement v^o at the end of the cylinder after thermally-induced preloading effects is given by eq. (142) with S equal to zero, i.e.,

$$v_T^o \Big|_{x \rightarrow \frac{L}{2}} = \frac{B_{16}}{A_{66}} \frac{dw_T^o}{dx} \Big|_{x \rightarrow \frac{L}{2}} \quad (176)$$

Under thermally-induced preloading effects and axial load, the simply supported and clamped boundary conditions are:

1) Simply Supported end (at $x = +L/2$):

$$v^o \Big|_{x \rightarrow \frac{L}{2}} = \frac{B_{16}}{A_{66}} \frac{dw^o}{dx} \Big|_{x \rightarrow \frac{L}{2}} + \frac{S}{A_{66}} \left(+\frac{L}{2} \right) = \frac{B_{16}}{A_{66}} \frac{dw_T^o}{dx} \Big|_{x \rightarrow \frac{L}{2}}, \quad (177a)$$

$$w^o \Big|_{x \rightarrow \frac{L}{2}} = w_T^o \Big|_{x \rightarrow \frac{L}{2}}, \quad (177b)$$

and

$$\left(D_{11} - \frac{B_{16}^2}{A_{66}} - \frac{B_{11}^2}{A_{11}} \right) \frac{d^2 w^o}{dx^2} \Big|_{x \rightarrow \frac{L}{2}} + \left(\frac{B_{11} A_{12}}{A_{11} R} - \frac{B_{12}}{R} \right) w^o \Big|_{x \rightarrow \frac{L}{2}} - \frac{B_{11}}{A_{11}} (N + N_x^T) + M_x^T = 0. \quad (177c)$$

2) Clamped end (at $x = +L/2$):

$$v^o \Big|_{x \rightarrow \frac{L}{2}} = \frac{B_{16}}{A_{66}} \frac{dw^o}{dx} \Big|_{x \rightarrow \frac{L}{2}} + \frac{S}{A_{66}} \left(+\frac{L}{2} \right) = \frac{B_{16}}{A_{66}} \frac{dw_T^o}{dx} \Big|_{x \rightarrow \frac{L}{2}}, \quad (178a)$$

$$w^o \Big|_{x \rightarrow \frac{L}{2}} = w_T^o \Big|_{x \rightarrow \frac{L}{2}}, \quad (178b)$$

and

$$\frac{dw^o}{dx} \Big|_{x \rightarrow \frac{L}{2}} = \frac{dw_T^o}{dx} \Big|_{x \rightarrow \frac{L}{2}}. \quad (178c)$$

where the subscript T denotes the value of the response due to thermally-induced preloading effects.

Obviously, since $w^o(x)$ and its first derivative are involved in the boundary conditions, the unknown constants F and G in the solutions for $w^o(x)$, eqs. (166), (167), and (168), can be solved for. Also, these two boundary conditions require that

a third unknown, the torsional load S be found. Therefore, three unknowns, F , G , and S , must be solved for using eqs. (177) and (178).

It is worth noting that in the case of clamped boundary conditions, the specification of v^o , eq. (178a), and specification of $\frac{dw^o}{dx}$, eq. (178c), both involve $\frac{dw_T^o}{dx}$ evaluated at $x = +L/2$. In fact, if eq. (178c) is multiplied by $\frac{B_{16}}{A_{66}}$ and the result is subtracted from eq. (178a), the solution

$$S = 0 \quad (179)$$

is found. Therefore, eq. (178a) can now be eliminated from the system of equations used to solve for F and G , leaving eq. (178b) and (178c) as the system of equations to be solved. The physical interpretation of this result is that for these particular unsymmetrically laminated cylinders (which result in certain B matrix terms not being zero), axial compression with clamped boundary conditions does not induce a torsional load S , while simple support boundary conditions will induce a nonzero S . This is a result of the definition of the tangential displacement $v^o(x)$ involving the slope $\frac{dw^o}{dx}$ and the value of the thermally-induced preloading torsional load, S_T , being equal to zero. If the boundary conditions during the cooling from consolidation temperature to ambient temperature were other than lubricated end conditions, i.e., if the ends were simply supported or clamped during the cooling procedure, a nonzero value for S_T would result for unsymmetrically laminated cylinders, and imposition of clamped boundary conditions during axial compression would result in an induced torsional load S .

H. Numerical Results for the Case of Thermally-Induced Preloading Effects and a Compressive Axial Load

Dimensionless axial, tangential, and radial displacements for cylinders with $[+45/-45/0_2]_{2S}$, $[+45/-45/0_2]_{4T}$, and $[0_2/-45/+45]_{4T}$ stacking sequences, with simply supported and clamped end conditions and varying load N , are presented in Fig. 14 through Fig. 31. The figures illustrate the variation of these displacements along the dimensionless half-length of the cylinders. The three families of figures illustrating the axial, tangential, and radial mid-surface displacement have common vertical scales for ease of comparison within these families.

The two axial load levels investigated are given by fractions of the load N^* , i.e., for $N=10\% N^*$ and $N=90\% N^*$. The quantity N^* is independent of boundary conditions and thermal preloading. Recall that the quantity N^* dictated the form of the roots of the characteristic equation, eq. (152). The values of N^* for the three cylinders are:

$$[+45/-45/0_2]_{2S} : -2271 \text{ lb/in,}$$

$$[+45/-45/0_2]_{4T} : -2241 \text{ lb/in,}$$

$$[0_2/-45/+45]_{4T} : -2771 \text{ lb/in.}$$

1. Simply Supported Boundary Conditions with Thermally-Induced Preloading Effects and a Compressive Axial Load

The dimensionless mid-surface displacements as a function of distance along the half length of these cylinders with simply supported ends are presented in Fig. 14 through Fig. 16 for $N=10\% N^*$, and Fig. 17 through Fig. 19 for $N=90\% N^*$. Comparison of

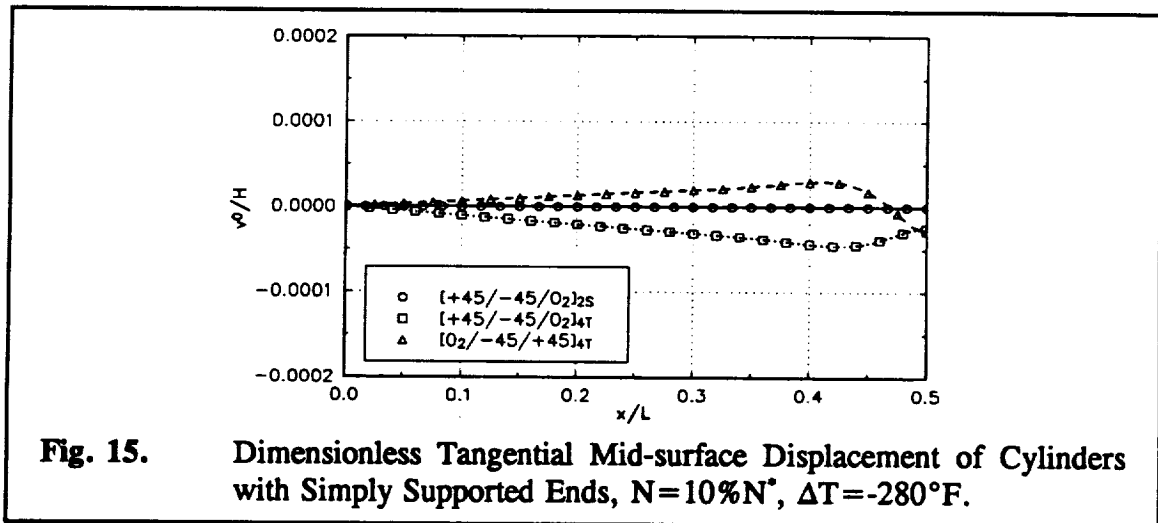
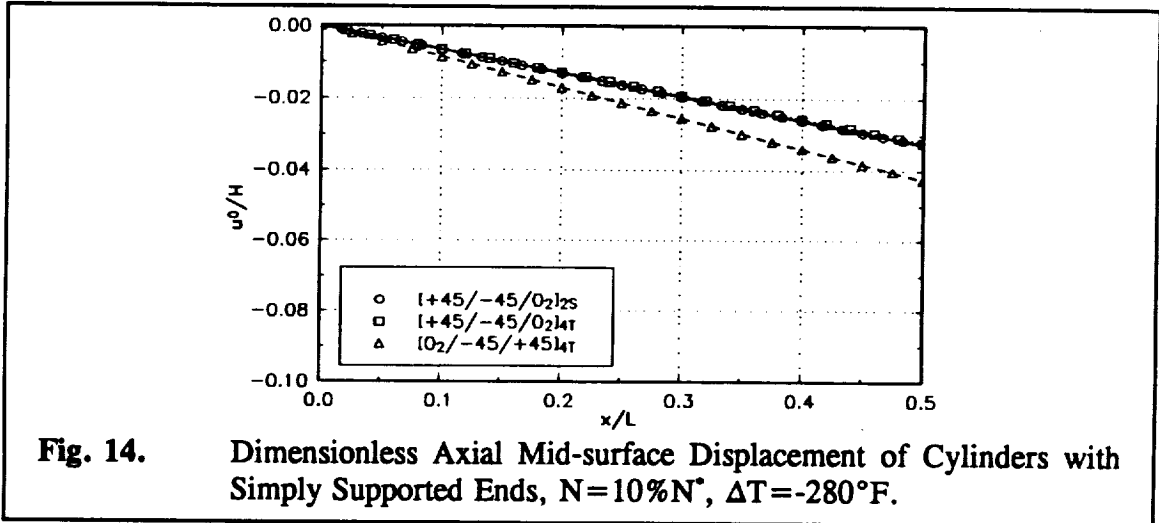
the results relative to the two load levels exhibits the change in the magnitude and shape of the responses. The difference in the shape of the responses is a result of the nonlinear nature of the governing equations. In particular, the length of the boundary layer increases with increasingly compressive axial load.

Fig. 19 illustrates that, at comparable load levels, the maximum value of the radial response of the $[+45/-45/0_2]_{4T}$ cylinder is significantly larger than that of the $[0_2/-45/+45]_{4T}$ cylinder. Note that the actual load $N = 90\% N^*$ on the $[+45/-45/0_2]_{4T}$ cylinder has a smaller magnitude than the load on the $[0_2/-45/+45]_{4T}$ cylinder, since the load N^* is larger in magnitude for the $[0_2/-45/+45]_{4T}$ cylinder and each cylinder in these figures is loaded axially based on the quantity N/N^* , with N^* being different for each cylinder.

The tangential displacement $v^o(x)$ is given by eq. (142). Note that the magnitude of A_{66} and the magnitude of B_{16} (presented in Table II) for the $[+45/-45/0_2]_{4T}$ and $[0_2/-45/+45]_{4T}$ cylinders are identical, while the sign of B_{16} for these two cylinders are opposite. Therefore, the difference in the magnitude of the tangential displacement, presented in Fig. 15 and Fig. 18, is a result of the difference in the magnitude of $\frac{dw^o}{dx}$ for these cylinders, while the difference in the sign of $v^o(x)$ is a result of the difference in the sign of B_{16} for these cylinders.

As illustrated in Fig. 14 and Fig. 17, the magnitudes of the axial displacements of the $[0_2/-45/+45]_{4T}$ cylinder are larger than the magnitudes of the axial displacements of the $[+45/-45/0_2]_{4T}$ and $[+45/-45/0_2]_{2S}$ cylinders. Since all three cylinders have identical inplane stiffnesses, as dictated by A_{11} , A_{12} , A_{22} , and A_{66} , and the fact that these figures

represent displacement data based on dimensionless loads N/N^* , this difference in magnitude is a consequence of the larger magnitude of N^* for the $[0_2/-45/+45]_{4T}$ cylinder.



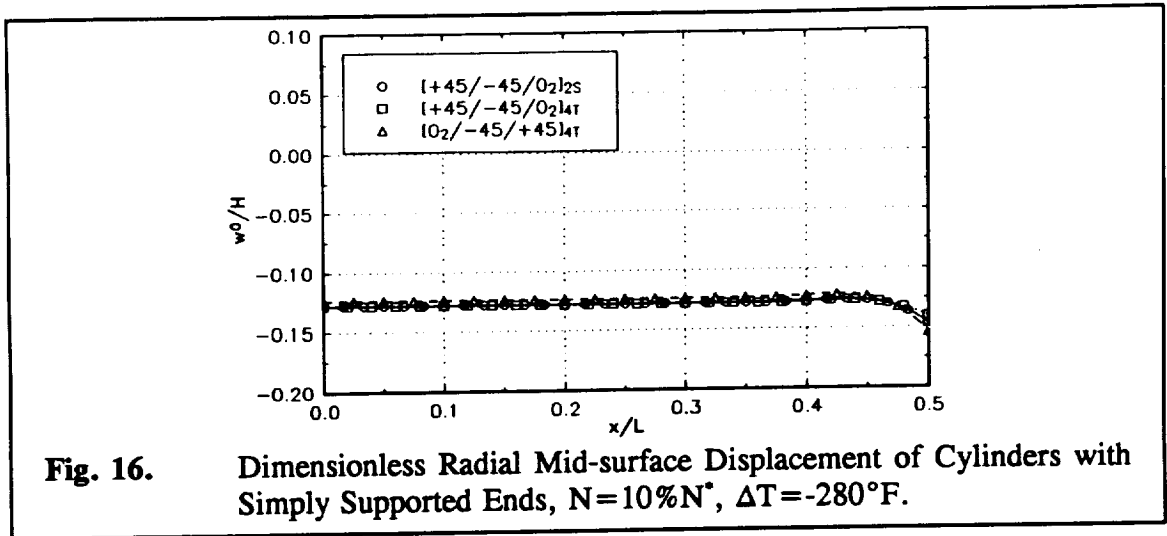


Fig. 16. Dimensionless Radial Mid-surface Displacement of Cylinders with Simply Supported Ends, $N=10\%N^*$, $\Delta T=-280^\circ\text{F}$.

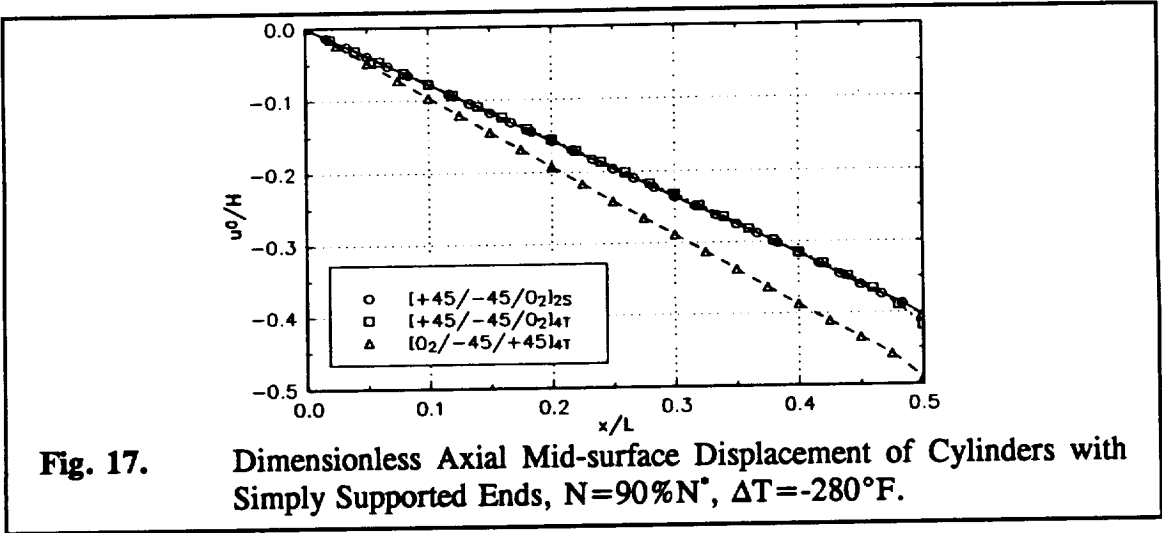


Fig. 17. Dimensionless Axial Mid-surface Displacement of Cylinders with Simply Supported Ends, $N=90\%N^*$, $\Delta T=-280^\circ\text{F}$.

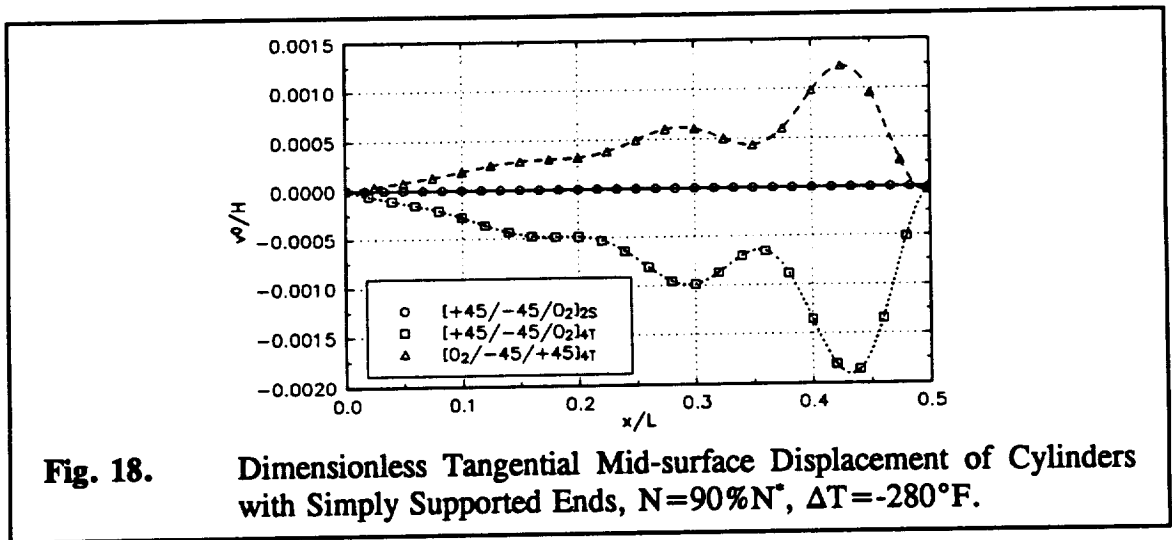
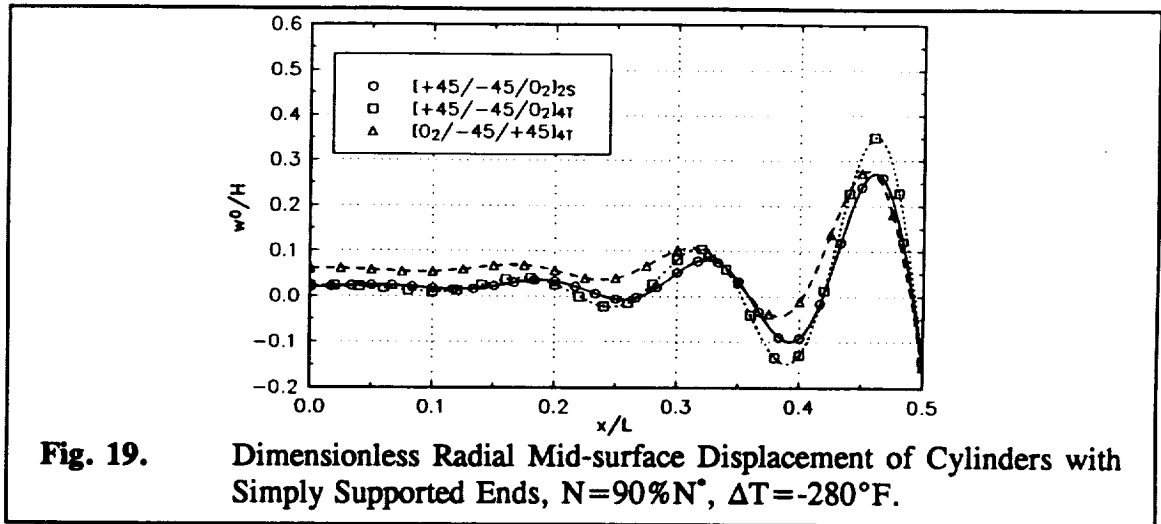


Fig. 18. Dimensionless Tangential Mid-surface Displacement of Cylinders with Simply Supported Ends, $N=90\%N^*$, $\Delta T=-280^\circ\text{F}$.



2. Clamped Boundary Conditions with Thermally-Induced Preloading Effects and a Compressive Axial Load

Since simply supported boundary conditions are difficult, if not impractical, to obtain in reality, and since the displacements of unsymmetrically laminated cylinders are large and rapidly changing near the ends of the cylinder, it is legitimate to ask if the responses of cylinders with clamped ends would be comparatively diminished.

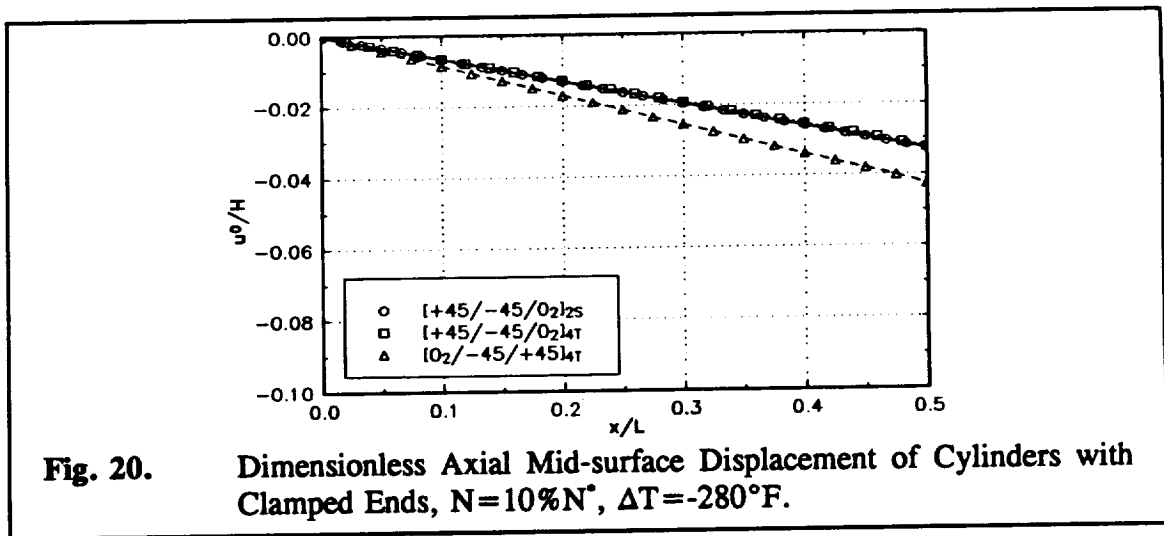
The dimensionless mid-surface displacements as a function of distance along the half length of cylinders with clamped ends are presented in Fig. 20 through Fig. 22 for $N=10\%N^*$, and Fig. 23 through Fig. 25 for $N=90\%N^*$.

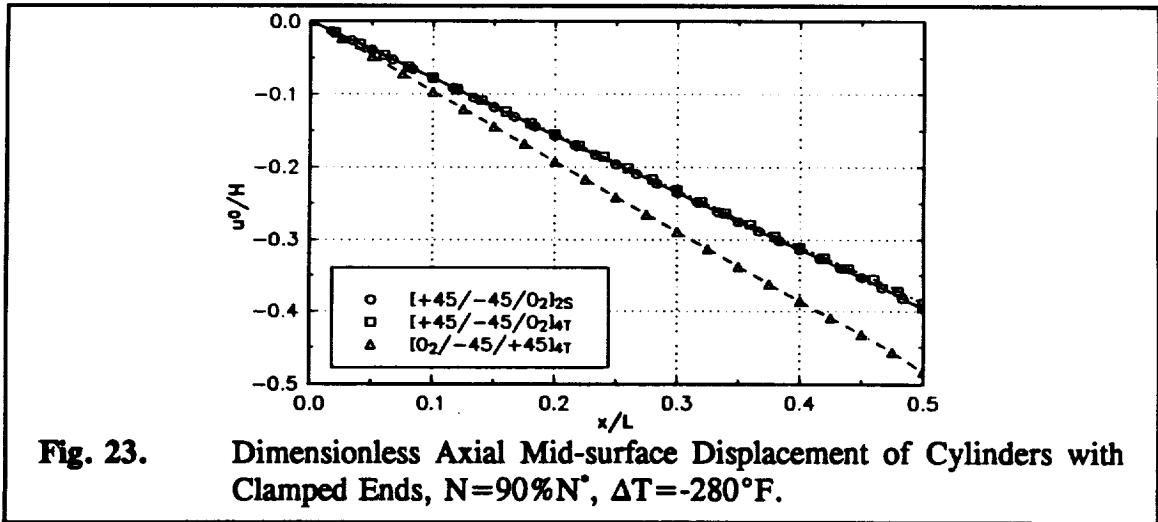
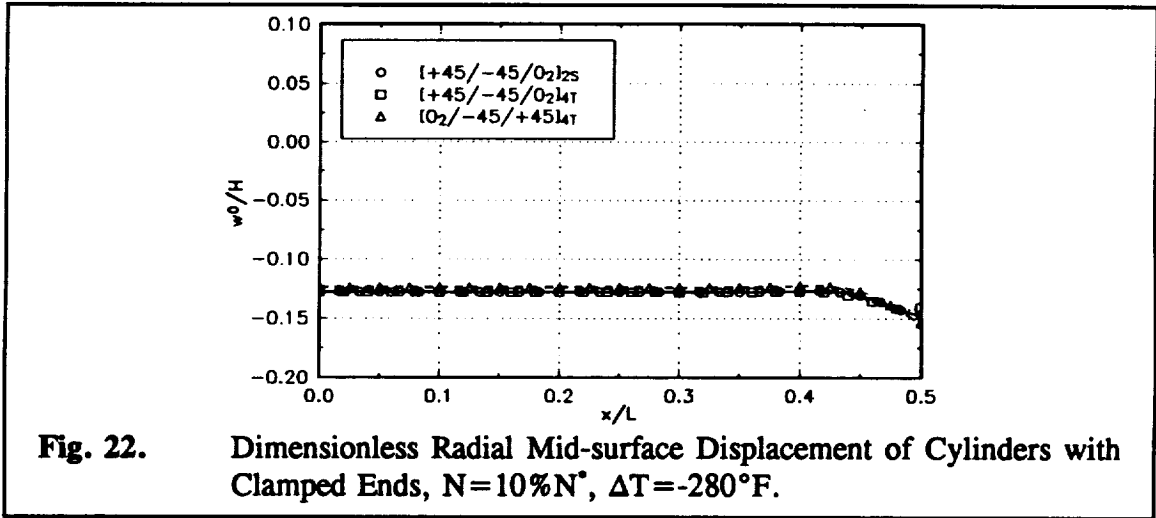
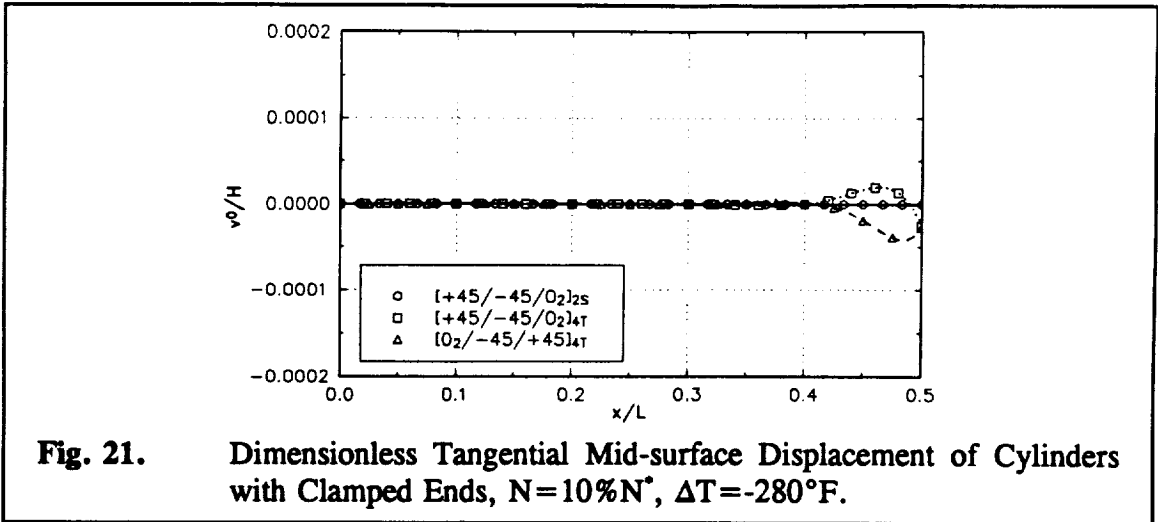
As was the case with simply supported ends, it is observed that the axial displacement is largest for the $[0_2/-45/+45]_{4T}$ cylinder. Again, this can be attributed to the fact that the value of the axial load N is significantly larger for this cylinder, relative to the other two, while the inplane stiffnesses of all three cylinders are identical.

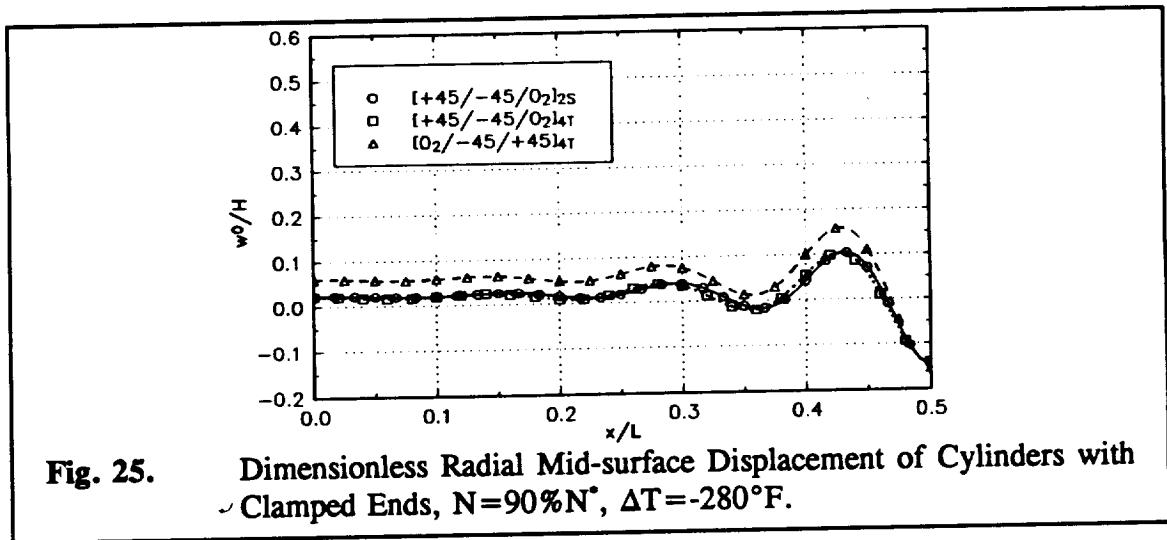
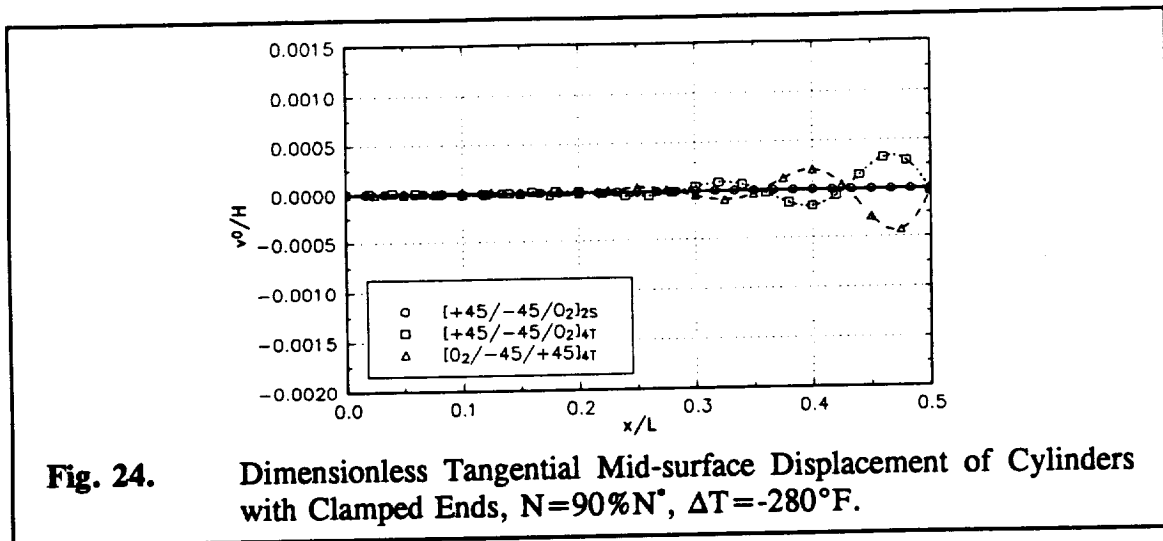
From Fig. 24 and Fig. 25, it is apparent that the maximum values of the tangential

and radial displacements of the $[0_2/-45/+45]_{4T}$ cylinder are larger than those of the $[+45/-45/0_2]_{4T}$ cylinder. This is converse to the results of the previous section, Fig. 18 and Fig. 19, where simply supported boundary conditions were imposed. In comparing the simply supported and clamped boundary condition results for $N = 90\% N^*$, it is also evident that the range of values for the tangential and radial response of the $[+45/-45/0_2]_{4T}$ and $[0_2/-45/+45]_{4T}$ cylinders with simply supported boundary conditions are broader than the range of values of these responses for the clamped boundary conditions.

Again, from Fig. 22 and Fig. 25, it can be observed that the length of the boundary layer increases with increasingly compressive axial load.







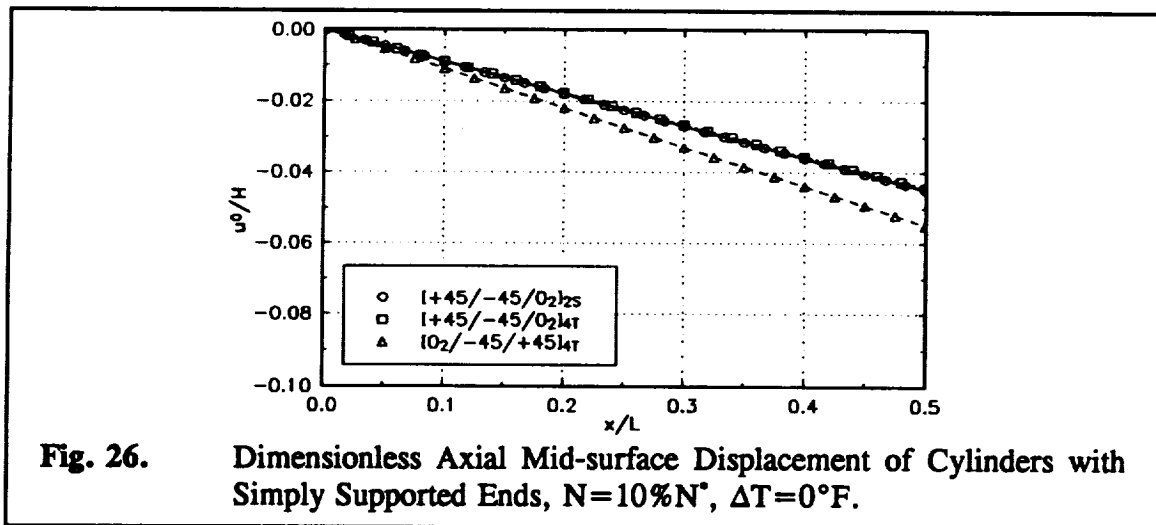
3. Effect of Neglecting to Include the Thermally-Induced Preloading Effects

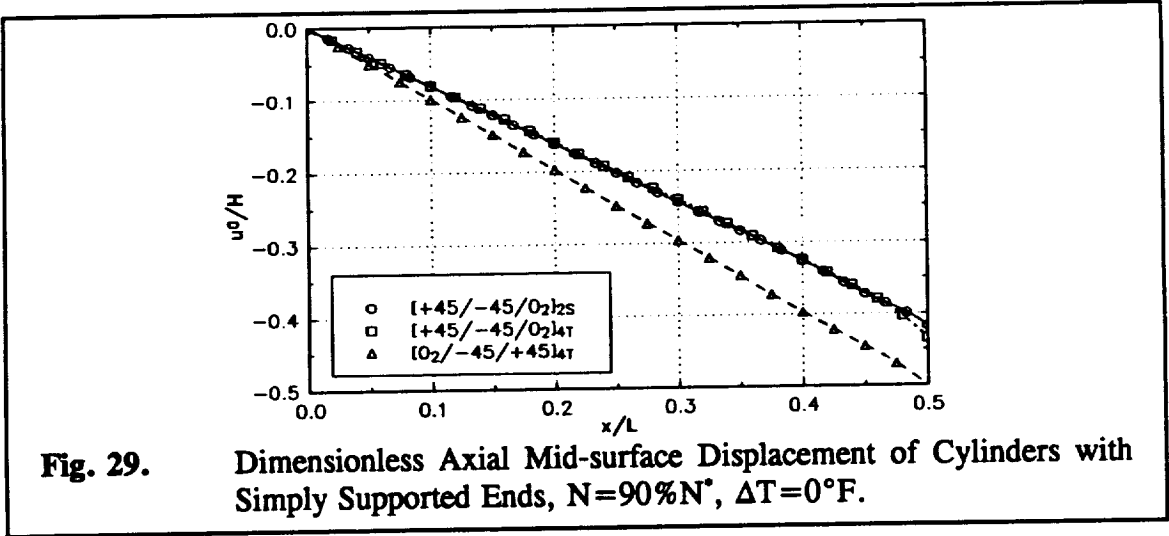
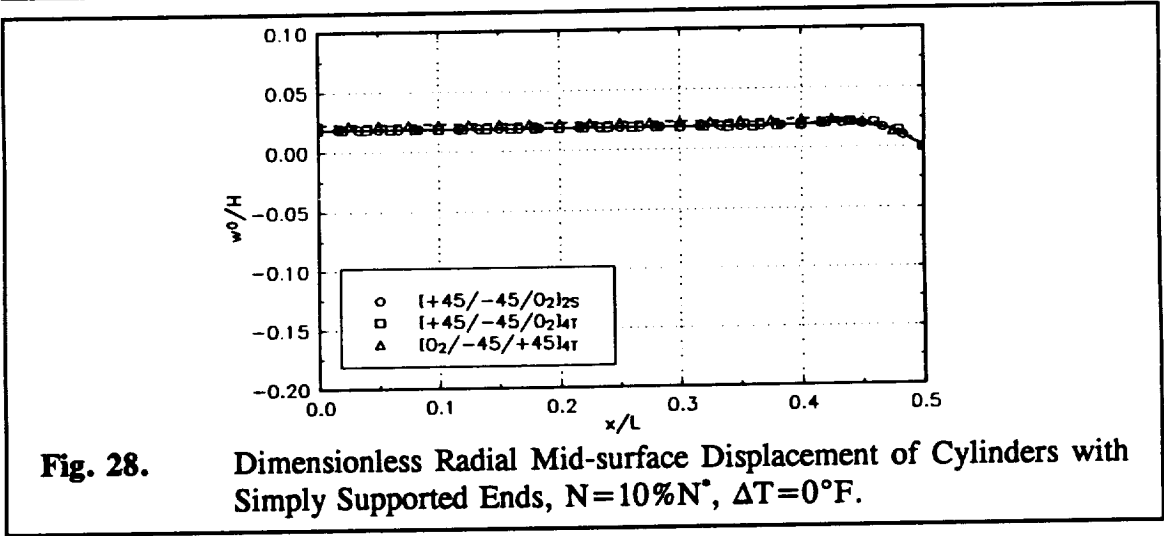
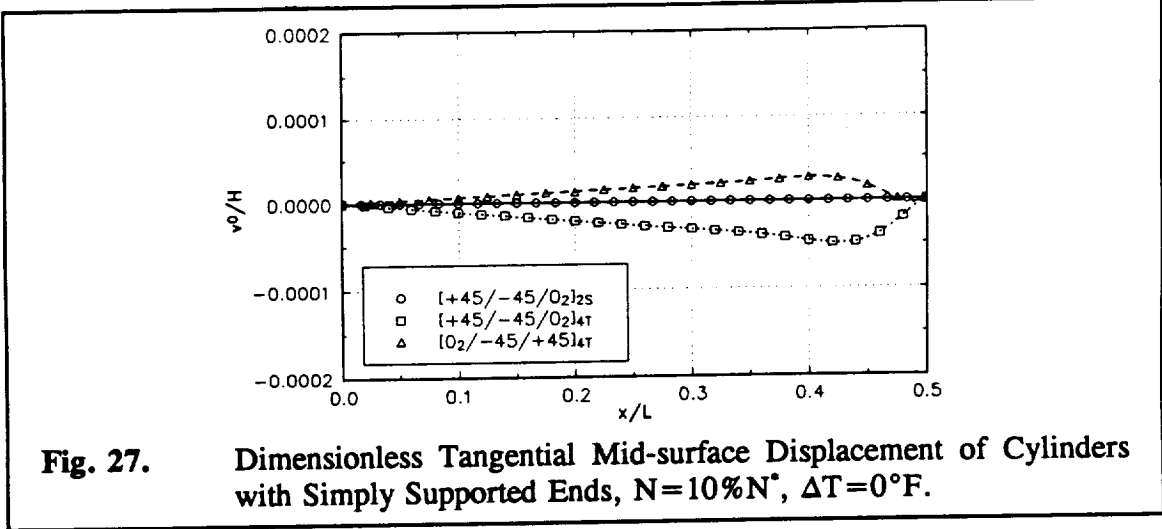
In Fig. 26 through Fig. 31, the dimensionless axial, tangential, and radial mid-surface displacements are presented for simply supported cylinders, subjected to the same axial loads as before, but neglecting to include the thermally-induced preloading effects.

Comparing the case of simply supported cylinders with thermal preloading and axial load to the case of axial load only for $N=90\%N^*$, i.e., Fig. 17 through Fig. 19 and

Fig. 29 through Fig. 31, it is evident that neglecting to include the thermally-induced preloading effects has a measurable effect on the predicted radial displacement response of the cylinders. There is not much difference in the axial or tangential displacement response. The tangential and radial responses at the mid-length of the cylinder differ between these two cases since the particular solution depends on the thermally-induced stress resultants N_x^T , N_θ^T , and M_x^T .

Fig. 32 and Fig. 33 represent the displacement responses for a $[0_8/90_8]_T$ cylinder using the same material properties as above. These figures illustrate the exaggerated effect of neglecting to include the thermally-induced preloading effects in the solution for the axially loaded case. There is a large difference between the results. This particular case was studied in ref. 1 without including thermal effects. Results such as shown in Fig. 32 and Fig. 33 certainly provide motivation to recompute the results of ref. 1 with thermal effects.





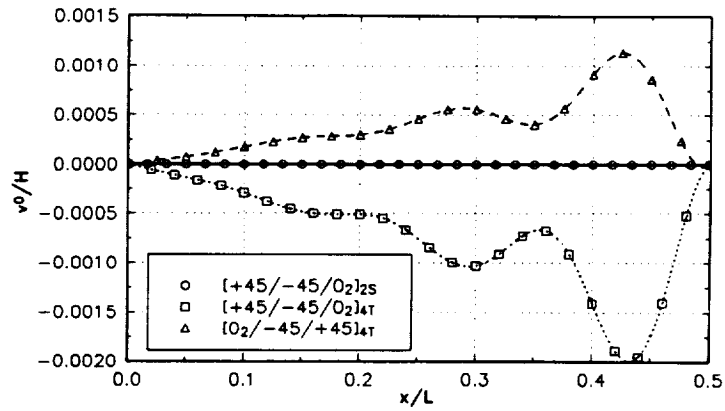


Fig. 30. Dimensionless Tangential Mid-surface Displacement of Cylinders with Simply Supported Ends, $N=90\%N^*$, $\Delta T=0^\circ\text{F}$.

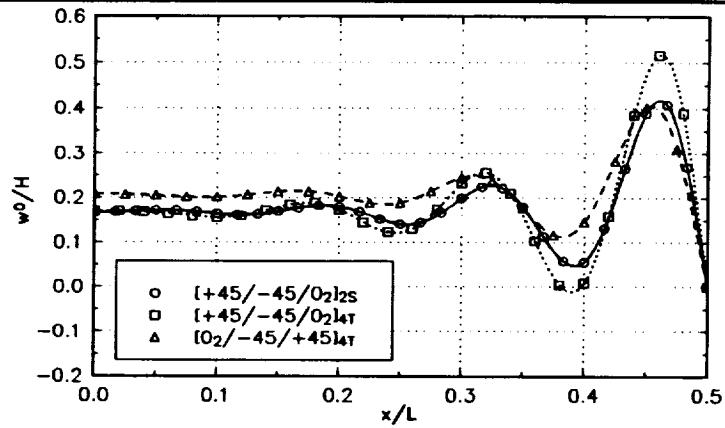


Fig. 31. Dimensionless Radial Mid-surface Displacement of Cylinders with Simply Supported Ends, $N=90\%N^*$, $\Delta T=0^\circ\text{F}$.

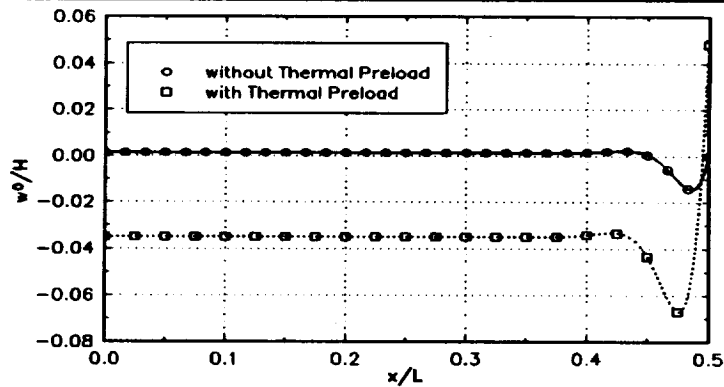


Fig. 32. Dimensionless Radial Mid-surface Displacement of a $[O_8/90_8]_T$ Cylinder with Simply Supported Ends, $N=10\%N^*$, $\Delta T=0^\circ\text{F}$ and $\Delta T=-280^\circ\text{F}$.

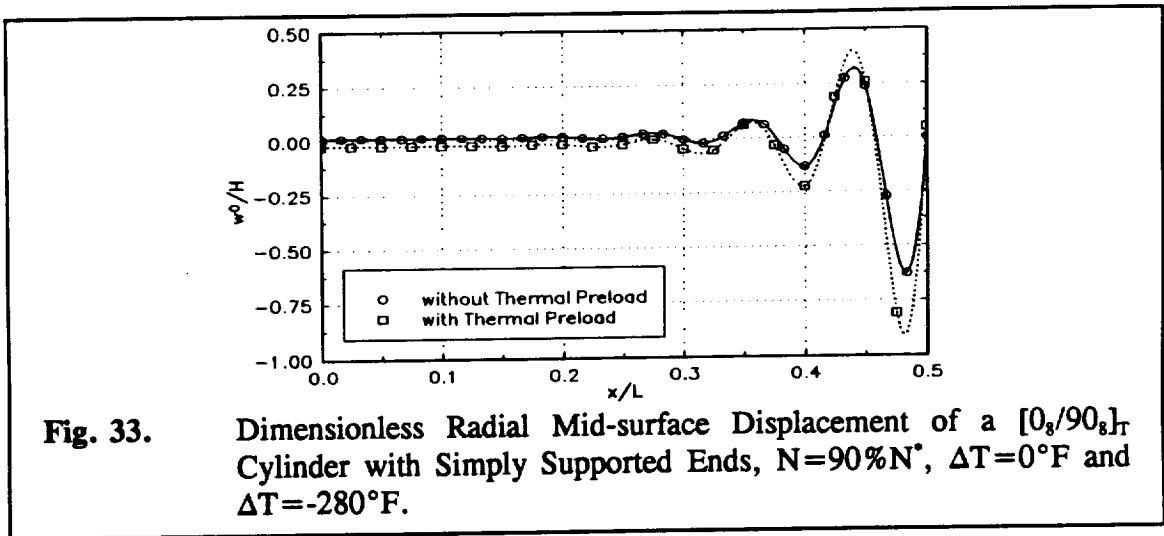


Fig. 33. Dimensionless Radial Mid-surface Displacement of a $[0_8/90_8]_T$ Cylinder with Simply Supported Ends, $N=90\%N^*$, $\Delta T=0^\circ\text{F}$ and $\Delta T=-280^\circ\text{F}$.

In the next chapter, the effects of unsymmetric stacking sequence and thermally-induced preloading on the intralaminar stress components will be investigated. The solutions to the axisymmetric problem presented thus far will be employed to compute the intralaminar stress components in the individual layers of cylinders.

IV. CALCULATION OF INTRALAMINAR STRESSES

In this chapter the equations used to calculate the principal material system stresses σ_{11} , σ_{22} , and τ_{12} within the wall of the $[+45/-45/0_2]_{2S}$, $[+45/-45/0_2]_{4T}$, and $[0_2/-45/+45]_{4T}$ cylinders will be presented, and numerical results with thermally-induced preloading effects and compressive axial load will be illustrated. The principal material system stress components σ_{11} , σ_{22} , and τ_{12} will be referred to as the principal material system intralaminar stresses. These stress components can be calculated from the principal material system strains, ϵ_{11} , ϵ_{22} , and γ_{12} , through constitutive relations. The other three stress components, $\tau_{\theta r}$, $\tau_{\theta z}$, and σ_r , are referred to as interlaminar stresses and will be discussed in a later chapter.

A. Equations Describing Intralaminar Stresses

Under the axisymmetric assumption of the previous chapter, the intralaminar strains ϵ_x , ϵ_θ , and $\gamma_{x\theta}$, in the cylinder coordinate system $x-\theta-r$ are given by eq. (12) and eq. (128), namely,

$$\begin{aligned}\epsilon_x &= \epsilon_x^o + z\kappa_x^o \\ \epsilon_\theta &= \epsilon_\theta^o + z\kappa_\theta^o \\ \gamma_{x\theta} &= \gamma_{x\theta}^o + z\kappa_{x\theta}^o,\end{aligned}$$

(12)

and

$$\begin{aligned}
 \beta_x^o &= -\frac{dw^o}{dx}; \quad \beta_\theta^o = 0 \\
 \epsilon_x^o &= \frac{du^o}{dx} + \frac{1}{2}\beta_x^{o^2}; \quad \epsilon_\theta^o = \frac{w^o}{R}; \quad \gamma_{x\theta}^o = \frac{dv^o}{dx} \\
 \kappa_x^o &= \frac{d\beta_x^o}{dx}; \quad \kappa_\theta^o = 0; \quad \kappa_{x\theta}^o = 0.
 \end{aligned}
 \tag{128}$$

In the previous chapter closed-form solutions for $u^o(x)$, $v^o(x)$, and $w^o(x)$ were presented. Therefore, the derivatives of these functions with respect to x are analytically obtainable, and the expressions in eq. (128) are known for a given temperature change, axial load, and boundary conditions.

The principal material strains can be calculated from the strains ϵ_x , ϵ_θ , and $\gamma_{x\theta}$ by coordinate transformation from the x - θ - z coordinate system to the 1-2-3 principal material coordinate system for each layer. These transformations are given by

$$\begin{Bmatrix} \epsilon_{11} \\ \epsilon_{22} \\ \frac{\gamma_{12}}{2} \end{Bmatrix} = \begin{bmatrix} \cos^2\theta & \sin^2\theta & -2\sin\theta\cos\theta \\ \sin^2\theta & \cos^2\theta & 2\sin\theta\cos\theta \\ \sin\theta\cos\theta & -\sin\theta\cos\theta & \cos^2\theta - \sin^2\theta \end{bmatrix} \begin{Bmatrix} \epsilon_x \\ \epsilon_\theta \\ \frac{\gamma_{x\theta}}{2} \end{Bmatrix}, \tag{180}$$

where θ is the angle measured from the x axis to the fiber direction (the 1-axis) of a given layer.

Once the total strains in the 1-2-3 coordinate system are known, the mechanical strains are obtained by subtracting the free thermal strains,

$$\begin{aligned}
 \epsilon_{11}^T &= \alpha_{11} \Delta T, \\
 \epsilon_{22}^T &= \alpha_{22} \Delta T,
 \end{aligned}
 \tag{181}$$

from the total strains given by eq. (180). By definition, an orthotropic layer does not have a free thermal shearing strain. Therefore, the mechanical strains are given by

$$\begin{aligned}\epsilon_{11}^M &= \epsilon_{11} - \alpha_{11} \Delta T, \\ \epsilon_{22}^M &= \epsilon_{22} - \alpha_{22} \Delta T, \\ \gamma_{12}^M &= \gamma_{12}.\end{aligned}\tag{182}$$

From these mechanical strains, the principal material system intralaminar stresses σ_{11} , σ_{22} , and τ_{12} can be calculated using the reduced stiffness matrix for each layer, i.e.,

$$\begin{Bmatrix} \sigma_{11} \\ \sigma_{22} \\ \tau_{12} \end{Bmatrix} = \begin{bmatrix} Q_{11} & Q_{12} & 0 \\ Q_{12} & Q_{22} & 0 \\ 0 & 0 & Q_{66} \end{bmatrix} \begin{Bmatrix} \epsilon_{11}^M \\ \epsilon_{22}^M \\ \gamma_{12}^M \end{Bmatrix}.\tag{183}$$

The reduced stiffnesses are

$$\begin{aligned}Q_{11} &= \frac{E_1}{1 - \nu_{12}\nu_{21}}, \\ Q_{12} &= \frac{\nu_{12}E_2}{1 - \nu_{12}\nu_{21}}, \\ Q_{22} &= \frac{E_2}{1 - \nu_{12}\nu_{21}}, \\ Q_{66} &= G_{12},\end{aligned}\tag{184}$$

where E_1 , E_2 , ν_{12} , and G_{12} are known for a given orthotropic layer and ν_{21} is calculated by

$$v_{21} = \frac{v_{12} E_2}{E_1} . \quad (185)$$

The values for the layer material properties used in these analyses were given in the previous chapter in Table I.

B. Numerical Results for Intralaminar Stresses: Case of Thermally-Induced Preloading Effects and a Compressive Axial Load with Clamped Boundary Conditions

Since clamped boundary conditions more closely represent actual applications of cylinders, the remainder of the analyses will focus on clamped boundary conditions. Again, the three cylinders of interest have a length to radius ratio of 3, a radius to thickness ratio of 125, and have $[+45/-45/0_2]_{2S}$, $[+45/-45/0_2]_{4T}$, and $[0_2/-45/+45]_{4T}$ stacking sequences. The thermal preloading effects are due to a temperature change, ΔT , equal to -280°F .

The numerical results to be presented in this chapter are principal material system intralaminar stresses in various groups of layers within the cylinder wall. The stresses are normalized by the quantity (N/H) , where N is the compressive axial load and H is the wall thickness, 0.080 in. The quantity (N/H) represents the average axial stress in the cylinder wall. The stress components are reported at the mid-thickness location of each layer. The two axial load levels investigated are given by fractions of the load N^* , i.e., $N = 10\% N^*$ and $N = 90\% N^*$.

For each cylinder and load case, six figures are presented. There are two figures for

each of the mid-layer principal material system intralaminar stress components, σ_{11} , σ_{22} , and τ_{12} ; one figure for the 0° layers and one figure for the $\pm 45^\circ$ layers. Due to the difference in magnitude of the respective stress components in these two groups of layers, two figures can be used. For each cylinder and load case the vertical scale of each of the six respective figures is the same for comparative purposes. Since the magnitudes of the stress components are largest near the ends of the cylinders, the horizontal scale includes only the portion of the half-length of the cylinder from $x/L=0.3$ to $x/L=0.5$. Where possible, the layer number in the stacking sequence is printed next to the respective layer's stress component relation in the figures. Where the relations are too closely spaced in the figures, the direction of increasing layer numbering in the stacking sequence is shown with arrows. Recall, layer no. 1 is at the inner most radial position.

The first three sets of figures, Fig. 34 through Fig. 36, represent principal material system intralaminar stress results for the three cylinders subjected to a compressive axial load of $N = 10\% N^*$, including thermally-induced preloading effects, i.e., with a temperature change, ΔT , equal to -280°F . The next three sets of figures, Fig. 37 through Fig. 39, represent principal intralaminar stress results for the three cylinders subjected to a compressive axial load of $N = 90\% N^*$, including thermally-induced preloading effects. The last set of figures, Fig. 40, represent principal intralaminar stress results for the $[+45/-45/0_2]_{4T}$ cylinder subjected to a compressive axial load of $N = 90\% N^*$, neglecting thermally-induced preloading effects, i.e., with a temperature change, ΔT , equal to 0° .

C. Discussion of Intralaminar Stress Results

For the low load level for the $[+45/-45/0_2]_{2S}$ laminate, Fig. 34, the fiber-direction stresses, σ_{11} , are higher in the $\pm 45^\circ$ layers than the 0° layers. Since the 0° layers are aligned with the applied load and thus will directly bear the load, it is surprising that the fiber-direction stresses are not higher in the 0° layers. This anomaly is no doubt due to the thermally-induced effects dominating at this low load level. This will be seen shortly. The intralaminar stresses perpendicular to the fibers, σ_{22} , are about the same for the 0° layers as for the $\pm 45^\circ$ layers. The shear stresses are small, being zero in the 0° layers and equal and opposite in the $\pm 45^\circ$ layers.

For the low load level, the stresses in the $[+45/-45/0_2]_{4T}$ laminate, Fig. 35, are similar in magnitude and spatial distribution to the stresses in the symmetric laminate. The primary difference between the unsymmetric laminate and the symmetric laminate is a minor level of shear stress in the 0° layers of the unsymmetric laminate.

The stress levels at the low load level in the $[0_2/-45/+45]_{4T}$ laminate, Fig. 36, are similar to the stresses in the $[+45/-45/0_2]_{2S}$ and $[+45/-45/0_2]_{4T}$ laminates. The fiber-direction stresses in the 45° layers, at the end of the cylinder, are somewhat lower for the $[0_2/-45/+45]_{4T}$ laminate than for the other two laminates. The compressive stresses perpendicular to the fibers, σ_{22} , are not as high as for the $[0_2/-45/+45]_{4T}$ laminate as for the other two. The same is true for the shear stresses in the $\pm 45^\circ$ layers, though the difference in stress levels for one laminate to the other two is of little consequence for this low load level.

For the high load level and the symmetrically laminated cylinder, Fig. 37, the fiber-

direction stress levels in the 0° layers, the load bearing layers, are higher than in the $\pm 45^\circ$ layers. Apparently, at the low load level, Fig. 34a and Fig. 34b, thermal effects do dominate but at the higher load level, they are in the background. This will be discussed more shortly.

The stress levels in the two unsymmetric laminates at the high load are quite similar to the stress levels in the symmetric laminate at that load level. The intralaminar stresses perpendicular to the fiber-direction, σ_{22} , are compressive, thus virtually eliminating the potential for micro-cracking due to this stress component. The shear stresses in the $\pm 45^\circ$ layers for the three laminates could lead to matrix cracking, but they are low, even for this high load level.

To provide an indication of the magnitude of the thermally-induced intralaminar stresses, the stresses in the $[+45/-45/0_2]_{4T}$ cylinder with the high load level but not including thermal effects are shown in Fig. 40. These should be compared directly with Fig. 38, the same laminate and same load level, but with thermal effects included. All stresses except the fiber-direction stress in the 0° layers shows some influence of the thermal effects. By comparing Fig. 38c and Fig. 38d with Fig. 40c and Fig. 40d, it appears as though the intralaminar stresses perpendicular to the fibers, σ_{22} , due to thermal effects, are compressive. Also, when comparing Fig. 38f with Fig. 40f, it can be concluded that thermal effects relieve somewhat the intralaminar stress in the $\pm 45^\circ$ layers.

It should be noted that the solutions for the intralaminar stresses obtained to this point can be used directly in a failure criterion associated with classical lamination theory

(CLT). However, since the failure of a cylinder on a material failure basis also consists of determining whether delamination occurs for a given load case, a method for determining the interlaminar stresses is needed.

In the following chapters, the analyses performed thus far will be used to derive solutions for the interlaminar stress components within the cylinder wall.

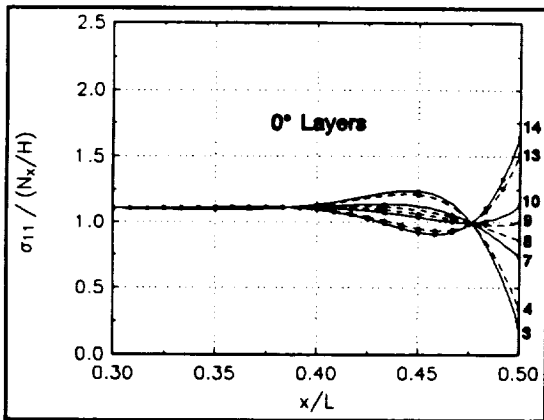


Fig. 34a. σ_{11} along x/L for 0° Layers of a $[+45/-45/0_2]_{2S}$ Cylinder, $N=10\%N^*$, $\Delta T=-280^\circ F$.

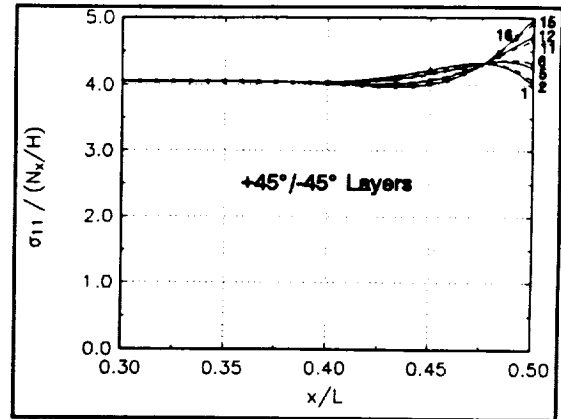


Fig. 34b. σ_{11} along x/L for 45° Layers of a $[+45/-45/0_2]_{2S}$ Cylinder, $N=10\%N^*$, $\Delta T=-280^\circ F$.

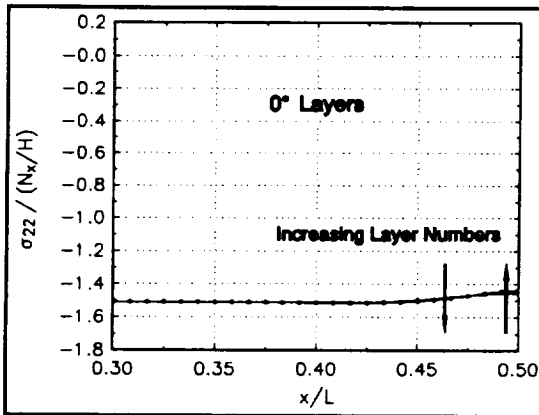


Fig. 34c. σ_{22} along x/L for 0° Layers of a $[+45/-45/0_2]_{2S}$ Cylinder, $N=10\%N^*$, $\Delta T=-280^\circ F$.

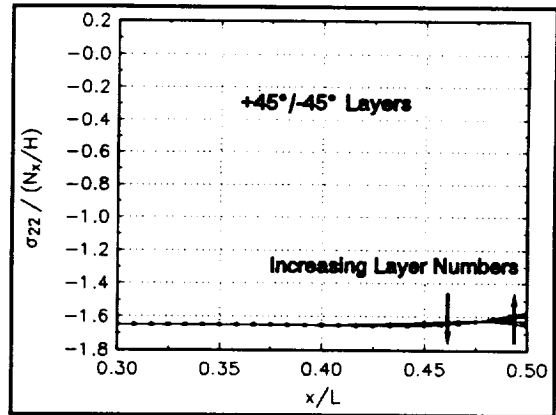


Fig. 34d. σ_{22} along x/L for 45° Layers of a $[+45/-45/0_2]_{2S}$ Cylinder, $N=10\%N^*$, $\Delta T=-280^\circ F$.

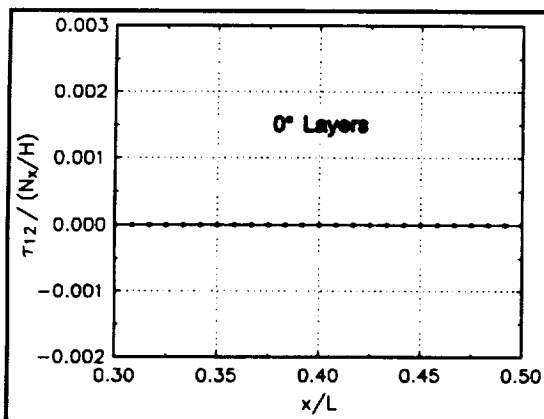


Fig. 34e. τ_{12} along x/L for 0° Layers of a $[+45/-45/0_2]_{2S}$ Cylinder, $N=10\%N^*$, $\Delta T=-280^\circ F$.

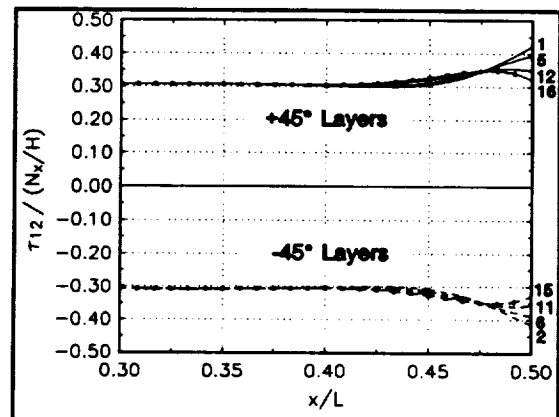


Fig. 34f. τ_{12} along x/L for 45° Layers of a $[+45/-45/0_2]_{2S}$ Cylinder, $N=10\%N^*$, $\Delta T=-280^\circ F$.

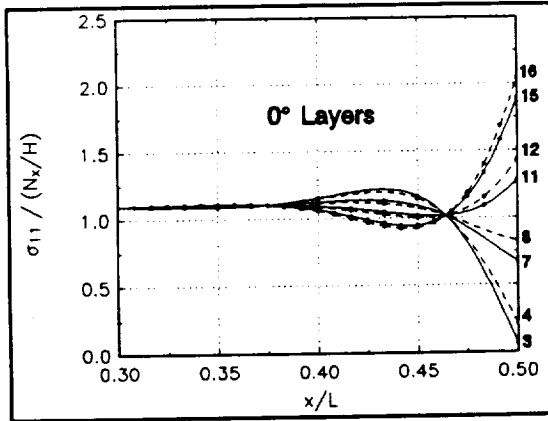


Fig. 35a. σ_{11} along x/L for 0° Layers of a $[+45/-45/0_2]_{4T}$ Cylinder, $N=10\%N^*$, $\Delta T=-280^\circ\text{F}$.

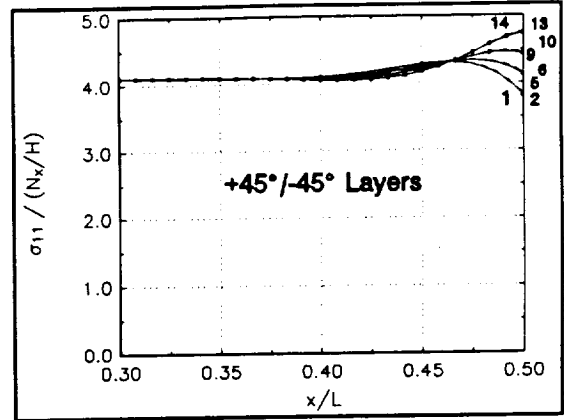


Fig. 35b. σ_{11} along x/L for 45° Layers of a $[+45/-45/0_2]_{4T}$ Cylinder, $N=10\%N^*$, $\Delta T=-280^\circ\text{F}$.

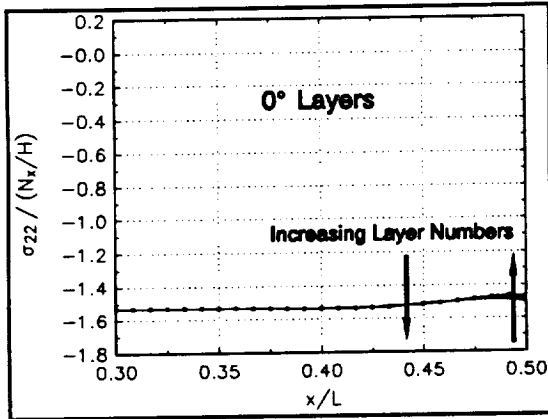


Fig. 35c. σ_{22} along x/L for 0° Layers of a $[+45/-45/0_2]_{4T}$ Cylinder, $N=10\%N^*$, $\Delta T=-280^\circ\text{F}$.

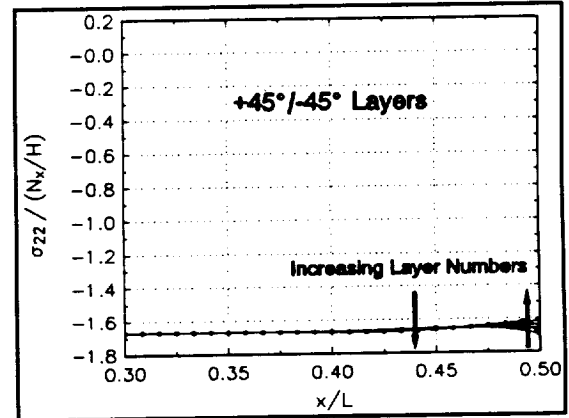


Fig. 35d. σ_{22} along x/L for 45° Layers of a $[+45/-45/0_2]_{4T}$ Cylinder, $N=10\%N^*$, $\Delta T=-280^\circ\text{F}$.

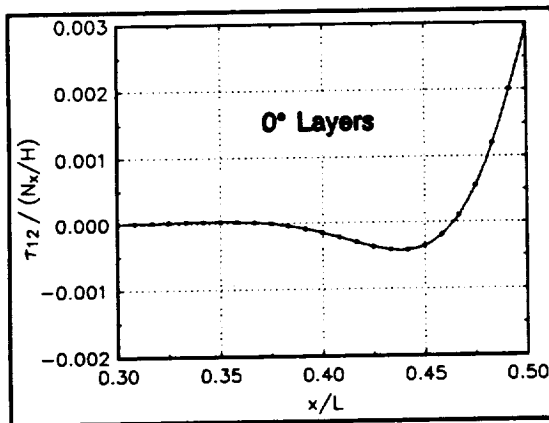


Fig. 35e. τ_{12} along x/L for 0° Layers of a $[+45/-45/0_2]_{4T}$ Cylinder, $N=10\%N^*$, $\Delta T=-280^\circ\text{F}$.

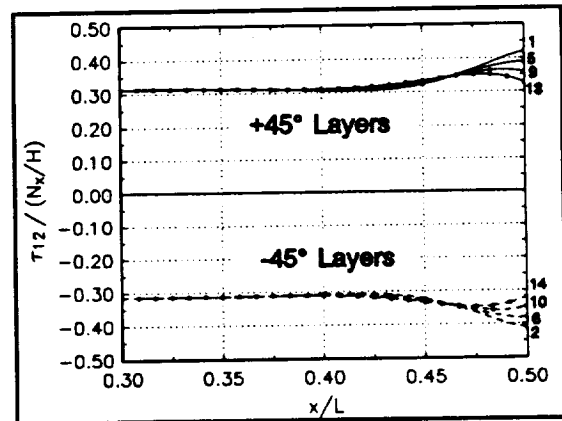


Fig. 35f. τ_{12} along x/L for 45° Layers of a $[+45/-45/0_2]_{4T}$ Cylinder, $N=10\%N^*$, $\Delta T=-280^\circ\text{F}$.

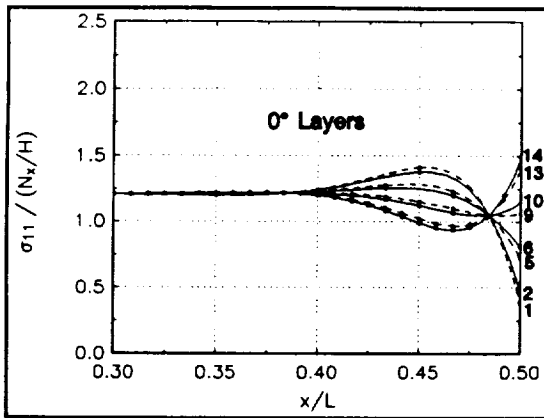


Fig. 36a. σ_{11} along x/L for 0° Layers of a $[0_2/-45/+45]_{4T}$ Cylinder, $N=10\%N^*$, $\Delta T=-280^\circ F$.

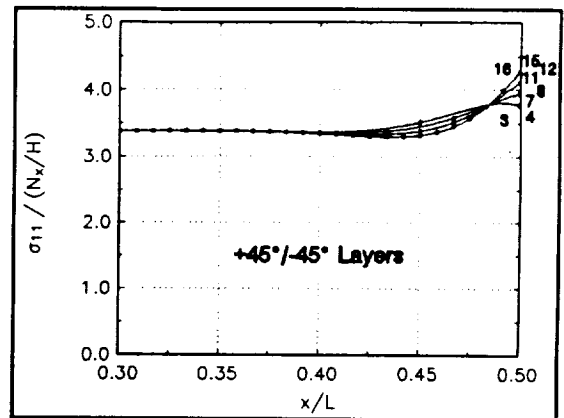


Fig. 36b. σ_{11} along x/L for 45° Layers of a $[0_2/-45/+45]_{4T}$ Cylinder, $N=10\%N^*$, $\Delta T=-280^\circ F$.

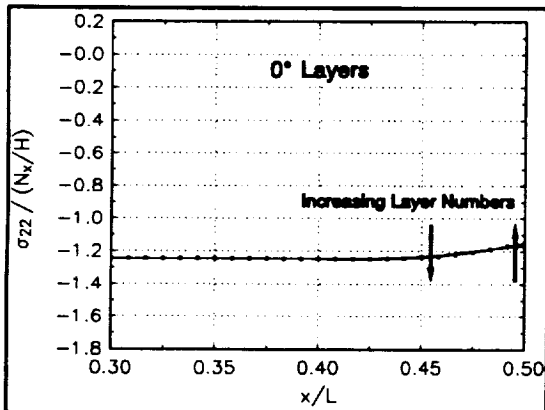


Fig. 36c. σ_{22} along x/L for 0° Layers of a $[0_2/-45/+45]_{4T}$ Cylinder, $N=10\%N^*$, $\Delta T=-280^\circ F$.

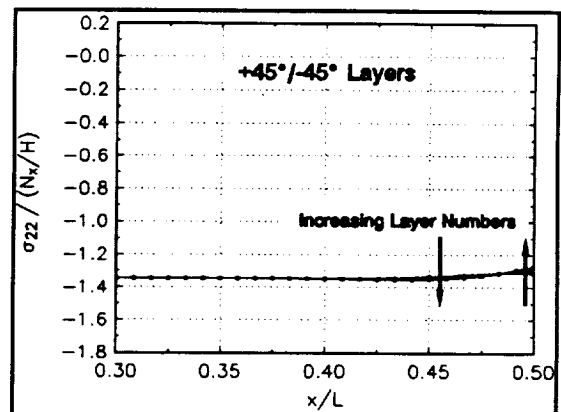


Fig. 36d. σ_{22} along x/L for 45° Layers of a $[0_2/-45/+45]_{4T}$ Cylinder, $N=10\%N^*$, $\Delta T=-280^\circ F$.

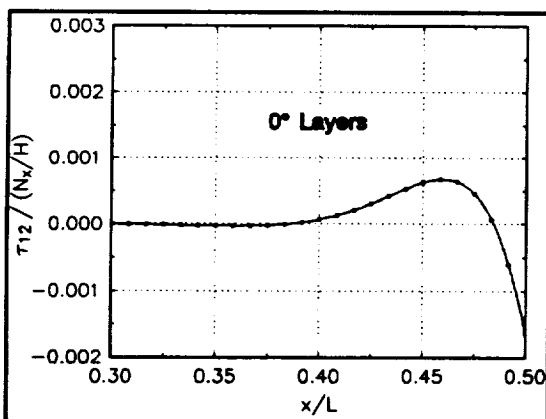


Fig. 36e. τ_{12} along x/L for 0° Layers of a $[0_2/-45/+45]_{4T}$ Cylinder, $N=10\%N^*$, $\Delta T=-280^\circ F$.

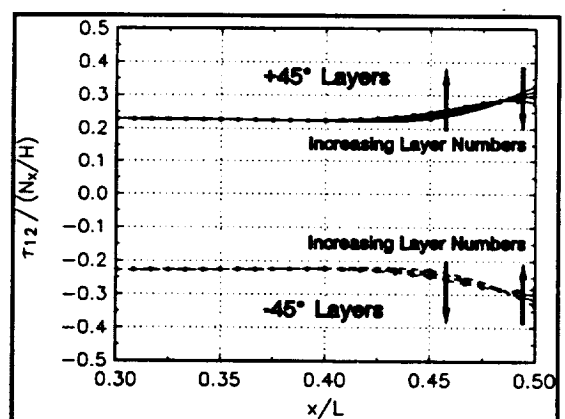


Fig. 36f. τ_{12} along x/L for 45° Layers of a $[0_2/-45/+45]_{4T}$ Cylinder, $N=10\%N^*$, $\Delta T=-280^\circ F$.

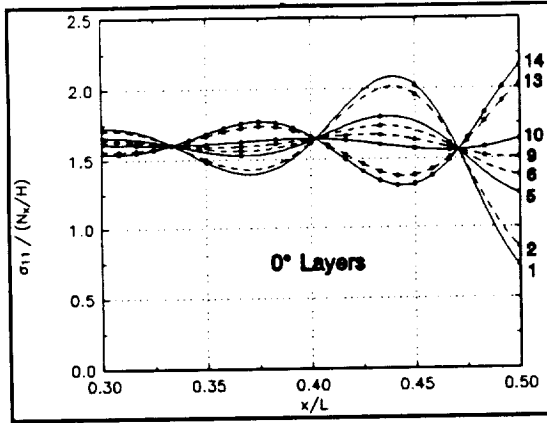


Fig. 37a. σ_{11} along x/L for 0° Layers of a $[+45/-45/0_2]_{2S}$ Cylinder, $N=90\%N^*$, $\Delta T=-280^\circ F$.

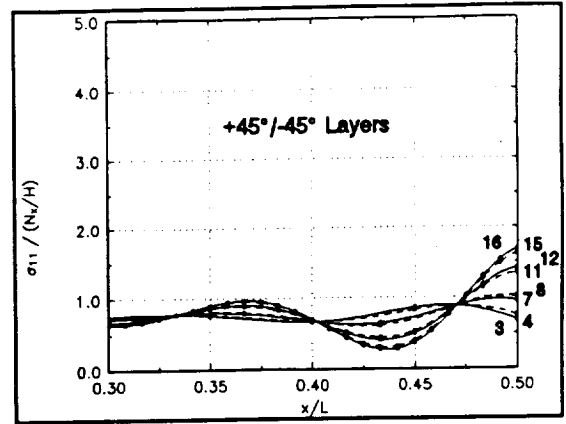


Fig. 37b. σ_{11} along x/L for 45° Layers of a $[+45/-45/0_2]_{2S}$ Cylinder, $N=90\%N^*$, $\Delta T=-280^\circ F$.

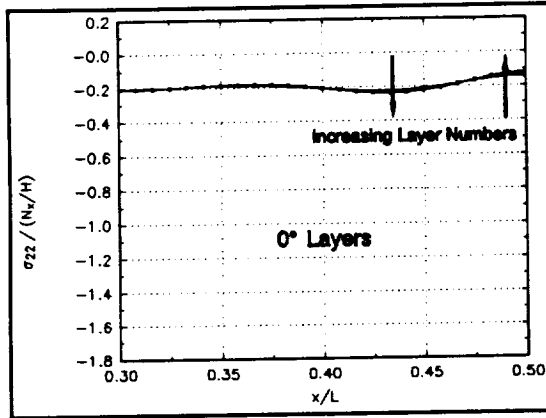


Fig. 37c. σ_{22} along x/L for 0° Layers of a $[+45/-45/0_2]_{2S}$ Cylinder, $N=90\%N^*$, $\Delta T=-280^\circ F$.

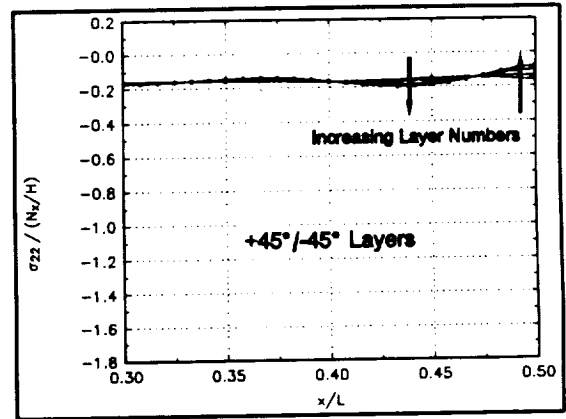


Fig. 37d. σ_{22} along x/L for 45° Layers of a $[+45/-45/0_2]_{2S}$ Cylinder, $N=90\%N^*$, $\Delta T=-280^\circ F$.

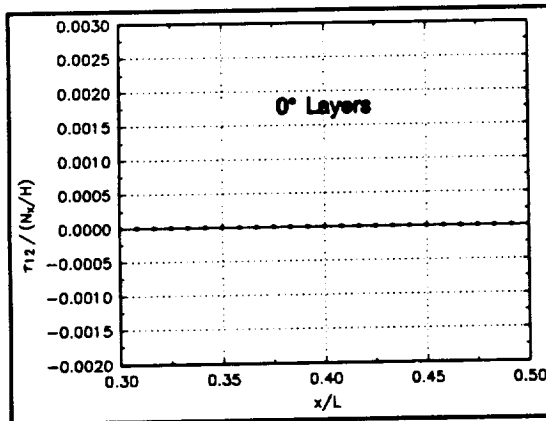


Fig. 37e. τ_{12} along x/L for 0° Layers of a $[+45/-45/0_2]_{2S}$ Cylinder, $N=90\%N^*$, $\Delta T=-280^\circ F$.

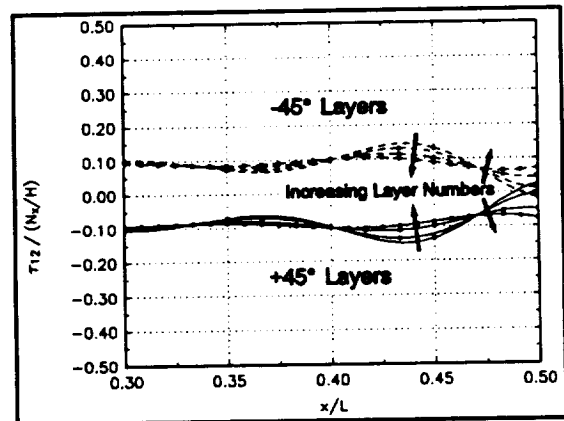


Fig. 37f. τ_{12} along x/L for 45° Layers of a $[+45/-45/0_2]_{2S}$ Cylinder, $N=90\%N^*$, $\Delta T=-280^\circ F$.

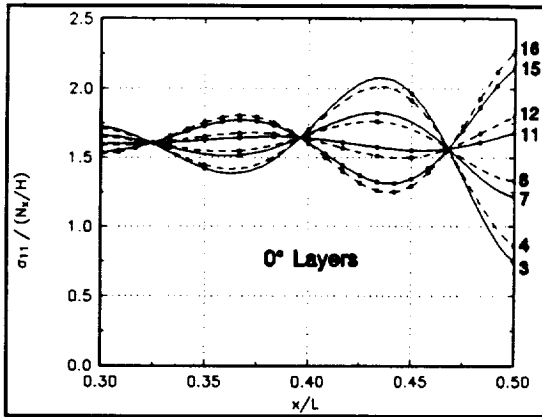


Fig. 38a. σ_{11} along x/L for 0° Layers of a $[+45/-45/0_2]_{4T}$ Cylinder, $N=90\%N^*$, $\Delta T=-280^\circ F$.

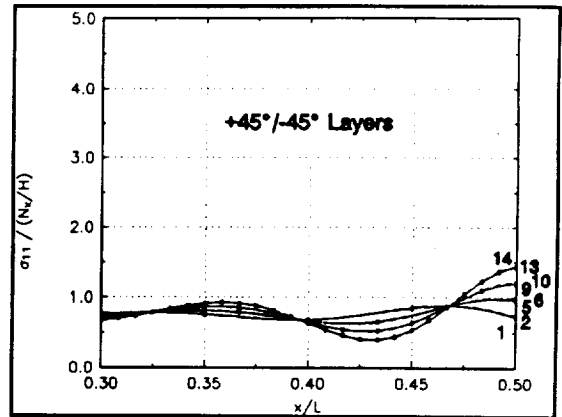


Fig. 38b. σ_{11} along x/L for 45° Layers of a $[+45/-45/0_2]_{4T}$ Cylinder, $N=90\%N^*$, $\Delta T=-280^\circ F$.

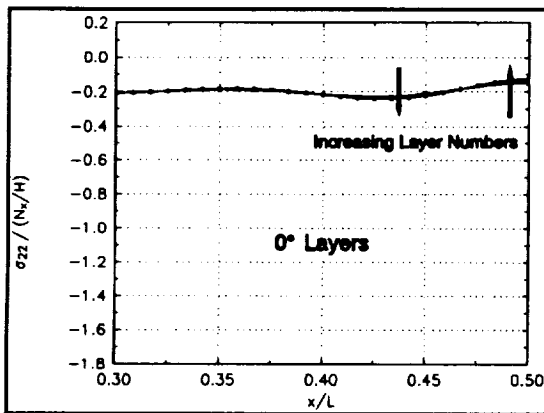


Fig. 38c. σ_{22} along x/L for 0° Layers of a $[+45/-45/0_2]_{4T}$ Cylinder, $N=90\%N^*$, $\Delta T=-280^\circ F$.

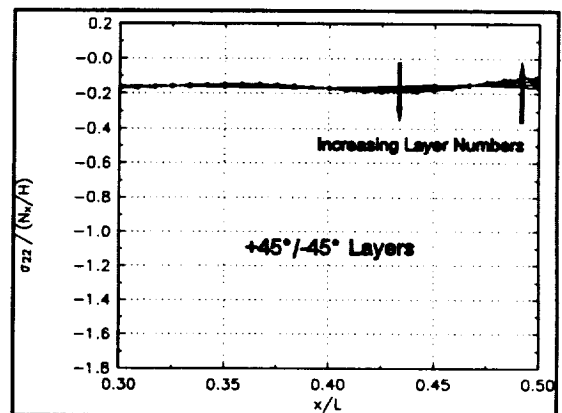


Fig. 38d. σ_{22} along x/L for 45° Layers of a $[+45/-45/0_2]_{4T}$ Cylinder, $N=90\%N^*$, $\Delta T=-280^\circ F$.

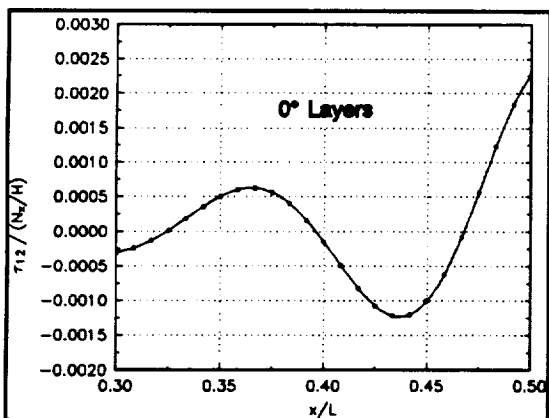


Fig. 38e. τ_{12} along x/L for 0° Layers of a $[+45/-45/0_2]_{4T}$ Cylinder, $N=90\%N^*$, $\Delta T=-280^\circ F$.

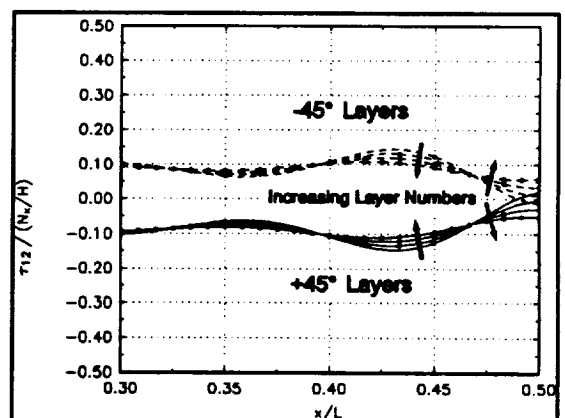


Fig. 38f. τ_{12} along x/L for 45° Layers of a $[+45/-45/0_2]_{4T}$ Cylinder, $N=90\%N^*$, $\Delta T=-280^\circ F$.

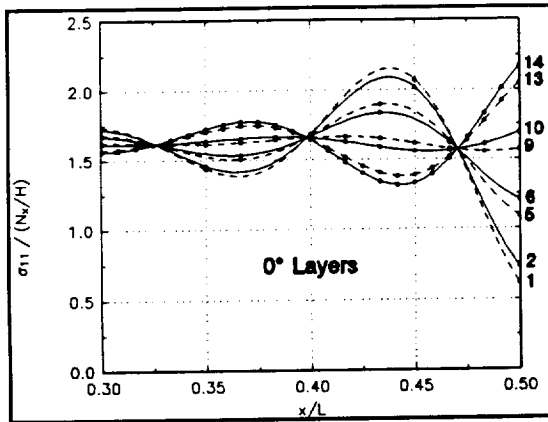


Fig. 39a. σ_{11} along x/L for 0° Layers of a $[0_2/-45/+45]_{4T}$ Cylinder, $N=90\%N^*$, $\Delta T=-280^\circ\text{F}$.

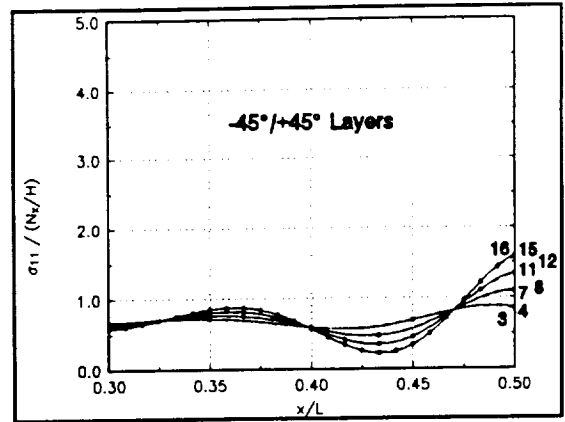


Fig. 39b. σ_{11} along x/L for 45° Layers of a $[0_2/-45/+45]_{4T}$ Cylinder, $N=90\%N^*$, $\Delta T=-280^\circ\text{F}$.

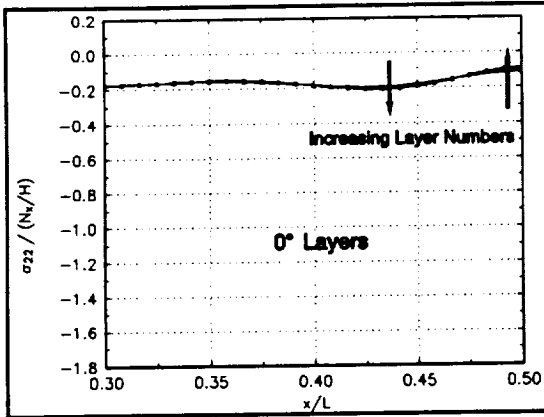


Fig. 39c. σ_{22} along x/L for 0° Layers of a $[0_2/-45/+45]_{4T}$ Cylinder, $N=90\%N^*$, $\Delta T=-280^\circ\text{F}$.

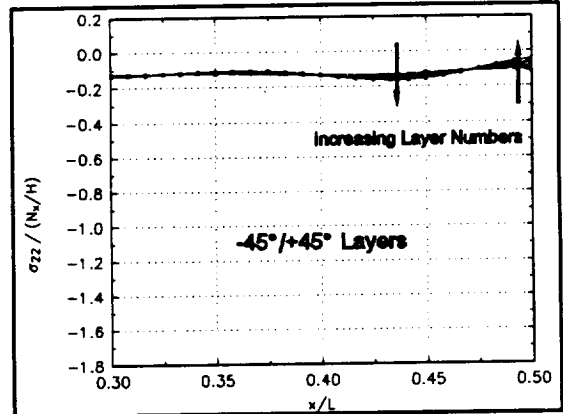


Fig. 39d. σ_{22} along x/L for 45° Layers of a $[0_2/-45/+45]_{4T}$ Cylinder, $N=90\%N^*$, $\Delta T=-280^\circ\text{F}$.

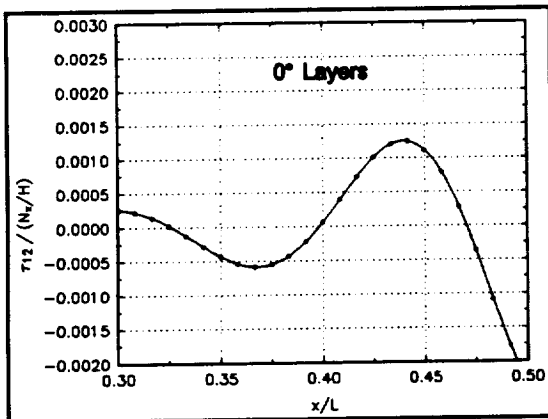


Fig. 39e. τ_{12} along x/L for 0° Layers of a $[0_2/-45/+45]_{4T}$ Cylinder, $N=90\%N^*$, $\Delta T=-280^\circ\text{F}$.

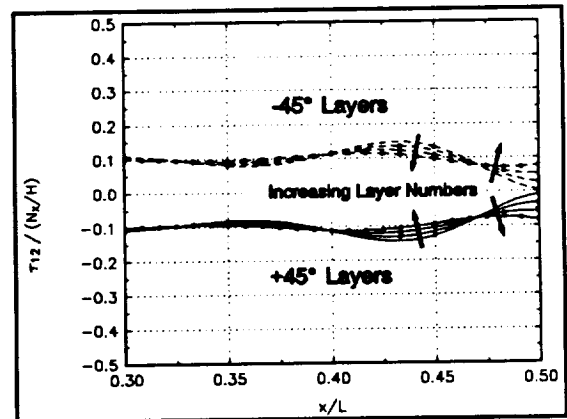


Fig. 39f. τ_{12} along x/L for 45° Layers of a $[0_2/-45/+45]_{4T}$ Cylinder, $N=90\%N^*$, $\Delta T=-280^\circ\text{F}$.

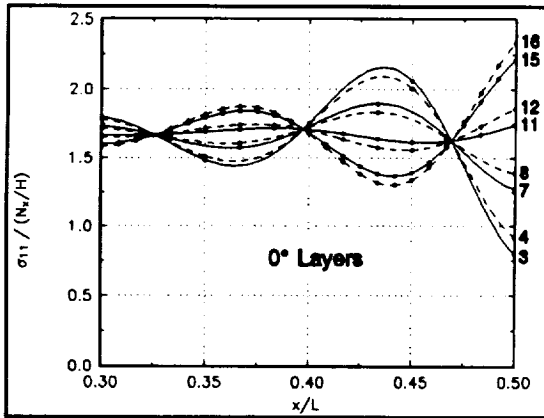


Fig. 40a. σ_{11} along x/L for 0° Layers of a $[+45/-45/0_2]_{4T}$ Cylinder, $N=90\%N^*$, $\Delta T=0^\circ F$.

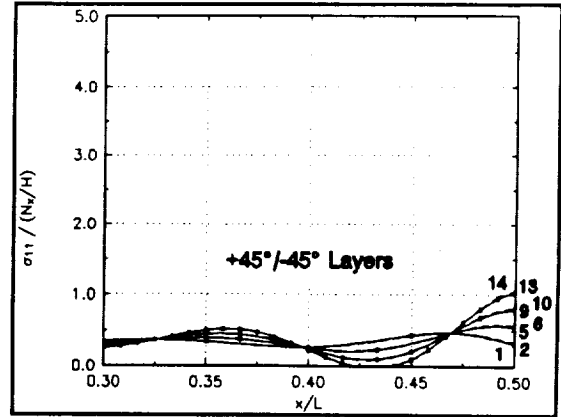


Fig. 40b. σ_{11} along x/L for 45° Layers of a $[+45/-45/0_2]_{4T}$ Cylinder, $N=90\%N^*$, $\Delta T=0^\circ F$.

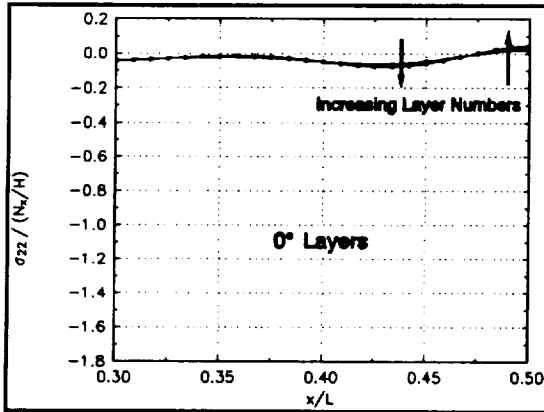


Fig. 40c. σ_{22} along x/L for 0° Layers of a $[+45/-45/0_2]_{4T}$ Cylinder, $N=90\%N^*$, $\Delta T=0^\circ F$.

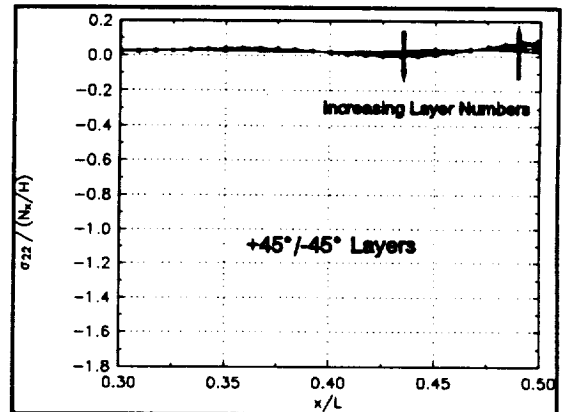


Fig. 40d. σ_{22} along x/L for 45° Layers of a $[+45/-45/0_2]_{4T}$ Cylinder, $N=90\%N^*$, $\Delta T=0^\circ F$.

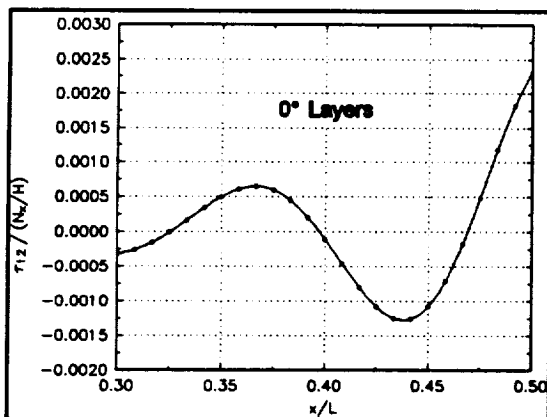


Fig. 40e. τ_{12} along x/L for 0° Layers of a $[+45/-45/0_2]_{4T}$ Cylinder, $N=90\%N^*$, $\Delta T=0^\circ F$.

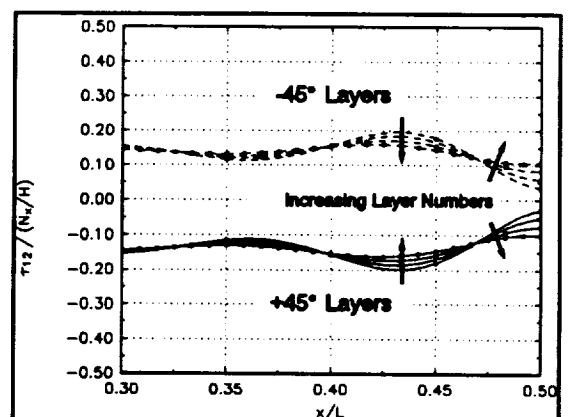


Fig. 40f. τ_{12} along x/L for 45° Layers of a $[+45/-45/0_2]_{4T}$ Cylinder, $N=90\%N^*$, $\Delta T=0^\circ F$.

V. DERIVATION OF THE THREE-DIMENSIONAL EQUILIBRIUM EQUATIONS IN CYLINDRICAL COORDINATES

In the previous chapters, the assumptions of thin shell theory and axisymmetry have been employed in order to obtain closed-form solutions for the response of composite cylinders. This method has provided relations for the displacements and intralaminar strains and stresses as functions of the axial and radial coordinates.

As a practical matter, it is important not to ignore the existence of the stresses at the layer-to-layer interfaces of the cylinder. These stress components are the shear stress components τ_{xz} and $\tau_{\theta r}$, and the normal stress σ_r . These three stresses will be referred to as interlaminar stresses. If acceptable levels for the interlaminar stresses are exceeded, delamination of the layers can result, leading to a structural failure. The theory presented thus far incorporates classical lamination theory (CLT) which assumes a state of plane stress, i.e., that the interlaminar stresses can be ignored. Therefore, a different set of governing equations is required in order to calculate the interlaminar stresses.

The aim of the remainder of this work is to calculate the interlaminar stresses by using the solutions for the intralaminar stresses derived in the previous chapters. The procedure used to this end consists of deriving the three-dimensional equilibrium equations and boundary conditions for a linear elastic body undergoing large deformations, simplifying these equations in accord with the pertinent assumptions of the previous chapters, and solving these equations using the solutions previously obtained for

the intralaminar stresses.

In the following section, the three-dimensional equilibrium equations and boundary conditions will be derived for the cylindrical coordinate system used thus far in the analyses. In a subsequent section, the displacement gradients and rotations will be derived for the cylindrical coordinate system. The equilibrium equations and boundary conditions will then be recast in a form which explicitly illustrates the terms which depend on the displacement gradients and rotations, then, the equations can be simplified in a rational manner based on the magnitude of the deformations and rotations at a point. In order to bring the three dimensional equilibrium equations, boundary conditions, and the displacement gradients and rotations into accord with the solutions for the intralaminar stresses, these relations will be simplified under the assumptions of axisymmetry. In addition, the displacement gradients and rotations will be simplified further under the assumption of Kirchhoff, i.e., that the displacements vary linearly through the thickness of each layer. The simplified relations for the displacement gradients and rotations for the three cylinders of the previous analyses will be used to quantify the relative magnitudes of the coefficients of the stress components appearing in the three-dimensional equilibrium equations. These results will be used to further simplify the equilibrium equations. Finally, in the next chapter, these simplified equilibrium equations will be solved for the interlaminar stresses and results for the three cylinders will be presented. The method of solution will incorporate the solutions of the previous chapter for the intralaminar stresses, in the manner described by Pagano (ref. 3).

A. Transformation of the Three-Dimensional Equations of a Linear Elastic Body in Rectangular Coordinates to Cylindrical Coordinates

The method of derivation of the three-dimensional equilibrium equations in cylindrical coordinates will begin with the derivation of the tensor form of the equilibrium equations in rectangular coordinates. These equations will then be transposed into the cylindrical coordinate system by methods of tensor analysis.

The total potential energy (ref. 4) for a linear elastic body in rectangular coordinates is

$$\Pi(\bar{u}) = \int_V \left(\frac{1}{2} \tau_{ij} e_{ij} - f_i u_i \right) dV - \int_{S_2} \hat{t}_i u_i dS . \quad (186)$$

If Green's Strain tensor,

$$e_{ij} = \frac{1}{2} (u_{i,j} + u_{j,i} + u_{p,i} u_{p,j}) , \quad (187)$$

is incorporated into eq. (186), and the first variation is taken with respect to the displacement tensor u_i , the Euler equations and variationally consistent natural boundary conditions are

$$(\tau_{ij} + \tau_{ip} u_{j,p})_{,i} + f_j = 0 \quad \text{in } V, \quad (188a)$$

and

$$t_j + t_p u_{j,p} = \hat{t}_j \quad \text{on } S_2 \quad (188b)$$

OR u_j is specified on S_2 ,

where τ_{ij} are the Kirchhoff stress tensor components, u_j are the displacement vector components, f_j are the components of the body force vector, \hat{t}_j are the tractions specified

on the surface S_2 of the total boundary S , and V is the volume containing the body. As essential boundary conditions, the displacements are assumed to be zero over the surface $S_1 \equiv S - S_2$, i.e.,

$$u_j = 0 \quad \text{on } S_1. \quad (188c)$$

The tensor t_j is defined as

$$t_j = \tau_{ij} n_i, \quad (189)$$

which acts over the surface S_2 , where n_i are the components of the surface normal vector. Therefore, from the definition of the principal of minimum total potential energy, equations (188) represent the equilibrium equations and variationally consistent boundary conditions governing the three-dimensional response of a linear elastic body undergoing large deformations in a rectangular coordinate system. It should be noted that these are tensor equations, therefore, they can be transposed into any specific curvilinear coordinates in Euclidean space through the rules of tensor analysis. Note also, that the covariant and contravariant components of the tensor quantities in these equations are identical, since the coordinate system is rectangular. In the following, these equations will be transposed into curvilinear coordinates, and the distinction between covariant and contravariant tensor components must be observed.

Eringen (ref. 5) notes that a tensor equation in rectangular coordinates can be resolved into curvilinear coordinates by enforcing the following two rules: "(a) The partial differentiation symbol (\cdot) must be replaced with covariant differentiation (\mid), and (b) The repeated indices must be on diagonal positions." Applying these rules to eqs.

(188a) and (188b) results in a different form of the tensor equations, i.e.,

$$(\sigma^{ij} + \sigma^{ip} u^j|_p)|_i + f^j = 0 \quad \text{in } V, \quad (190a)$$

and

$$t^j + t^p u^j|_p = \hat{t}^j \quad \text{on } S_2, \quad (190b)$$

where covariant differentiation of contravariant tensors is now involved. The tensor calculus involved in carrying out these differentiations depends on the base vectors \bar{g}_k , the metric tensor g_H , and the Christoffel symbols of the second kind $\left\{ \begin{matrix} k \\ ij \end{matrix} \right\}$ related to the transformation from rectangular to cylindrical coordinates. For the coordinate system used so far in the analysis, i.e., the coordinate system presented in Fig. 1, the base vectors are

$$\begin{aligned} \bar{g}_1 &= \bar{i}_1 \\ \bar{g}_2 &= (r \cos \theta) \bar{i}_2 - (r \sin \theta) \bar{i}_3 \\ \bar{g}_3 &= (\sin \theta) \bar{i}_2 + (\cos \theta) \bar{i}_3 \end{aligned} \quad (191)$$

where \bar{i}_1 , \bar{i}_2 , and \bar{i}_3 are the unit base vectors of the global rectangular coordinate system. Therefore, the metric tensor is

$$||g_H|| = \begin{bmatrix} 1 & 0 & 0 \\ 0 & r^2 & 0 \\ 0 & 0 & 1 \end{bmatrix}, \quad (192)$$

and the nonzero Christoffel symbols of the second kind are

$$\begin{aligned} \left\{ \begin{matrix} 2 \\ 23 \end{matrix} \right\} &= \frac{1}{r} = \left\{ \begin{matrix} 2 \\ 32 \end{matrix} \right\}, \\ \left\{ \begin{matrix} 3 \\ 22 \end{matrix} \right\} &= -r. \end{aligned} \quad (193)$$

Carrying out the differentiation in eq. (190a), according to the rules of covariant differentiation results in a tensor equation involving only partial derivatives, namely,

$$\begin{aligned}
& \frac{1}{g^{ll}} \left(\tau^{lj}{}_{,l} + \left\{ \begin{matrix} i \\ in \end{matrix} \right\} \tau^{nj} + \left\{ \begin{matrix} j \\ in \end{matrix} \right\} \tau^{in} \right) + (\tau^{ip} u_{j,p})_{,j} + \left\{ \begin{matrix} i \\ if \end{matrix} \right\} \tau^{fp} u_{j,p} \\
& + \left\{ \begin{matrix} p \\ if \end{matrix} \right\} \tau^{if} u_{j,p} - \left\{ \begin{matrix} q \\ jp \end{matrix} \right\} u_q \left(\tau^{ip}{}_{,i} + \left\{ \begin{matrix} i \\ if \end{matrix} \right\} \tau^{fp} + \left\{ \begin{matrix} p \\ if \end{matrix} \right\} \tau^{if} \right) \\
& - \left\{ \begin{matrix} r \\ jp \end{matrix} \right\}{}_{,i} \tau^{ip} u_r - \left\{ \begin{matrix} r \\ jp \end{matrix} \right\} \tau^{ip} u_{r,i} + \left\{ \begin{matrix} r \\ ji \end{matrix} \right\} \tau^{ip} \left(\left\{ \begin{matrix} s \\ rp \end{matrix} \right\} u_s - u_{r,p} \right) \\
& + \left\{ \begin{matrix} r \\ pi \end{matrix} \right\} \tau^{ip} \left(\left\{ \begin{matrix} s \\ jr \end{matrix} \right\} u_s - u_{j,r} \right) + f^j = 0 .
\end{aligned} \tag{194}$$

The underscore of the superscripts of g^{ll} signify that the summation is suspended. In the following, the components of the body force, f^j , are assumed to be zero.

By expanding the tensor equation, eq. (194), for $j=1$, substituting the values of the metric tensor and Christoffel symbols derived above, collecting terms, and simplifying, the first equilibrium equation is

$$\begin{aligned}
& r \left[\tau^{11} (1 + u_{1,1}) + \tau^{12} u_{1,2} + \tau^{13} u_{1,3} \right]_{,1} \\
& + r \left[\tau^{21} (1 + u_{1,1}) + \tau^{22} u_{1,2} + \tau^{23} u_{1,3} \right]_{,2} \\
& + \left[r (\tau^{31} (1 + u_{1,1}) + \tau^{32} u_{1,2} + \tau^{33} u_{1,3}) \right]_{,3} = 0 .
\end{aligned} \tag{195a}$$

Likewise, for $j=2$,

$$\begin{aligned}
& \left[\tau^{11} u_{2,1} + \tau^{12} (r^2 + u_{2,2} + r u_3) + \tau^{13} u_{2,3} - \frac{1}{r} \tau^{13} u_2 \right]_{,1} \\
& + \left[\tau^{21} u_{2,1} + \tau^{22} (r^2 + u_{2,2} + r u_3) + \tau^{23} u_{2,3} - \frac{1}{r} \tau^{23} u_2 \right]_{,2} \\
& + \left[\tau^{31} u_{2,1} + \tau^{32} (r^2 + u_{2,2} + r u_3) + \tau^{33} u_{2,3} - \frac{1}{r} \tau^{33} u_2 \right]_{,3} \\
& + r \tau^{21} u_{3,1} + \tau^{22} (r u_{3,2} - u_2) + \tau^{23} (r + r u_{3,3}) = 0 ,
\end{aligned} \tag{195b}$$

and for $j=3$,

$$\begin{aligned}
& r \left[\tau^{11} u_{3,1} + \tau^{12} \left(u_{3,2} - \frac{1}{r} u_2 \right) + \tau^{13} (1 + u_{3,3}) \right]_{,1} \\
& + r \left[\tau^{21} u_{3,1} + \tau^{22} \left(u_{3,2} - \frac{1}{r} u_2 \right) + \tau^{23} (1 + u_{3,3}) \right]_{,2} \\
& + \left[r \left(\tau^{31} u_{3,1} + \tau^{32} \left(u_{3,2} - \frac{1}{r} u_2 \right) + \tau^{33} (1 + u_{3,3}) \right) \right]_{,3} \\
& - \frac{1}{r} \tau^{21} u_{2,1} - \tau^{22} (r^2 + u_{2,2} + r u_3) - \tau^{23} \left(u_{2,3} - \frac{1}{r} u_2 \right) = 0 .
\end{aligned} \tag{195c}$$

It is important to realize that these equations involve tensor components τ^{ij} and u_i and not the physical components of the stresses and displacements. The physical components of stress will be denoted by σ^{ij} as given by

$$\sigma^{ij} = \sqrt{g_{ii}} \sqrt{g_{jj}} \tau^{ij} \quad \text{or} \quad \tau^{ij} = \sqrt{g^{ii}} \sqrt{g^{jj}} \sigma^{ij} , \tag{196}$$

where

$$g_{ii} = \frac{1}{g^{ii}} \tag{197}$$

for orthogonal coordinate systems. Since the cylindrical coordinate system in this

analysis is orthogonal, then by eqs. (192) and (197),

$$g^{11} = 1 = g^{33}, \quad \text{and} \quad g^{22} = \frac{1}{r^2}. \quad (198)$$

The physical components of the displacement tensor u_i are \bar{u}_i as given by

$$\bar{u}_i = \sqrt{g^{ii}} u_i \quad \text{or} \quad u_i = \sqrt{g_{ii}} \bar{u}_i. \quad (199)$$

Using the above relations to obtain the physical components of the stress and displacement tensors, and

(a) substituting x for the superscript 1, θ for 2, and r for 3 in eqs. (195),

(b) substituting u for \bar{u}_1 , v for \bar{u}_2 , and w for \bar{u}_3 , and

(c) replacing the partial derivative notation according to $\frac{\partial(\)}{\partial x} \equiv (\)_{,1}$,

$$\frac{\partial(\)}{\partial \theta} \equiv (\)_{,2}, \quad \text{and} \quad \frac{\partial(\)}{\partial r} \equiv (\)_{,3},$$

a more standard form of the equilibrium equations can be obtained, namely,

$$\begin{aligned} & r \frac{\partial}{\partial x} \left[\left(1 + \frac{\partial u}{\partial x} \right) \sigma^{xx} + \frac{1}{r} \frac{\partial u}{\partial \theta} \tau^{x\theta} + \frac{\partial u}{\partial r} \tau^{xr} \right] \\ & + \frac{\partial}{\partial \theta} \left[\left(1 + \frac{\partial u}{\partial x} \right) \tau^{x\theta} + \frac{1}{r} \frac{\partial u}{\partial \theta} \sigma^{\theta\theta} + \frac{\partial u}{\partial r} \tau^{\theta r} \right] \\ & + \frac{\partial}{\partial r} r \left[\left(1 + \frac{\partial u}{\partial x} \right) \tau^{xr} + \frac{1}{r} \frac{\partial u}{\partial \theta} \tau^{\theta r} + \frac{\partial u}{\partial r} \sigma^{rr} \right] = 0, \end{aligned} \quad (200a)$$

$$\begin{aligned}
& r \frac{\partial}{\partial x} \left[\frac{\partial v}{\partial x} \sigma^{xx} + \left(1 + \frac{1}{r} \frac{\partial v}{\partial \theta} + \frac{w}{r} \right) \tau^{x\theta} + \frac{\partial v}{\partial r} \tau^{xr} \right] \\
& + \frac{\partial}{\partial \theta} \left[\frac{\partial v}{\partial x} \tau^{x\theta} + \left(1 + \frac{1}{r} \frac{\partial v}{\partial \theta} + \frac{w}{r} \right) \sigma^{\theta\theta} + \frac{\partial v}{\partial r} \tau^{\theta r} \right] \\
& + \frac{\partial}{\partial r} r \left[\frac{\partial v}{\partial x} \tau^{xr} + \left(1 + \frac{1}{r} \frac{\partial v}{\partial \theta} + \frac{w}{r} \right) \tau^{\theta r} + \frac{\partial v}{\partial r} \sigma^{rr} \right] \\
& + \frac{\partial w}{\partial x} \tau^{x\theta} + \frac{1}{r} \left(\frac{\partial w}{\partial \theta} - v \right) \sigma^{\theta\theta} + \left(1 + \frac{\partial w}{\partial r} \right) \tau^{\theta r} = 0 ,
\end{aligned} \tag{200b}$$

and

$$\begin{aligned}
& r \frac{\partial}{\partial x} \left[\frac{\partial w}{\partial x} \sigma^{xx} + \frac{1}{r} \left(\frac{\partial w}{\partial \theta} - v \right) \tau^{x\theta} + \left(1 + \frac{\partial w}{\partial r} \right) \tau^{xr} \right] \\
& + \frac{\partial}{\partial \theta} \left[\frac{\partial w}{\partial x} \tau^{x\theta} + \frac{1}{r} \left(\frac{\partial w}{\partial \theta} - v \right) \sigma^{\theta\theta} + \left(1 + \frac{\partial w}{\partial r} \right) \tau^{\theta r} \right] \\
& + \frac{\partial}{\partial r} r \left[\frac{\partial w}{\partial x} \tau^{xr} + \frac{1}{r} \left(\frac{\partial w}{\partial \theta} - v \right) \tau^{\theta r} + \left(1 + \frac{\partial w}{\partial r} \right) \sigma^{rr} \right] \\
& - \frac{\partial v}{\partial x} \tau^{x\theta} - \left(1 + \frac{1}{r} \frac{\partial v}{\partial \theta} + \frac{w}{r} \right) \sigma^{\theta\theta} - \frac{\partial v}{\partial r} \tau^{\theta r} = 0 .
\end{aligned} \tag{200c}$$

In the last step, symmetry of the stress tensor was used in order to emphasize that six stress components, not nine, are involved. The fact that component designation of the stresses are superscripts is an artifact of the contravariant tensor of eqs. (195). However, since the stress components in eqs. (200) are physical components, they are not tensor components, and therefore, the terms covariant and contravariant have no meaning in this context. Hence, the difference between a superscript and subscript notation for the stress components is superficial.

In a similar manner to that used for the equilibrium equations, the natural boundary condition equation, eq. (190b), can be transposed into the cylindrical coordinate system. The result, in the physical components of stress and displacement, is

$$\begin{aligned}
& \left[\left(1 + \frac{\partial u}{\partial x} \right) \sigma^{xx} + \frac{1}{r} \frac{\partial u}{\partial \theta} \tau^{x\theta} + \frac{\partial u}{\partial r} \tau^{xr} \right] \bar{n}_x \\
& + \left[\left(1 + \frac{\partial u}{\partial x} \right) \tau^{x\theta} + \frac{1}{r} \frac{\partial u}{\partial \theta} \sigma^{\theta\theta} + \frac{\partial u}{\partial r} \tau^{\theta r} \right] \bar{n}_\theta \\
& + \left[\left(1 + \frac{\partial u}{\partial x} \right) \tau^{xr} + \frac{1}{r} \frac{\partial u}{\partial \theta} \tau^{\theta r} + \frac{\partial u}{\partial r} \sigma^{rr} \right] \bar{n}_r = \bar{t}^x \quad \text{on } S_2
\end{aligned} \tag{201a}$$

OR u is specified on S_2 ,

and

$$\begin{aligned}
& \left[\frac{\partial v}{\partial x} \sigma^{xx} + \left(1 + \frac{1}{r} \frac{\partial v}{\partial \theta} + \frac{w}{r} \right) \tau^{x\theta} + \frac{\partial v}{\partial r} \tau^{xr} \right] \bar{n}_x \\
& + \left[\frac{\partial v}{\partial x} \tau^{x\theta} + \left(1 + \frac{1}{r} \frac{\partial v}{\partial \theta} + \frac{w}{r} \right) \sigma^{\theta\theta} + \frac{\partial v}{\partial r} \tau^{\theta r} \right] \bar{n}_\theta \\
& + \left[\frac{\partial v}{\partial x} \tau^{xr} + \left(1 + \frac{1}{r} \frac{\partial v}{\partial \theta} + \frac{w}{r} \right) \tau^{\theta r} + \frac{\partial v}{\partial r} \sigma^{rr} \right] \bar{n}_r = \bar{t}^\theta \quad \text{on } S_2
\end{aligned} \tag{201b}$$

OR v is specified on S_2 ,

and

$$\begin{aligned}
& \left[\frac{\partial w}{\partial x} \sigma^{xx} + \frac{1}{r} \left(\frac{\partial w}{\partial \theta} - v \right) \tau^{x\theta} + \left(1 + \frac{\partial w}{\partial r} \right) \tau^{xr} \right] \bar{n}_x \\
& + \left[\frac{\partial w}{\partial x} \tau^{x\theta} + \frac{1}{r} \left(\frac{\partial w}{\partial \theta} - v \right) \sigma^{\theta\theta} + \left(1 + \frac{\partial w}{\partial r} \right) \tau^{\theta r} \right] \bar{n}_\theta \\
& + \left[\frac{\partial w}{\partial x} \tau^{xr} + \frac{1}{r} \left(\frac{\partial w}{\partial \theta} - v \right) \tau^{\theta r} + \left(1 + \frac{\partial w}{\partial r} \right) \sigma^{rr} \right] \bar{n}_r = \bar{t}^r \quad \text{on } S_2
\end{aligned} \tag{201c}$$

OR w is specified on S_2 ,

where the bar over the surface tractions \bar{t}^x , \bar{t}^θ , and \bar{t}^r , and surface normals \bar{n}_x , \bar{n}_θ , and \bar{n}_r , in eqs. (201) signify that these are the physical components of these quantities.

In summary, the equilibrium equations for the three-dimensional stress state of a body in cylindrical coordinates undergoing large deformation are three coupled, nonlinear

partial differential equations. The boundary condition relations are also coupled, nonlinear equations.

B. Derivation of the Displacement Gradients and Rotation Components of the Finite Strain Tensor in Cylindrical Coordinates

The equilibrium equations and boundary conditions just presented will later be simplified by rewriting them such that the coefficients of the stress components are cast in a form which reflects the contributions of the displacement gradients and rotations, in accord with the method presented by Novozhilov (ref. 6). This method enables one to simplify the equilibrium equations in a rational manner by eliminating certain terms based on the relative magnitudes of the products of the displacement gradients and/or rotations and stress components.

First, the displacement gradients and rotations will be derived for the cylindrical coordinate system used thus far in the analyses. Eringen (Ref. 5) gives the following definitions for the displacement gradients, or infinitesimal strains, and the rotations, respectively, as

$$e_{kl} = \frac{1}{2} (u_{k|l} + u_{l|k}) \quad , \quad r_{kl} = \frac{1}{2} (u_{k|l} - u_{l|k}) \quad , \quad (202a)$$

where

$$u_{k|l} \equiv u_{k,l} - \left\{ \begin{matrix} m \\ k \ l \end{matrix} \right\} u_m \quad . \quad (202b)$$

If eq. (202b) is substituted into eq. (202a), the symmetry of the Christoffel symbols of the second kind is recognized, and the result is expanded, the following expressions for

the displacement gradient and rotations result

$$\begin{aligned}
 e_{kl} &= \frac{1}{2} \left(u_{k,l} + u_{l,k} - 2 \left\{ \begin{matrix} m \\ kl \end{matrix} \right\} u_m \right), & r_{kl} &= \frac{1}{2} (u_{k,l} - u_{l,k}), \\
 e_{lk} &= e_{kl} \text{ for all } k,l; & r_{lk} &= -r_{kl} \text{ for } k \neq l, \\
 & & r_{kl} &= 0 \text{ for } k=0.
 \end{aligned} \tag{203}$$

These definitions can be expressed in terms of their physical components by using the relation

$$\bar{e}_{ij} = \sqrt{g^{ii}} \sqrt{g^{jj}} e_{ij}, \quad \bar{r}_{ij} = \sqrt{g^{ii}} \sqrt{g^{jj}} r_{ij}. \tag{204}$$

The displacements appearing in eq. (203) may also be expressed in terms of their physical components, as given by eq. (199). Therefore, the physical components of the displacement gradients and rotations in terms of the physical components of the displacements, can be shown to be

$$\begin{aligned}
 \bar{e}_{11} &= \bar{u}_{1,1}, & \bar{r}_{12} &= \frac{1}{2} \left(\frac{1}{r} \bar{u}_{1,2} - \bar{u}_{2,1} \right) = -\bar{r}_{21}, \\
 \bar{e}_{12} &= \frac{1}{2} \left(\frac{1}{r} \bar{u}_{1,2} + \bar{u}_{2,1} \right), & \bar{r}_{13} &= \frac{1}{2} (\bar{u}_{1,3} - \bar{u}_{3,1}) = -\bar{r}_{31}, \\
 \bar{e}_{13} &= \frac{1}{2} (\bar{u}_{1,3} + \bar{u}_{3,1}), & \bar{r}_{23} &= \frac{1}{2} \left(\frac{\bar{u}_2}{r} + \bar{u}_{2,3} - \frac{1}{r} \bar{u}_{3,2} \right) = -\bar{r}_{32}, \\
 \bar{e}_{22} &= \frac{1}{r} (\bar{u}_{2,2} + \bar{u}_3), & & \\
 \bar{e}_{23} &= \frac{1}{2} \left(\bar{u}_{2,3} + \frac{2}{r} \bar{u}_{3,2} - \frac{\bar{u}_2}{r} \right), & & \\
 \bar{e}_{33} &= \bar{u}_{3,3}. & &
 \end{aligned} \tag{205}$$

These relations can be expressed in the terminology of the cylindrical coordinate system by substituting, as before, the definitions $u \equiv \bar{u}_1$, $v \equiv \bar{u}_2$, and $w \equiv \bar{u}_3$, and writing the partial differentials using the definitions $\frac{\partial(\)}{\partial x} \equiv (\)_{,1}$, $\frac{\partial(\)}{\partial \theta} \equiv (\)_{,2}$, $\frac{\partial(\)}{\partial r} \equiv (\)_{,3}$. These substitutions result in the following form of the displacement gradient and rotation definitions:

$$\begin{aligned}
 e_{xx} &= \frac{\partial u}{\partial x}, & 2r_{x\theta} &= \frac{1}{r} \frac{\partial u}{\partial \theta} - \frac{\partial v}{\partial x} = -2r_{\theta x}, \\
 2e_{x\theta} &= \frac{1}{r} \frac{\partial u}{\partial \theta} + \frac{\partial v}{\partial x}, & 2r_{xr} &= \frac{\partial u}{\partial r} - \frac{\partial w}{\partial x} = -2r_{rx}, \\
 2e_{xr} &= \frac{\partial u}{\partial r} + \frac{\partial w}{\partial x}, & 2r_{\theta r} &= \frac{v}{r} + \frac{\partial v}{\partial r} - \frac{1}{r} \frac{\partial w}{\partial \theta} = -2r_{r\theta}, \\
 e_{\theta\theta} &= \frac{1}{r} \frac{\partial v}{\partial \theta} + \frac{w}{r}, & & \\
 2e_{\theta r} &= \frac{\partial v}{\partial r} + \frac{1}{r} \frac{\partial w}{\partial \theta} - \frac{v}{r}, & & \\
 e_{rr} &= \frac{\partial w}{\partial r}. & &
 \end{aligned} \tag{206}$$

The displacement gradients and rotations can be combined in order to make substitution into the equilibrium equations more obvious. Useful combinations of the displacement gradients and rotations are:

$$\begin{aligned}
\frac{\partial u}{\partial x} &= e_{xx} \ , \\
\frac{1}{r} \frac{\partial u}{\partial \theta} &= e_{x\theta} + r_{x\theta} \ , \\
\frac{\partial u}{\partial r} &= e_{xr} + r_{xr} \ , \\
\frac{\partial v}{\partial x} &= e_{x\theta} - r_{x\theta} \ , \\
\frac{1}{r} \left(\frac{\partial v}{\partial \theta} + w \right) &= e_{\theta\theta} \ , \\
\frac{\partial v}{\partial r} &= e_{\theta r} + r_{\theta r} \ , \\
\frac{\partial w}{\partial x} &= e_{xr} - r_{xr} \ , \\
\frac{1}{r} \left(\frac{\partial w}{\partial \theta} - v \right) &= e_{\theta r} - r_{\theta r} \ , \\
\frac{\partial w}{\partial r} &= e_{rr} \ .
\end{aligned} \tag{207}$$

Substituting these combinations into the equilibrium equations, eqs.(200), derived in the previous section results in

$$\begin{aligned}
& r \frac{\partial}{\partial x} [(1 + e_{xx})\sigma^{xx} + (e_{x\theta} + r_{x\theta})\tau^{x\theta} + (e_{xr} + r_{xr})\tau^{xr}] \\
& + \frac{\partial}{\partial \theta} [(1 + e_{xx})\tau^{x\theta} + (e_{x\theta} + r_{x\theta})\sigma^{\theta\theta} + (e_{xr} + r_{xr})\tau^{\theta r}] \\
& + \frac{\partial}{\partial r} r [(1 + e_{xx})\tau^{xr} + (e_{x\theta} + r_{x\theta})\tau^{\theta r} + (e_{xr} + r_{xr})\sigma^{rr}] = 0 \ ,
\end{aligned} \tag{208a}$$

$$\begin{aligned}
& r \frac{\partial}{\partial x} [(e_{x\theta} - r_{x\theta}) \sigma^{xx} + (1 + e_{\theta\theta}) \tau^{x\theta} + (e_{\theta r} + r_{\theta r}) \tau^{xr}] \\
& + \frac{\partial}{\partial \theta} [(e_{x\theta} - r_{x\theta}) \tau^{x\theta} + (1 + e_{\theta\theta}) \sigma^{\theta\theta} + (e_{\theta r} + r_{\theta r}) \tau^{\theta r}] \\
& + \frac{\partial}{\partial r} r [(e_{x\theta} - r_{x\theta}) \tau^{xr} + (1 + e_{\theta\theta}) \tau^{\theta r} + (e_{\theta r} + r_{\theta r}) \sigma^{rr}] \\
& + (e_{xr} - r_{xr}) \tau^{x\theta} + (e_{\theta r} - r_{\theta r}) \sigma^{\theta\theta} + (1 + e_{rr}) \tau^{\theta r} = 0 ,
\end{aligned} \tag{208b}$$

and

$$\begin{aligned}
& r \frac{\partial}{\partial x} [(e_{xr} - r_{xr}) \sigma^{xx} + (e_{\theta r} - r_{\theta r}) \tau^{x\theta} + (1 + e_{rr}) \tau^{xr}] \\
& + \frac{\partial}{\partial \theta} [(e_{xr} - r_{xr}) \tau^{x\theta} + (e_{\theta r} - r_{\theta r}) \sigma^{\theta\theta} + (1 + e_{rr}) \tau^{\theta r}] \\
& + \frac{\partial}{\partial r} r [(e_{xr} - r_{xr}) \tau^{xr} + (e_{\theta r} - r_{\theta r}) \tau^{\theta r} + (1 + e_{rr}) \sigma^{rr}] \\
& - (e_{x\theta} - r_{x\theta}) \tau^{x\theta} - (1 + e_{\theta\theta}) \sigma^{\theta\theta} - (e_{\theta r} + r_{\theta r}) \tau^{\theta r} = 0 .
\end{aligned} \tag{208c}$$

In a similar manner, the natural boundary condition relations, eqs. (201), can be rewritten by substituting the combinations of displacement gradients and rotations of eq. (207), i.e.,

$$\begin{aligned}
& [(1 + e_{xx}) \sigma^{xx} + (e_{x\theta} + r_{x\theta}) \tau^{x\theta} + (e_{xr} + r_{xr}) \tau^{xr}] \bar{n}_x \\
& + [(1 + e_{xx}) \tau^{x\theta} + (e_{x\theta} + r_{x\theta}) \sigma^{\theta\theta} + (e_{xr} + r_{xr}) \tau^{\theta r}] \bar{n}_\theta \\
& + [(1 + e_{xx}) \tau^{xr} + (e_{x\theta} + r_{x\theta}) \tau^{\theta r} + (e_{xr} + r_{xr}) \sigma^{rr}] \bar{n}_r = \bar{t}^x \quad \text{on } S_2
\end{aligned} \tag{209a}$$

OR u is specified on S_2 ,

and

$$\begin{aligned}
& [(e_{x\theta} - r_{x\theta}) \sigma^{xx} + (1 + e_{\theta\theta}) \tau^{x\theta} + (e_{\theta r} + r_{\theta r}) \tau^{xr}] \bar{n}_x \\
& + [(e_{x\theta} - r_{x\theta}) \tau^{x\theta} + (1 + e_{\theta\theta}) \sigma^{\theta\theta} + (e_{\theta r} + r_{\theta r}) \tau^{\theta r}] \bar{n}_\theta \\
& + [(e_{x\theta} - r_{x\theta}) \tau^{xr} + (1 + e_{\theta\theta}) \tau^{\theta r} + (e_{\theta r} + r_{\theta r}) \sigma^{rr}] \bar{n}_r = \bar{t}^\theta \quad \text{on } S_2
\end{aligned} \tag{209b}$$

OR v is specified on S_2 ,

and

$$\begin{aligned}
& \left[(e_{xr} - r_{xr}) \sigma^{xx} + (e_{\theta r} - r_{\theta r}) \tau^{x\theta} + (1 + e_{rr}) \tau^{xr} \right] \bar{n}_x \\
& + \left[(e_{xr} - r_{xr}) \tau^{x\theta} + (e_{\theta r} - r_{\theta r}) \sigma^{\theta\theta} + (1 + e_{rr}) \tau^{\theta r} \right] \bar{n}_\theta \\
& + \left[(e_{xr} - r_{xr}) \tau^{xr} + (e_{\theta r} - r_{\theta r}) \tau^{\theta r} + (1 + e_{rr}) \sigma^{rr} \right] \bar{n}_r = \bar{i}^r \quad \text{on } S_2 \quad (209c)
\end{aligned}$$

OR w is specified on S_2 .

To summarize the results of this section, relations between the displacement gradients and rotations and the partial derivatives appearing in the equilibrium equations for a cylindrical body undergoing large deformations, i.e., eqs. (200), and the natural boundary conditions, eqs. (201), have been obtained. These results were substituted into the equilibrium equations and natural boundary conditions derived in the previous section. In a subsequent section, the equilibrium equations and natural boundary conditions will be simplified through a rational method of comparison of the relative magnitudes of the displacement gradients and rotations in the coefficients of the stresses in these equations.

C. Specialization of the Displacement Gradients and Rotations Under the

Assumption of Axisymmetry

Since the results of the previous chapters will be used to calculate the portions of the three-dimensional equilibrium equations just presented, the relations for the displacement gradients and rotations will be specialized under the assumption of axisymmetric response and loading, so that they will be in accord with the previous analyses.

The assumption of axisymmetric response and loading is defined by

$$\frac{\partial(\quad)}{\partial\theta} = 0, \quad (210)$$

() being any response quantity. By enforcing this definition, the displacement gradients and rotations of the previous section, eqs. (206), become

$$\begin{aligned} e_{xx} &= \frac{\partial u}{\partial x}, & 2r_{x\theta} &= -\frac{\partial v}{\partial x} = -2r_{\theta x}, \\ 2e_{x\theta} &= \frac{\partial v}{\partial x}, & 2r_{xr} &= \frac{\partial u}{\partial r} - \frac{\partial w}{\partial x} = -2r_{rx}, \\ 2e_{xr} &= \frac{\partial u}{\partial r} + \frac{\partial w}{\partial x}, & 2r_{\theta r} &= \frac{v}{r} + \frac{\partial v}{\partial r} = -2r_{r\theta}, \\ e_{\theta\theta} &= \frac{w}{r}, & & \\ 2e_{\theta r} &= \frac{\partial v}{\partial r} - \frac{v}{r}, & & \\ e_{rr} &= \frac{\partial w}{\partial r}. & & \end{aligned} \quad (211)$$

D. Simplification of the Axisymmetric Displacement Gradients and Rotations Under the Assumptions of Kirchhoff and Donnell

In order to incorporate the analyses of the previous chapters, the axisymmetric displacement gradients and rotations must be simplified by utilizing the relations describing the displacements from the previous chapters, i.e.,

$$\begin{aligned} u(x,\theta,r) &= u^o(x,\theta) + z\beta_x^o(x,\theta) \\ v(x,\theta,r) &= v^o(x,\theta) + z\beta_\theta^o(x,\theta) \\ w(x,\theta,r) &= w^o(x,\theta), \end{aligned}$$

(7)

and

$$\begin{aligned}\beta_x^o &= -\frac{\partial w^o}{\partial x} \\ \beta_\theta^o &= -\frac{\partial w^o}{R\partial\theta},\end{aligned}\tag{9}$$

which describe the displacement field in general according to the Kirchhoff assumption, and eqs. (173a), (173b), and (166) which are the solutions for $u^o(x)$, $v^o(x)$, and $w^o(x)$ for $0 \geq N > N^*$, eqs. (174a), (174b), and (167) which are the solutions for $u^o(x)$, $v^o(x)$, and $w^o(x)$ for $N = N^*$, and eqs. (175a), (175b), and (168) which are solutions for $u^o(x)$, $v^o(x)$, and $w^o(x)$ for $N < N^*$. Additionally, the assumption of Donnell was incorporated in the analyses of the previous chapters, namely, that for thin shells, the variable r can be replaced by the mean radius R .

Under the conditions imposed by the Kirchhoff and Donnell assumptions, the partial differentials which make up the axisymmetric displacement gradients and rotations listed in eq. (211) simplify to

$$\begin{aligned}e_{xx} &= \frac{du^o}{dx} - z \frac{d^2w^o}{dx^2}, & 2r_{x\theta} &= -\frac{dv^o}{dx} = -2r_{\theta x}, \\ 2e_{x\theta} &= \frac{dv^o}{dx}, & 2r_{xr} &= -2\frac{dw^o}{dx} = -2r_{rx}, \\ 2e_{xr} &= 0, & 2r_{\theta r} &= \frac{v^o}{R} = -2r_{r\theta}, \\ e_{\theta\theta} &= \frac{w^o}{R}, \\ 2e_{\theta r} &= \frac{v^o}{R}, \\ e_{rr} &= 0.\end{aligned}\tag{212}$$

Note that under these assumptions,

$$r_{x\theta} = -e_{x\theta}, \quad \text{and} \quad r_{\theta r} = -e_{\theta r}. \quad (213)$$

E. Specialization of the Three-Dimensional Equilibrium Equations and Boundary Conditions Under the Assumption of Axisymmetry

The analyses previous to this chapter have been made under the assumption of axisymmetry. Since the solutions obtained in the previous chapters are to be incorporated into the three-dimensional equations derived previously in this chapter, the last form of the equilibrium equations and boundary conditions, i.e., eq. (208) and (209), will be specialized under the assumption of axisymmetry.

Enforcing the conditions for axisymmetry, eq. (210), into the equilibrium equations of the previous section, i.e., eqs. (200), results in

$$\begin{aligned} & r \frac{\partial}{\partial x} [(1 + e_{xx}) \sigma^{xx} + r_{xr} \tau^{xr}] \\ & + \frac{\partial}{\partial r} r [(1 + e_{xx}) \tau^{xr} + r_{xr} \sigma^{rr}] = 0, \end{aligned} \quad (214a)$$

$$\begin{aligned} & r \frac{\partial}{\partial x} [e_{x\theta} \sigma^{xx} + (1 + e_{\theta\theta}) \tau^{x\theta}] \\ & + \frac{\partial}{\partial r} r [e_{x\theta} \tau^{xr} + (1 + e_{\theta\theta}) \tau^{\theta r}] \\ & - r_{xr} \tau^{x\theta} + e_{\theta r} \sigma^{\theta\theta} + \tau^{\theta r} = 0, \end{aligned} \quad (214b)$$

and

$$\begin{aligned}
& r \frac{\partial}{\partial x} [(-r_{xr}) \sigma^{xx} + (2e_{\theta r}) \tau^{x\theta} + \tau^{xr}] \\
& + \frac{\partial}{\partial r} r [(-r_{xr}) \tau^{xr} + (2e_{\theta r}) \tau^{\theta r} + \sigma^{rr}] \\
& - 2e_{x\theta} \tau^{x\theta} - (1 + e_{\theta\theta}) \sigma^{\theta\theta} - 2e_{\theta r} \tau^{\theta r} = 0 .
\end{aligned} \tag{214c}$$

Enforcing eq. (210) on the natural boundary condition equations, eqs. (201), results

in

$$\begin{aligned}
& [(1 + e_{xx}) \sigma^{xx} + r_{xr} \tau^{xr}] \bar{n}_x + [(1 + e_{xx}) \tau^{x\theta} + r_{xr} \tau^{\theta r}] \bar{n}_\theta \\
& + [(1 + e_{xx}) \tau^{xr} + r_{xr} \sigma^{rr}] \bar{n}_r = \hat{t}^x \quad \text{on } S_2
\end{aligned} \tag{215a}$$

OR u is specified on S_2 ,

and

$$\begin{aligned}
& [(2e_{x\theta}) \sigma^{xx} + (1 + e_{\theta\theta}) \tau^{x\theta}] \bar{n}_x \\
& + [(2e_{x\theta}) \tau^{x\theta} + (1 + e_{\theta\theta}) \sigma^{\theta\theta}] \bar{n}_\theta \\
& + [(2e_{x\theta}) \tau^{xr} + (1 + e_{\theta\theta}) \tau^{\theta r}] \bar{n}_r = \hat{t}^\theta \quad \text{on } S_2
\end{aligned} \tag{215b}$$

OR v is specified on S_2 ,

and

$$\begin{aligned}
& [(-r_{xr}) \sigma^{xx} + (2e_{\theta r}) \tau^{x\theta} + \tau^{xr}] \bar{n}_x \\
& + [(-r_{xr}) \tau^{x\theta} + (2e_{\theta r}) \sigma^{\theta\theta} + \tau^{\theta r}] \bar{n}_\theta \\
& + [(-r_{xr}) \tau^{xr} + (2e_{\theta r}) \tau^{\theta r} + \sigma^{rr}] \bar{n}_r = \hat{t}^r \quad \text{on } S_2
\end{aligned} \tag{215c}$$

OR w is specified on S_2 .

F. Simplification of the Equilibrium Equations and Boundary Conditions Through Elimination of Terms of Relatively Small Magnitude

At this point, the three-dimensional equilibrium equations and boundary conditions have been simplified so that the solutions of the previous chapters can be used to evaluate

the displacement gradients, rotations, and intralaminar stresses at any point within the cylinder wall. It should be noted that these quantities are obtained from CLT. The solutions of the previous chapter are being used in order to later derive recursive closed-form relations for the interlaminar stresses at a given point along the length of the cylinder.

In an attempt to further simplify the equilibrium equations, eqs. (214), and boundary condition relations, eqs. (215), a study will be conducted of the relative magnitudes of the terms which are being differentiated in the equilibrium equations. This is similar to the method implemented by Novozhilov (Ref. 6) to simplify the three-dimensional equilibrium equations based on the relative magnitude of the displacement gradients and rotations appearing in these equations in order to rationally obtain equations relevant to small deformations and small rotations. To be conservative, no assumptions will be made as to whether a term can be eliminated under a general case of cylinder stacking sequence, constitutive properties, geometry, boundary condition, or load level. Otherwise, the study will be conducted based on these parameters as they will occur in the subsequent calculation of the interlaminar stresses. This precaution is being taken due to the nonlinear nature of the CLT solutions presented in the previous chapters.

The cylinders to be analyzed in the rest of this work are the same cylinders which were analyzed in the previous chapter on intralaminar stresses. Likewise, only clamped boundary conditions will be investigated. Thermally-induced preloading effects with $\Delta T = -280^\circ\text{F}$ will be used in the CLT solutions.

The maximum absolute values of the displacement gradients and rotations for the

cylinders subjected to compressive axial loads of $N = 10\% N^*$, $N = 90\% N^*$, and $N = 99\% N^*$ are presented in Table III. As can be seen, the displacement gradients and rotations are considerably smaller than unity.

Table III. Maximum Values of Displacement Gradients and Rotations

Cylinder & Load	$ e_{xx} _{\max}$	$ e_{xx} _{\max}$	$ e_{\theta\theta} _{\max}$	$ \Gamma_{xr} _{\max}$	$ e_{x\theta} _{\max}$	$ e_{\theta r} _{\max}$
	$r=r_{\text{inner}}$	$r=r_{\text{outer}}$			$ \Gamma_{x\theta} _{\max}$	$ \Gamma_{\theta r} _{\max}$
$[\pm 45/0_2]_{2S}$ $N=10\%N^*$	$.20 \cdot 10^{-3}$	$.29 \cdot 10^{-3}$	$.12 \cdot 10^{-2}$	$.11 \cdot 10^{-2}$	0	0
$[\pm 45/0_2]_{4T}$ $N=10\%N^*$	$.20 \cdot 10^{-3}$	$.31 \cdot 10^{-3}$	$.11 \cdot 10^{-2}$	$.11 \cdot 10^{-2}$	$.40 \cdot 10^{-5}$	$.10 \cdot 10^{-6}$
$[0_2/\mp 45]_{4T}$ $N=10\%N^*$	$.27 \cdot 10^{-3}$	$.31 \cdot 10^{-3}$	$.12 \cdot 10^{-2}$	$.18 \cdot 10^{-2}$	$.28 \cdot 10^{-5}$	$.17 \cdot 10^{-6}$
$[\pm 45/0_2]_{2S}$ $N=90\%N^*$	$.29 \cdot 10^{-2}$	$.32 \cdot 10^{-2}$	$.12 \cdot 10^{-2}$	$.15 \cdot 10^{-1}$	0	0
$[\pm 45/0_2]_{4T}$ $N=90\%N^*$	$.29 \cdot 10^{-2}$	$.29 \cdot 10^{-2}$	$.11 \cdot 10^{-2}$	$.14 \cdot 10^{-1}$	$.28 \cdot 10^{-4}$	$.14 \cdot 10^{-5}$
$[0_2/\mp 45]_{4T}$ $N=90\%N^*$	$.35 \cdot 10^{-2}$	$.38 \cdot 10^{-3}$	$.13 \cdot 10^{-2}$	$.18 \cdot 10^{-1}$	$.35 \cdot 10^{-4}$	$.18 \cdot 10^{-5}$
$[\pm 45/0_2]_{2S}$ $N=99\%N^*$	$.37 \cdot 10^{-2}$	$.35 \cdot 10^{-2}$	$.15 \cdot 10^{-2}$	$.21 \cdot 10^{-1}$	0	0
$[\pm 45/0_2]_{4T}$ $N=99\%N^*$	$.36 \cdot 10^{-2}$	$.32 \cdot 10^{-2}$	$.15 \cdot 10^{-2}$	$.20 \cdot 10^{-1}$	$.30 \cdot 10^{-4}$	$.18 \cdot 10^{-5}$
$[0_2/\mp 45]_{4T}$ $N=99\%N^*$	$.44 \cdot 10^{-2}$	$.42 \cdot 10^{-2}$	$.21 \cdot 10^{-2}$	$.25 \cdot 10^{-1}$	$.39 \cdot 10^{-4}$	$.24 \cdot 10^{-5}$

1. Simplification of the First Equilibrium Equation

The derivative with respect to x in the first equilibrium equation, eq. (214a), is

$$\frac{\partial}{\partial x} [(1 + e_{xx})\sigma^{xx} + r_{xr}\tau^{xr}] . \quad (216)$$

For the range of load levels investigated, the maximum absolute value of the displacement gradient e_{xx} is less than 10^{-2} . Therefore, e_{xx} is small enough relative to 1 such that it can be neglected, and the coefficient of σ^{xx} becomes 1. Since the magnitude of τ^{xr} is expected to be small relative to the magnitude of σ^{xx} , and since the rotation r_{xr} is small relative to 1 for these load cases, it can be reasonably assumed that σ^{xx} is sufficiently large compared to $r_{xr}\tau^{xr}$ to warrant the elimination of the latter term from the derivative with respect to x .

The derivative with respect to r in the first equilibrium equation, eq. (214a), is

$$\frac{\partial}{\partial r} r [(1 + e_{xx})\tau^{xr} + r_{xr}\sigma^{rr}] . \quad (217)$$

As with the derivative with respect to x , e_{xx} can be neglected such that the coefficient of τ^{xr} is 1. Also, the interlaminar stress component σ^{rr} is expected to be small relative to τ^{xr} . Therefore, it can reasonably be assumed that τ^{xr} is sufficiently large compared to $r_{xr}\sigma^{rr}$ to warrant the elimination of the latter from the derivative with respect to r .

In light of these results, the first equilibrium equation becomes

$$r \frac{\partial \sigma^{xx}}{\partial x} + \frac{\partial (r \tau^{xr})}{\partial r} = 0 , \quad (218)$$

which is a linear partial differential equation.

2. Simplification of the Second Equilibrium Equation

The derivative with respect to x in the second equation, eq. (214b), is

$$\frac{\partial}{\partial x} [e_{x\theta} \sigma^{xx} + (1 + e_{\theta\theta}) \tau^{x\theta}] . \quad (219)$$

Referring to Table III, the maximum absolute value of $e_{\theta\theta}$ for the load levels investigated is on the order of 10^{-3} . Therefore, it can be neglected in the coefficient of $\tau^{x\theta}$ in the derivative with respect to x and the coefficient of $\tau^{\theta r}$ in the derivative with respect to r . The maximum absolute value of $e_{x\theta}$ is less than 10^{-4} . Therefore, in the derivative with respect to x , the maximum absolute value of the coefficient of σ^{xx} is less than 10^{-4} and the coefficient of $\tau^{x\theta}$ is 1. The intralaminar stress component $\tau^{x\theta}$ is, in general, one or two orders of magnitude smaller than σ^{xx} . Therefore, it can reasonably be assumed that $\tau^{x\theta}$ is sufficiently large relative to $e_{x\theta} \sigma^{xx}$ in the derivative with respect to x such that the latter term can be eliminated.

The derivative with respect to r in the second equilibrium equation is

$$\frac{\partial}{\partial r} [e_{x\theta} \tau^{xr} + (1 + e_{\theta\theta}) \tau^{\theta r}] . \quad (220)$$

Based on the observations for the derivatives with respect to x , the coefficient of $\tau^{\theta r}$ in the derivative with respect to r is 1 and the coefficient of τ^{xr} has a maximum absolute value of 10^{-4} . The interlaminar stress components τ^{xr} and $\tau^{\theta r}$ are expected to differ by several orders of magnitude. Therefore, it is reasonable to assume that $\tau^{\theta r}$ is sufficiently large relative to $e_{x\theta} \tau^{xr}$ in the derivative with respect to r such that the latter term can be eliminated.

The terms in the second equilibrium equation that are not differentiated are

$$-r_{xr} \tau^{x\theta} + e_{\theta r} \sigma^{\theta\theta} + \tau^{\theta r} . \quad (221)$$

Since the magnitudes of the intralaminar stress components $\sigma^{\theta\theta}$ and $\tau^{x\theta}$ are about the same, and the maximum absolute value of r_{xr} is approximately 0.025 for the load cases investigated while the maximum absolute value of $e_{\theta r}$ is less than 10^{-5} , it can reasonably be assumed that the term $r_{xr} \tau^{x\theta}$ is sufficiently large compared to $e_{\theta r} \sigma^{\theta\theta}$ such that the latter term can be eliminated. Since the interlaminar stress component $\tau^{\theta r}$ is expected to be several orders of magnitude smaller than $\tau^{x\theta}$, the magnitude of the term $r_{xr} \tau^{x\theta}$ may be comparable to the magnitude of $\tau^{\theta r}$.

Based on these assumptions, the second equilibrium equation becomes

$$r \frac{\partial \tau^{x\theta}}{\partial x} + \frac{\partial (r \tau^{\theta r})}{\partial r} - r_{xr} \tau^{x\theta} + \tau^{\theta r} = 0 , \quad (222)$$

which is a nonlinear partial differential equation.

3. Simplification of the Third Equilibrium Equation

The derivative with respect to x in the third equilibrium equation, eq. (214c), is

$$\frac{\partial}{\partial x} [(-r_{xr}) \sigma^{xx} + (2e_{\theta r}) \tau^{x\theta} + \tau^{xr}] . \quad (223)$$

The maximum absolute value of the displacement gradient $e_{\theta r}$ is less than 10^{-5} and the maximum absolute value of the rotation r_{xr} is 0.025. Therefore, the magnitude of the $(-r_{xr}) \sigma^{xx}$ term can be assumed to be sufficiently large compared to the $(2e_{\theta r}) \tau^{x\theta}$ term such that the latter term can be eliminated. However, since τ^{xr} is expected to be several orders of magnitude smaller than σ^{xx} , the magnitude of $(-r_{xr}) \sigma^{xx}$ can be expected to be comparable to the magnitude of τ^{xr} . Therefore, based on these observations, the

derivative with respect to x becomes

$$\frac{\partial}{\partial x} [(-r_{xr})\sigma^{xx} + \tau^{xr}] . \quad (224)$$

The derivative with respect to r in the third equilibrium equation is

$$\frac{\partial}{\partial r} r [(-r_{xr})\tau^{xr} + (2e_{\theta r})\tau^{\theta r} + \sigma^{rr}] . \quad (225)$$

Since the interlaminar stress components τ^{xr} and $\tau^{\theta r}$ are expected to differ by several orders of magnitude, and in light of the magnitudes of the coefficients of these components, it can be assumed that $(-r_{xr})\tau^{xr}$ is sufficiently large compared to $(2e_{\theta r})\tau^{\theta r}$ such that the latter term can be eliminated. The interlaminar stress component σ^{rr} is expected to be small relative to τ^{xr} . Therefore, the magnitude of the $(-r_{xr})\tau^{xr}$ term can be assumed to be comparable to the magnitude of the σ^{rr} term. Based on these observations, the derivative with respect to r becomes

$$\frac{\partial}{\partial r} r [(-r_{xr})\tau^{xr} + \sigma^{rr}] . \quad (226)$$

The terms in the third equilibrium equation that are not differentiated are

$$-2e_{x\theta}\tau^{x\theta} - (1 + e_{\theta\theta})\sigma^{\theta\theta} - 2e_{\theta r}\tau^{\theta r} . \quad (227)$$

Due to the magnitudes of the absolute values of the displacement gradients $e_{x\theta}$ and $e_{\theta r}$, the terms $-2e_{x\theta}\tau^{x\theta}$ and $-2e_{\theta r}\tau^{\theta r}$ can be neglected with respect to the term $(1 + e_{\theta\theta})\sigma^{\theta\theta}$. Also, due to the magnitude of $e_{\theta\theta}$ relative to 1, it can be neglected in the latter term.

Based on the observations of the relative magnitudes of the terms in the third

equilibrium equation, it can be simplified to

$$r \frac{\partial}{\partial x} [(-r_{xr}) \sigma^{xx} + \tau^{xr}] + \frac{\partial}{\partial r} r [(-r_{xr}) \tau^{xr} + \sigma^{rr}] - \sigma^{\theta\theta} = 0 . \quad (228)$$

4. Simplification of the Natural Boundary Conditions

Since the terms which appear as coefficients of the surface normals \bar{n}_x and \bar{n}_r in the natural boundary condition relations, eqs. (215), are identical to the terms being differentiated with respect to x and r , respectively, in the equilibrium equations, eqs. (214), the results of the previous sections where the equilibrium equations were simplified can be used directly to simplify the natural boundary condition relations. Therefore, based on the magnitude study for the equilibrium equations, the natural boundary condition relations become

$$[\sigma^{xx}] \bar{n}_x + [(1 + e_{xx}) \tau^{x\theta} + r_{xr} \tau^{\theta r}] \bar{n}_\theta + [\tau^{xr}] \bar{n}_r = \hat{t}^x \quad \text{on } S_2 \quad (229a)$$

OR u is specified on S_2 ,

and

$$[\tau^{x\theta}] \bar{n}_x + [(2e_{x\theta}) \tau^{x\theta} + (1 + e_{\theta\theta}) \sigma^{\theta\theta}] \bar{n}_\theta + [\tau^{\theta r}] \bar{n}_r = \hat{t}^\theta \quad \text{on } S_2 \quad (229b)$$

OR v is specified on S_2 ,

and

$$\begin{aligned} & [(-r_{xr}) \sigma^{xx} + \tau^{xr}] \bar{n}_x \\ & + [(-r_{xr}) \tau^{x\theta} + (2e_{\theta r}) \sigma^{\theta\theta} + \tau^{\theta r}] \bar{n}_\theta \\ & + [(-r_{xr}) \tau^{xr} + \sigma^{rr}] \bar{n}_r = \hat{t}^r \quad \text{on } S_2 \end{aligned} \quad (229c)$$

OR w is specified on S_2 .

However, the coefficients of the surface normal \bar{n}_θ must be analyzed as to the relative

magnitudes of the terms in these coefficients. In the coefficient of \bar{n}_θ in the first natural boundary condition relation, eq. (229a), e_{xx} can be neglected relative to 1 in the coefficient of $\tau^{x\theta}$. Since the interlaminar stress component $\tau^{\theta r}$ is expected to be small relative to the intralaminar stress component $\tau^{x\theta}$, the term $\tau^{x\theta}$ can be assumed sufficiently large compared to $r_{xr}\tau^{\theta r}$ such that the later term can be eliminated. Based on these observations, the first natural boundary condition relation becomes

$$[\sigma^{xx}]\bar{n}_x + [\tau^{x\theta}]\bar{n}_\theta + [\tau^{xr}]\bar{n}_r = \bar{t}^x \quad \text{on } S_2 \quad (230a)$$

OR u is specified on S_2 .

In the coefficient of \bar{n}_θ in the second natural boundary condition relation, $e_{\theta\theta}$ is small relative to 1 such that it can be ignored in the coefficient of $\sigma^{\theta\theta}$. Also, since the maximum absolute value of $e_{x\theta}$ is less than 10^{-4} , it can be assumed that the term $\sigma^{\theta\theta}$ is sufficiently large compared to the term $(2e_{x\theta})\tau^{x\theta}$ such that the latter term can be eliminated. Therefore, the second natural boundary condition becomes

$$[\tau^{x\theta}]\bar{n}_x + [\sigma^{\theta\theta}]\bar{n}_\theta + [\tau^{\theta r}]\bar{n}_r = \bar{t}^\theta \quad \text{on } S_2 \quad (230b)$$

OR v is specified on S_2 .

In the coefficient of \bar{n}_θ in the third boundary condition relation, the term $(2e_{\theta r})\sigma^{\theta\theta}$ can assumed to be small relative to the other two terms, since $e_{\theta r}$ is small. However, although $\tau^{\theta r}$ is expected to be small relative to the intralaminar stress component $\tau^{x\theta}$, and since the maximum absolute value of r_{xr} is approximately 0.025, the magnitude of the term $(-r_{xr})\tau^{x\theta}$ can be assumed comparable to the magnitude of the term $\tau^{\theta r}$.

Therefore, the third natural boundary condition relation becomes

$$\begin{aligned} & [(-r_{xr})\sigma^{xx} + \tau^{xr}]\bar{n}_x \\ & + [(-r_{xr})\tau^{x\theta} + \tau^{\theta r}]\bar{n}_\theta \\ & + [(-r_{xr})\tau^{xr} + \sigma^{rr}]\bar{n}_r = \hat{t}^r \quad \text{on } S_2 \end{aligned} \quad (230c)$$

OR w is specified on S_2 .

In summary, after simplification by the consideration of the relative magnitudes of the terms appearing in the equilibrium equations under the assumptions of axisymmetric response and loading, and the assumptions of Kirchhoff and Donnell, these equations are

$$r \frac{\partial \sigma^{xx}}{\partial x} + \frac{\partial (r\tau^{xr})}{\partial r} = 0 , \quad (231a)$$

$$r \frac{\partial \tau^{x\theta}}{\partial x} + \frac{\partial (r\tau^{\theta r})}{\partial r} - r_{xr}\tau^{x\theta} + \tau^{\theta r} = 0 , \quad (231b)$$

and

$$r \frac{\partial}{\partial x} [(-r_{xr})\sigma^{xx} + \tau^{xr}] + \frac{\partial}{\partial r} r [(-r_{xr})\tau^{xr} + \sigma^{rr}] - \sigma^{\theta\theta} = 0 . \quad (231c)$$

By the same method, the natural boundary conditions become

$$[\sigma^{xx}]\bar{n}_x + [\tau^{x\theta}]\bar{n}_\theta + [\tau^{xr}]\bar{n}_r = \hat{t}^x \quad \text{on } S_2 \quad (232a)$$

OR u is specified on S_2 ,

and

$$[\tau^{x\theta}]\bar{n}_x + [\sigma^{\theta\theta}]\bar{n}_\theta + [\tau^{\theta r}]\bar{n}_r = \hat{t}^\theta \quad \text{on } S_2 \quad (232b)$$

OR v is specified on S_2 ,

and

$$\begin{aligned} & [(-r_{xr})\sigma^{xx} + \tau^{xr}] \bar{n}_x \\ & + [(-r_{xr})\tau^{x\theta} + \tau^{\theta r}] \bar{n}_\theta \\ & + [(-r_{xr})\tau^{xr} + \sigma^{rr}] \bar{n}_r = \bar{t}^r \quad \text{on } S_2 \end{aligned} \tag{232c}$$

OR w is specified on S_2 .

In the following chapter, these equations will be solved and the interlaminar stresses will be calculated for the three cylinders of interest.

VI. SOLUTION OF THE THREE-DIMENSIONAL EQUILIBRIUM EQUATIONS FOR THE INTERLAMINAR STRESSES

In chapter five, the three-dimensional equilibrium equations and boundary conditions were derived for a linear elastic body in cylindrical coordinates for finite strains, under the assumption of axisymmetric loading and response, and under Kirchhoff's and Donnell's assumptions for the displacement variables. These steps were performed in order to obtain three-dimensional equilibrium equations and boundary conditions compatible with the assumptions and solutions of the previous chapters, which concluded with the derivation of the intralaminar stress relations. Under these conditions, the closed-form intralaminar stress relations can be used in the solution of the interlaminar stress components, analogous to the method implemented by Pagano (Ref. 3).

In this chapter, the first of the equilibrium equations, i.e.

$$r \frac{\partial \sigma^{xx}}{\partial x} + \frac{\partial (r \tau^{xr})}{\partial r} = 0, \quad (233)$$

will be solved for the interlaminar stress component τ^{xr} . Since $\sigma^{xx}(x,r)$ is known at any point along the length of the cylinder and at any point through its thickness from closed-form relations obtained previously, the partial derivative with respect to x of σ^{xx} is also known through analytical differentiation of the closed-form solution to $\sigma^{xx}(x,r)$.

The interlaminar stress components $\tau^{\theta r}$ and σ^{rr} are assumed to be small relative to the interlaminar stress component τ^{xr} . For an axisymmetric response, $\tau^{\theta r}$ would be expected to be small. Other researchers (ref. 7) have found σ^{rr} to be small for

the case of cylinder bending, and that is assumed to be the case for the cylinder compression problem studied here. Therefore, $\tau^{\theta r}$ and σ^{rr} will not be solved for or calculated in this work. However, the solution method to be presented for the determination of the interlaminar stress component τ^{xr} from the first equilibrium equation is directly applicable to the determination of the other two interlaminar stress components.

A. Solution of the First Equilibrium Equation

The differentiation implicit in eq. (233) can be distributed, and the result simplified to give

$$\frac{\partial \tau^{xr}}{\partial r} + \frac{\tau^{xr}}{r} = - \frac{\partial \sigma^{xx}}{\partial x} . \quad (234)$$

As mentioned previously, the partial derivative appearing on the right-hand side of this equation can be calculated from the closed-form relation for $\sigma^{xx}(x,r)$. For a given layer, the intralaminar stress component $\sigma^{xx}(x,r)$ is given by eqs. (19) and (20), which are the CLT stress-strain relations, and eqs. (12) and (128), which are the axisymmetric kinematic relations. They are repeated here for convenience:

CLT Stress-Strain Relations:

$$\begin{aligned} \sigma_x &= \bar{Q}_{11} \epsilon_x + \bar{Q}_{12} \epsilon_\theta + \bar{Q}_{16} \gamma_{x\theta} - \sigma_x^T \\ \sigma_\theta &= \bar{Q}_{12} \epsilon_x + \bar{Q}_{22} \epsilon_\theta + \bar{Q}_{26} \gamma_{x\theta} - \sigma_\theta^T \\ \tau_{x\theta} &= \bar{Q}_{16} \epsilon_x + \bar{Q}_{26} \epsilon_\theta + \bar{Q}_{66} \gamma_{x\theta} - \tau_{x\theta}^T, \end{aligned} \quad (19)$$

where

$$\begin{aligned}
\sigma_x^T &= (\bar{Q}_{11}\alpha_x + \bar{Q}_{12}\alpha_\theta + \bar{Q}_{16}\alpha_{x\theta})\Delta T \\
\sigma_\theta^T &= (\bar{Q}_{12}\alpha_x + \bar{Q}_{22}\alpha_\theta + \bar{Q}_{26}\alpha_{x\theta})\Delta T \\
\tau_{x\theta}^T &= (\bar{Q}_{16}\alpha_x + \bar{Q}_{26}\alpha_\theta + \bar{Q}_{66}\alpha_{x\theta})\Delta T.
\end{aligned}
\tag{20}$$

Axisymmetric Kinematic Relations:

$$\begin{aligned}
\varepsilon_x &= \varepsilon_x^o + z \kappa_x^o \\
\varepsilon_\theta &= \varepsilon_\theta^o + z \kappa_\theta^o \\
\gamma_{x\theta} &= \gamma_{x\theta}^o + z \kappa_{x\theta}^o,
\end{aligned}
\tag{12}$$

where

$$\begin{aligned}
\beta_x^o &= -\frac{dw^o}{dx}; \quad \beta_\theta^o = 0 \\
\varepsilon_x^o &= \frac{du^o}{dx} + \frac{1}{2}\beta_x^{o2}; \quad \varepsilon_\theta^o = \frac{w^o}{R}; \quad \gamma_{x\theta}^o = \frac{dv^o}{dx} \\
\kappa_x^o &= \frac{d\beta_x^o}{dx}; \quad \kappa_\theta^o = 0; \quad \kappa_{x\theta}^o = 0.
\end{aligned}
\tag{128}$$

In order to proceed with the solution process, the first of eqs. (19) must be differentiated with respect to x . Since the transformed reduced stiffnesses \bar{Q}_{ij} are assumed constant along the length of the cylinder, the partial derivative of σ^{xx} with respect to x , in terms of the strain components is

$$\frac{\partial \sigma^{xx}}{\partial x} = \bar{Q}_{11} \frac{\partial \varepsilon_x}{\partial x} + \bar{Q}_{12} \frac{\partial \varepsilon_\theta}{\partial x} + \bar{Q}_{16} \frac{\partial \gamma_{x\theta}}{\partial x}. \tag{235}$$

Therefore, the partial derivatives of the inplane strain components given in eqs. (12) and (128) are required. Performing the differentiation results in

$$\begin{aligned}
\frac{\partial \epsilon_x}{\partial x} &= \frac{d^2 u^o}{dx^2} + \frac{dw^o}{dx} \frac{d^2 w^o}{dx^2} - z \frac{d^3 w^o}{dx^3}, \\
\frac{\partial \epsilon_\theta}{\partial x} &= \frac{1}{R} \frac{dw^o}{dx}, \\
\frac{\partial \gamma_{x\theta}}{\partial x} &= \frac{d^2 v^o}{dx^2}.
\end{aligned} \tag{236}$$

These partial derivatives involve the derivatives of the solutions for the reference surface displacements $u^o(x)$, $v^o(x)$, and $w^o(x)$. For instance, the first of eqs. (236) involves the second derivative of $u^o(x)$. This term can most easily be derived from the definition of N_x for the axisymmetric problem, given in eq. (134) as

$$N_x = A_{11} \epsilon_x^o + A_{12} \frac{w^o}{R} - B_{11} \frac{d^2 w^o}{dx^2} - N_x^T, \tag{237}$$

where ϵ_x^o is given by eq. (13) as

$$\epsilon_x^o = \frac{du^o}{dx} + \frac{1}{2} \beta_x^{o^2} = \frac{du^o}{dx} + \frac{1}{2} \left(\frac{dw^o}{dx} \right)^2. \tag{238}$$

Substituting eq. (238) into eq. (237), and solving for $\frac{du^o}{dx}$ results in

$$\frac{du^o}{dx} = \frac{1}{A_{11}} (N_x + N_x^T) - \frac{A_{12}}{A_{11}R} w^o + \frac{B_{11}}{A_{11}} \frac{d^2 w^o}{dx^2} - \frac{1}{2} \left(\frac{dw^o}{dx} \right)^2. \tag{239}$$

Differentiating the above expression once results in

$$\frac{d^2 u^o}{dx^2} = -\frac{A_{12}}{A_{11}R} \frac{dw^o}{dx} + \frac{B_{11}}{A_{11}} \frac{d^3 w^o}{dx^3} - \frac{dw^o}{dx} \frac{d^2 w^o}{dx^2}. \tag{240}$$

Since the solution for $w^o(x)$ is known and it is continuous, its derivatives are obtainable

and the expression in eq. (240) is known for any point along the half-length of the cylinder.

Substituting eq. (240) into eq. (236) results in an expression for $\frac{\partial \epsilon_x}{\partial x}$ in terms of derivatives of $w^o(x)$, i.e.,

$$\frac{\partial \epsilon_x}{\partial x} = \left[-\frac{A_{12}}{A_{11}R} \frac{dw^o}{dx} + \frac{B_{11}}{A_{11}} \frac{d^3 w^o}{dx^3} - \frac{dw^o}{dx} \frac{d^2 w^o}{dx^2} \right] + \frac{dw^o}{dx} \frac{d^2 w^o}{dx^2} + z \left(-\frac{d^3 w^o}{dx^3} \right)$$

or

$$\frac{\partial \epsilon_x}{\partial x} = -\frac{A_{12}}{A_{11}R} \frac{dw^o}{dx} + \frac{B_{11}}{A_{11}} \frac{d^3 w^o}{dx^3} + z \left(-\frac{d^3 w^o}{dx^3} \right). \quad (241)$$

Since eq. (234) involves differentiation with respect to r , it will be necessary to express the above equation in terms of r instead of z . This is easily accomplished by substituting the definition of the local z coordinate, i.e.,

$$z = r - R, \quad (242)$$

into the last expression in eq. (241), which results in

$$\frac{\partial \epsilon_x}{\partial x} = -\frac{A_{12}}{A_{11}R} \frac{dw^o}{dx} + \left(\frac{B_{11}}{A_{11}} + R \right) \frac{d^3 w^o}{dx^3} + r \left(-\frac{d^3 w^o}{dx^3} \right). \quad (243)$$

The partial derivative of ϵ_θ in eqs. (236) involves the constant R , the mean radius of the cylinder, and the second derivative of $w^o(x)$, which can be obtained through differentiation of the solution for $w^o(x)$, derived in chapter 3.

The partial derivative of $\gamma_{x\theta}$ in eq. (236), i.e., $\frac{\partial \gamma_{x\theta}}{\partial x}$, can be obtained by differentiating the equation for $\gamma_{x\theta}$ in terms of $w^o(x)$ given by eq. (135b), namely,

$$\gamma_{x\theta}^o = \left(\frac{B_{16}}{A_{66}} \frac{d^2 w^o}{dx^2} + \frac{S}{A_{66}} \right). \quad (135b)$$

Differentiating this equation once with respect to x results in

$$\frac{\partial \gamma_{x\theta}}{\partial x} = \frac{B_{16}}{A_{66}} \frac{d^3 w^o}{dx^3}. \quad (244)$$

Substituting the expressions for the partial derivatives of the inplane strain components with respect to x , eqs. (243), (244), and (236), into the expression describing the partial derivative of σ^{xx} , eq. (235), results in

$$\begin{aligned} \frac{\partial \sigma^{xx}}{\partial x} = & \left\{ \bar{Q}_{11} \left[-\frac{A_{12}}{A_{11}R} \frac{dw^o}{dx} + \left(\frac{B_{11}}{A_{11}} + R \right) \frac{d^3 w^o}{dx^3} \right] \right. \\ & \left. + \bar{Q}_{12} \left[\frac{1}{R} \frac{dw^o}{dx} \right] + \bar{Q}_{16} \left[\frac{B_{16}}{A_{66}} \frac{d^3 w^o}{dx^3} \right] \right\} \\ & + r \left\{ -\bar{Q}_{11} \left[\frac{d^3 w^o}{dx^3} \right] \right\}. \end{aligned} \quad (245)$$

This expression can be rewritten in the form

$$\frac{\partial \sigma^{xx}}{\partial x} = \left\{ \frac{d \sigma^{xx^M}}{dx} \right\} + r \left\{ \frac{d \sigma^{xx^B}}{dx} \right\}, \quad (246)$$

where

$$\begin{aligned} \frac{d \sigma^{xx^M}}{dx} = & \left\{ \bar{Q}_{11} \left[-\frac{A_{12}}{A_{11}R} \frac{dw^o}{dx} + \left(\frac{B_{11}}{A_{11}} + R \right) \frac{d^3 w^o}{dx^3} \right] \right. \\ & \left. + \bar{Q}_{12} \left[\frac{1}{R} \frac{dw^o}{dx} \right] + \bar{Q}_{16} \left[\frac{B_{16}}{A_{66}} \frac{d^3 w^o}{dx^3} \right] \right\}, \end{aligned} \quad (247a)$$

and

$$\frac{d \sigma^{xx^b}}{dx} = \left\{ -\bar{Q}_{11} \left[\frac{d^3 w^o}{dx^3} \right] \right\} . \quad (247b)$$

Therefore, at any axial location along the length of the cylinder, the derivatives defined in eqs. (247) can be calculated from the derivatives of the solution for $w^o(x)$ and the transformed reduced stiffnesses \bar{Q}_{ij} for the layer which corresponds to the coordinate r . It should be noted that the derivatives in eqs. (247) are known functions of the x coordinate. In order to make this point clear and to simplify the notation, the definitions

$$m(x) = \frac{d \sigma^{xx^M}}{dx} = \left\{ \bar{Q}_{11} \left[-\frac{A_{12}}{A_{11}R} \frac{dw^o}{dx} + \left(\frac{B_{11}}{A_{11}} + R \right) \frac{d^3 w^o}{dx^3} \right] + \bar{Q}_{12} \left[\frac{1}{R} \frac{dw^o}{dx} \right] + \bar{Q}_{16} \left[\frac{B_{16}}{A_{66}} \frac{d^3 w^o}{dx^3} \right] \right\} , \quad (248a)$$

and

$$b(x) = \frac{d \sigma^{xx^b}}{dx} = \left\{ -\bar{Q}_{11} \left[\frac{d^3 w^o}{dx^3} \right] \right\} \quad (248b)$$

are introduced. Substituting eqs. (246) and (247) into eq. (234) using the definitions in eqs. (248) results in the partial differential equation

$$\frac{\partial \tau^{xr}(x,r)}{\partial r} + \frac{\tau^{xr}(x,r)}{r} = -\{m(x) + r[b(x)]\} . \quad (249)$$

For a specified temperature change, boundary condition, axial load level N_x , and axial position $x = \bar{x}$, the terms $m(x)$ and $b(x)$ are known quantities. Therefore, at a specified axial location $x = \bar{x}$, eq. (249) becomes a nonhomogeneous ordinary differential equation.

That is,

$$\frac{d\tau^{xr}(\bar{x}, r)}{dr} + \frac{\tau^{xr}(\bar{x}, r)}{r} = -\{m(\bar{x}) + r[b(\bar{x})]\} . \quad (250)$$

Equation (250) is of the form

$$\frac{dF}{dr} + \frac{F}{r} = g + hr , \quad (251)$$

where the substitutions

$$F = F(r) \equiv \tau^{xr}(\bar{x}, r) ; \quad g \equiv -m(\bar{x}) ; \quad h = -b(\bar{x}) \quad (252)$$

have been made. By introducing a change of variable according to

$$r = e^z , \quad (253)$$

eq. (251) becomes

$$\frac{dF}{dz} + F = g e^z + h e^{2z} . \quad (254)$$

This differential equation has a homogeneous solution of the form

$$F_{\text{homo.}} = A e^{-z} \quad \text{or} \quad F_{\text{homo.}} = \frac{A}{r} , \quad (255)$$

where A is an unknown constant to be determined, and the particular solution

$$F_{\text{part.}} = s e^z + 2t e^{2z} . \quad (256)$$

Substituting eq. (256) into eq. (254) results in

$$(2s) e^z + (3t) e^{2z} = g e^z + h e^{2z} \quad \rightarrow \quad 2s = g ; \quad 3t = h . \quad (257)$$

Therefore, the particular solution is

$$F_{part.} = \frac{g}{2} e^z + \frac{h}{3} e^{2z} \quad (258)$$

or

$$F_{part.} = \frac{g}{2} r + \frac{h}{3} r^2 .$$

Hence, the solution to the nonhomogeneous ordinary differential equation (251) is

$$F(r) = \frac{A}{r} + \frac{g}{2} r + \frac{h}{3} r^2 . \quad (259)$$

Since the step relating the partial differential equation (249) to the ordinary differential equations (250) and (251) was taken by restricting eqs. (250) and (251) to a particular x location, it must be realized that the constants A , g , and h appearing in eq. (259) are unique for each x location. Therefore, g and h in eq. (259) vary along the length of the cylinder and are known quantities obtained by the relations in eqs. (248), and $A = A(x)$ is a unique constant for each x location, which will be determined later. Thus, by using the definitions from eq. (252), and noting that $A = A(x)$, for a particular axial location $x = \bar{x}$, the solution presented above in eq. (259) becomes

$$\tau^{xr}(\bar{x}, r) = \frac{A(\bar{x})}{r} - \frac{m(\bar{x})}{2} r - \frac{b(\bar{x})}{3} r^2 . \quad (260)$$

It should be noted that since the stress-strain relations of eq. (19) apply only within a given layer, the solution given in eq. (260) also applies only within a given layer. To make this distinction clear, a superscript (k), which denotes the layer number from $k = 1$ at the inner layer to $k = K$ at the outer layer, will be used from this point onward. For example, eq. (260) will now be written

$$\tau^{xr^{(k)}}(\bar{x}, r) = \frac{A^{(k)}(\bar{x})}{r} - \frac{m^{(k)}(\bar{x})}{2} r - \frac{b^{(k)}(\bar{x})}{3} r^2, \quad (261)$$

which is valid in the range

$$r^{(k-1)} \leq r \leq r^{(k)}. \quad (262)$$

Therefore, for a cylinder with K layers, there are K constants $A^{(k)}(\bar{x})$ to be determined in as many equations (261). In eq. (262), the superscript on r can take on the range from 0 to K , with $r^{(0)} \equiv \left(R - \frac{H}{2}\right)$ being the radius of the inner surface of the cylinder, and $r^{(K)} \equiv \left(R + \frac{H}{2}\right)$ being the radius of the outer surface of the cylinder. Therefore, $r^{(k)}$ corresponds to the k^{th} layer interface.

Thus far, the pertinent kinematic relations, constitutive relations, and the first equilibrium equation have been used to derive the solution form of τ^{xr} . Next, the boundary condition relations of eqs. (232) must be satisfied for each layer of the cylinder. However, this is a trivial matter since the displacements are specified everywhere within the cylinder and on its boundaries due to the assumptions of the CLT analysis.

In this analysis, the adjacent layers are assumed to have a perfect bond at the layer interface. This implies that all of the displacement components and interlaminar stress components are continuous across the interfaces of adjacent layers. As noted in the previous paragraph, the displacements are continuous across the interfaces since they have been prescribed to vary linearly through the thickness of the cylinder wall in the CLT analysis of chapters 2, 3, and 4. However, the interface condition for the continuity of the interlaminar stress components has not yet been addressed. In order to

solve for the unknown constants $A^{(k)}(\bar{x})$, the interface continuity of the interlaminar stress component τ^{xr} will be used. For the $k=1$ through K layers, there are $(K-1)$ interface continuity conditions and two surfaces on which τ^{xr} can be specified, namely the surfaces at the inner and outer radii of the cylinder. This results in $(K+1)$ conditions from which the K unknown constants $A^{(k)}(\bar{x})$ can be determined. Since the interface conditions for τ^{xr} must be satisfied in order to comply with the assumption of perfectly bonded layers mentioned previously, the boundary condition for τ^{xr} at either the inner or outer radius will have to be ignored. Since the axial loading investigated thus far in this work does not consist of an applied traction on either the inner or outer surfaces of the cylinder, the condition

$$\tau^{xr^{(k-1)}}(\bar{x}, r^{(0)}) = 0 , \quad (263)$$

will be imposed. Therefore, for a particular axial location, $x = \bar{x}$, the equation describing τ^{xr} for the first layer at the inner radius can be written as

$$\tau^{xr^{(1)}}(\bar{x}, r^{(0)}) = \frac{A^{(1)}(\bar{x})}{r^{(0)}} - \frac{r^{(0)}}{2} m^{(1)}(\bar{x}) - \frac{(r^{(0)})^2}{3} b^{(1)}(\bar{x}) = 0 . \quad (264)$$

This equation can be solved for $A^{(1)}(\bar{x})$ to give

$$A^{(1)}(\bar{x}) = \frac{(r^{(0)})^2}{2} m^{(1)}(\bar{x}) + \frac{(r^{(0)})^3}{3} b^{(1)}(\bar{x}) , \quad (265)$$

where the constants $m^{(1)}(\bar{x})$ and $b^{(1)}(\bar{x})$ are calculated from eqs. (248) using values for the transformed reduced stiffnesses \bar{Q}_{ij} for the first (inner) layer of the cylinder.

The interface continuity condition for τ^{xr} is

$$\tau^{xr^{(k+1)}}(\bar{x}) = \tau^{xr^{(k)}}(\bar{x}) \quad (266)$$

over the range of $k = 1$ to $K-1$. Substituting eq. (261) into eq. (266) results in

$$\begin{aligned} & \frac{A^{(k+1)}(\bar{x})}{r^{(k)}} - \frac{r^{(k)}}{2} m^{(k+1)}(\bar{x}) - \frac{(r^{(k)})^2}{3} b^{(k+1)}(\bar{x}) \\ &= \frac{A^{(k)}(\bar{x})}{r^{(k)}} - \frac{r^{(k)}}{2} m^{(k)}(\bar{x}) - \frac{(r^{(k)})^2}{3} b^{(k)}(\bar{x}) \quad , \end{aligned} \quad (267)$$

which can be rearranged to provide a recursive relation for $A^{(k+1)}(\bar{x})$, i.e.,

$$\begin{aligned} A^{(k+1)}(\bar{x}) = & \\ & A^{(k)}(\bar{x}) + \frac{(r^{(k)})^2}{2} [m^{(k+1)}(\bar{x}) - m^{(k)}(\bar{x})] + \frac{(r^{(k)})^2}{3} [b^{(k+1)}(\bar{x}) - b^{(k)}(\bar{x})] \quad . \end{aligned} \quad (268)$$

Hence, the K constants $A^{(k)}(\bar{x})$ in the equations describing $\tau^{xr}(\bar{x}, r)$ are known quantities and the interlaminar stress component τ^{xr} can be calculated at any radial location r at a specified axial location $x = \bar{x}$ where the CLT solutions have been previously calculated.

B. Calculation of the Interlaminar Stress Component τ^{xr}

In the following, numerical results will be presented which illustrate the relations between the interlaminar stress component τ^{xr} and the radial coordinate r for the three cylinders analyzed in this investigation. Clamped boundary conditions are enforced, compressive axial loads of $N = 10\% N^*$ and $N = 90\% N^*$ are applied, and thermally-induced preloading effects corresponding to a temperature change of -280°F are included in the CLT solutions used for the calculation of the terms of the solution of τ^{xr} involving the intralaminar stress component σ^{xx} . As noted in the previous section, the solution for $\tau^{(k)}(\bar{x}, r)$ is calculable only after an axial position $x = \bar{x}$ has been selected and the

derivatives appearing in the definitions of the "constants" $A^{(k)}(\bar{x})$, $m^{(k)}(\bar{x})$, and $b^{(k)}(\bar{x})$ have been calculated for each layer. The axial positions investigated will be: (a) The end of the cylinder at $x=+L/2$; (b) The axial position x where the rotation r_{xr} has a maximum absolute value, and; (c) The axial position x where the interlaminar shear stress resultant, Q_x , has a maximum absolute value. An expression relating Q_x to the CLT solution is contained in the axisymmetric version of eq. (126b), namely,

$$Q_x = \frac{dM_x}{dx} + N_x \frac{dw}{dx} . \quad (269)$$

The term $\frac{dM_x}{dx}$ can be calculated from the expression for M_x in eq. (134), i.e.,

$$M_x = B_{11} \epsilon_x^o + \frac{B_{12}}{R} w^o + B_{16} \gamma_{x\theta}^o - D_{11} \frac{d^2 w^o}{dx^2} - M_x^T , \quad (270)$$

which, by substituting the expressions relating ϵ_x^o and $\gamma_{x\theta}^o$ to the solution for $w^o(x)$ and its derivatives, i.e., eqs. (135), and differentiating the result once with respect to x becomes

$$\frac{dM_x}{dx} = \left(\frac{B_{11}^2}{A_{11}} + \frac{B_{16}^2}{A_{66}} - D_{11} \right) \frac{d^3 w^o}{dx^3} + \left(\frac{B_{12}}{R} - \frac{B_{11} A_{12}}{A_{11} R} \right) \frac{dw^o}{dx} . \quad (271)$$

The linear form of Q_x is obtained by eliminating the second term in eq. (269), i.e.,

$$Q_{x(\text{linear})} = \frac{dM_x}{dx} , \quad (272)$$

as given by equation (271). Since the solution for τ^{xr} was obtained from the linearized form of the first equilibrium equation, then it is expected that the formal definition of the resultant Q_x , i.e.,

$$Q_x \equiv \sum_{k=1}^K \left[\int_{r^{(k-1)}}^{r^{(k)}} \tau^{xr^{(k)}} dr \right] \quad (273)$$

should agree with the expression for $Q_{x(\text{max})}$ given in eqs. (271) and (272).

Therefore, the axial position x corresponding to the largest absolute value of

$$Q_{x(\text{max})} = \left(\frac{B_{11}^2}{A_{11}} + \frac{B_{16}^2}{A_{66}} - D_{11} \right) \frac{d^3 w^o}{dx^3} + \left(\frac{B_{12}}{R} - \frac{B_{11} A_{12}}{A_{11} R} \right) \frac{dw^o}{dx} , \quad (274)$$

will be one of the axial locations used to calculate the relation between τ^{xr} and r . Hence, as a check of the interlaminar stress calculation for τ^{xr} , the values of τ^{xr} will be numerically integrated along the radial direction as shown in eq. (273), and the result will be compared to that calculated through eq. (274).

C. Numerical Results for the Interlaminar Stress Component τ^{xr} : Case of Thermally-Induced Preloading Effects and a Compressive Axial Load with Clamped Boundary Conditions

Fig. 41 through Fig. 45 illustrate the relationship between the normalized interlaminar shear stress and the radial coordinate ρ for the compressive axial load levels $N = 10\% N^*$ and $N = 90\% N^*$ at various locations along the length of the three cylinders. The shear stress τ^{xr} has been normalized by the quantity (N/H) , as the intralaminar stress components were in chapter 4. The radial coordinate has been redefined as ρ , where

$$\rho = \frac{r - R}{H} = \frac{z}{H} \quad (275)$$

and
$$-0.5 \leq \rho \leq +0.5 . \quad (276)$$

Each figure represents the interlaminar shear stress response of the three cylinders for the two load cases and a particular axial location. In each of the figures, horizontal grid lines and symbols are used to designate the 15 layer interfaces. Fig. 41 illustrates the shear stress response at the end of the cylinders, $x = +L/2$, associated with the low axial load level. While distribution of the shear stress in the symmetric laminate is shown to be symmetric about the mean radius, $\rho = 0$, the distributions of the shear stress in the two unsymmetric cylinders are skewed, with the shear stress having larger magnitudes to either side of the mean radius. For instance, the $[0_2/-45/+45]_{4T}$ laminate has a peak shear stress magnitude at a radius two layer thicknesses inside of the mean radius. This behavior leads to larger slope discontinuities in the interlaminar shear stress at the interface of layers of differing orientations on the side of the mean radius to which the response is skewed. Conversely, the slope discontinuities are smaller to the other side of the maximum response location. Due to the opposite signs of the **B** matrix terms, the $[+45/-45/0_2]_{4T}$ laminate has a peak interlaminar shear stress at a radial location outside of the mean radius. These trends can be observed for the higher load level as well, i.e., the case represented in Fig. 42, which also represents the interlaminar stress component at the end of the cylinder. However, partly due to the scale used to illustrate the higher load level response plots, the effects appear to be smaller. It is also seen that the shear stress at the end of the cylinder for the $[0_2/-45/+45]_{4T}$ laminate is larger for both the low

and high load levels then for the other two laminates.

For the low load level, the axial location of the maximum shear stress resultant Q_x is at the ends of all three cylinders. However, for the high load level the axial location of the largest Q_x occurs at $x/L=0.480$ for the $[+45/-45/0_2]_{2S}$ and $[0_2/-45/+45]_{4T}$ cylinders and at $x/L=0.478$ for the $[+45/-45/0_2]_{4T}$ cylinder. The interlaminar shear stress response for this case is presented in Fig. 43. Again, the $[0_2/-45/+45]_{4T}$ cylinder has the largest shear stress magnitude. Shown in this plot is the fact that the shear stress of all three cylinders at this axial location is also skewed relative to the mean radius of the cylinder. The reason for this behavior is not immediately apparent, but it could be a function of the magnitudes of the first and third derivatives of $w^o(x)$ at axial locations away from the end of the cylinders, as they appear in the relations for the solution for τ^{xr} , relative to the magnitudes of these terms at the ends of the cylinders.

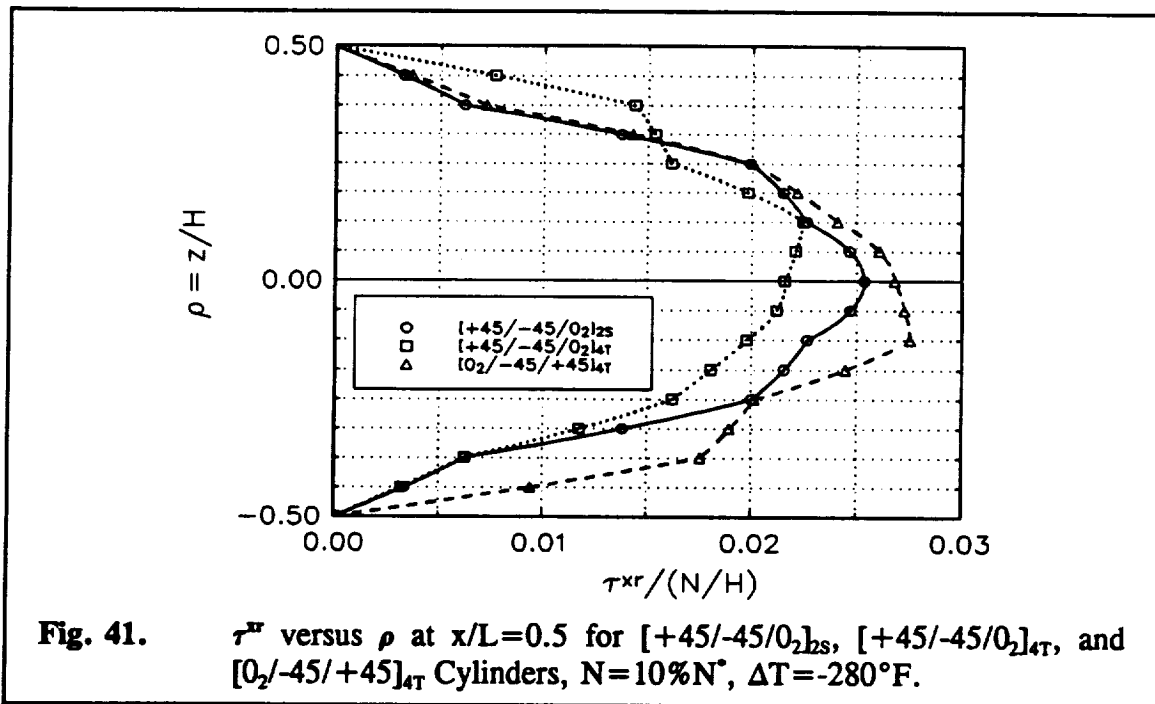
Fig. 44 and Fig. 45 represent the interlaminar shear stress response at axial locations for which the cylinders possess peak magnitudes of the rotation, r_{xr} , for the low and high load levels, respectively. These axial locations are in the vicinity of $x/L=.470$ for all three laminates at the high load level, and at $x/L=0.480$ for the $[+45/-45/0_2]_{2S}$ and $[0_2/-45/+45]_{4T}$ cylinders and at $x/L=0.5$ for the $[+45/-45/0_2]_{4T}$ cylinder at the low load level. Again, it is noted that the response of all three cylinders is skewed relative to the mean radius. For the shear stress results previously discussed, i.e., at the low and high load level and where the axial locations were that of maximum Q_x and the cylinders' end, the $[0_2/-45/+45]_{4T}$ cylinder has the largest overall shear stress magnitude of the two three cylinders. This is also true for the high load level where the axial location is that

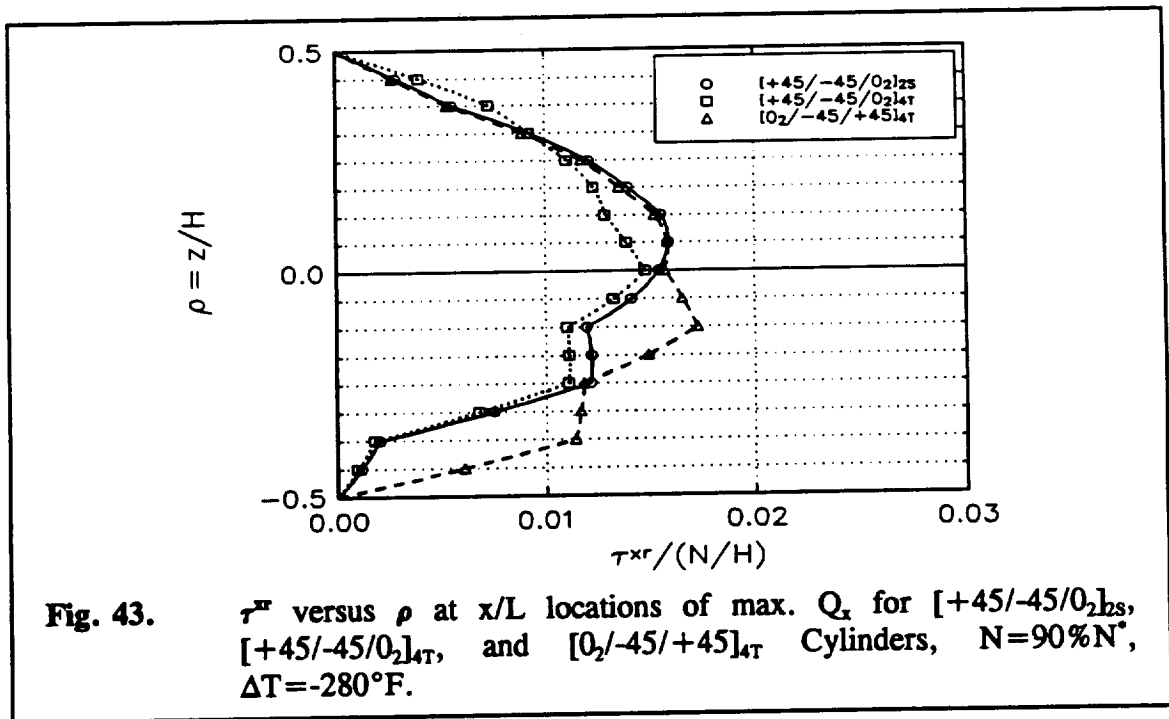
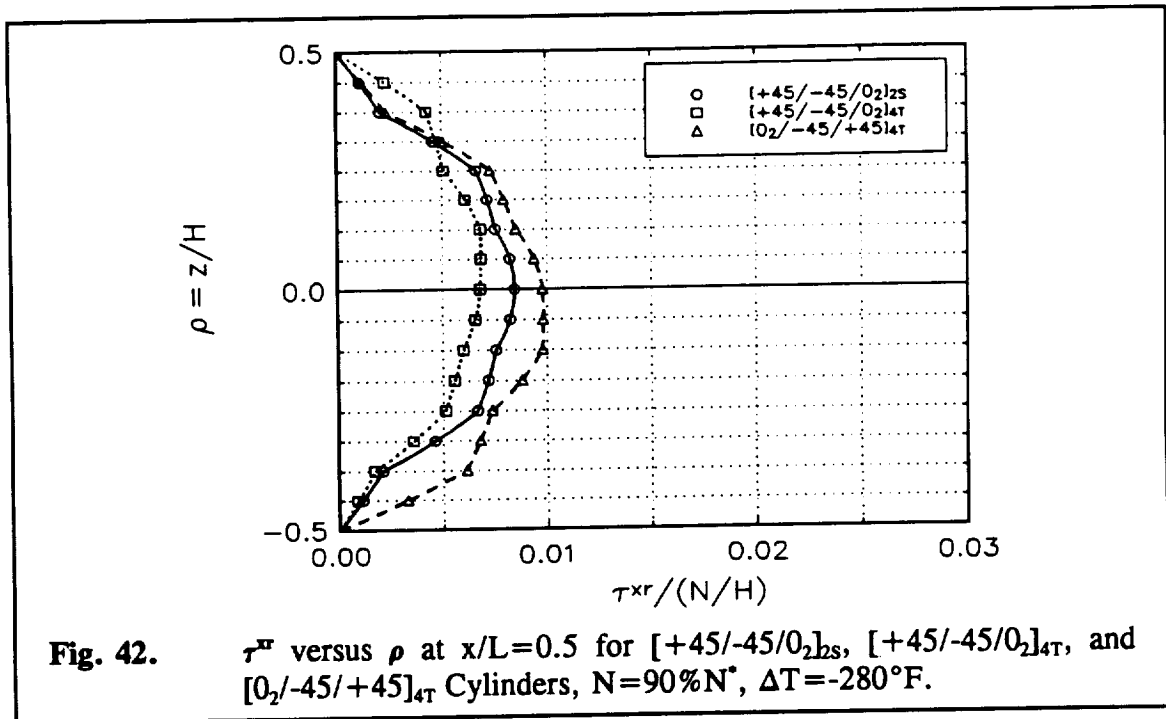
of the maximum rotation r_{xr} , as seen in Fig. 45. However, for the low load level and at the axial location of maximum rotation r_{xr} , the overall magnitude of the shear stress for the $[+45/-45/0_2]_{4T}$ cylinder is larger than the overall magnitude for the $[0_2/-45/+45]_{4T}$ cylinder. This reversal in trend indicates that the thermally-induced preloading effects dominate the response at the low load level. This characteristic was observed with the interlaminar stresses discussed in chapter 4.

The responses shown in Fig. 41 through Fig. 45 were numerically integrated using Simpson's 1/3 quadrature rule. Since the relation describing τ^{xr} as a function of r is parabolic in r , and Simpson's quadrature involves approximation of the data by a series of parabolic segments, the results of the numerical integration by Simpson's rule are independent of the number of data points used. The results presented in the figures were numerically integrated on a layer-by-layer basis and the integration results were summed, as indicated in eq. (273). Also, the linearized relation for the shear resultant Q_x , given by eq. (274) was calculated at the axial location corresponding to that at which the τ^{xr} data was obtained for each relation in each figure. These steps were conducted as a check of the accuracy of the solution for τ^{xr} . The results of these calculations are presented in Table IV. The right-most column of Table IV is the CLT relation for the shear resultant Q_x as given in eq. (274), and the second column from the right is the result of Simpson's quadrature on the τ^{xr} data. It is seen that there is excellent agreement between the two relations for all load cases and axial locations investigated. This result suggests that the solution for τ^{xr} derived from the linearized version of the first equilibrium equation, eq. (233), is accurate for these cylinders under the load levels

and boundary conditions studied.

This chapter brings to a close the investigation of the displacement and stress response of unsymmetrically laminated cylinders. Though specific cylinders were considered, general conclusions can be drawn from the results presented. A discussion of these conclusions is the subject of the final chapter.





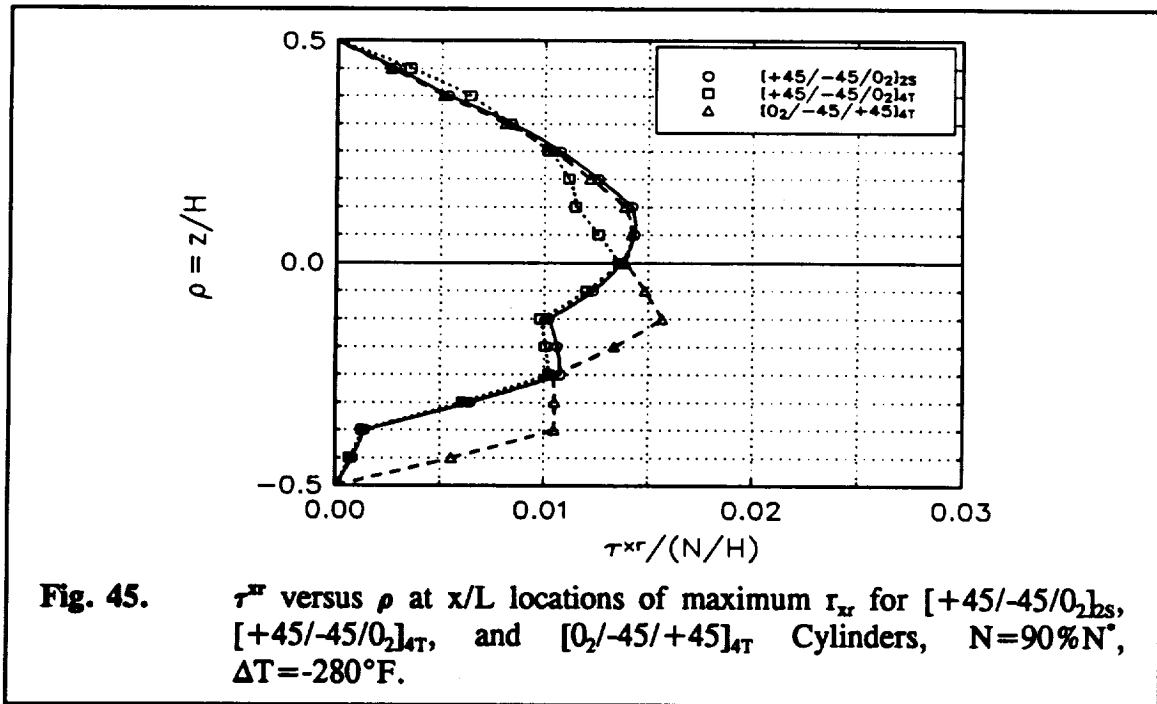
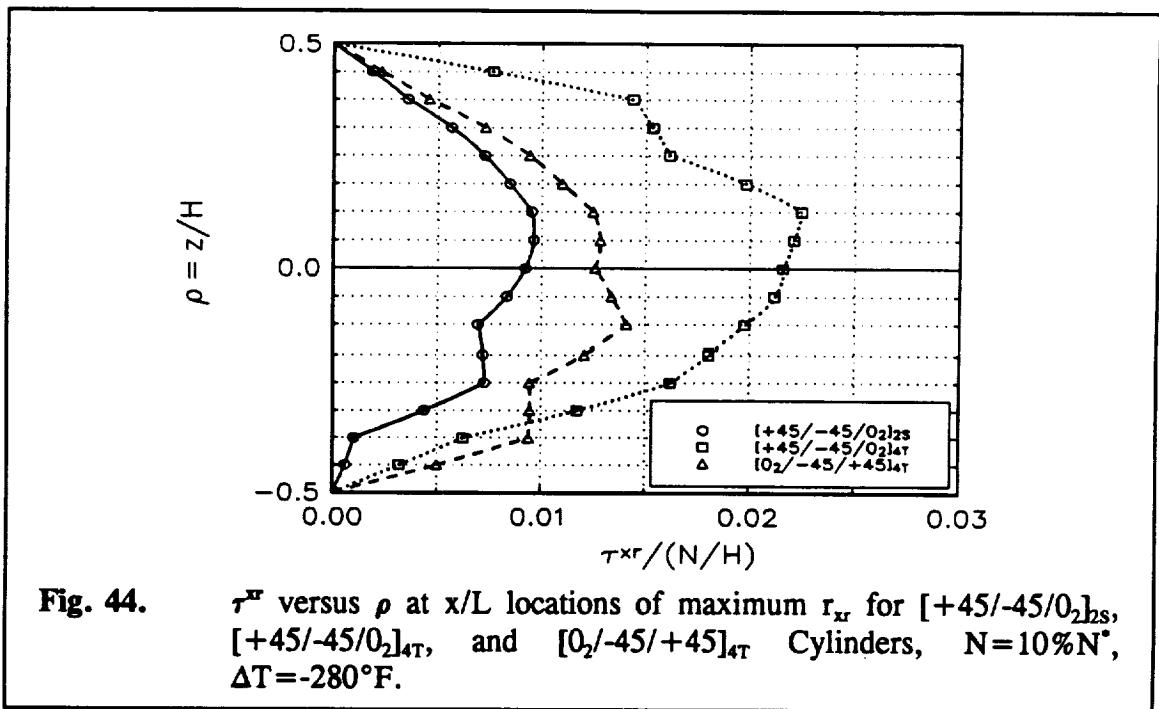


Table IV. Comparison of the Shear Resultant Q_x as Calculated from the Interlaminar Shear Stress τ^{xr} and the Derivative of the CLT Relation for M_x .

Cylinder Stacking Sequence	Axial Load Level, N/N^*	Axial Location Criterion	Axial Location, x/L	$\int \frac{\tau^{xr}}{(N/H)} d\rho$	$\frac{dM_x^1}{dx}$
[+45/-45/0 ₂] _{2S}	10%	Cyl. End	0.5	0.0157	0.0158
[+45/-45/0 ₂] _{4T}	10%	Cyl. End	0.5	0.0149	0.0149
[0 ₂ /-45/+45] _{4T}	10%	Cyl. End	0.5	0.0182	0.0183
[+45/-45/0 ₂] _{2S}	10%	Max. r_{xr}	0.477	0.00572	0.00572
[+45/-45/0 ₂] _{4T}	10%	Max. r_{xr}	0.5	0.0149	0.0149
[0 ₂ /-45/+45] _{4T}	10%	Max. r_{xr}	0.485	0.00909	0.00913
[+45/-45/0 ₂] _{2S}	90%	Cyl. End	0.5	0.00524	0.00524
[+45/-45/0 ₂] _{4T}	90%	Cyl. End	0.5	0.00454	0.00456
[0 ₂ /-45/+45] _{4T}	90%	Cyl. End	0.5	0.00650	0.00654
[+45/-45/0 ₂] _{2S}	90%	Max. r_{xr}	0.470	0.00846	0.00851
[+45/-45/0 ₂] _{4T}	90%	Max. r_{xr}	0.468	0.00798	0.00803
[0 ₂ /-45/+45] _{4T}	90%	Max. r_{xr}	0.470	0.01010	0.01014
[+45/-45/0 ₂] _{2S}	90%	Max. Q_x	0.480	0.00954	0.00954
[+45/-45/0 ₂] _{4T}	90%	Max. Q_x	0.478	0.00888	0.00892
[0 ₂ /-45/+45] _{4T}	90%	Max. Q_x	0.480	0.01119	0.00127

¹ normalized to correlate with $\int \frac{\tau^{xr}}{(N/H)} d\rho$

VII. CONCLUSIONS

A. Discussion of Displacement Results

In chapter 3, results were presented for the mid-plane displacements $u^o(x)$, $v^o(x)$, and $w^o(x)$ as they vary along the length of one symmetrically laminated cylinder and two unsymmetrically laminated cylinders with equal and opposite **B** matrix terms. From the results for the preloading response due to thermal effects, it was observed that all of the cylinders expand axially due to the negative value of the effective axial thermal expansion coefficient of the cylinders and the negative temperature change, ΔT , from consolidation temperature to ambient temperature. In addition, all three cylinders respond to the temperature change by a reduction in the radii of the cylinders. For the symmetric cylinder, the tangential displacement is zero and radial displacement is constant along the cylinder's length. For the unsymmetric cylinders, the tangential and radial displacements vary along the cylinders' length, particularly near the ends. These two cylinders' ends "curl" radially and twist, producing a boundary layer effect. The direction of the curl for the cylinders is opposite, depending on the sign of the thermally induced moment M_x^T , which is a consequence of the opposite signs of the **B** matrix terms for these two unsymmetric cylinders. Any unsymmetric laminate will exhibit this characteristic. This thermally induced curl and twist must be accounted for in the boundary conditions for subsequent axial loading and could have an effect on the onset of buckling of the cylinders. This is because the radius at the end of an unsymmetric cylinder through which the axial load is applied is different from the radius away from the ends.

Displacement results of the case of compressive axial load, including the thermally-induced preloading effects discussed above, indicate that the thermal effects have a measurable influence on the radial displacements under axial load. Neglecting the thermally-induced preloading effects results in smaller radial deformations. For a highly unsymmetric stacking sequence, the effects become larger. The load-induced axial and tangential displacements appear to be relatively unaffected by the thermally-induced preloading effects.

The shape and magnitude of the tangential and radial displacement responses change as the level of the compressive axial load increases. In particular, the length of the boundary layer, where the variation of the tangential and radial displacements fluctuate, increases as the load level increases. The axial displacement remains virtually linear along the axial direction, even at the high load level.

Comparison of the displacement results for simply supported and clamped boundary conditions reveal that the simply supported case yields a larger range of tangential and radial displacements for each cylinder although the axial displacement response is about the same.

An important conclusion is that if unsymmetrically laminated cylinders are to be analyzed or manufactured, it is important to include the thermally-induced preloading effects not only in the prediction of the overall displacement behavior of the cylinder under compressive axial loading, but also in the specification of the end conditions for both the analysis and the fixture design. The extent to which these effects are important depends on the material properties, stacking sequence, and the axial load level.

B. Discussion of Intralaminar Stress Results

An interesting observation was made of the intralaminar stress results in chapter 4. At the low load level investigated, $N = 10\% N^*$, the fiber-direction stresses, σ_{11} , in the $\pm 45^\circ$ layers is larger than the fiber-direction stresses in the 0° degree layers of the $[+45/-45/0_2]_{2S}$, $[+45/-45/0_2]_{4T}$, and $[0_2/-45/+45]_{4T}$ cylinders. This is surprising since the 0° layers have fibers aligned with the axial load and are expected to bear the majority of the axial load. This result indicates that at low load levels the thermally-induced preloading effects dominate the fiber-direction intralaminar stress response. The intralaminar stress component perpendicular to the fibers, σ_{22} , and the intralaminar shear stress component, τ_{12} , are small relative to the fiber-direction stresses.

When the axial load level is increased to $N = 90\% N^*$, the thermally-induced preloading effects are seen to be in the background, based on the observation that now the 0° layers have a larger fiber-direction magnitude than the $\pm 45^\circ$ layers, as would be expected for a cylinder subject to large axial loads. The intralaminar stress component perpendicular to the fibers, σ_{22} , is observed to be compressive. This result virtually eliminates the potential for matrix micro-cracking due to this stress component. The possibility of inplane shear failure also seems low, since the magnitude of τ_{12} is observed to be low, even for this high load level. It should be noted that the application of the relations for the principal material stress components presented in chapter 4 to conventional CLT plane-stress failure theories can easily be accomplished, although it was not done as part of this work.

C. Discussion of Interlaminar Stress Results

In order to more fully develop the relations for the material failure modes of the composite cylinders, a solution for the interlaminar shear stress τ^{zr} was developed and used to calculate the interlaminar shear stress for the cylinders and load cases investigated for the intralaminar stresses. It was reasoned that the remaining interlaminar stresses $\tau^{\theta r}$ and σ^{rr} are small relative to τ^{zr} in the context of axisymmetric loading. The solution for the interlaminar shear stress τ^{zr} was derived through a rational simplification of the three-dimensional equilibrium equation for the axial direction. Based on the excellent comparison between the results of numerically integrating the interlaminar shear stresses and the relation for the linearized shear stress resultant Q_x from the CLT solution of the third chapter, it is recognized that the solution obtained for the intralaminar shear stress was accurate. It was hoped that this would be the case since the method used to simplify the three-dimensional equilibrium equation, and the solution used to obtain the other stress component appearing in the equilibrium equation, σ_{xx} , both utilized the assumptions of Kirchhoff and Donnell.

It is observed that at the ends of the cylinders, the interlaminar shear stress response of the symmetric cylinder is symmetric with respect to the mean radius, R , or $\rho = 0$. The two unsymmetric cylinders, with $[0_2/-45/+45]_{4T}$ and $[+45/-45/0_2]_{4T}$ stacking sequences and equal but opposite B matrix terms, have peak interlaminar shear stresses at radial locations to the inside and outside of the mean radius. However, the shape of the interlaminar shear stress response through the cylinder wall is seen to vary along the length of the cylinder. In particular, for both the low and high load levels, the location

of peak interlaminar stress for the symmetric cylinder is seen to move away from the mean radius as the axial location at which the response is calculated is varied from the end of the cylinder, $x/L=0.5$, to the axial location of peak rotation, r_{xr} . This is also true as the axial location is varied from the end of the cylinder to the axial location of peak Q_x , for the high load level.

It is also observed that the axial location of peak Q_x occurs at the end of the cylinder, $x/L=0.5$, for the low load level, while the axial location of peak r_{xr} is at $x/L \approx 0.48$ for the high load level. For this load level the interlaminar shear stress response is skewed relative to the mean radius.

Comparing the results for the interlaminar shear stress calculated at the axial location of peak rotation, r_{xr} , for the low and high load levels, reveals that the $[+45/-45/0_2]_{4T}$ cylinder has the largest shear stress for the low load level, while the other unsymmetric cylinder has the largest shear stress for the high load level. This difference is yet again an indication of the thermally-induced preloading effects dominating the cylinder response at low load levels.

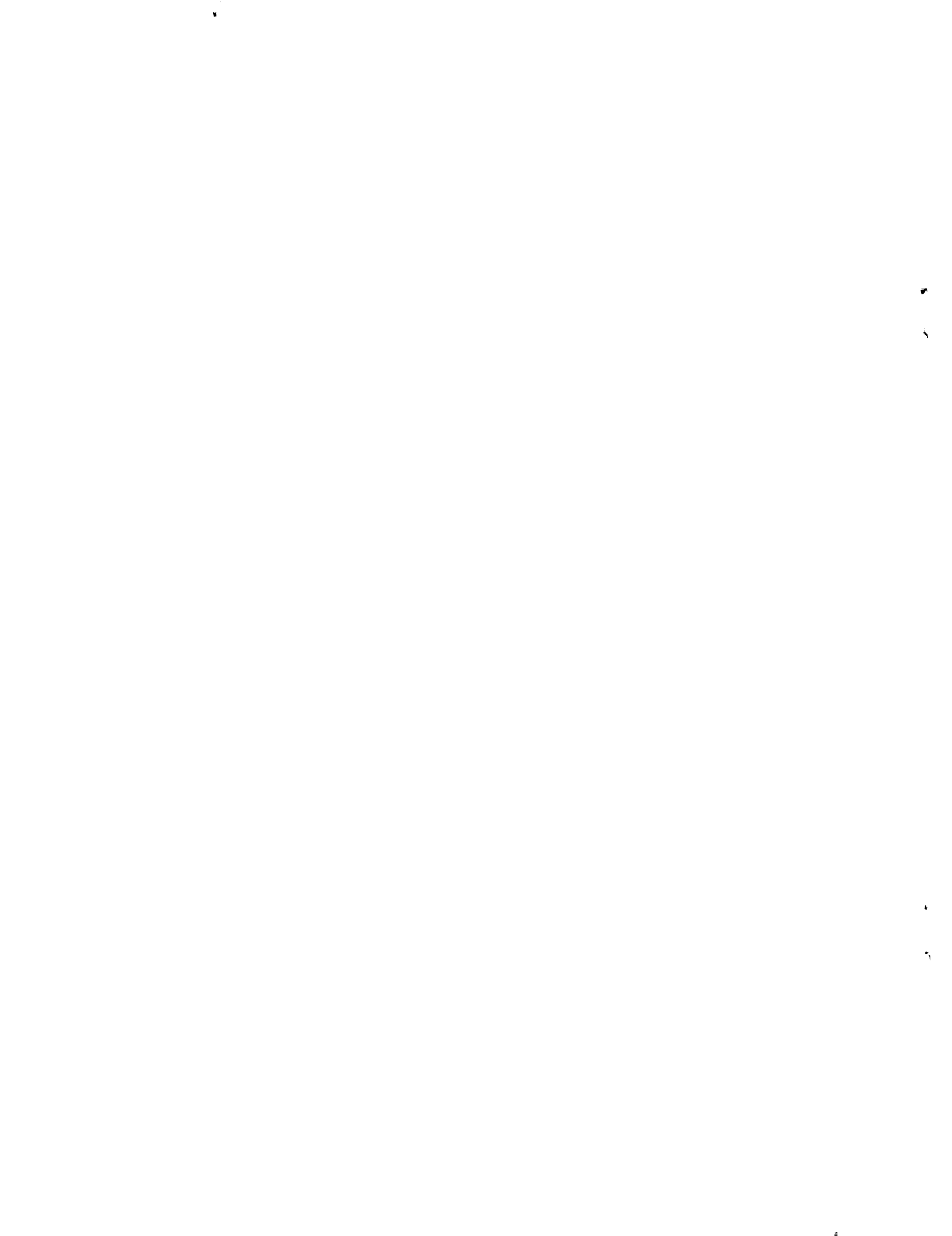
REFERENCES

1. Jones, R. M. and Hennemann, J. C. F., "Effect of Prebuckling Deformations on Buckling of Laminated Composite Circular Cylindrical Shells," AIAA Journal, vol. 18, no. 1, Jan. 1980, pp. 110-115.
2. Booton, M., "Buckling of Imperfect Anisotropic Cylinders Under Combined Loading," University of Toronto Institute of Aerospace Studies Report, UTIAS Report No. 203, CN ISSN 0082-5255, 1976.
3. Pagano, N. J., "Exact Solutions for Composite Laminates in Cylindrical Bending", J. Composite Materials, vol. 3, July 1969, pp. 398-411.
4. Reddy, J. N., Energy and Variational Methods in Applied Mechanics, John Wiley and Sons, 1984, p. 112.
5. Eringen, A. C., Mechanics of Continua, Robert E. Krieger Publishing Co., 1980.
6. Novozhilov, V. V., Foundations of the Nonlinear Theory of Elasticity, Graylock Press, 1953.
7. Fuchs, H. P., and Hyer, M. W., "Bending Response of Thin-walled Laminated Composite Cylinders," J. Composite Structures, vol. 22, 1992, pp. 87-107.

THIS PAGE INTENTIONALLY LEFT BLANK.

INITIAL DISTRIBUTION

Copies	Agency	Name	CENTER DISTRIBUTION		
			Copies	Code	Name
1	ONT 233	G. Remmers			
1	ONR 1132SM		1	0112	Douglas
			1	0114	Becker
6	NAVSEA		1	60	Wacker
1	05M	Kaznoff	1	60D	Krenzke
1	05P	Malakhoff	1	601	Morton
1	05P1	Packard	1	65	Rockwell
1	05P2	McCarthy	1	65	Jones
1	05R	Capt. R. Percival	1	65R	W. Brown
1	05U	Capt. J. Gillard	1	65.1	Tinley
			10	65.1	Paraska
3	DARPA		1	65.2	Phyllaier
1	AVSTO	James J. Kelly	1	65.2	Bonanni
1	RMO	Technical Library	1	65.2	Charette
			1	65.2	Garalla
1	NASA Headquarters	RM	1	65.2	Hoffman
			1	65.3	Nishida
1	NASA Langley Research Center		1	65.4	Wiggs
1	MS 190	M. Nemeth	1	66.2	Critchfield
			1	69.4	UERD Tech Ref. Ctr.
1	HERCULES AERO, INC.				
	P.O. Box 98		1	342.4	TIC (C)
	Magna, UT 84044-0098		1	342.5	TIC (A)
1	MS N2EA16	D. Cohen			
5	VPI&SU, ESM Department				
	Blacksburg, Virginia 24061-0219				
1		Z. Grdal			
1		Prof. O. Hayden Griffin			
1		Tamara Knott			
2		Prof. M. W. Hyer			
1	VPI&SU, Aerospace Engin. Dept.				
	Blacksburg, Virginia 24061-0219				
1		Eric Johnson			







DEPARTMENT OF THE NAVY
NAVAL SURFACE WARFARE CENTER
CARDEROCK DIVISION

CARDEROCK DIVISION HEADQUARTERS
DAVID TAYLOR MODEL BASIN
BETHESDA, MD 20084-5000

9110/subs
Ser 65-13
01 Apr 1993

From: Commander, Carderock Division, Naval Surface Warfare Center
To: Distribution

Subj: THERMAL AND COMPRESSION RESPONSE OF UNSYMMETRICALLY
LAMINATED CYLINDERS

Encl: (1) "Axisymmetric Deformations and Stresses of
Unsymmetrically Laminated Composite Cylinders in Axial
Compression with Thermally-Induced Preloading Effects",
by Peter J. Paraska

1. The analytical response of unsymmetrically laminated,
monocoque composite cylinders under axial loading must take into
account the non-uniform preloading shape brought about by the
temperature change from cure temperature to ambient temperature.

2. This report documents an analytical study of the response of
unsymmetrically laminated cylinders subjected to thermally-induced
preloading effects and compressive axial load. Closed-form
solutions are obtained for the displacements and intralaminar
stresses and recursive relations for the interlaminar shear stress
solutions. For the closed-form intralaminar stress
solutions. For the cylinder geometries and stacking sequence
examples analyzed, several important and as yet undocumented
effects of including thermally-induced preloading in the analysis
are observed. It should be noted that this work is easily extended
to include uniform internal and/or external pressure loadings and
the application of strain and stress failure theories.

3. This effort was funded under Survivability, Structures, and
Materials Directorate Job Order number 4-1700-001-41 and NASA Grant
NAG-1-901.

Martin A. Kienzke
MARTIN A. KIENZKE
By direction

Enclosure (1) has been assigned CARDEROCKDIV-U-SSM-65-93/03

Writer: Paraska/code 65.1
Typist: Paraska/x71650/29 MAR 1993

157798
11-11-93